

HEPATIC CLEARANCE OF DRUGS: DISCRIMINATION BETWEEN TWO MODELS
AND IMPLICATIONS IN PHARMACOKINETICS AND THERAPEUTICS

by

Kim-Ching Sandy Pang
B.Sc.Pharm., University of Toronto, 1971.

DISSERTATION

Submitted in partial satisfaction of the requirements for the degree of

DOCTOR OF PHILOSOPHY

in

PHARMACEUTICAL CHEMISTRY

in the

GRADUATE DIVISION

(San Francisco)

of the

UNIVERSITY OF CALIFORNIA

Approved:

Malcolm Rowland
Leslie B. Bent
D. K. Kirby

Committee in Charge

Deposited in the Library, San Francisco Medical Center:

Date

Librarian

JAN 4 1976

Degree Conferred:

ABSTRACT

The disposition of lidocaine (L) and its monodeethylated metabolite, monoethylglycine xylidide (MEGX) were studied in the perfused rat liver in situ preparation in an attempt to discriminate between two widely used models of hepatic clearance. In one model (Model I), the liver is regarded as a well stirred compartment with the effluent unbound drug concentration in equilibrium with that in the liver. In the other (Model II), the liver is regarded as a large number of parallel identical units with enzyme distributed evenly throughout the units.

A theoretical analysis of the response of various parameters to changes in organ blood flow, plasma protein binding and/or blood cell partitioning and a hepatocellular enzymatic activity term, A' indicate that the two models behave differently and that maximum discrimination is achieved by monitoring the influence of blood flow and plasma protein binding and/or blood cell partition on the availability of a highly cleared drug under steady state and linear conditions. Under conditions where $a, \lambda = 1$ discrimination between Models I and II was performed by monitoring the influence of hepatic blood flow on the availability or the effluent concentration of a highly cleared drug under steady state and linear conditions.

The perfused rat liver in situ preparation was viable for at least 2.5 hours. In single passage perfusion experiments, the extraction of L,

judged by measurements of the difference in concentration of drug across the liver and lack of uptake by the liver, was greater than 99.5%. Steady state was achieved within 20 minutes and the system was linear at influent concentrations below 7 mg/L. When operating under steady state and linear conditions for L, the response of the availability of L and the resultant effluent concentration of MEGX to a stepwise change in hepatic blood flow (10-16 ml/s/min/liver) were best predicted by Model I. The analysis is based on the assumption that the hepatocellular enzymatic activity remains constant with time and changes in blood flow. To exclude the last possibility, the influence of hepatic blood flow on the clearance of a poorly cleared drug antipyrine was studied.

Theoretically, according to both Models I and II, the clearance of a poorly cleared drug equals the term A' and is independent of perfusion. Single passage and recirculating experiments indicated that the extraction ratio of antipyrine ranged between 0.04-0.08. In confirmation of the prediction, the hepatic clearance of antipyrine in recirculating experiments did not vary with changes in blood flow between 8-16 ml/s/min/liver.

When the metabolite, MEGX, was infused alone into the rat liver preparation under steady state and linear conditions concentrations (concentrations <0.5 mg/L), the extraction ratio ranged between 0.7-0.9. This information together with the MEGX effluent concentration following infusions of L, suggest that at least 30% of L is deethylated to MEGX in the rat. In some single passage experiments, the availability of MEGX with blood flow changes between 10-16 ml/s/min/liver were best predicted by

Model I. In other experiments, neither Model I nor II satisfactorily predicted the observations. The explanation for this discrepancy remains unresolved.

The appearance of the metabolite (MEGX) in the perfusate generated from L with flow changes under linear kinetic conditions for L and MEGX was again better predicted by Model I. The analysis is based on the assumption that the fractional conversion of lidocaine to MEGX is constant and that the models can adequately describe the kinetics of MEGX.

Several single passage experiments were performed with L and MEGX separately using input concentrations (4-84 mg/L) which capacity limited the enzyme system(s). Attempts to satisfactorily fit the observations based on Models I and II, assuming a single-enzyme system, were partially successful, although predictions based on Model I tended to give a better fit of the data. Various explanations for the discrepancy are proposed, including deterioration of the liver preparation with time or high concentration of drug, the presence of multiple enzyme system of widely differing values of V_{max} and K_m , and end product inhibition. The possibility of MEGX diminishing the clearance of L was investigated by adding varying concentrations of MEGX (0-13 mg/L) to the perfusate containing a low concentration of L in three single passage experiments. A concentration dependent inhibition of L by metabolite MEGX was demonstrated in all cases, although considerable variation existed between experiments.

All the data with L, MEGX and antipyrine point to an acceptance of a

model of hepatic drug clearance which conceives of the liver acting operationally as a well stirred single compartment, with the effluent drug concentration in equilibrium with that in the liver (Model I). The implications of this model in pharmacokinetics, therapeutics and drug metabolism are several fold. For hepatically cleared drugs given orally on fixed dose-fixed interval dosage regimen, the plateau plasma concentration is independent of hepatic blood flow, and depends only on the rate of drug administration and the intrinsic hepatocellular activity term A' and the degree of protein binding (α) and/or blood cell partitioning (function λ). Thus for such drugs, whether highly or poorly cleared, the sole source of variation in the plateau concentration in a population receiving the same rate of administration result from variation in the term A' , α or λ . Similarly, according to Model I, the total area under a blood concentration-time curve following oral administration also depends only A' , α and λ and is independent of hepatic blood flow. Estimates of V_{max} , K_m are frequently made from peripheral plasma or blood concentration-time data. Estimates of V_{max} are essentially independent of the model used, but according to Model I, there is an overestimation of K_m for highly hepatically cleared drugs. An estimate of the true K_m can be made if V_{max} and hepatic blood flow are known.

O.K.

Y.T. Banet
for Malcolm Rowland

ACKNOWLEDGEMENTS

To the doctors of philosophy, I would like to express my appreciation to those who have formally instructed me, interacted with me and befriended me. I would like to express my gratitude to their criticism, suggestions, time and patience.

To the graduate students, I would like to express my thanks to their friendship and encouragement for making these four years of graduate school a very pleasant four.

Lastly and most important of all, I would like to say thanks to the many rats that I have sacrificed, especially to those which worked for making the present investigation a possibility.

TABLE OF CONTENTS

	Page
ACKNOWLEDGMENTS	1
LIST OF TABLES	viii
LIST OF FIGURES	x
I. INTRODUCTION.....	1
A. History: Clearance - A Concept.....	1
B. Clearance Concepts in Pharmacokinetics and Therapeutics	2
1. As a Determinant of Half-Life.....	3
2. As a Determinant of Plateau Concentration.....	3
3. As an Assessment of Availability.....	4
4. As an Assessment of Organ Function.....	5
C. The Liver: An Eliminating Organ.....	6
1. Anatomy.....	6
2. Histology	8
3. Function of the Liver.....	9
4. Hepatic Clearance and Oral Availability.....	9
D. Factors Affecting Hepatic Clearance of Drugs.....	10
1. Liver Mass.....	11
2. Blood Flow.....	11
3. Oxygen.....	12
4. Temperature.....	13
5. Plasma Protein Binding.....	13
E. Measurement of Hepatic Clearance.....	14
1. Measurement <u>In vivo</u>	14
2. Measurement <u>In vitro</u>	15
F. The Perfused Liver Preparation.....	15
II. THEORETICAL.....	17
A. Models of Hepatic Clearance.....	17
1. Brauer's Description of Hepatic Clearance.....	21
2. Model I.....	23
3. Model II.....	28

TABLE OF CONTENTS (continued)

	Page
a. Changing Hepatic Blood Flow.....	37
1) Model I.....	37
a) Extraction Ratio.....	39
b) Clearance.....	39
c) Availability.....	40
d) Area under the Blood-Concentration-Time Curve Following a Single Oral Dose.....	40
e) Area under the Blood-Concentration-Time Curve Following a Single Intravenous Dose..	41
f) Steady State Drug Concentration in Blood Following Constant Oral Administration.....	41
g) Steady State Drug Concentration in Blood Following Constant Drug Infusion.....	42
2) Model II.....	45
a) Extraction Ratio.....	45
b) Clearance.....	46
c) Availability.....	46
d) Area under the Blood-Concentration-Time Curve Following a Single Oral Dose.....	47
e) Area under the Blood-Concentration-Time Curve Following a Single Intravenous Dose..	47
f) Steady State Drug Concentration in Blood Following Constant Oral Administration.....	48
g) Steady State Drug Concentration in Blood Following Constant Drug Infusion.....	51
b. Changing $\frac{a}{A}$	51
1) Model I.....	52
a) Extraction Ratio.....	53
b) Clearance.....	54
c) Availability.....	54
d) Area under the Blood-Concentration-Time Curve Following a Single Oral Dose.....	55
e) Area under the Blood-Concentration-Time Curve Following a Single Intravenous Dose..	55
f) Steady State Drug Concentration in Blood Following Constant Oral Administration.....	56
g) Steady State Drug Concentration in Blood Following Constant Infusion.....	56
2) Model II.....	58

TABLE OF CONTENTS (continued)

	Page
a) Extraction Ratio.....	58
b) Clearance.....	59
c) Availability.....	59
d) Area under the Blood-Concentration-Time Curve Following a Single Oral Dose.....	60
e) Area under the Blood-Concentration-Time Curve Following a Single Intravenous Dose..	61
f) Steady State Drug Concentration in Blood Following Constant Oral Administration.....	61
g) Steady State Drug Concentration in Blood Following Constant Drug Infusion.....	62
 c. Changing A'.....	62
1) Model I.....	64
2) Model II.....	64
 B. Discrimination between Models I and II.....	66
1. By the Alteration of Blood Flow under Linear Kinetic Conditions.....	68
2. By the Alteration of Protein Binding and/or Blood Cell Partitioning under Linear Kinetic Conditions...	70
3. By the Alteration of Eliminating Capacity (A') under Linear Kinetic Conditions.....	73
4. By Graphical Discrimination - Fitting Data to Linearized Equations for Models I and II.....	74
a. Changing Blood Flow under Linear Conditions (Low concentrations to the Liver; g is held Constant)..	74
b. Changing the Degree of Protein Binding (Low Concentration to the Liver; Blood Flow Is Constant)	75
c. Changing the Input Drug Concentration to the Liver Such that the Velocity of Removal Approaches the Vmax of the System (Blood Flow Is Constant).....	77
 III. STATEMENT OF PURPOSE OF INVESTIGATION.....	79
 IV. EXPERIMENTAL.....	81
A. Material.....	81
B. Procedure.....	84
 I. Biological.....	84
a. Preparation of the Perfusion Medium.....	85
b. The Apparatus.....	86
c. Operative Procedure.....	90
d. Method and Time of Sampling.....	92

TABLE OF CONTENTS (continued)

	Page
1) Blood.....	92
a) Single Passage (Steady State Experiments)	92
b) Recirculating Experiments.....	93
2) Bile.....	93
3) Liver.....	93
2. Chemical.....	94
a. Lidocaine Assay in Blood, Bile and Liver.....	94
b. Antipyrine Assay in Blood and Bile.....	99
c. MEGX Assay in Blood, Bile and Liver.....	103
d. Protein Determination.....	105
e. Analysis of the Biochemistry of the Perfusion Medium.....	109
3. Physical.....	109
a. Method of Protein Binding Determination.....	109
b. Measurements of Oxygen Tension and pH.....	114
c. Measurement of Perfusion Pressure.....	115
d. Electron Microscopy.....	115
V. RESULTS AND DISCUSSION.....	116
A. Analytical.....	116
1. Biological.....	116
2. Chemical.....	117
a. Lidocaine Assay.....	117
1) Stability and Reproducibility.....	117
2) Specificity.....	119
3) Sensitivity.....	120
b. Antipyrine Assay.....	120
1) Stability and Reproducibility.....	120
2) Specificity.....	121
3) Sensitivity.....	121
c. MEGX Assay.....	121
1) Stability and Reproducibility.....	122
2) Specificity.....	123
3) Sensitivity.....	123

TABLE OF CONTENTS (continued)

	Page
B. Discussion of the Experimental Procedure.....	124
1. Protein Binding.....	124
2. Discrimination between Models I and II by Changing Hepatic Blood Flow of a Highly Cleared Drug at a Concentration to the Liver below the Km of the System	127
a. Lidocaine, a Highly Cleared Compound.....	127
b. Viability, Stability and Steady State.....	129
c. Linearity.....	137
d. Experimental Design.....	138
e. Results and Treatment of Data for the Flow-Change Experiments Conducted at Constant Influent Lidocaine Concentrations at or below 4 mg/L.....	142
f. Mass Balance with Liver Analysis.....	148
3. Clearance of a Poorly Cleared Compound with Changes in Blood Flow.....	151
4. Discrimination between Models I and II by Changing the Influent Lidocaine Concentration Delivered at Constant Blood flow to the Liver When Operating under Non-linear Conditions.....	160
5. Further Discrimination between Models I and II by the Formation of the Metabolite (MEGX) from the Parent Compound (Lidocaine) with Flow Changes under Linear Conditions.....	172
a. Linearity of MEGX Extraction under Constant Blood Flow.....	172
b. Effect of Flow Changes on the Extraction of MEGX under Linear Kinetic Conditions.....	172
c. Generation of MEGX from Lidocaine at a Constant Low Concentration of Lidocaine to the Liver with Changes in Blood Flow.....	177
6. Fitting of Data from the Literature into the Models..	192
VI. CONCLUSIONS	200
A. Implications of Model I in Pharmacokinetics and Therapeutics Under Linear Kinetic Conditions.....	202
1. Hepatic Blood Flow.....	203
2. Protein Binding or Blood Cell Partitioning	209
3. Hepatocellular Activity or Eliminating Capacity of the System (Term A').....	213
4. Generation of Metabolites.....	215
5. Estimation of <u>In vivo</u> Vmax and Km.....	218
B. Qualifying Remarks	224

TABLE OF CONTENTS (continued)

	Page
Appendix I.....	225
Appendix II.....	227
Appendix III.....	228
Appendix IV.....	230
Appendix V.....	232
Appendix VI.....	234
Appendix VII.....	238
Appendix VIII.....	242
Appendix IX.....	246
Appendix X.....	249
Appendix XI.....	251
Appendix XII.....	253
REFERENCES.....	256 •

LIST OF TABLES

Table	Page
1. Interrelations between A' , α , λ and \dot{V}_B and Various Pharmacokinetics Parameters for Models I and II.....	36
2. A comparison of Predicted Pharmacokinetics Parameters in Terms of \dot{V}_B , α , λ and A' for Models I and II.....	67
3. List of Compounds Used.....	81
4. Composition of the Perfusion Medium.....	84
5. Stability of Lidocaine in Liver Tissue Stored in 10% NaOH.....	118
6. Binding of Lidocaine to Perfusate Components.....	125
7. Binding of MEGX to Perfusate Components.....	126
8. Lidocaine Elimination by Bile.....	131
9. The Biochemistry of the Perfusate Medium.....	132
10. Oxygen Tension in Arterial and Venous Blood at Various Flow Rates.....	134
11. Flow-Pressure Relationship of the Perfused Rat Liver <u>in situ</u> Preparation.....	136
12. Constant Extraction of Lidocaine with Influent Concentration below 7 mg/L.....	138
13. Influence of Hepatic Blood Flow on the Extraction of Lidocaine.....	139
14. Regression Analysis of Data and Comparison of the Slopes to Slope = 1.....	147
15. Liver Analysis of Lidocaine and the Partition of Lidocaine in Liver with Respect to Effluent Drug Concentration in the Blood.....	149
16. Various Parameters Calculated for Antipyrine in Recirculating Experiments.....	158
17. Effect of Influent Lidocaine Concentration on Its Hepatic Extraction under Constant Blood Flow (10 ml/min) - Studies I and II.....	161

LIST OF TABLES (continued)

	Page
18. Regression Analyses and Curve Fitting by NONLIN Performed on Studies I and II for Models I and II.....	163
19. Generation of MEGX with High Concentration of Lidocaine - Studies I and II.....	168
20. Inhibition of Metabolism of Lidocaine by MEGX - Studies I, II and III.....	171
21. Statistical Parameters from Regression Analysis and the Comparison of Slopes on the Predicted and Observed Effluent MEGX Concentrations for Models I and II.....	176
22. Statistical Parameters from Regression Analyses and the Comparison of Slopes in the Predicted and Observed Data for Model I (Effluent MEGX Concentration) and Model II (Ratio of Effluent MEGX and Lidocaine Concentrations)	186
23. Computer fitting by NONLIN of data from Brauer and Whitsett.....	194

LIST OF FIGURES

Figure	Page
1. Blood Supply of the liver.....	7
2. Elimination of Drugs across the liver as viewed as A) Mass balance across the Liver, B) Mass balance expressed relative to rate of drug entry and C) Mass balance expressed relative to input drug concentration.....	18
3. Diagrammatic representation of the liver, an eliminating organ and the reservoir (body), a non-eliminating organ as a two compartment model with elimination from the peripheral (liver) compartment.....	20
4. Diagrammatic representation of Model I - the liver is conceived as a well stirred compartment.....	24
5. Diagrammatic representation of Model II - liver sinusoids as parallel tubes.....	29
6. A unit of the Model (Model II).....	30
7. Influence of Hepatic blood flow on pharmacokinetic parameters A) ER, B) \dot{V}_{cl} and C) F according to Model I....	43
8. Influence of hepatic blood flow on pharmacokinetic parameters A) AUC_{oral} , B) AUC_{IV} , C) $C_{B,ss,oral}$, and D) $C_{B,ss,inf}$ according to Model I.....	44
9. Influence of hepatic blood flow on pharmacokinetic parameters A) ER, B) \dot{V}_{cl} and C) F according to Model II... .	49
10. Influence of hepatic blood flow on pharmacokinetic parameters A) AUC_{oral} , B) AUC_{IV} , C) $C_{B,ss,oral}$ and D) $C_{B,ss,inf}$ according to Model II.....	50
11. Influence of the ratio $\frac{a}{b}$ on pharmacokinetic parameters A) ER or \dot{V}_{cl} B) F C) AUC_{oral} or $C_{B,ss,oral}$ and B) AUC_{IV} or $C_{B,ss,inf}$ according to Model I.....	57
12. Influence of the ratio $\frac{a}{b}$ on pharmacokinetic parameters A) ER or \dot{V}_{cl} B) F C) AUC_{oral} or $C_{B,ss,oral}$ and D) AUC_{IV} or $C_{B,ss,inf}$ according to Model II.....	63

LIST OF FIGURES (continued)

	Page
13. Influence of the eliminating capacity (A') on A) ER or \dot{V}_{Cl} according to Model I B) ER or \dot{V}_{Cl} according to Model II and C) ratio ER ₁ /ER _{II} or $\dot{V}_{Cl1}/\dot{V}_{ClII}$	65
14. Ratio of the anticipated values of various pharmacokinetic parameters with changes in hepatic flow.....	71
15. Ratio of the anticipated values of various pharmacokinetic parameters with changes in the ratio $\frac{a}{X}$	72
16A. Linearized transformation of Equation 19 (Model I) ($\frac{a}{X}$ is held constant).....	74
16B. Linearized transformation of Equation 27 (Model II) ($\frac{a}{X}$ is held constant).....	75
17A. Linearized transformation of Equation 19 (Model I) (\dot{V}_B is held constant).....	76
17B. Linearized transformation of Equation 27 (Model II) (\dot{V}_B is held constant).....	76
18A. Linearized transformation of Equation 15 (Model I) at High Input Concentration to the Liver ($\frac{a}{X}$ and \dot{V}_B are held constant).....	78
18B. Linearized transformation of Equation 26 (Model II) at High Input Concentration to the Liver ($\frac{a}{X}$ and \dot{V}_B are held constant).....	78
19. Schematic representation of the assembly of the Perfusion Apparatus.....	87
20. The Liver Perfusion Apparatus.....	88
21. Parts of the Perfusion Apparatus A) Harvard Peristaltic Pump B) Bentley by-pass filter and C) Oxygenator and Bubble Trap.....	89
22. Chromatograms obtained when blank blood (A), 1 mcg lidocaine hydrochloride monohydrate and 1 mcg Br-DEA in blood (B), and 1 mcg lidocaine hydrochloride monohydrate and 1 mcg WI2714 in blood (C) were taken through the assay procedure.....	97
23. Calibration curve for lidocaine.....	98

LIST OF FIGURES (continued)

Page

24. Chromatograms obtained when blank blood (A) and blood containing 5 mcg antipyrine and 10 mcg 4-bromo-antipyrine (B) were taken through the antipyrine assay.....	101
25. Calibration curve for antipyrine.....	102
26. Chromatograms obtained when 2 ml blank blood (A) and the same volume of blood containing 750 ng MEGX and 500 ng internal standard (B) were taken through the assay.....	106
27. Calibration curve for MEGX in blood.....	107
28. Calibration curve for protein.....	110
29. Attainment of equilibrium during equilibrium dialysis.....	113
30. Viability of the Preparation.....	130
31. Schematic representation of the design of experiments used to discriminate between two models of hepatic drug clearance with alterations in blood flow.....	141
32. The Predicted and observed lidocaine data for Models I and II when blood flow is changed to 12, 14 and 16 mls/min from the control flow rate of 10 mls/min (Study I-Appendix IX).	143
33. Predicted versus observed effluent lidocaine concentrations for Model I for a series of nine experiments performed at a low influent lidocaine concentration (4 mg/L) with alterations of blood flow.....	145
34. Predicted versus observed effluent lidocaine concentrations for Model II for a series of nine experiments performed at a low influent lidocaine concentration (4 mg/L) with alterations of blood flow.....	146
35. Exponential decay of the concentration of antipyrine in the reservoir with time under constant blood flow (10 mls/min) to the liver preparation in a recirculating experiment (Study I).....	154
36. Exponential decay of the concentration of antipyrine in the reservoir with time under constant blood flow (10 mls/min) to the liver preparation in a recirculating experiment (Study II).....	155
37. The lack of effect of changes in hepatic blood flow on the exponential decay of the concentration of antipyrine in the reservoir with time in a recirculating experiment (Study III).....	156

LIST OF FIGURES (continued)

Figure	Page
38. The lack of effect of changes in hepatic blood flow in the exponential decay of the concentration of antipyrine in the reservoir with time in a recirculating experiment (Study IV)	157
39. A plot of the predicted and observed effluent MEGX concentrations with blood flow changes at constant low influent MEGX concentration for Model I	174
40. A plot of predicted versus observed effluent MEGX concentrations with blood flow changes at constant low influent MEGX concentrations for Model II..... (-g/V _B)	175
41. A plot of (1-e ^{-g/V_B})/g against g	185
42. Predicted MEGX effluent concentrations versus the observed data for Model I for the same nine experiments performed with low influent lidocaine concentration with alterations in blood flow.....	188
43. Predicted MEGX effluent concentrations versus the observed data for Model II for the same nine experiments performed with low influent lidocaine concentration with alterations in blood flow.....	189
44. NONLIN computer curve fitting of data from Brauer for Models I and II	195
45. NONLIN computer curve fittings of data from Whitsett for Models I and II	196
46. Plot of weighted residual against the predicted value of the data from Brauer and Whitsett for Models I and II	198

1. INTRODUCTION

A. History: Clearance - A Concept

The concept of comparing simultaneous blood and urine concentrations of a given marker as an index of renal function appears to have been introduced by Gréhant in 1904 (1), who used the ratio of urinary urea to blood urea concentrations as an index of renal functional capacity. The effect of changing the volume of urine on the concentration of urea was however, disregarded. Ambard and Weill (2) were the first to include both urea output and urine volume in an attempt to relate urea excretion quantitatively to urea content of blood, and so paved the way for the clearance formula. Although the actual clearance formula was first suggested by Thomas Addis in 1917 (3), the term was first used by Möller and co-workers in 1929 (4). They defined the clearance of any substance as the volume of biological fluid that is cleared of the drug per unit time. This is not a real volume. As blood passes through the kidneys, no single ml of blood has all of its urea removed in one transit through the kidney; rather a little urea is removed from each of the many ml of blood perfusing the kidneys. One may add up this urea and express it as though it were derived by completely clearing a much smaller volume of all of its contained urea.

The concept of clearance not only applies to the kidneys but to other eliminating organs irrespective of the process or mechanism involved. The concept of hepatic clearance appears to have been first introduced by

Lewis (5) and related to the ability of the liver to eliminate drugs.

Clearances of bases by the stomach have been reported in dogs when drugs are given intravenously (6) while the lung as a clearing organ for endogenous (7,8,9) and exogenous compounds (10) has been well documented.

Strictly speaking, clearance should be defined with respect to the eliminating organ, the sampling site and the elimination process involved. For example, the clearance of a drug associated with metabolism by the liver and measured in blood is its hepatic blood metabolic clearance. Generally, plasma is the site sampled and reference is always made to plasma clearance unless stated otherwise. Blood clearance can be calculated directly if the concentration in blood is measured, or from plasma clearance when the ratio of the concentration of drug in blood to plasma is known (11).

Drugs are eliminated in various ways and by different organs. Total clearance is a term used to denote the sum of the clearances by each eliminating organ. Total clearance is usually determined from intravenous bolus or constant intravenous infusion studies (12, 13). Although clearance can be determined at any instant by a direct measurement of the drop in concentration across an organ, what usually determined is the time-average value (14) and when the system is linear, the time-average clearance equals the steady state clearance (14).

B. Clearance Concepts in Pharmacokinetics and Therapeutics

Clearance concepts play an important role in pharmacokinetics and biopharmaceutics.

1. As a Determinant of Half-Life

Irrespective of any model, the rate of elimination of a drug by an organ is the product of its clearance and entering concentration. In the simplest case, the linear open one compartment model, clearance (\dot{V}_{Cl}) can be expressed as

$$\dot{V}_{Cl} = k \cdot V_d$$

Equation 1

$$= \frac{0.693 \cdot V_d}{t_{1/2}}$$

where k is the elimination rate constant, V_d is the volume of distribution and $t_{1/2}$ is the half-life of the drug, that is, the time it takes for the amount of drug in the body (or plasma concentration) to fall by one-half. And so, for a given clearance, the larger the volume of distribution, the longer the half-life of the drug.

In linear multicompartment models, the relationship between clearance and the half-life associated with the majority of drug elimination is more complex, but a strong dependence of this half-life on clearance still exists (15).

2. As a Determinant of the Plateau Concentration

Following a constant intravenous infusion, the steady state concentration is controlled only the rate of infusion and the total clearance

of the drug (12). A correction must be made for the availability (F) when a drug is administered extravascularly. An understanding of the factors which influence drug clearance allows reasonable predictions of steady state drug concentration under a number of conditions (16, 17, 18, 19). Knowing the total clearance the equations relating steady state concentration to infusion rate have been extended to predictions of plateau concentrations achieved with fixed dose-fixed time interval dosage regimens (20). Here the plateau concentration is the time-average concentration during the dosing interval at the plateau (12). These equations, or modifications thereof have been some of the most widely used in the clinical application of pharmacokinetics (21).

3. As an Assessment of Availability

Clearance can influence and is used to assess the availability of a drug. Availability is defined as the extent to which an administered material reaches the point of measurement, usually a peripheral venous site. The route of administration can influence drug availability. The intravenous route of administration circumvents the process of absorption by introducing the drug directly into the blood stream. Most drugs, however, are given orally, and some of them are poorly available. This may be due to the failure to cross gastrointestinal epithelium (22), degradation in the lumen of the gastrointestinal tract (23), or complexation with the luminal contents of the gastrointestinal tract and hence removal with the feces (24, 25). Other compounds (26) may be poorly available because a significant fraction is removed by hepatic extraction before the drug reaches the systemic circulation, a phenomenon known as the "first-pass effect" (27).

For any linear kinetic model availability (F) is related to dose, the total area under the blood-concentration-time (AUC) and the blood clearance of the unchanged drug by: (20)

$$F = \frac{AUC \cdot V_{cl}}{\text{Dose}} \quad \text{Equation 2}$$

For drugs given intravenously, F is unity so that the ratio of the availability between extravascular and intravenous dose gives the absolute value for the availability of the extravascular dose. Relative availability is the ratio of the availability of two extravascularly administered dosage forms. In either case, the most common method of assessing the ratio is based on Equation 2, and compares the AUC following the different routes of administration or different dosage forms and correcting for differences in the dose (20). This method is applicable to single or multiple situations (12) but in each case it is assumed that total clearance is constant with concentration and time. Assuming that the ratio of renal to total clearance remains constant, drug availability has also been conveniently determined by comparing the ratio of the cumulative amount of drug excreted unchanged in urine (20) for both single dose and multiple dose studies.

4) As an Assessment of Organ Function

A variety of tests, based on clearance considerations have been devised to assess the degree of impairment of organ function. Urea and inulin (28) have been used to assess the glomerular filtration rate. The hepatic clearance of bromosulphalein (BSP) (29, 30, 31) indocyanine green (32,33),

galactose (34,35,36) and antipyrine (37) have been used as measurements of liver function. The efficiency of hepatic extraction of colloidal chromic phosphate CrPO_4 (38), colloidal gold (39) and thorotrust (40) have also been used as tests for liver function.

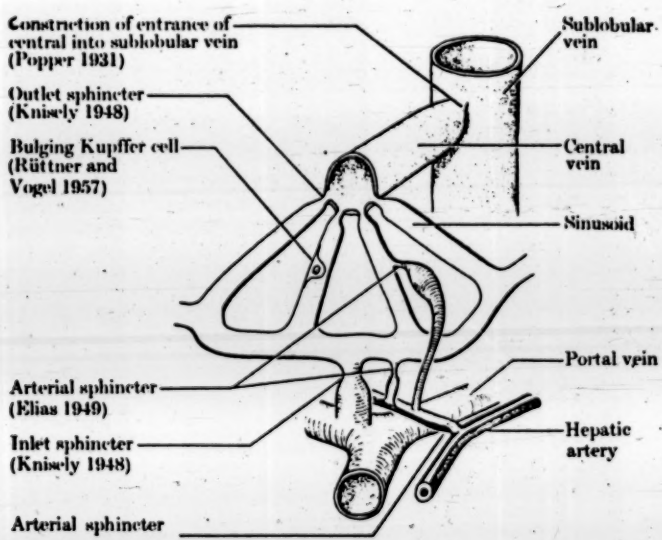
C. The Liver: An Eliminating Organ

1. Anatomy

The liver is the major organ for metabolism of most compounds and together with the excretory function of the kidney, plays an important role in the elimination of drugs. Anatomically, the liver is a lobular organ interposing between the gastrointestinal tract and the general circulation. It is the largest organ in the body, about 3% of the total body weight (14) and receives a total blood flow of about 1 ml/min/gm liver of which 20-30% is supplied by the hepatic artery. The remainder enters as deoxygenated blood at low pressure and in a steady non-pulsatile stream via the portal vein, which drains blood from the spleen, pancreas, and gastrointestinal tract (42,43). The normal portal vein pressure in the rat is 12-14 cm blood and in man is 7-10 mm Hg (44). The portal venous tree branches out to an extraordinarily high degree (Figure 1) (45). This highly ramified portal tree in turn pours its contents into a sinusoidal bed which forms a continuous meshwork of interconnected blood spaces, interpenetrated by an equally continuous system of convoluted sheets of liver parenchyma cells, and lined by a delicate endothelial cell sheet. Any element of blood within the sinusoidal bed can reach another part of the sinusoidal bed within the organ.

Figure 1. Blood supply of the liver (45)

The relationship between portal venous and hepatic arterial supply is shown; both systems supply the sinusoids which separate sheets of liver parenchyma cells.



without leaving this section of the vascular tree.

The hepatic artery arises from the coeliac axis, a branch of the aorta that arises just beneath the diaphragm. It is not only connected to the portal vein by cross anastomoses but also supplies a capillary plexus which enmeshes the bile ducts in particular and drains into the portal vein or to a smaller extent into the sinusoids (46).

Venous blood emerges from the sinusoids to enter the hepatic veins. These vessels have a very short course outside the liver before entering the inferior vena cava.

2. Histology

Histologically, the liver is a continuous mass of parenchyma cells (about 60% of cell population) tunneled by vessels and sinusoids. Apart from the liver parenchyma cells, there are flat "littoral" or Kupffer cells (30%) which line the sinusoids and have a phagocytic action (47). Connective tissue, substances which occupy space and resist deformation are present in the liver. This connective tissue is divided into lobular, vascular and capsular portions. The greater part of the noncapsular collagen of the liver is found associated with vessels larger than the sinusoids. Reticular scaffolding of lobular portions of the liver i.e. parenchyma adjacent to the sinusoids, appear slight. The slightly scaffolded plates of parenchyma, with their endothelial lining, are suspended in their blood matrix between the meshes of a network of rather solid portal tracts

Interlaced by a corresponding network of hepatic vein branches.

3. Function of the Liver

The liver plays an important role in almost all phases of intermediary metabolism and assists in the regulation of body fluids. It is the major organ for drug biotransformation (48). During their passage through the liver, substances are generally converted by a multi-enzyme system to more polar excretable forms. Additionally they may be excreted via the bile, a complex isotonic solution containing pigments (derived from the breakdown of porphyrins), bile salts, cholesterol and lecithins in the micellar form and inorganic electrolytes. Discrete transport mechanisms are present which control the secretion of a wide range of endogenous and foreign substances into the bile. The secreted substances can be reabsorbed through the gastrointestinal tract back into the blood stream and thereby completing an enterohepatic process (49). There is also a copious lymphatic drainage to the liver, in the Spaces of Disse and beneath the liver capsule. However lymph flow is more sluggish than bile flow and hence is viewed as an insignificant route of drainage (45).

4. Hepatic Clearance and Oral Availability

When given orally, some compounds which are highly extracted by the liver may be transformed to inert or less active metabolites and hence fail to reach an effective concentration in the blood (50, 51). This is due to the "first-pass effect". After this initial extraction by the

liver, the fraction of the dose that is available or the extent of availability (F) is given by:

$$F = 1 - ER$$

Equation 3

For highly cleared drugs, variations in the extraction ratio (ER) will cause large variations in the availability.(52). Availability can be estimated by the comparison of the AUC for a single oral to that of an intravenous dose for the same amount of dose given. A correction for the doses needs to be made if different doses are used. The basis of the comparison of the AUC's for the estimation of F is that total clearance is constant with concentration and time. Gibaldi *et al* also showed a method for the estimation of F under the same assumptions using only oral data (AUC_{oral}), hepatic blood flow and the dose (27)..

D. Factors Affecting the Hepatic Clearance of Drugs

Hepatic clearance is dependent upon the mass of functional cellular elements available as well as upon circulating factors and regulatory mechanisms. The interrelationships between these variables are depicted schematically (53)

$$\text{Hepatic clearance} = \text{Total Hepatic}$$

$$\text{Blood Flow} \quad \times \quad \text{Extraction Ratio}$$

$$= \text{Liver Mass} \times \text{Tissue Perfusion} \quad \times \quad \text{Extraction Ratio}$$

$$= \text{Liver Mass} \times \text{Perfused Fraction} \quad \times \quad \text{Effective Tissue Perfusion}$$

$$\times \quad \text{Extraction Ratio}$$

1. Liver Mass

Liver Mass

Most hepatic processes involve enzymatic mechanisms. Therefore, an upper limit for reaction velocity must exist for each process. These maximal velocity must exist for each process. These maximal velocities are proportional to the functional liver mass, which depends not only on the total cellular amount of enzymes, but also on the evenness of perfusion and the presence of inhibitory or accelerating factors (54).

2. Blood Flow

Hepatic clearance can also be influenced by liver blood flow. Liver blood flow can be estimated by injection of substances such as indocyanine green (ICG) (55), bromosulphalein (BSP), ¹³¹I rose bengal, ¹⁹⁸Au (56) and ethanol (57). Liver blood flow as reported by Brauer is 1.0 to 1.5 ml/min/gm liver in man, dog and the rat (58). Fischer reported the work of eighteen investigators on hepatic blood flow in dogs to be 34.6 ml/min/Kg of body weight (1.1 ml/min/gm liver) (44). Greenway and Stark reported similar findings in conscious dogs and for cats the value is 1:34 ml/min/gm liver and for man, 1.04 ml/min/gm liver (42).

Blood flow to the liver is known to be affected by blood pressure (53, 59) metabolic and nervous control (42, 44), as well as some pharmacological agents. Blood flow seems to be affected by posture; as the upright position decreases hepatic blood flow by 40% as compared to the supine (60). Pathological conditions are known to cause decreases in hepatic blood flow. Disease states as cardiac failure (61), liver cirrhosis (62) and

hepatitis (44) all result in a decrease in hepatic blood flow. In some cases, a decrease to one-third of the normal value was reported. However, liver blood flow can increase upon the administration of substances as phenobarbital (63) and cortisone (44). Thus within the realm of physiological interplay, the range of hepatic blood flow varies from 0.5 to 2 ml/min/gm liver.

3. Oxygen

Oxygen is a prerequisite for integral cellular function. Most of the oxygen supply to the liver comes via the hepatic arterial flow rather than the portal vein. Hepatic oxygen consumption as measured by the sum of (hepatic arterial flow X hepatic artery-hepatic vein difference) and (portal venous flow X portal vein-hepatic vein difference) in the dog is 1.9 ml/min/kg of body weight (2.0 mcMole/min/gm liver) (44). The isolated rat liver preparation has a similar value of 2.2 mcMole/min/gm liver (45). Cumming and Mannerling (64) found that in both the intact rat and the isolated rat liver preparation that the rate of hexobarbital metabolism was constant when the oxygen tension in the arterial blood was maintained above 45 mm Hg. Below an oxygen tension of 45 mm Hg in the arterial blood, a decline in the rate of hexobarbital metabolism was observed. The effect of hypoxia on liver function was also studied in the isolated perfused pig liver preparation (65). No functional parameter, including galactose elimination capacity (GEC) as a measure of functional hepatic mass, showed any significant change when the pO_2 in the hepatic veins

exceeded 30 mm Hg. Below this value, parallel decreases in GEC, oxygen uptake, ATP in liver tissue and ATP/ADP occurred while AMP in liver tissue and lactate/pyruvate ratio increased.

4. Temperature

Little is known about the sensitivity of the hepatic clearance of drugs to temperature. A drop in the temperature from 37°C to 20°C resulted in a decrease in blood flow, bile flow as well as extraction of radiocolloid chromic phosphate in the isolated rat liver preparation (66). Temporary cooling produced no permanent changes, and recovery upon rewarming was complete. Other studies (67, 68) which utilized hypothermic perfusion as a method of liver storage found no irreversible damage when function was assessed.

5. Plasma Protein Binding

Most drugs are bound to plasma proteins. The degree of binding varies with the drug, protein involved, and the concentration of both species. Binding may be influenced by the presence of other drugs (67) and disease states (70,71,72). Equilibrium between the small drug molecule and macromolecule is generally established within milliseconds and movement on and off proteins is easily facilitated. Whether changes in plasma protein binding will influence the hepatic clearance of a drug depends on its hepatic extraction (73). Alterations of protein binding are unlikely to

affect the hepatic clearance of highly extracted compounds such as lidocaine and propranolol (74, 75). It is only with the poorly cleared compounds that a dependence of clearance on plasma protein binding is anticipated. An example is warfarin, whose hepatic extraction ratio is only 0.0003. A linear relationship exists between its hepatic clearance and the fraction of unbound drug in plasma (76). The situation is analogous to the renal handling of a drug which is glomerularly filtered but neither secreted nor reabsorbed (77).

E. Measurement of Hepatic Clearance

I. Measurement in vivo

Difficulties arise in measuring hepatic clearance in vivo and usually it is measured indirectly. Thus, it is taken as the difference between the total and renal clearance, assuming all extrarenal elimination is via the liver. This assumption is sometimes invalid. The kidney is known to metabolize drugs (78, 79) and blood is also known to be a clearing "organ" for some compounds, e.g. acetylsalicylic acid (80).

Direct measurement of in vivo hepatic clearance requires direct sampling of the portal vein or the hepatic artery and the hepatic vein, and a knowledge of hepatic blood flow (26). The direct method gives a higher estimate of hepatic clearance (compared to the hepatic clearance estimated by the AUC method) when the drug undergoes enterohepatic recycling.

2. Measurement in vitro

A widely used in vitro technique is the liver perfusion preparation. Here, the liver remains intact. Fluid or blood, carrying nutrients and oxygen to sustain the liver in a viable state is mechanically circulated through the hepatic vascular bed. The techniques of liver perfusion are

- (1) isolated, where the liver is removed from the donor during perfusion.
- (2) in situ, where the liver remains in its natural anatomical position with the donor. For (1) and (2), the portal vein is cannulated as the inflow and the inferior vena cava as the outflow.
- (3) hepatic artery cannulation instead of the portal vein cannulation and
- (4) retrograde perfusion in which the inferior vena cava serves as the inflow while the outflow is via the portal vein (45).

F. The Perfused Liver Preparation

The perfused liver preparation, though employed as an in vitro technique, fulfills certain criteria for liver functions, and can survive for a sufficiently long period to allow study of its properties. The

properties of the perfused liver preparations were explored by the early work of Brauer and coworkers on bile production (82), portal pressure (82), temperature (66), and flow-pressure relationships (59) with the use of radiocolloid chromic phosphate.

The comparison of the functions of the isolated perfused pig liver to that of the in vivo pig liver (34) was done by more recent work by Tygstrup and Winkler (35) and other investigators (29). Herz et al (83) studied the excretory capacity of the isolated perfused liver to excrete bromosulfphthalein (BSP) and compared it to the in vivo preparation and found that there was no significant difference between the two preparations. Protein synthesis (84) as well as protein catabolism (85, 86) were demonstrated in the isolated perfused rat liver (87).

This preparation is widely utilized to study biochemical pathways, intermediary metabolism and the regulation of endogenous compounds (88,89,90,91). Drugs studied include nortriptyline (92), phenylbutazone (93), hexobarbital (94,95), imipramine and desmethylimipramine (96, 97). Other investigators have utilized this preparation to study altered metabolism of a drug with the use of an inhibitor or an enhancer (98, 99, 100).

1). THEORETICALA. Models of Hepatic Clearance

If one considers mass balance across the liver (Figure 2), the rate of drug removal or velocity (v) is given by the difference between the rate of drug input (blood flow (\dot{V}_B) X influent drug concentration (C_I)) and the rate of drug output (blood flow (\dot{V}_B) X effluent drug concentration (C_O)):

$$v = \dot{V}_B \cdot (C_I - C_O)$$

Equation 4

When the velocity is expressed relative to the rate of input ($\dot{V}_B \cdot C_I$), elimination is now expressed in terms of the extraction ratio (ER) of the drug, thus

$$\frac{v}{\dot{V}_B \cdot C_I} = \frac{(C_I - C_O)}{C_I} = ER \quad \text{Equation 5}$$

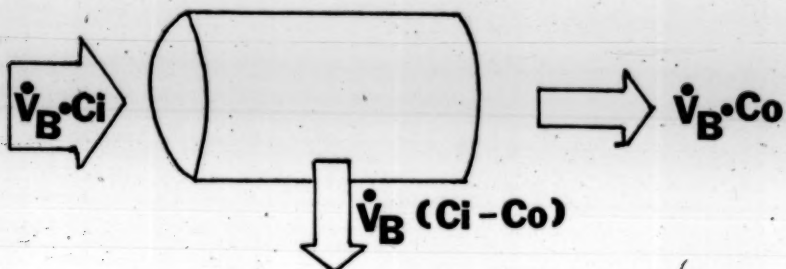
Alternately when the velocity is expressed relative to the influent drug concentration (C_I), the efficiency of elimination is expressed as the product of blood flow and the extraction ratio, which is the blood clearance (\dot{V}_{Cl}) of the drug.

$$\frac{v}{C_I} = \frac{\dot{V}_B (C_I - C_O)}{C_I} = \dot{V}_B ER = \dot{V}_{Cl} \quad \text{Equation 6}$$

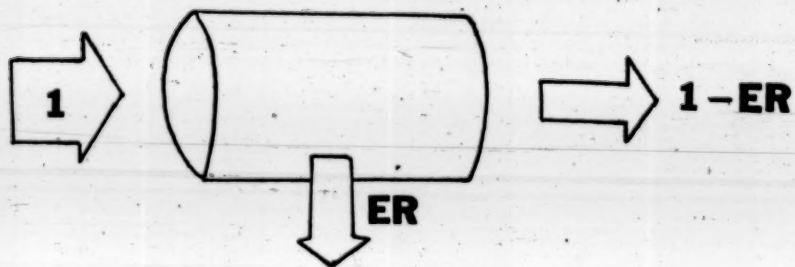
Figure 2. Elimination of drugs across the liver as viewed in

- A) Mass balance across the liver
- B) Mass balance expressed relative to rate of drug entry ($V_B \cdot C_I$)
- C) Mass balance expressed relative to input drug concentration (C_I)

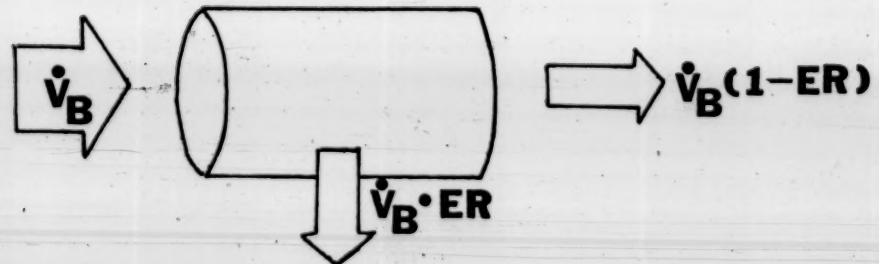
Mass balance across the liver



Mass balance expressed relative to
rate of drug entry ($\dot{V}_B \cdot C_i$)



Mass balance expressed relative to
input drug concentration (C_i)



Diagrammatically, the liver, an eliminating compartment is connected to a non-eliminating compartment (the reservoir, or the body compartment) via the blood stream as depicted in Figure 3. It is assumed that the concentration of drug in blood entering the liver (C_l) equals that in the reservoir (C_R) and similarly concentration in blood leaving the organ (C_o) and entering the reservoir are equal. Elimination can occur by metabolism or biliary excretion in the liver. This model assumes the liver as the only eliminating organ.

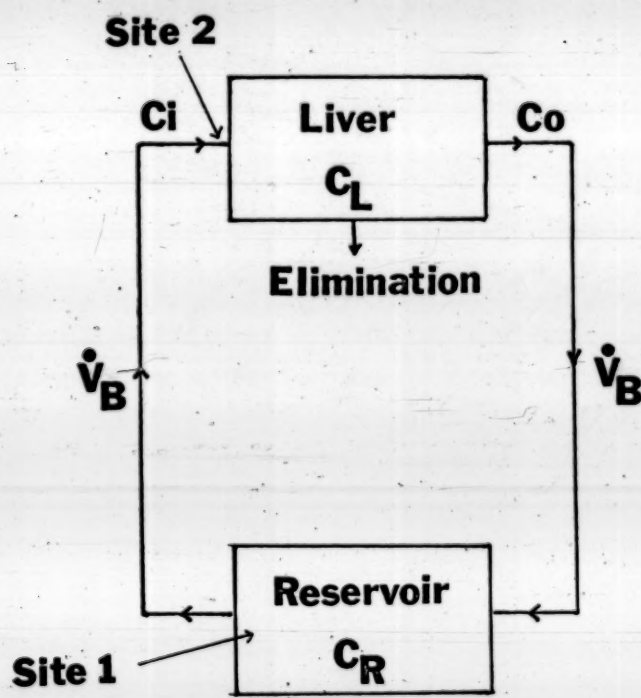
The introduction of a bolus of drug into the reservoir (site 1 in Figure 3) is analogous to intravenous administration of the drug. Here the drug initially distributes into the reservoir (body) before it reaches the eliminating organ. When the drug is introduced at a site just prior to the liver (site 2 in Figure 3), a situation analogous to the oral administration of a dose is created. The drug undergoes elimination by the liver before it reaches its site of sampling, usually at a remote venous site (reservoir). Thus only a fraction of the orally administered dose reaches the sampling site. This fraction is the extent of availability (F) as described earlier (page 4).

Pharmacokinetic parameters can be obtained viewing this liver model. The extraction ratio can be obtained by the assessment of the concentrations of the drug before and after the eliminating organ. Their difference divided by the influent concentration gives the fraction of the drug extracted during its passage through the liver, or the extraction ratio (ER) of the drug.

The clearance of the drug (\dot{V}_{C_l}) can be directly assessed from the product of hepatic blood flow and the extraction ratio. An alternative method of estimating clearance involves dividing the intravenously

Figure 3. Diagrammatic representation of the liver, an eliminating organ and the reservoir (body), a non-eliminating organ as a two compartment model with elimination from the peripheral (liver) compartment.

The arrows indicate the direction of blood flow (\dot{V}_B)
 C_I , C_0 , C_L and C_R are concentrations of the drug in blood to the liver away from the liver, in the liver and in the reservoir respectively.



administered dose by the area under the blood-concentration-time curve.

The area under the blood-concentration-time curve (AUC) is obtained by sampling the reservoir at appropriate times. An integration of the concentration of drug in the blood with time ($\int C dt$) gives the area under the curve.

The extent of availability (F) for an orally administered dose is given by (I-ER), or by a comparison of the area under the curve for an orally administered dose to that for an intravenously administered dose, correcting for the doses given. A measure of F is also given when the hepatic blood flow and the area under the curve for the orally administered dose is known (the method of Gibaldi) (27).

Constant oral administration (site 2 in Figure 3) and constant drug infusion (site 1 in Figure 3) give rise to steady state conditions. The steady state blood concentration ($C_{B,ss}$) is the concentration of the drug in the blood (reservoir) when the rate of drug administration equals to the rate of elimination such that the concentration of drug in the blood remains constant.

1. Brauer's Description of Hepatic Clearance

Early work by Brauer et al showed that an increase in blood flow decreased the hepatic extraction ratio of radiocolloid chromic phosphate (101). In an attempt to describe the hepatic uptake of this compound, these workers developed a model based on the following assumptions:

- (1) Chromic phosphate is taken up by the Kupffer cells lining the sinusoids.

(2) Chromic phosphate elimination may be described by first order kinetics.

(3) Clearance is constant and independent of concentration and previous exposure of the liver to the radiocolloid.

Evidence for linear kinetics was demonstrated by the log-linear disappearance of chromic phosphate in the perfusate in a recirculating experiment, that is:

$$[\text{CrPO}_4]_{t_2} = [\text{CrPO}_4]_{t_1} e^{-K(t_2-t_1)} \quad \text{Equation 7}$$

where $[\quad]$ denotes concentration at various times t_2 and t_1 , K is the rate constant for drug disappearance, and t_2, t_1 denote times ($t_2 > t_1$). Brauer et al (102) interpreted K to be a constant incorporating the rate constant for the basic reaction and the surface to volume ratio (or the "concentration of active surface") in that particular segment. However, in making their interpretation, they appeared to have erroneously extrapolated the above equation to describe the loss of chromic phosphate across the liver. They did this by assuming that t_1 represented the time in the portal vein and t_2 the time that the material would appear in the hepatic vein so (t_2-t_1) is the mean transit time for the material in the liver. Even so, their model has many characteristics in common with Model II to be described subsequently.

2) Model I

A model based on steady state considerations was constructed by Rowland et al (14) on the hepatic clearance of drugs. The basic assumptions are:



- (1) The liver is viewed as a single, well stirred compartment.
- (2) Distribution of drug into the eliminating organ is perfusion rate limited.
- (3) The concentration of drug in the eliminating organ is in equilibrium with that in the effluent venous blood.

A diagrammatic representation is depicted in Figure 4.

If one considers mass balance, by Fick's Principle, the rate of drug removal (v) is represented by:

$$v = \dot{V}_B \cdot (C_l - C_o) = \text{Metabolism} + \text{Uptake} + \text{Biliary Excretion} \quad \text{Equation 8}$$

At steady state, when uptake is essentially complete, the velocity or rate of removal is due to metabolism and biliary excretion. These processes of metabolism and excretion in turn are described by Michaelis-Menten kinetics.

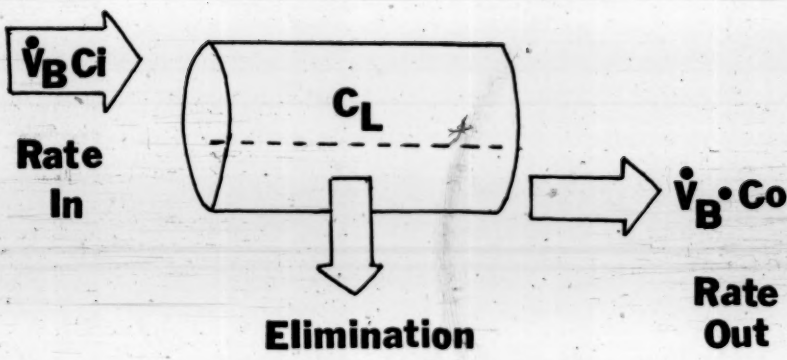
Figure 4. Diagrammatic representation of Model I -- the Liver is conceived as a well stirred single compartment.

$\dot{V}_B \cdot C_I$ is the rate of drug input

$\dot{V}_B \cdot C_o$ is the rate of drug output

C_L is the concentration of drug in the liver

Model I



$$v = \dot{V}_B \cdot (C_L - C_0) = \sum_{i=1}^n \frac{V_{max,i} \cdot C_L}{K_{m,i} + C_L} \quad \text{Equation 9}$$

where $K_{m,i}$ and $V_{max,i}$ are the Michaelis-Menten constant and the velocity maximum for the i th enzymatic or excretory process.

Since equilibrium is assumed to exist between the concentration of drug in the liver (C_L) and that of the effluence (C_0), C_L/C_0 can be represented by a constant R for a particular set of conditions. The value of R can vary with concentration. Equation 9 can now be represented by:

$$\dot{V}_B \cdot (C_L - C_0) = \sum_{i=1}^n \frac{V_{max,i} \cdot C_0}{\frac{K_{m,i}}{R} + C_0} \quad \text{Equation 10}$$

and

$$\dot{V}_B \cdot \frac{(C_L - C_0)}{C_0} = \sum_{i=1}^n \frac{V_{max,i}}{\frac{K_{m,i}}{R} + C_0} = A \quad \text{Equation 11}$$

The term A is the summation $\sum_{i=1}^n \frac{V_{max,i}}{\frac{K_{m,i}}{R} + C_0}$ and denotes the

enzymatic and excretory capacity of the system. Upon rearrangement,

Equation 11 can be expressed in terms of the extraction ratio.

Thus

$$ER = \frac{A}{A + \dot{V}_B} \quad \text{Equation 12}$$

from which it may be seen that the extraction ratio is influenced by hepatic blood flow. The corresponding expression for clearance becomes

$$\dot{V}_{Cl} = \dot{V}_B \cdot \frac{A}{A + \dot{V}_B} \quad \text{Equation 13}$$

The effect of protein binding has not been included in the general equations for the extraction ratio and clearance (Equations 12 and 13). A more complete description of the model would be to include protein binding as an additional variable (102).

The unbound species is considered as the species that is in equilibrium within tissues. Thus the unbound drug concentration in the liver should equal the unbound drug concentration in the plasma in the effluent, i.e. $C_L, \text{ unbound} = C_o, \text{ unbound in plasma}$. Since it is only the unbound species that is eliminated, a re-examination of Equation 10 yields

$$\dot{V}_B \cdot (Cl - Co) = \sum_{i=1}^n \frac{V_{maxi} \cdot C_{L, \text{ unbound}}}{K_{m_i} + C_{L, \text{ unbound}}} \quad \text{Equation 14}$$

$$\frac{V_B \cdot (C_1 - C_0)}{C_0, \text{ unbound in plasma}} = \sum_{i=1}^n \frac{V_{max,i}}{K_m,i + C_0, \text{ unbound in plasma}}$$

Equation 15

where $C_0, \text{ unbound in plasma} = \alpha \cdot C_0, \text{ plasma}$ and α is the fraction of drug unbound in plasma.

If the drug partitions into red blood cells such that λ is the ratio of concentration of drug in blood to that of the plasma (C_B/C_p), then a correction must be made, and

$$C_0, \text{ unbound in plasma} = \frac{\alpha}{\lambda} C_0, \text{ blood} \quad \text{Equation 16}$$

The function λ is related to the hematocrit (H), and α , the fraction of unbound drug in plasma and β , the ratio of concentration of drug in blood cell to that in plasma as seen in the following relationship.

Consider mass balance for the amount of drug in blood.

$$C_B \cdot V_B = V_B \cdot (1-H) \cdot C_p, \text{ unbound} + V_B \cdot (1-H) \cdot C_p, \text{ bound} + H \cdot V_B \cdot C_{\text{blood cells}}$$

Equation 17

$$\frac{\text{amount in blood}}{V_B} = \frac{\text{amount in plasma that is unbound}}{(1-H)} + \frac{\text{amount in plasma that is bound}}{(1-H)} + \frac{\text{amount in blood cells}}{H}$$

where V_B is the blood volume. Rearranging Equation 17 gives

$$\lambda = 1 - H + H \cdot \frac{C_{\text{blood cells}}}{C_p} \quad \text{Equation 18}$$

Equation 18

When $C_{\text{blood cells}}/C_p$ is the unity, then $\lambda = 1$. The degree of plasma protein binding will alter the ratio $C_{\text{blood cells}}/C_p$ as the unbound moiety, the species that equilibrates between tissue, is altered with changes in α . By substituting Equation 17 into Equation 15 and rearranging, the general equation for the extraction ratio for Model I is expressed as:

$$ER = \frac{\frac{\alpha}{\lambda} A'}{\frac{\alpha}{\lambda} A' + \dot{V}_B} \quad \text{Equation 19}$$

where $A' = V_{\text{max}}/K_m$. Clearance (\dot{V}_{cl}) is given by:

$$\dot{V}_{\text{cl}} = \dot{V}_B \cdot \frac{\frac{\alpha}{\lambda} A'}{\frac{\alpha}{\lambda} A' + \dot{V}_B} \quad \text{Equation 20}$$

3. Model II

Another simple model (Model II) was developed by Winkler and co-workers (54) using assumptions made by Goresky *et al* (103) for pulse studies and applying them to steady state conditions. Liver sinusoids are depicted as a series of cylindrical tubes as shown in Figures 5 and 6. The basic assumptions of the model are:

- (1) The liver is composed of a number of identical and parallel cylindrical tubes.
- (2) The enzyme is uniformly distributed in the sheet of parenchyma

Figure 5. Diagrammatic representation of Model II - Liver sinusoids as parallel tubes.

$\dot{V}_B \cdot C_l$ is the rate of drug input

$\dot{V}_B \cdot C_o$ is the rate of drug output

C_l is the concentration of drug in the liver

Model II

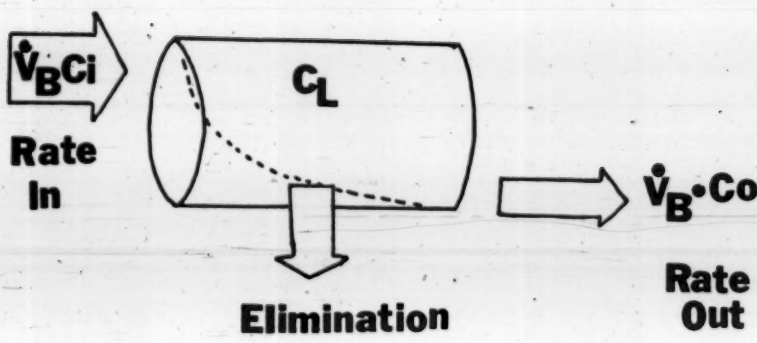




Figure 6. A unit of the model (Modell II)

\dot{V}_B , C_I is the rate of input into the unit

\dot{V}_B , C_O is the rate of drug output from the unit

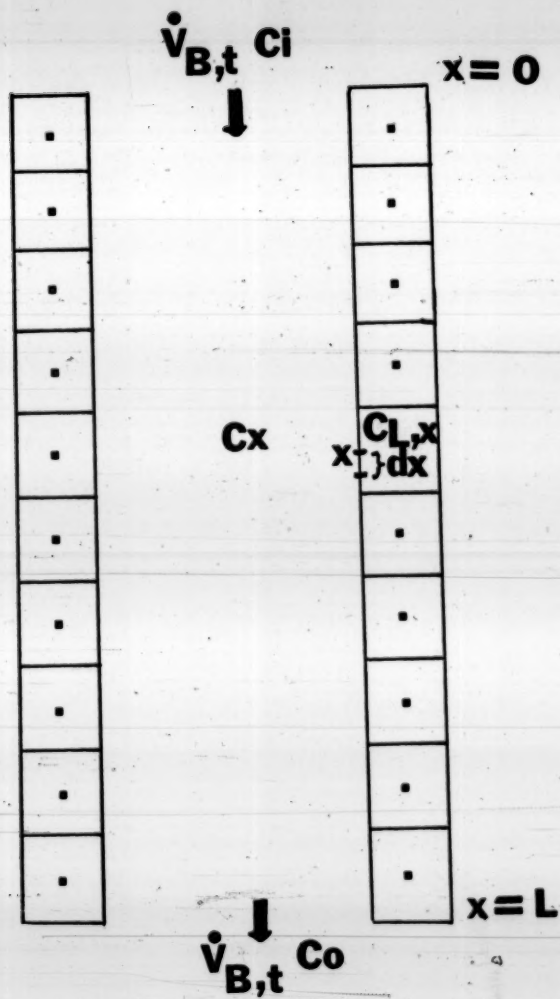
C_x is the concentration of drug in the sinusoid at point x.

$C_{L,x}$ is the concentration of drug in the hepatocyte at point x.

L is the length of the unit

$\dot{V}_{B,t}$ is the blood flow to the unit.

dx is a small increment in length from point x.



cells, while the substrate is distributed in each cross-section of the sinusoidal vascular and perisinusoidal space.

- (3) The total liver enzymatic activity (elimination rate) v , with a maximum velocity (V_{max}) is the sum of the individual enzymatic activity for each cylinder.
- (4) Transverse diffusion is instantaneous.
- (5) Transport of substrate between the perfusate in the sinusoid and the parenchyma cells containing the enzyme does not rate-limit the eliminating process.
- (6) At any point along the cylinder, the ratio of drug concentration in the hepatocyte ($C_{L,x}$) to that of the sinusoid (C_x) is a constant.

Consider one of these tubes of length L , having an enzyme system characterized by a corresponding V_{max} and K_m . At steady state, over any distance dx , the rate of metabolism (v_x) is given by

$$v_x = \frac{dx}{L} \cdot \frac{V_{max} \cdot C_x}{\frac{K_m}{R} + C_x} = -\dot{V}_{B,t} \cdot dC_x \quad \text{Equation 21}$$

where C_x is the concentration of drug in the tube at any point x , $\dot{V}_{B,t}$ is the blood flow along the tube and R is the ratio of $C_{L,x}/C_x$.

At low concentrations of the drug where $(K_m/R) \gg C_x$, the rate of metabolism along the entire tube, (\dot{V}_t) is given on integration of equation 21 (104)

$$\dot{V}_t = \dot{V}_{B,t} \cdot C_t \cdot (1 - e^{-\frac{A_t}{\dot{V}_{B,t}}}) \quad \text{Equation 22}$$

where A_t is the enzymatic capacity of the tube ($V_{max,t}/(K_m/R)$). For k numbers of identical tubes present in the liver.

$$A_t = A/k, \quad \dot{V}_{B,t} = \dot{V}_B / k, \quad V_{max,t} = V_{max}/k$$

The rate of loss from the entire liver is the sum of the rates of loss from all the tubes, and, since all the tubes are identical, it is k times the rate of loss from one tube. Therefore,

$$\begin{aligned} \text{Rate of loss from liver} &= k \cdot \dot{V}_{B,t} \cdot C_t \cdot (1 - e^{-\frac{A_t}{\dot{V}_{B,t}}}) \\ &= \dot{V}_B C_t (1 - e^{-\frac{A}{\dot{V}_B}}) \quad \text{Equation 23} \end{aligned}$$

Thus the extraction ratio at steady state is given by:

$$ER = (1 - e^{-\frac{A}{\dot{V}_B}}) \quad \text{Equation 24}$$

and clearance under steady state is

$$\dot{V}_{Cl} = \dot{V}_B (1 - e^{-(A/\dot{V}_B)}) \quad \text{Equation 25}$$

The term A has the same meaning as in Model I and is $\sum_{i=1}^n \frac{V_{max_i}}{K_m_i + C_0}$

for multi enzyme systems. At low concentrations of drugs to the liver,

A is a constant and is $\sum_{i=1}^n \frac{V_{max_i}}{K_m_i} \cdot \frac{R}{R}$.

For a uni-enzyme system when $C_{L,x} \gg K_m$, Integration of Equation 21 yields (104)

$$\ln\left(\frac{C_0}{C_1}\right) + \frac{V_{max}}{\dot{V}_B \cdot \frac{K_m}{R}} = \frac{C_1 - C_0}{K_m/R} \quad \text{Equation 26}$$

A more complete description for Model II would be to include the effect of protein binding. Again, the unbound species would be the equilibrating as well as the eliminated species. After correction for plasma protein binding and blood cell partitioning, the general equation for Model II for the extraction ratio is now:

$$ER = (1 - e^{-(\frac{\alpha}{\lambda} A' / \dot{V}_B)}) \quad \text{Equation 27}$$

where $A' = V_{max}/K_m$. Clearance (\dot{V}_{Cl}) is given by:

$$\dot{V}_{Cl} = \dot{V}_B (1 - e^{-(\frac{\alpha}{\lambda} A' / \dot{V}_B)}) \quad \text{Equation 28}$$

As shown previously, the extraction ratios and hence clearances in the two models differ (Equations 19, 20, 27 and 28). The variables that can influence hepatic clearance of drugs in both models are:

- (1) hepatic blood flow
- (2) plasma protein binding and blood cell partitioning
- (3) the enzymatic activity (A') within the liver cells.

The term A' is also referred to as the intrinsic liver or metabolic clearance(105, 106, 107) and

- (4) the drug concentration at the enzyme site.

The term (A') is a variable, but at low concentration of drug in the liver ($C_{L,X} \ll Km$), (A') is reduced to a constant and the kinetics of the drug are linear. The influence of hepatic blood flow, plasma protein binding and blood cell partitioning as well as the enzymatic activity (A') on hepatic drug clearance is better elucidated under these conditions. Thus discussion is mainly restricted to describe the influence of these factors on hepatic clearance at low concentrations of drug to the liver. Their influence on other important pharmacokinetic parameters as the extent of availability (F), the areas under the blood-concentration-time curve (AUC) for single oral and intravenous doses, and the steady state blood concentration ($C_{B,ss}$) after constant oral administration and constant infusion under linear kinetic conditions are also discussed. Influence of these factors is made assuming that the liver is the only eliminating organ.

Once again, the fundamental equation for the extraction ratios for

Models I and II are

$$\text{Model I} \quad ER = \frac{\frac{\alpha}{\lambda} A'}{\frac{\alpha}{\lambda} A' + \dot{V}_B}$$

$$\text{Model II} \quad ER = (1 - e^{-\frac{\alpha}{\lambda} A' / \dot{V}_B})$$

The influence of hepatic blood flow (\dot{V}_B), plasma protein binding and blood cell partitioning (α, λ), and the enzymatic activity (A') of the liver cells on various pharmacokinetic parameters at low concentration of drug to the liver for Models I and II is summarized in the following table.

Table I: Interrelations between A' , α , λ and \dot{V}_B and Various Pharmacokinetic Parameters for Models I and II

Parameter	Model I	Model II	Derivation of Equation
ER	$\frac{\alpha A'_I}{\lambda A'_I + \dot{V}_B}$	$(1 - e^{-\frac{(\alpha A'_I)}{\lambda A''_I} / \dot{V}_B})$	
\dot{V}_{cl}	$\dot{V}_B \left(\frac{\alpha A'_I}{\lambda A'_I + \dot{V}_B} \right)$	$\dot{V}_B (1 - e^{-\frac{(\alpha A'_I)}{\lambda A''_I} / \dot{V}_B})$	$\dot{V}_B \cdot ER$
F	$\frac{\dot{V}_B}{\frac{\alpha A'_I}{\lambda A'_I} + \dot{V}_B}$	$e^{-\frac{(\alpha A'_I)}{\lambda A''_I} / \dot{V}_B}$	$1 - ER$
AUC_{oral}	$\frac{Dose}{\frac{\alpha A'_I}{\lambda A'_I}}$	$\frac{Dose \cdot e^{-\frac{(\alpha A'_I)}{\lambda A''_I} / \dot{V}_B}}{\dot{V}_B (1 - e^{-\frac{(\alpha A'_I)}{\lambda A''_I} / \dot{V}_B})}$	$\frac{F \cdot Dose}{\dot{V}_{cl}}$
AUC_{IV}	$\frac{Dose}{\dot{V}_B \left(\frac{\alpha A'_I}{\lambda A'_I} + \dot{V}_B \right)}$	$\frac{Dose}{\dot{V}_B (1 - e^{-\frac{(\alpha A'_I)}{\lambda A''_I} / \dot{V}_B})}$	$\frac{Dose}{\dot{V}_{cl}}$
$C_{B,ss}_{oral}$	$\frac{Dose / \tau}{\frac{\alpha A'_I}{\lambda A'_I}}$	$\frac{(Dose / \tau) \cdot e^{-\frac{(\alpha A'_I)}{\lambda A''_I} / \dot{V}_B}}{\dot{V}_B (1 - e^{-\frac{(\alpha A'_I)}{\lambda A''_I} / \dot{V}_B})}$	$\frac{F \cdot (Dose / \tau)}{\dot{V}_{cl}}$
$C_{B,ss}_{inf}$	$\frac{R^o}{\dot{V}_B \left(\frac{\alpha A'_I}{\lambda A'_I} + \dot{V}_B \right)}$	$\frac{R^o}{\dot{V}_B (1 - e^{-\frac{(\alpha A'_I)}{\lambda A''_I} / \dot{V}_B})}$	$\frac{R^o}{\dot{V}_{cl}}$

a. Changing Hepatic Blood Flow

The following analysis of the influence of hepatic blood flow on a variety of parameters assumes that the substrate concentration in the liver (C_L) is much less than the K_m of the enzyme system. Then the term (A') reduces to

$$A' = \sum_{i=1}^n \frac{V_{max,i}}{K_m,i}$$

Under these conditions the kinetics and the extraction ratio are independent of drug concentration. The situation becomes more complicated in those cases where C_L approaches or exceeds K_m . Under these circumstances all parameters will be concentration dependent.

1) Model I

The predictions for the influence of blood flow on the extraction ratio, clearance, availability, the area under the blood-concentration time curve for a single oral and intravenous dose, and the steady state blood concentrations following constant oral administration and constant intravenous infusion for Model I are shown in Figures 7 and 8. The value of $\frac{a}{\lambda}$ is set equal to one.

The calculations for the predicted values are made as follows: A reference point (the value of the extraction ratio at a hepatic blood

flow of 1.0 ml/min/gm liver is established and used to calculate the value for (A_1') as in Equation 19. ($\frac{a}{A} = 1$). This value of (A_1') is in turn used to predict changes in the extraction ratio of hepatic blood flows of 0.5, 1.5 and 2.0 ml/min/gm liver. As an example, the reference point has an extraction ratio of 0.9 at blood flow of 1.0 ml/min/gm liver. The value for (A_1') can be obtained using Equation 19.

$$0.9 = \frac{A_1'}{A_1' + 1.0}$$

$$0.1 \cdot A_1' = 0.9$$

$$\text{and} \quad A_1' = 9.0$$

The extraction ratio at hepatic blood flow of 0.5 ml/min/gm liver is given by:

$$ER = \frac{9.0}{9.0 + 0.5} = 0.9474$$

Similarly, the extraction ratios at hepatic blood flows of 1.5 and 2.0 ml/min/gm liver are 0.8571 and 0.8182 respectively. A curve is generated by connecting these four points. A family curve is thus constructed by utilizing different reference points ranging from 0.1 to 0.999. The predicted values for the other parameters as clearance, availability, area under the blood-concentration-time curve and the steady state blood concentration are obtained in the same manner using appropriate equations in Table I.

a) Extraction Ratio

The influence of blood flow on the extraction ratio of a drug operating under linear kinetic conditions is shown in Figure 7A. For drugs with very high extraction ratios (> 0.95) at a blood flow of 1.0 ml/min/gm liver, the extraction ratio is unresponsive to changes in blood flow ($A' \gg \dot{V}_B$ and $ER = 1$) as predicted from Equation 19. When the extraction ratio is low (< 0.2), the extraction ratio changes inversely with blood flow ($\dot{V}_B \gg A'$ and $ER = \frac{A'}{\dot{V}_B}$) as predicted from Equation 19. For drugs with intermediate extraction ratios (0.2-0.7), the extraction ratio responds to changes in blood flow in a non-linear manner as predicted in Equation 19.

b) Clearance

The influence of blood flow on the clearance of drugs is shown in Figure 7B. As expected from Equation 20, drugs with high extraction ratios (> 0.95) have clearances approaching blood flow (ER approaches unity). At low extraction ratios (< 0.2), clearance becomes equal to A' ($\dot{V}_B \gg A'$), in which case, clearance is insensitive to changes in blood flow. It is the intermediate range of the extraction ratio (0.2-0.7) that clearance responds to changes in blood flow in a non-linear fashion.

c) Availability

In the context of this thesis, availability (F) is defined as the fraction of the drug which survives a single passage through the liver. According to Model 1, availability is given by:

$$\text{Availability (F)} = 1 = \text{ER}$$

$$= \frac{\dot{V}_B}{A' + \dot{V}_B} \quad \text{Equation 29}$$

The manner in which availability changes with blood flow for drugs having different reference extraction ratios is depicted in Figure 7C. For highly cleared drugs, when the eliminating capacity (term A') greatly exceeds the value of blood flow (ER \approx 1), Equation 29 reduces to

$$F = \frac{\dot{V}_B}{A'} \quad \text{Equation 30}$$

in which case availability varies directly with blood flow. At the other extreme, when ER is low (< 0.2) availability is unaffected by changes in blood flow ($\dot{V}_B \gg A'$, $F = 1$).

d) Area under the Blood-Concentration-Time Curve Following a Single Oral Dose

For a single oral dose, only a fraction (F) of the dose is available.

$$F \cdot \text{Dose} = \dot{V}_{cl} \cdot \text{AUC}_{\text{oral}} \quad \text{Equation 31}$$

When appropriately substituting for F and \dot{V}_{cl} , it is seen that Equation 31 simplifies to

$$AUC_{oral} = \frac{Dose}{A'}$$

Equation 32

from which it is seen that AUC_{oral} should depend only on dose and the enzymatic activity and not blood flow as shown in Figure 8A (105).

e) Area under the Blood-Concentration-Time Curve Following a Single Intravenous Dose

The area under the blood-concentration-time curve following a single intravenous dose is given by:

$$AUC_{IV} = \frac{Dose}{\dot{V}_{cl}} = \frac{Dose}{\dot{V}_B (A' + \dot{V}_B)}$$

The area under the curve is influenced mostly where clearance approaches blood flow, i.e. when the extraction of the drug is high. At low extraction ratios, the influence of blood flow on AUC_{IV} is insignificant ($\dot{V}_{cl} \approx A'$). The greater the extraction ratio of the drug, the greater the influence of blood flow on AUC_{IV} (Figure 8B).

f) Steady State Drug Concentration in Blood Following Constant Oral Administration

When a drug is given orally at a fixed dose-fixed time interval (of duration τ), the concentration in the blood accumulates until a

plateau is reached. At the plateau, the rate of entry of drug into the body ($F \cdot \text{Dose}/\tau$) is matched by the rate of elimination ($\dot{V}_{cl} \cdot C_{B,ss,oral}$) where $C_{B,ss,oral}$ refers to the time-averaged blood concentration of drug at the plateau. Hence the value for the steady state concentration is given by:

$$C_{B,ss,oral} = \frac{F \cdot (\text{Dose}/\tau)}{\dot{V}_{cl}} \quad \text{Equation 34}$$

Substitution of Equations 28 and 29 into Equation 34 yields

$$C_{B,ss,oral} = \frac{(\text{Dose}/\tau)}{A'} \quad \text{Equation 35}$$

which shows that the steady state concentration depends only on the rate of drug administration and the eliminating capacity (A') and is independent of blood flow (Figure 8C). This situation is analogous to the lack of influence of blood flow on AUC_{oral} .

g) Steady State Drug Concentration in Blood Following Constant Drug Infusion

When a drug is infused directly into the general circulation, $F = 1$. At steady state, the rate of drug infusion (R^*) is matched by the rate of elimination. The steady state concentration in blood ($C_{B,ss,inf}$) is given by:

$$C_{B,ss,inf} = \frac{R^*}{\dot{V}_{cl}} \quad \text{Equation 36}$$

Figure 7. Influence of hepatic blood flow on pharmacokinetic parameters

A) ER

B) \dot{V}_{cl}

C) F

according to Model 1.

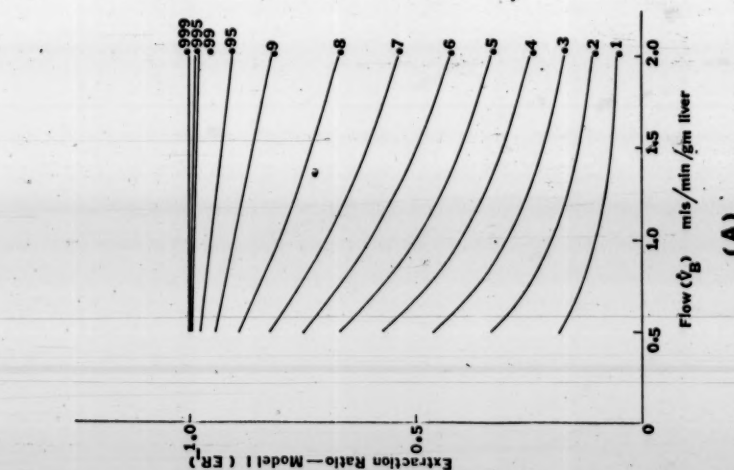
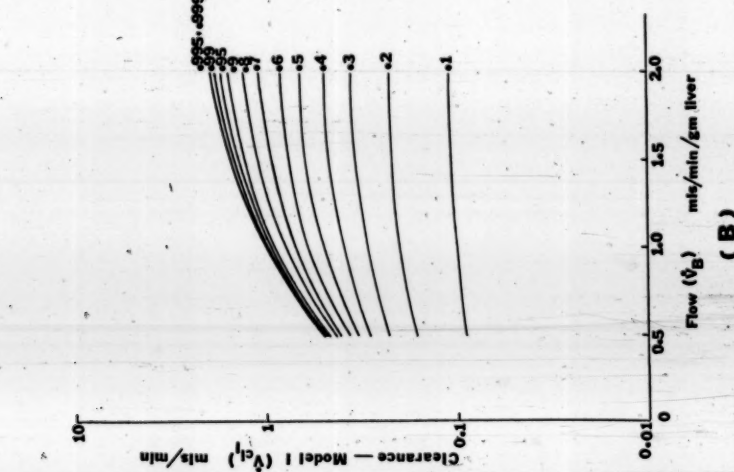
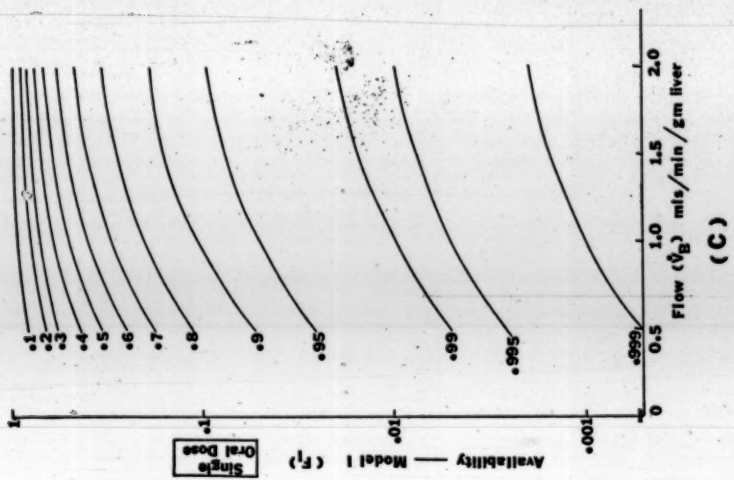
The numbers (0.1 to 0.999) next to each curve on the graph

indicate the extraction ratios at the reference blood flow

of 1.0 ml/min/gm liver. This reference point is used to

generate other points on the curve, ($\frac{a}{\lambda} = 1$) for all

calculation. The calculated values are given in Appendix IIIA.



(A)

(B)

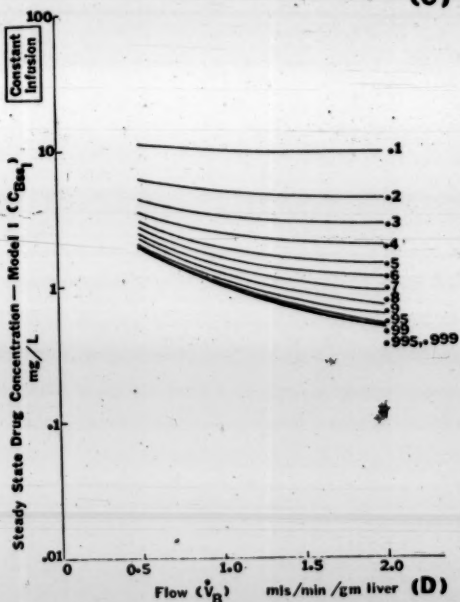
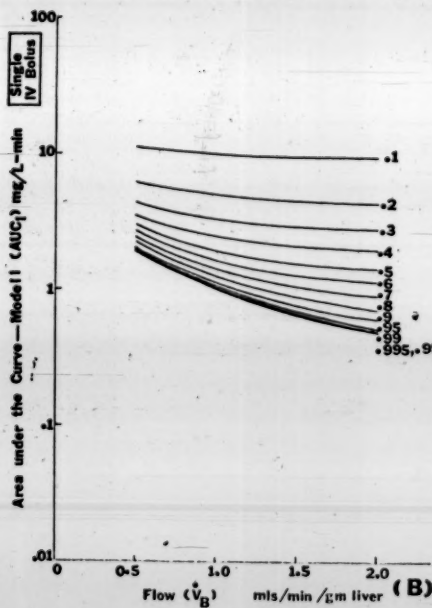
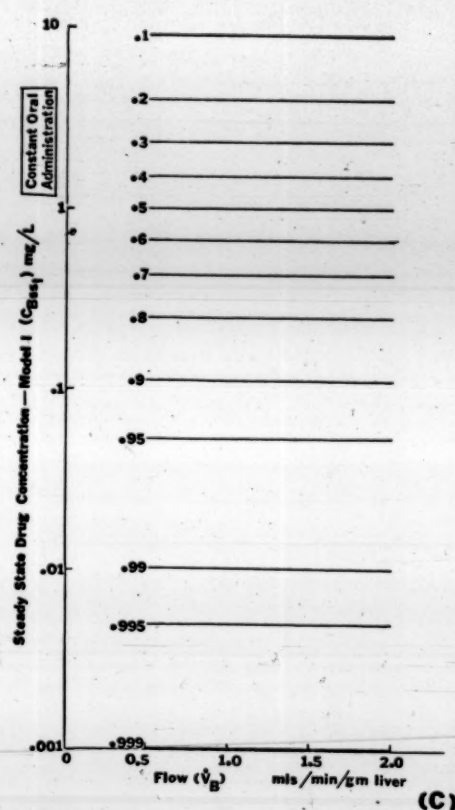
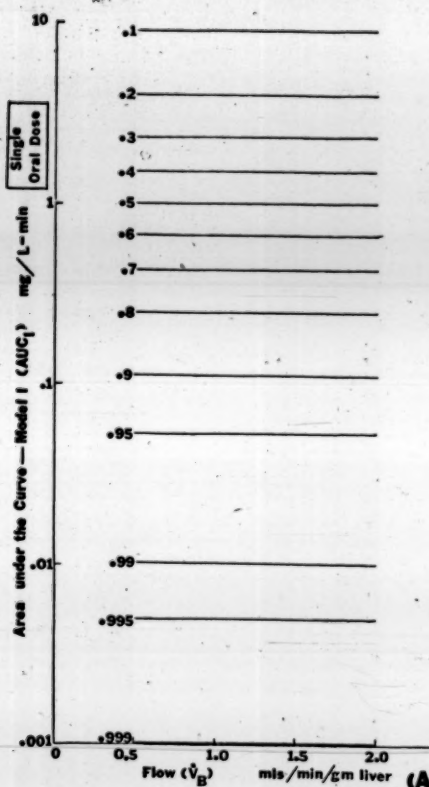
(C)

Figure 8. Influence of hepatic blood flow on pharmacokinetic parameter

- A) AUC_{oral}
- B) AUC_{IV}
- C) $C_{B,ss}_{oral}$
- D) $C_{B,ss}_{inf}$

according to Model I

The numbers (0.1 to 0.999) next to each curve on the graph
~~indicate~~
Indicate the extraction ratios at the reference blood flow
of 1.0 ml/min/gm liver. This reference point is used to
generate other points on the curve, $\frac{a}{\lambda} = 1$ for all calculation.
The calculated values are given in Appendix IIIB.



As expected blood flow exerts its influence on the steady state concentration the greatest for highly extracted compounds where clearance approaches blood flow ($ER = 1$) whereas the steady state concentration is independent of blood flow for poorly extracted drugs ($\dot{V}_{cl} = A'$). These relations are depicted on Figure 8D.

2) Model II

The predictions for the influence of blood flow on the pharmacokinetic parameters (ER , \dot{V}_{cl} , F AUC and $C_{B,ss}$) for Model II are shown in Figures 9 and 10. For all calculations, the value of $\frac{a}{\lambda}$ is again set equal to one. The method used in calculations is the same as Model I. The initial calculations for A'_{11} and ER are based on substitution into Equation 27 instead of Equation 19 for Model II. The predicted values for the other parameters as clearance, availability, the area under the blood-concentration-time curve and the steady blood concentration are obtained in the same manner using appropriate equations in Table I.

a) Extraction Ratio

The influence of blood flow on the extraction ratio of a drug operating under linear kinetic conditions for Model II is shown in Figure 9A. For drugs with very high extraction ratios (> 0.95) the influence of blood flow on the extraction ratio is relatively insigni-

ficant ($A' \gg V_B$ and $ER \approx 1$) as predicted in Equation 27. When the extraction ratio is low (< 0.2), blood flow and the extraction ratio are related exponentially (Equation 27).

b) Clearance

The influence of blood flow on the clearance of drugs with different extraction ratios is shown in Figure 9B. As expected from Equation 28, drugs with high extraction ratios (> 0.95) have clearances approaching blood flow (ER approaches unity). At low extraction ratios (< 0.2) clearance equals A' ($V_B > A'$), in which case clearance is insensitive to changes in blood flow. For drugs in the intermediate range of extraction ratio (0.2-0.7), clearance responds to changes in blood flow in a non-linear fashion.

c) Availability

According to Model II, availability (F) is given by:

$$F = 1 - ER$$

$$= e^{-(A'/V_B)}$$

$$= e$$

Equation 37

The influence of blood flow on the availability for drugs with different extraction ratios is shown in Figure 9C. Availability is seen to vary exponentially with blood flow as in Equation 37. For highly extracted drugs, the influence of blood flow on F is more

dramatic than for poorly extracted compounds. (A' is a larger term for highly extracted drugs and is related to F exponentially). For poorly extracted compounds, (small A'), F is hardly affected by changes in blood flow.

(d) Area under the Blood-Concentration-Time Curve Following a Single Oral Dose

The area under the blood-concentration-time curve for a single oral dose (AUC_{oral}) is given by:

$$AUC_{oral} = \frac{F \text{ Dose}}{V_{cl}} \cdot \frac{e^{-(A'/V_B) \cdot \text{Dose}} - (1 - e^{-(A'/V_B) \cdot \text{Dose}})}{V_B(1 - e^{-(A'/V_B)})} \quad \text{Equation 38}$$

The effects of blood flow on AUC_{oral} follow closely the effects of blood flow on F and V_{cl} . Thus large variations on AUC_{oral} are expected for highly cleared drugs on changing blood flow. For poorly cleared compounds, clearance approaches the term A' and availability is hardly affected by blood flow. Thus AUC_{oral} for the poorly cleared compound (Equation 38) is insensitive to changes in blood flow (Figure 10A).

(e) Area under the Blood-Concentration-Time Curve Following a Single Intravenous Dose

The area under the blood-concentration-time curve for a single intravenous dose is given by:

$$AUC_{IV} = \frac{Dose}{V_{cl}} = \frac{Dose}{V_B(1 - e^{-\frac{V_A}{V_B}})} \quad \text{Equation 39}$$

and the influence of blood flow on AUC_{IV} for drugs with different extraction ratios is depicted in Figure 10B. The AUC_{IV} bears an inverse relationship to clearance. As expected, for highly cleared compounds (clearance approaches blood flow), AUC_{IV} bears an inverse relationship with blood flow. For poorly cleared compounds, (clearance approaches the term A'), AUC_{IV} is insensitive to changes in blood flow. For drugs with intermediate extraction ratios (0.2-07), the effect of blood flow on the AUC_{IV} is greater with increasing extraction ratio of the drug.

f) Steady State Drug Concentration in Blood Following Constant Oral Administration

The steady state concentration of drug in the blood on repetitive oral administration is given:

$$C_{B,ss_{oral}} = \frac{F \cdot (Dose/\tau)}{V_{cl}} \quad \text{Equation 40}$$

A situation similar to the effects of blood flow on AUC_{oral} is seen for $C_{B,ss_{oral}}$. Large variations in $C_{B,ss_{oral}}$ are expected for highly cleared drugs on changing blood flow. For poorly cleared compounds, the steady state blood concentration is insensitive to changes in

Figure 9. Influence of hepatic blood flow on pharmacokinetic parameters

A) ER

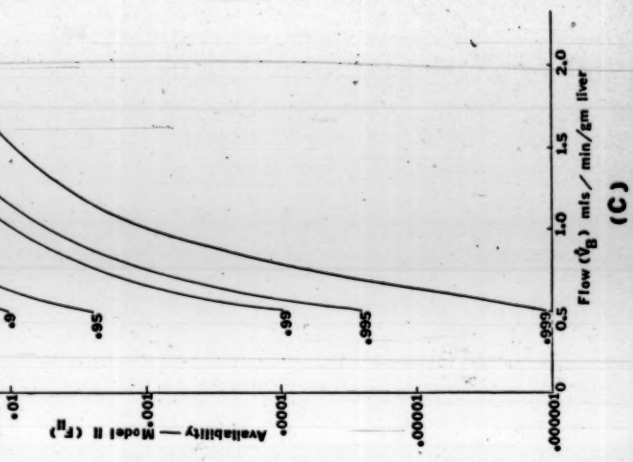
B) \dot{V}_{cl}

C) F

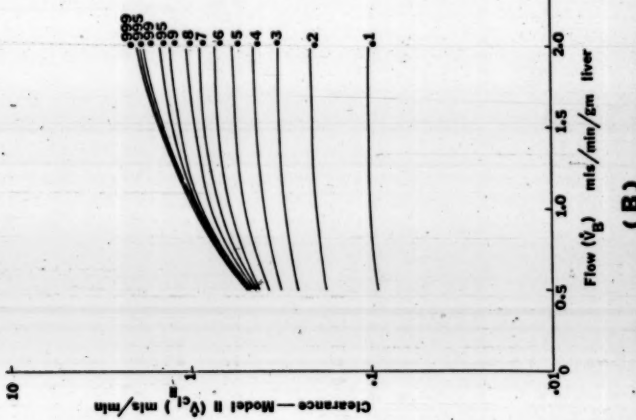
according to Model II

The numbers (0.1 to 0.999) next to each curve on the graph indicate the extraction ratios at the reference blood flow of 1.0 ml/min/gm liver. This reference point is used to generate other points on the curve. $\frac{a}{A} = 1$ for all calculation. The calculated values are given in Appendix IVA.

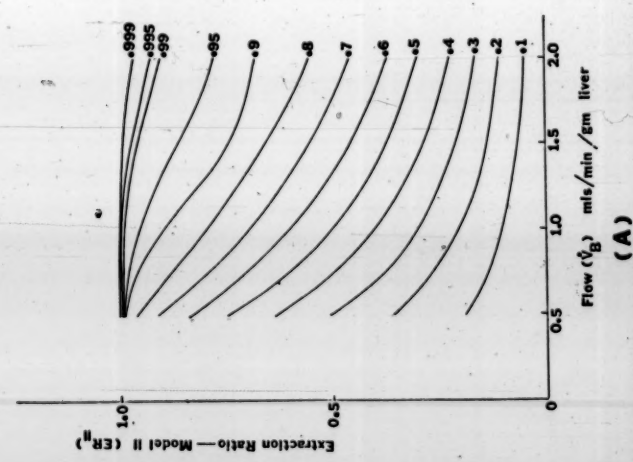
(C)



(B)



(A)



(A)

(A)

(A)

(A)

(A)

(A)

(A)

(A)

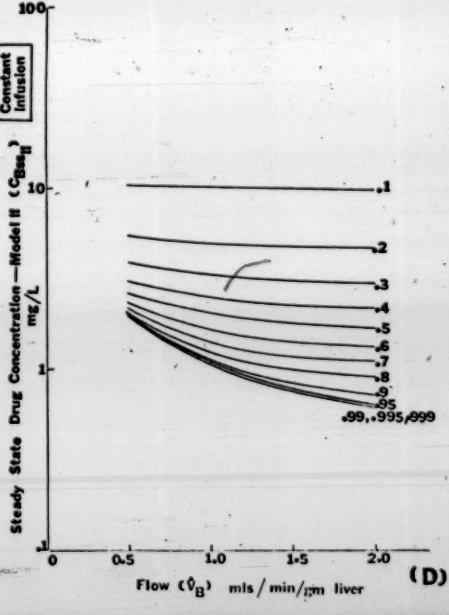
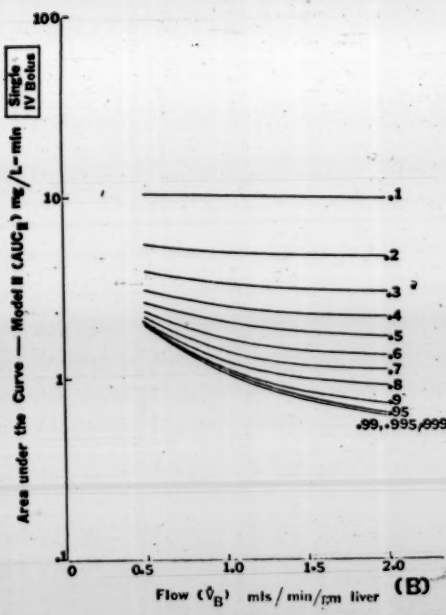
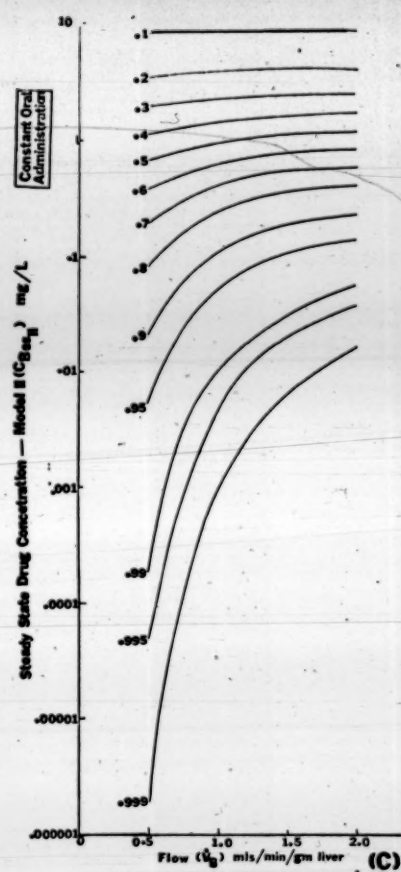
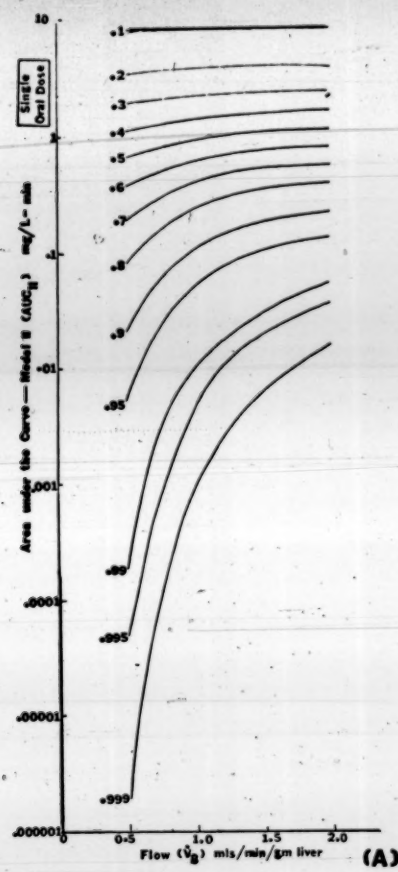
Figure 10. Influence of hepatic blood flow on pharmacokinetic parameters

- A) AUC_{oral}
- B) AUC_{IV}
- C) $C_{B,ssoral}$
- D) $C_{B,ssInf}$

according to Model II.

The numbers (0.1 to 0.999) next to each curve on the graph indicate the extraction ratios at the reference blood flow of 1.0 ml/min/gm liver. The reference point is used to generate other points on the curve, $\frac{a}{\lambda} = 1$ for all calculations.

The calculated values are given in Appendix IVB.



blood flow. The influence of blood flow on the steady state blood concentration following constant oral administration for drugs with different extraction ratios is shown in Figure 10C.

g) Steady State Drug Concentration in Blood Following Constant Drug Infusion

The steady state concentration of drug in blood following constant intravenous infusion is given by:

$$C_{B,ss,inf} = \frac{R^o}{V_{cl}}$$

Equation 41

Large variations in the steady state concentration with blood flow are anticipated for highly cleared compounds (clearance approaches blood flow) in contrast to the poorly cleared compounds (clearance approaches the term A') where blood flow does not affect the steady state blood concentration. For drugs with intermediate extraction ratios, the change in the steady state concentration is non-linear. The influence of flow on the steady state concentrations for drugs with different extraction ratios is shown in Figure 10D.

b. Changing $\frac{a}{\lambda}$

The following analysis of the influence of protein binding and blood cell partitioning on the various pharmacokinetic parameters assumes again that the substrate concentration in the liver (C_L) is

much less than the K_m of the enzyme system. The term (A') is a constant, and under these conditions the kinetics and extraction ratio are independent of drug concentration. In cases where C_L approaches or exceeds K_m , all parameters will be concentration dependent.

1) Model I

The predictions for the influence of protein binding (measured as fraction of drug unbound in plasma α) and blood cell partitioning (measured as the function λ) on the extraction ratio, clearance, availability, area under the blood-concentration-time curve for a single oral and intravenous dose, and the steady state blood concentrations following constant oral and constant intravenous infusion for Model I are shown in Figure II. The value of hepatic blood flow is held constant at 1.0 ml/min/gm liver for all calculations. The calculations for the predicted values are as follows:

A reference point (the value of extraction ratio at hepatic blood flow of 1.0 ml/min/gm liver and when $\frac{\alpha}{\lambda} = 1$) is established and used to calculate the value for (A') as in Equation 19. This value of (A') is in turn used to predict changes in the extraction ratio upon changing the ratio $\frac{\alpha}{\lambda}$ from 0.1 to 1.0 with blood flow kept constant at 1.0 ml/min/gm liver. As an example, the reference point has an extraction ratio of 0.9 at blood flow of 1.0 ml/min and

when $\frac{a}{\lambda} = 1$. The value for (A_1) can be obtained as in Equation 19.

$$0.9 = \frac{1 \cdot A_1}{1 \times A_1 + 1.0}$$

$$0.9 + 0.9A_1 = A_1$$

$$A_1 = 9.0$$

...

The extraction ratio when $\frac{a}{\lambda} = 0.1$ is given by:

$$ER = \frac{0.1 \times 9.0}{0.1 \times 9.0 + 1.0} = 0.4737$$

Similarly, the extraction ratios when the ratio $\frac{a}{\lambda}$ is 0.2, 0.3 and 0.4 are 0.6429, 0.7297 and 0.7826 respectively. A curve is generated by connecting the values of ER when $\frac{a}{\lambda}$ ranges from 0.1 to 1.0 at 0.1 increments. A family curve is thus constructed using different reference points. The predicted values for the other parameters such as clearance, availability, area under the blood-concentration-time curve and the steady state blood concentration are obtained in the same manner using appropriate equations (Table I).

a) Extraction Ratio

The influence of plasma protein binding and blood cell partitioning on the extraction ratio of a drug operating under linear kinetic conditions is shown in Figure 11A. For drugs with high

extraction ratios, (> 0.95 at flow of $1.0 \text{ ml/min/gm liver}$), the extraction ratio is relatively unresponsive to changes in the ratio $\frac{a}{\lambda} (\frac{a}{\lambda} A' \gg \dot{V}_B \text{ and } ER = 1)$. At low extraction ratios (< 0.2), the extraction ratio changes directly with $\frac{a}{\lambda} (\dot{V}_B \gg \frac{a}{\lambda} A' \text{ and } ER = \frac{a}{\lambda} A')$ as predicted from Equation 19. For a drug with intermediate extraction ratios (0.2-0.7), the extraction ratio responds to changes in $\frac{a}{\lambda}$ in a non-linear manner.

b) Clearance

The influence of $\frac{a}{\lambda}$ on clearances of drugs is the same as its influence on extraction ratios at constant hepatic blood flow as anticipated in Equation 20. This is depicted in Figure 11A. (Hepatic blood flow is constant at $1.0 \text{ ml/min/gm liver}$).

c) Availability

The manner in which availability changes with the ratio $\frac{a}{\lambda}$ for drugs with different extraction ratios is depicted in Figure 11B. For highly cleared drugs $\frac{a}{\lambda} A'$ greatly exceeds the value of blood flow, and the availability bears an inverse relationship with $\frac{a}{\lambda}$ ($F = \frac{\dot{V}_B}{\frac{a}{\lambda} A'}$). For poorly cleared compounds, the ratio $\frac{a}{\lambda}$ does not affect F ($\dot{V}_B \gg \frac{a}{\lambda} A', F = 1$). For drugs with intermediate extraction ratios, F changes in a non-linear fashion with $\frac{a}{\lambda}$ as anticipated in the general equation in Table I.

d) Area under the Blood-Concentration-Time Curve Following a Single Oral Dose

For drugs given orally, only a fraction (F) of the dose is available. When appropriately substituting for F and \dot{V}_{cl} (Table 1) into Equation 31, the area under the curve for a single oral dose is given by:

$$AUC_{oral} = \frac{Dose}{\frac{a}{\lambda} A'} \quad \text{Equation 42}$$

from which it is seen that AUC_{oral} changes inversely with the ratio $\frac{a}{\lambda}$ for all extraction ratios as shown in Figure 11C.

e) Area under the Blood-Concentration-Time Curve Following a Single Intravenous Dose

The area under the blood-concentration-time curve for a single intravenous dose is given by:

$$AUC_{IV} = \frac{Dose}{\dot{V}_{cl}} = \frac{Dose}{\dot{V}_B \frac{a}{\lambda} A'} \quad \text{Equation 43}$$

$$\left(\frac{\frac{a}{\lambda} A'}{\dot{V}_B} \right)$$

and is inversely related to clearance. The influence of the ratio $\frac{a}{\lambda}$ on the area under the curve following a single intravenous dose for

drugs with different extraction ratios is shown in Figure IID. As predicted, for highly cleared compounds ($ER > 0.95$), where clearance is unaffected by changes in $\frac{a}{\lambda}$, AUC_{IV} is independent of $\frac{a}{\lambda}$. For the poorly cleared compounds ($ER < 0.2$), where the clearance changes directly with $\frac{a}{\lambda}$, AUC_{IV} will change inversely with $\frac{a}{\lambda}$. For drugs with intermediate extraction ratios (0.2-0.7), clearance changes in a non-linear fashion with $\frac{a}{\lambda}$.

f) Steady State Drug Concentration in Blood Following Constant Oral Administration

When a drug is given at a fixed rate of administration ($Dose/\tau$),

the concentration of drug in blood at steady state is given by:

$$CB_{ss,oral} = \frac{(Dose/\tau)}{\frac{a}{\lambda} A'} \quad \text{Equation 44}$$

and changes inversely with $\frac{a}{\lambda}$ for all extraction ratios as shown in Figure IIC.

g) Steady State Drug Concentration in Blood on Constant Drug Infusion

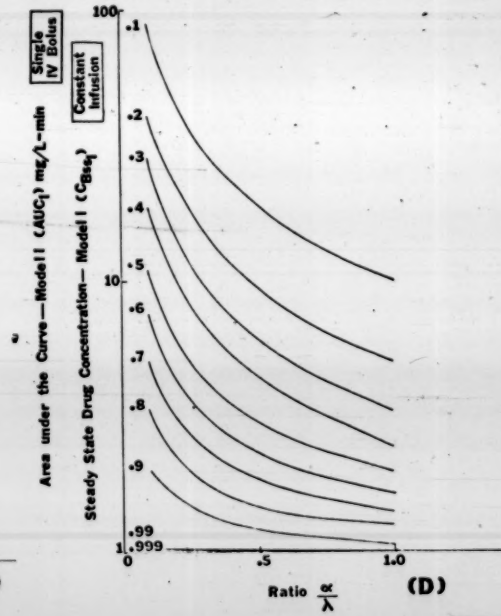
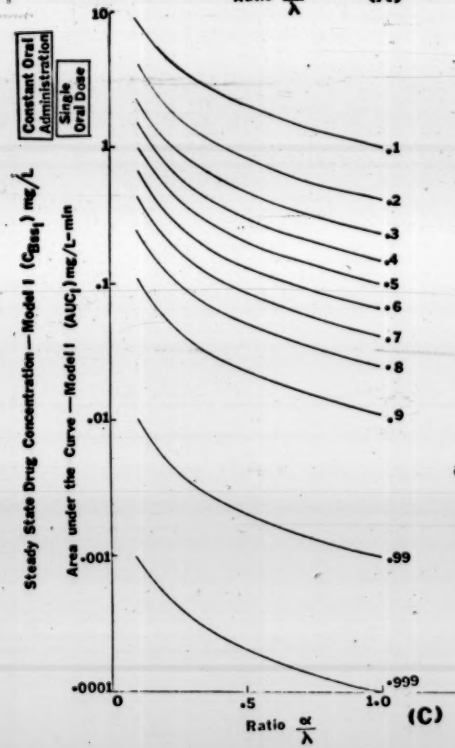
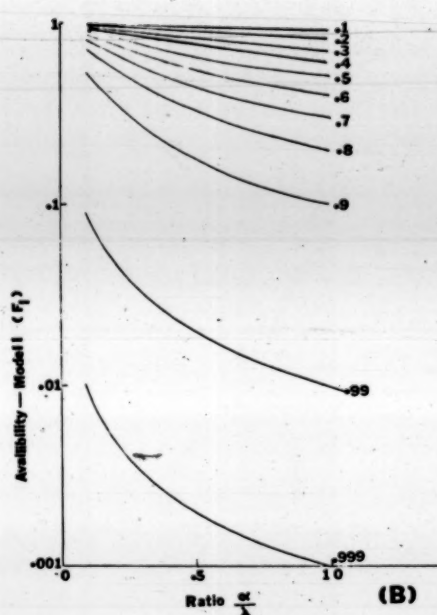
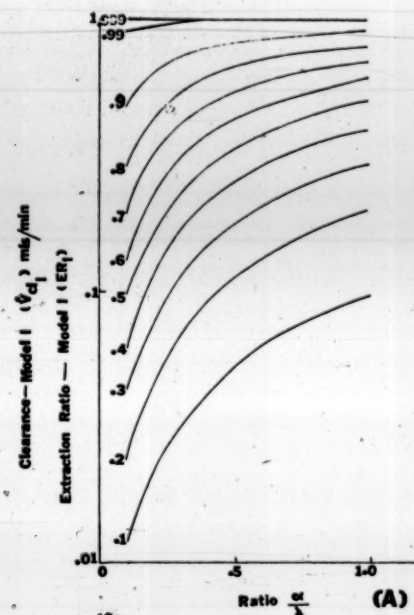
The steady state concentration of drug in blood following constant intravenous infusion is given by:

Figure 11. Influence of the ratio $\frac{\alpha}{\lambda}$ on pharmacokinetic parameters

- A) ER and \dot{V}_{Cl}
- B) F
- C) AUC_{oral} and $C_{B,ss}_{oral}$
- D) AUC_{ly} and $C_{B,ss}_{inf}$

according to Model I.

The numbers (0.1 to 0.999) appearing next to the curves on the graph indicate the extraction ratios at the reference point ($\frac{\alpha}{\lambda} = 1$; hepatic blood flow = 1.0 ml/min/gm liver). This reference point is used to generate other points on the curve. Hepatic blood flow = 1.0 ml/min/gm liver for all calculations. The calculated values for A, B, C, and D are given in Appendix VIA-D respectively.



$$C_{B,ss,inf} = \frac{R^*}{\dot{V}_{cl}} = \frac{R^*}{\dot{V}_B \left(\frac{a}{\lambda} A' \right) \left(\frac{a}{\lambda} A' + V_B \right)} \quad \text{Equation 45}$$

The change in the steady state concentration with $\frac{a}{\lambda}$ is analogous to the situation for AUC_{IV} with $\frac{a}{\lambda}$. The same trend is observed. This is depicted in Figure 11D.

2) Model II

The predictions for the influence of $\frac{a}{\lambda}$ on the extraction ratio, clearance, availability, and other pharmacokinetic parameter, e.g. AUC_{oral} , AUC_{IV} , $C_{B,ss,oral}$ and $C_{B,ss,inf}$ according to Model II are shown in Figure 12. The method used for the predicted values is the same as Model I. The initial calculations for A'_{II} and ER are based on substitution into Equation 27 instead of Equation 19 for Model II. The predicted values for other pharmacokinetic parameters as \dot{V}_{cl} , F, AUC and $C_{B,ss}$ are obtained in the same manner using appropriate equations (Table 1).

a) Extraction Ratio

The influence of plasma protein binding and blood cell parti-

tioning on the extraction ratio of a drug operating under linear kinetic conditions according to Model II is shown in Figure 12A. At high eliminating capacity of the liver (drugs with high $ER, \frac{a}{\lambda} A'$ is large compared to \dot{V}_B), the ratio $\frac{a}{\lambda}$ does not affect the extraction ratio of the drug. At low extraction ratios, increasing the ratio $\frac{a}{\lambda}$ greatly increases the extraction ratio of the drug ($A' \frac{a}{\lambda}$ is small compared to \dot{V}_B).

b) Clearance

The influence of $\frac{a}{\lambda}$ on clearance of drugs for drugs with different extraction ratios is the same as its influence on extraction ratios as shown in Figure 12A. (Hepatic blood flow is held constant at 1.0 ml/min/gm liver).

c) Availability

The availability of a drug according to Model II is given by:

$$F = e^{-\left(\frac{a}{\lambda} A' / \dot{V}_B\right)} \quad \text{Equation 46.}$$

and is related exponentially to \dot{V}_B for drugs with different extraction ratios as shown in Figure 12B. For highly extracted compounds, availability changes very drastically upon changing $\frac{a}{\lambda}$. This is so because the value

of A' is large. For poorly cleared compounds, though availability still changes exponentially with $\frac{\alpha}{\lambda}$, the value of A' is small, such that changes in with $\frac{\alpha}{\lambda}$ are small.

d) Area under the Blood-Concentration-Time Curve Following A Single Oral Dose.

The AUC_{oral} following a single oral dose is given by:

$$AUC_{oral} = \frac{F \cdot \text{Dose}}{V_{cl}} = \frac{e^{-(\frac{\alpha}{\lambda} A' / V_B)} \cdot \text{Dose}}{V_B (1 - e^{-(\frac{\alpha}{\lambda} A' / V_B)})} \quad \text{Equation 47}$$

according to Model II. The influence of $\frac{\alpha}{\lambda}$ on AUC_{oral} for drugs with different extraction ratios is shown in Figure 12C. Drugs that are highly cleared have clearances approaching blood flow (unaffected by $\frac{\alpha}{\lambda}$). Thus AUC_{oral} for these compounds will change with $\frac{\alpha}{\lambda}$ the same way F changes with $\frac{\alpha}{\lambda}$. For highly cleared compounds, large variations in AUC_{oral} occur (an increase in the ratio $\frac{\alpha}{\lambda}$ decreases AUC_{oral} exponentially). For poorly cleared compounds, F does not change with $\frac{\alpha}{\lambda}$ whereas clearance increases exponentially with increase in $\frac{\alpha}{\lambda}$. Since AUC_{oral} and clearance are inversely related, AUC_{oral} decreases with increase in the ratio $\frac{\alpha}{\lambda}$.

e) Area Under the Blood-Concentration-Time Curve Following a Single Intravenous Dose

The influence of $\frac{a}{\lambda}$ on AUC_{IV} for drugs with different extraction ratios is shown in Figure 12D. The area under the curve following a single intravenous dose is given by:

$$AUC_{IV} = \frac{Dose}{V_{cl}} = \frac{Dose}{V_B(1-e^{-(\frac{a}{\lambda} V_B/V_B)})} \quad \text{Equation 48}$$

and it is seen that AUC_{IV} and clearance are inversely related. For highly cleared compounds, clearance is not much affected by $\frac{a}{\lambda}$.

The AUC_{IV} for the poorly cleared compounds is very much influenced by changes in $\frac{a}{\lambda}$ (decreases drastically with $\frac{a}{\lambda}$ as V_{cl} changes exponentially with $\frac{a}{\lambda}$).

f) Steady State Drug Concentration in Blood Following Constant Oral Administration

The steady state drug concentration in blood following constant oral administration is given by:

$$C_{B,ss,inf} = \frac{F(Dose/\tau)}{V_{cl}} = \frac{Dose/\tau}{V_B(1-e^{-(\frac{a}{\lambda} V_B/V_B)})}$$

Equation 49

and is influenced by $\frac{F}{V_{cl}}$, a situation analogous to the influence of $\frac{\alpha}{\lambda}$ on AUC_{oral} . The influence of $\frac{\alpha}{\lambda}$ on $C_{B,ss,oral}$ for drug with different extraction ratios is seen in Figure 12C.

g) Steady State Drug Concentration In Blood Following Constant Drug Infusion

The steady state concentration of drug in blood following constant intravenous infusion is given by:

$$C_{B,ss,inf} = \frac{R^*}{V_{cl}} \cdot \frac{\frac{R^*}{V_B(1 - e^{-\frac{\alpha}{\lambda} t})}}{1 - (\frac{\alpha}{\lambda} A' / V_B)} \quad \text{Equation 50}$$

and varies inversely with clearance. The influence of $\frac{\alpha}{\lambda}$ on $C_{B,ss,inf}$ for drugs with different extraction ratios is shown in Figure 12D.

The situation is analogous to the influence of $\frac{\alpha}{\lambda}$ on AUC_{IV} .

c. Changing A'

The following analysis of the influence of the eliminating capacity (term A') assumes that the substrate concentration in the liver (C_L) is much less than the K_m of the enzyme system, in which case, the term A' is the sum of the V_{max}/K_m for all enzymes. Under these conditions, the kinetics and extraction ratio are independent of drug concentration. In cases where C_L approaches or exceeds the

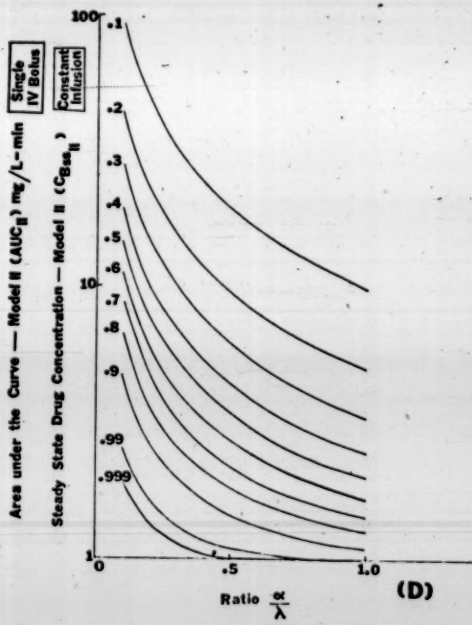
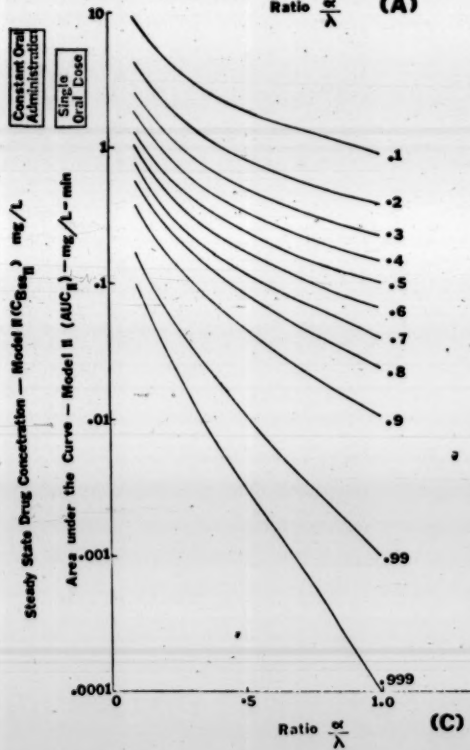
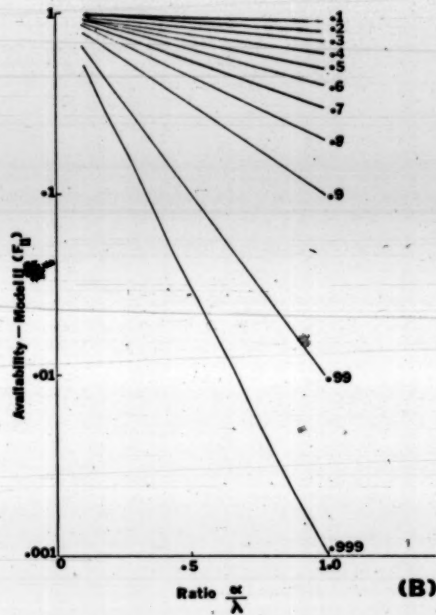
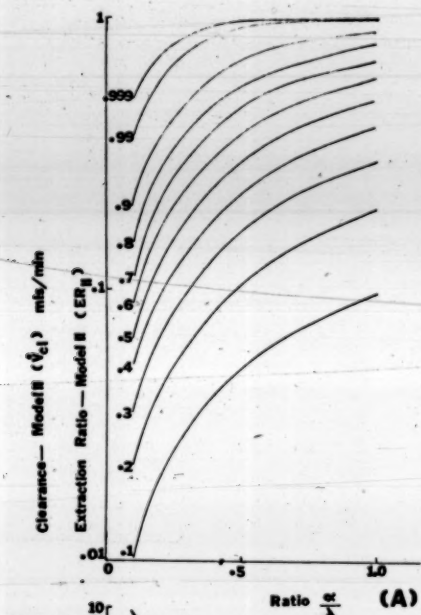
Figure 12. Influence of the ratio $\frac{\alpha}{\lambda}$ on pharmacokinetic parameters

- A) ER and $\frac{V}{Cl}$
- B) F
- C) AUC_{oral} and $C_{B,ss,oral}$
- D) AUC_{IV} and $C_{B,ss,inf}$

according to Model II

The numbers (0.1 to 0.999) next to each curve on the graph indicate the extraction ratios at the reference point $\frac{\alpha}{\lambda} = 1$; hepatic blood flow = 1.0 ml/min/gm liver). The reference point is used to generate other points on the curve. Hepatic blood flow is held constant at 1.0 ml/min/gm liver for all calculations.

The calculated values for A, B, C, and D are given in Appendix VIIA-D respectively.



K_m , the situation is more complex and all parameters will be concentration dependent.

1) Model I

The predictions for the influence of the term (A') on the extraction ratio and clearance of a drug is shown in Figure 13A. This graph depicts situation when the ratio $\frac{a}{\lambda}$ is set equal to one. Hepatic blood flow is taken to be 1.0 ml/min/gm liver and A' is expressed as multiples of blood flow. When A' greatly exceeds $\frac{a}{\lambda}$, i.e. for drugs with high extraction ratios, the extraction ratio approaches unity and clearance approaches blood flow. At low values of A' , the extraction ratio and clearance varies directly with A' , as shown by the initial slope of the curve. This is the case for drugs with low extraction ratios.

2) Model II

The predictions for the influence of the term (A') on the extraction ratio and clearance of a drug is shown in Figure 13B. This graph depicts a situation when the ratio $\frac{a}{\lambda}$ is set equal to one; hepatic blood flow assumes a value of 1.0 ml/min/gm liver and A' is expressed as multiples of blood flow. At low values of A' (poorly cleared compounds), the extraction ratio changes directly with A' and clearance approaches A' . The asymptotic value of one

Figure 13. Influence of the enzymatic capacity (A') on

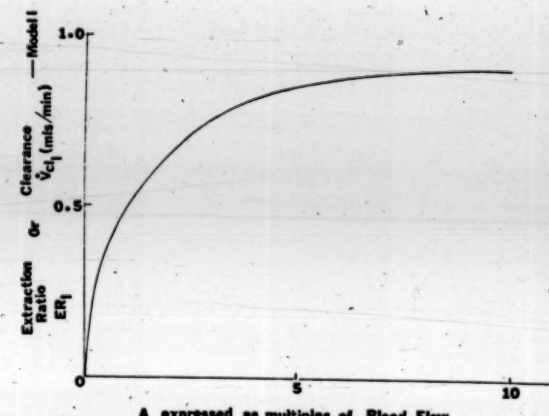
A) ER and \dot{V}_{Cl} according to Model I

B) ER and \dot{V}_{Cl} according to Model II

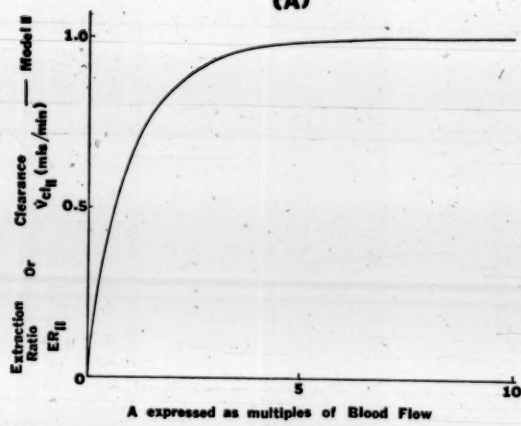
C) Ratio $\frac{ERI}{ERII}$ or $\frac{\dot{V}_{ClI}}{\dot{V}_{ClII}}$

The value of $\frac{\alpha}{\lambda} = 1$; hepatic blood flow = 1.0 ml/min/gm

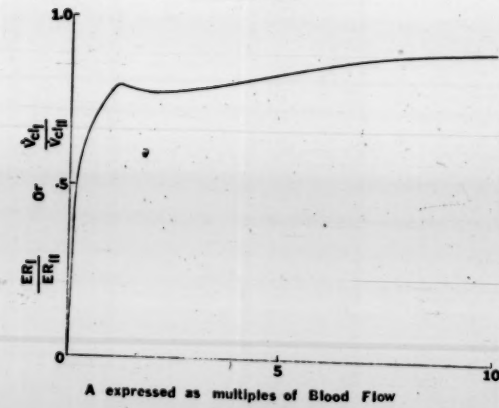
liver for all calculations.



(A)



(B)



(C)

for the extraction ratio is quickly reached with increases in A' .
in which case clearance approaches blood flow.

B) Discrimination between Models I and II

Discrimination is most readily performed under steady state and linear conditions when the term (A') is a constant. The following analysis examines the sensitivity of various parameters as discriminators.

A comparison of the predicted values of extraction ratio, clearance, area under the curve and steady state blood concentration for Model I and II is shown in Table 2.

Table 2. A Comparison of the Predicted Pharmacokinetic Parameters
In Terms of \dot{V}_B , α , λ and A' for Models I and II

ER_I/ER_{II}	$\left(\frac{\frac{\alpha}{\lambda} A'_I}{\frac{\alpha}{\lambda} A'_I + \dot{V}_B} \right)$	$\left(1 - e^{-\left(\frac{\alpha}{\lambda} A'_{II}/\dot{V}_B \right)} \right)$
$\dot{V}_{cI}/\dot{V}_{cII}$	$\left(\frac{\frac{\alpha}{\lambda} A'_I}{\frac{\alpha}{\lambda} A'_I + \dot{V}_B} \right)$	$\left(1 - e^{-\left(\frac{\alpha}{\lambda} A'_{II}/\dot{V}_B \right)} \right)$
F_I/F_{II}	$\left(\frac{\dot{V}_B}{\frac{\alpha}{\lambda} A'_I + \dot{V}_B} \right)$	$\left(e^{-\left(\frac{\alpha}{\lambda} A'_{II}/\dot{V}_B \right)} \right)$
AUC_{oralI}/AUC_{oralII}	$\frac{1}{\frac{\alpha}{\lambda} A'_I}$	$\frac{e^{-\left(\frac{\alpha}{\lambda} A'_{II}/\dot{V}_B \right)}}{\dot{V}_B \left(1 - e^{-\left(\frac{\alpha}{\lambda} A'_{II}/\dot{V}_B \right)} \right)}$
AUC_{IVI}/AUC_{IVII}	$\frac{1}{\left(\frac{\alpha}{\lambda} A'_I + \dot{V}_B \right)}$	$\frac{1}{\dot{V}_B \left(1 - e^{-\left(\frac{\alpha}{\lambda} A'_{II}/\dot{V}_B \right)} \right)}$
$C_{B,ss_{oralI}}/C_{B,ss_{oralII}}$	$\frac{1}{\frac{\alpha}{\lambda} A'_I}$	$\frac{e^{-\left(\frac{\alpha}{\lambda} A'_{II}/\dot{V}_B \right)}}{\dot{V}_B \left(1 - e^{-\left(\frac{\alpha}{\lambda} A'_{II}/\dot{V}_B \right)} \right)}$
$C_{B,ss_{infI}}/C_{B,ss_{infII}}$	$\frac{1}{\left(\frac{\alpha}{\lambda} A'_I + \dot{V}_B \right)}$	$\frac{1}{\dot{V}_B \left(1 - e^{-\left(\frac{\alpha}{\lambda} A'_{II}/\dot{V}_B \right)} \right)}$

It can be seen from Table 2 that ER_1/ER_{11} equals $\dot{V}_{Cl_1}/\dot{V}_{Cl_{11}}$,
 $AUC_{oral_1}/AUC_{oral_{11}}$ equals $C_{B,ss_{oral_1}}/C_{B,ss_{oral_{11}}}$ and $AUC_{IV_1}/AUC_{IV_{11}}$
>equals $C_{B,ss_{inf_1}}/C_{B,ss_{inf_{11}}}$. Furthermore, ER_1/ER_{11} or $\dot{V}_{Cl_1}/\dot{V}_{Cl_{11}}$
>is just the reciprocal of $AUC_{IV_1}/AUC_{IV_{11}}$ or $C_{B,ss_{inf_1}}/C_{B,ss_{inf_{11}}}$.

The ratio of F_1/F_{11} can be shown equal to Co_1/Co_{11} where (Co) is
>the effluent drug concentration from the liver ($Co = Cl \cdot (1-ER)$
>or $Cl:F$. Thus $F_1/F_{11} = Co_1/Co_{11}$).

I. By the Alteration of Blood Flow under Linear Kinetic Conditions

A comparison of the ratios for Models I and II of the anticipated

- (1) steady state extraction ratio or clearance
- (2) the availability or steady state effluent drug concentration
- (3) the total area under the blood-concentration-time curve for a single oral dose or the steady state drug concentration following constant oral administration and
- (4) the total area under the blood-concentration-time curve following a single intravenous dose or the steady state drug concentration in blood following constant intravenous infusion

upon changes in hepatic blood flow from 0.5 to 2.0 ml/min/gm liver is graphically displayed in Figure 14A, B, C and D respectively.

It is seen that the change in the ratio of the steady state extraction ratio (ER_1/ER_{11}) or clearance ($\dot{V}_{cl1}/\dot{V}_{cl11}$) is maximal for ratios of ER or \dot{V}_{cl} obtained from reference points having ER values of 0.7-0.9 at 1.0 ml/min/gm liver (Figure 14A). But even then it is only a 30% change. Since the ratio (AUC_{IV1}/AUC_{IV11}) or ($C_{B,ss1}/C_{B,ss11}$) is merely the reciprocal of ER_1/ER_{11} or $\dot{V}_{cl1}/\dot{V}_{cl11}$, a maximum of 30% difference is anticipated upon changes in blood flow as shown in Figure 14D.

In contrast, the ratio of the anticipated availability (F) or the steady state effluent drug concentration (Co) changes over a thousand fold with a fourfold change in blood flow (50% decrease or 100% increase from the normal value of 1.0 ml/min/gm liver) for drugs with extremely high extraction ratios (0.999 at 1.0 ml/min/gm liver (Figure 14B)). This magnitude of change is also found to be the case for ratios of the area under the curve (AUC_{oral1}/AUC_{oral11}) for a single oral dose or the steady state blood concentrations following constant oral administration ($C_{B,ssoral1}/C_{B,ssoral11}$) upon changes in blood flow. Again for highly extracted compounds (ER = 0.999 at 1.0 ml/min/gm liver) the ratios have the maximum range of a thousand fold.

These findings show that the steady state effluent drug concentration (C_o) or the extent of availability (F), the area under the blood-concentration-time curve for single oral dose (AUC_{oral}) and the steady state blood concentration on constant oral administration ($C_{B,ss,oral}$) would serve as sensitive indices for the discrimination of the two models upon changes in blood flow. Also the more highly extracted the compound, the greater the ability to discern between the models.

2. By the Alteration of Protein Binding and/or Blood Cell Partitioning under Linear Kinetic Conditions

A comparison of the ratios for Models I and II of the anticipated (1) ER or \dot{V}_{cl} (2) F or C_o , (3) AUC_{oral} or $C_{B,ss,oral}$ and (4) AUC_{IV} or $C_{B,ss,inf}$ upon changes in the ratio (λ) from 0.1 to 1.0 and at constant hepatic blood flow at 1.0 ml/min/gm liver is graphically displayed in Figures 15A, B, C and D respectively.

It is seen that the change in the ratio of the steady state extraction ratio (ER_I/ER_{II}) or clearance ($\dot{V}_{cl_I}/\dot{V}_{cl_{II}}$) is maximal with reference points having high extraction ratios (0.9) (Figure 15A). A 2.5 fold difference change in the ratio is obtained at maximum. Since the ratio ($AUC_{IV_I}/AUC_{IV_{II}}$) or ($C_{B,ss,inf_I}/C_{B,ss,inf_{II}}$) is the reciprocal of ER_I/ER_{II} or $\dot{V}_{cl_I}/\dot{V}_{cl_{II}}$, changes of similar magnitude are anticipated (Figure 15D).

Figure 14. Ratio of the anticipated values of various pharmacokinetic parameters with changes in hepatic blood flow. These ratios are:

- A) ER_1/ER_{11} or $\dot{V}_{cl_1}/\dot{V}_{cl_{11}}$
- B) C_0_1/C_0_{11} or F_1/F_{11}
- C) $AUC_{oral_1}/AUC_{oral_{11}}$ or $C_{B,ss,oral_1}/C_{B,ss,oral_{11}}$
- D) $AUC_{IV_1}/AUC_{IV_{11}}$ or $C_{B,ss,inf_1}/C_{B,ss,inf_{11}}$

The numbers (0.1 to 0.999) next to each curve on the graph

Indicate the extraction ratios at the reference point

$\frac{a}{\lambda} = 1$; hepatic blood flow = 1.0 ml/min/gm liver.

$\frac{a}{\lambda} = 1$ for all calculations. The ratio of ER , \dot{V}_{cl} and F for Models I and II are calculated from the predicted values of these parameters (Appendix IIIA and IVA) and is given in Appendix VA.

The ratio of AUC_{oral} , $C_{B,ss,oral}$, AUC_{IV} and $C_{B,ss,inf}$ for Models I and II are calculated from the predicted values of these parameters (Appendices IIIB and IVB) and is given in Appendix VB.

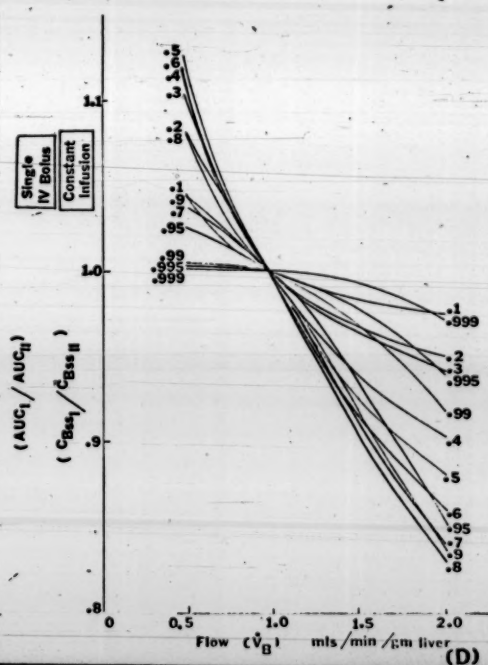
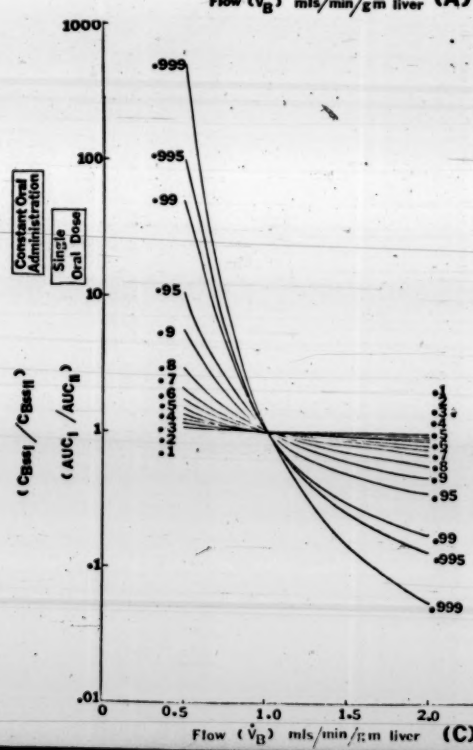
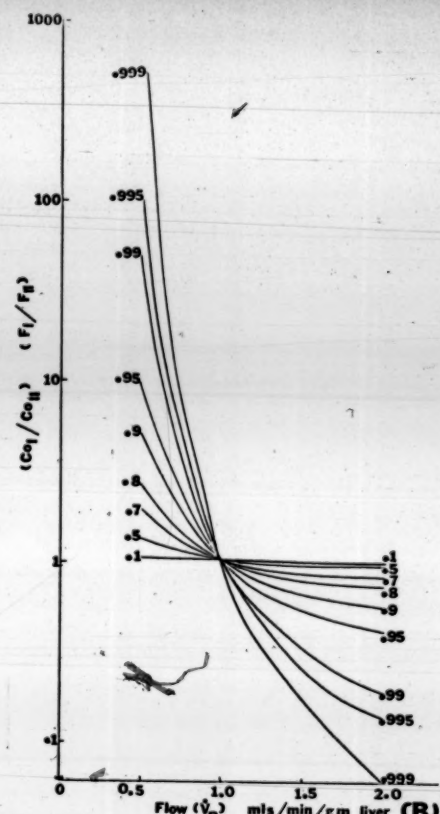
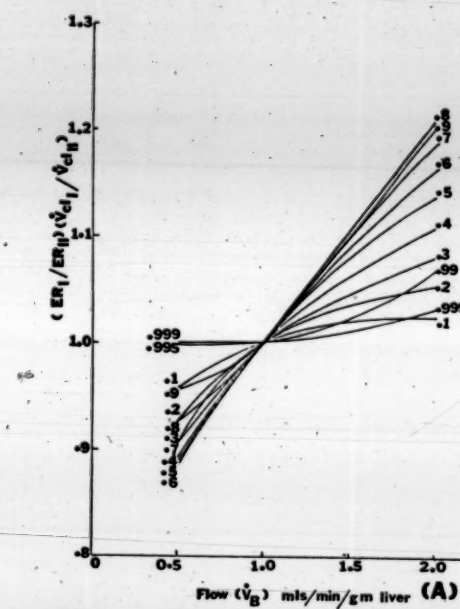
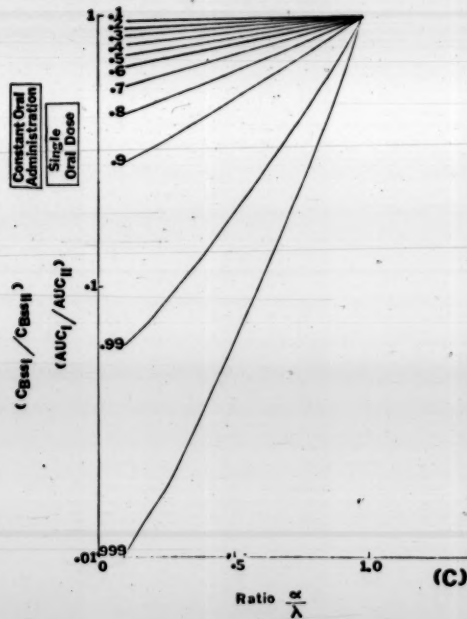
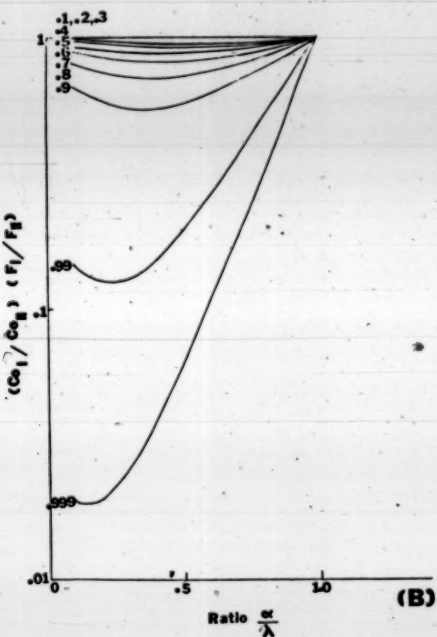
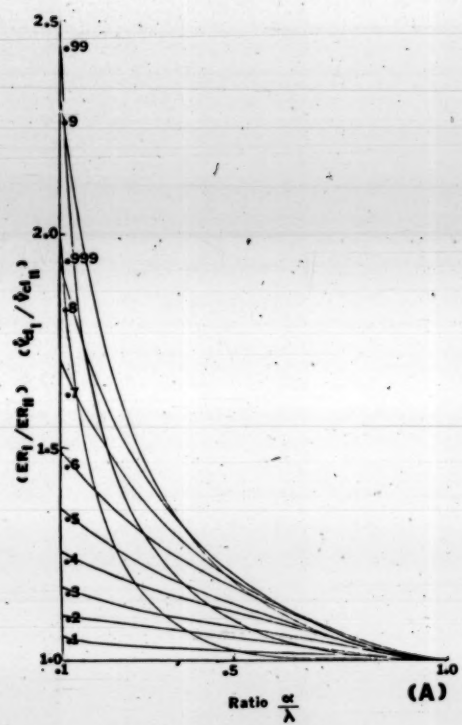


Figure 15. Ratio of the anticipated values of various pharmacokinetic parameters with changes in the ratio $(\frac{\alpha}{\lambda})$. These are:

- A) ER_1/ER_{11} or $\dot{V}_{Cl_1}/\dot{V}_{Cl_{11}}$
- B) C_0_1/C_0_{11} or F_1/F_{11}
- C) AUC_{oral1}/AUC_{oral11} or $C_{B,ssoral1}/C_{B,ssoral11}$
- D) AUC_{IV1}/AUC_{IV11} or $C_{B,ssinf1}/C_{B,ssinf11}$

The numbers (0.1 to 0.999) next to the curves on the graph

indicate the extraction ratios at the reference point ($\frac{\alpha}{\lambda} = 1$;
hepatic blood flow = 1.0 ml/min/gm liver). $\frac{\alpha}{\lambda} = 1$ for all
calculations. The ratio of ER or \dot{V}_{Cl} , F , AUC_{oral} or $C_{B,ssoral}$
and AUC_{IV} or $C_{B,ssinf}$ for Models I and II are calculated
from the predicted values of these parameters (Appendices VI
A-D and VII A-D) and is given in Appendix VIIA-D respectively.



In contrast, the ratio of the anticipated availability (F) or the steady state effluent drug concentration (C_0) for Models I and II changes over a hundred fold when $(\frac{\alpha}{\lambda})$ changes from 0.1 to 1.0 for drugs with high ER (> 0.9) (Figure 15B). This magnitude of change is also found for the ratio of the area under the blood-concentration-time curve following a single oral dose (AUC_{oral}) or the steady state blood concentration following constant oral administration ($C_{B,ss,oral}$) for Models I and II upon changing $\frac{\alpha}{\lambda}$ for highly cleared compounds.

These findings show that C_0 or F, AUC_{oral} or $C_{B,ss,oral}$ would serve as sensitive indices for the discrimination between the two models upon changing the ratio $\frac{\alpha}{\lambda}$ only for drugs with high extraction ratios (> 0.9).

3. By the Alteration of the Eliminating Capacity (A') under Linear Kinetic Conditions

Under linear conditions, the term A' is a constant. The ratio ER_1/ER_{II} or $\dot{V}_{cl,1}/\dot{V}_{cl,II}$ as function of A' which is expressed as multiples of blood flow (ml/min/gm liver) is depicted in Figure 13C (page 65). It is seen that at high values of A' , the ratios gradually approach the value of one and hence at that region, A' is a poor discriminator. At low values of A' , ($A' < 2 \times \dot{V}_B$) the values of ER_1/ER_{II} or $\dot{V}_{cl,1}/\dot{V}_{cl,II}$ are quite different from the value of one. Even then, the

maximum change only 70%. Hence A' is a poor discriminator at its best.

4. By Graphical Discrimination-Fitting Data to Linearized Equations for Models I and II

a. Changing Blood Flow under Linear Conditions (Low Concentrations to the Liver, $\frac{a}{\lambda}$ is Held Constant)

A linearized plot is obtained from Equation 19 for Model I by plotting $1/ER$ vs \dot{V}_B . If Model I holds, a straight line with y intercept = 1 and slope $1/(\frac{a}{\lambda} A')$ should be obtained (Figure 16A).

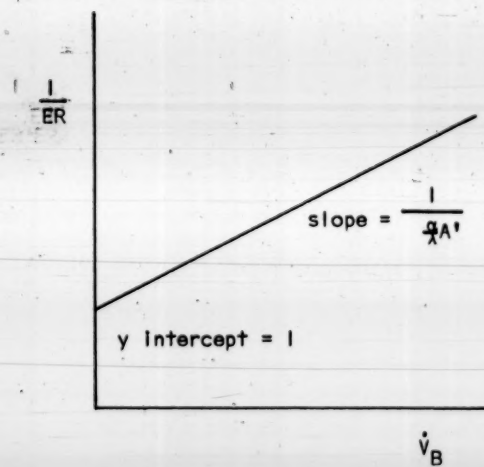


Figure 16A. Linearized transformation of Equation 19 (Model I)
 $\frac{a}{\lambda}$ is constant)

A similar linearized form from Equation 27 for Model II is obtained by plotting $\ln(1-ER)$ vs \dot{V}_B . If Model II holds, a straight line with a negative slope equal to $-\frac{\alpha}{\lambda} A'$ should be obtained (Figure 16B).

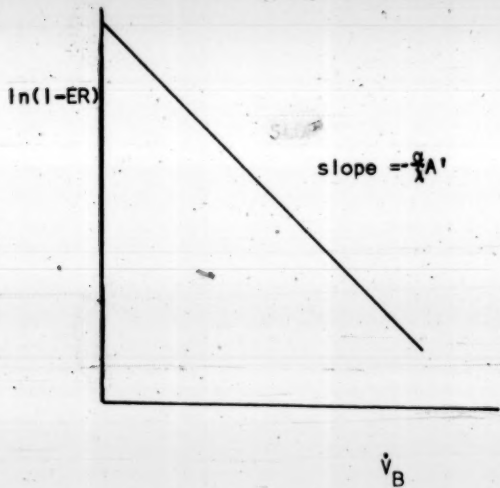


Figure 16B. Linearized transformation of Equation 27 (Model II)

$(\frac{\alpha}{\lambda} \text{ is constant})$

b. Changing the Degree of Protein Binding (Low Concentrations to the Liver; Blood Flow Is Held Constant)

If Model I holds, a plot of $1/ER$ vs $\frac{\alpha}{\lambda}$ would be a straight line with slope $= \dot{V}_B/A'$ and y intercept $= 1$ (Equation 19)(Figure 17A).

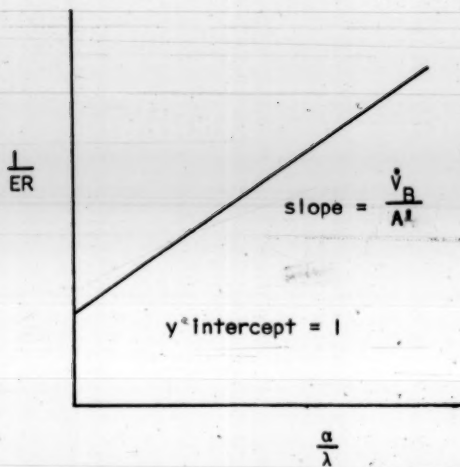


Figure 17A. Linearized transformation of Equation 19 (Model I)
(\dot{V}_B is constant)

Whereas if Model II holds, upon transformation of Equation 27 a straight line with negative slope of A'/\dot{V}_B is obtained on plotting $\ln(1-ER)$ against $\frac{\alpha}{\lambda}$ as shown in Figure 17B.

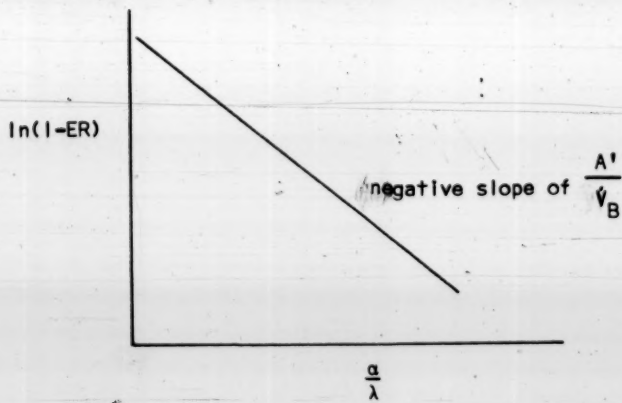


Figure 17B. Linearized transformation of Equation 27 (Model II)
(\dot{V}_B is constant)

c. Changing the Input Drug Concentration to the Liver Such that the Velocity of Removal Approaches the V_{max} of the System
(Blood Flow is Constant)

At a sufficiently high input concentration to the liver, the concentration of drug in liver (C_L) exceeds the value of K_m and the velocity of elimination approaches the V_{max} of the system. If only one enzyme is involved in drug elimination, or several enzyme systems can be suitably "lumped" so as to be characterized by a simple average K_m and V_{max} , then the data at steady state can be analyzed to discriminate between Models I and II. The value of $\frac{\alpha}{\lambda}$ should be constant under the concentration range studied for this analysis. The input concentration is varied while maintaining a constant hepatic blood flow.

If Model I holds, then by rearrangement of Equation 15 and with proper substitution of Equation 17, it may be seen that a straight line of slope of \dot{V}_B/V_{max} and y intercept of $(\frac{\lambda}{\alpha} K_m/V_{max})$ should be obtained when $(C_0/(C_i - C_0))$ is plotted against C_0 (Figure 18A). Whereas if Model II holds, a straight line will only be obtained when $\ln(C_0/C_i)$ is plotted against $(C_i - C_0)$ (Equation 26). The slope equals $1/(-\alpha K_m)$ and the negative y intercept is $V_{max}/(\dot{V}_B + \frac{\lambda}{\alpha} K_m)$ after correcting for protein binding and blood cell partitioning (Figure 18B).

Figure 18A: Linear transformation of Equation 15 (Model I)

at high input concentrations to the liver.

Source: www.ncbi.nlm.nih.gov/pmc/articles/PMC2625733/

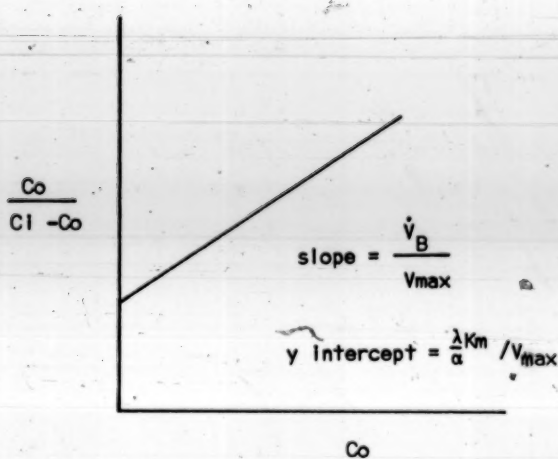


Figure 18A. Linearized transformation of Equation 15 (Model I) at High Input Concentration to the Liver ($\frac{\alpha}{\lambda}$ and \dot{V}_B are constant)

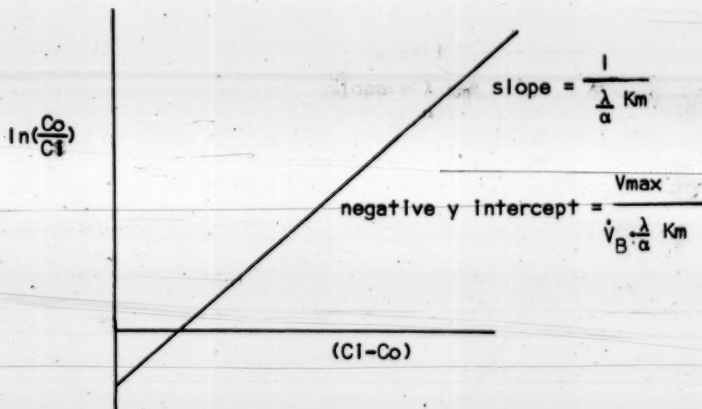


Figure 18B. Linearized transformation of Equation 26 (Model II) at High Input Concentration to the Liver ($\frac{\alpha}{\lambda}$ and \dot{V}_B are constant)

III. STATEMENT OF PURPOSE OF INVESTIGATION

The importance of clearance in pharmacokinetics and therapeutics is well established. The importance of the liver as a clearing organ for drugs and its unique anatomical position with regard to orally administered drugs are also well recognized. Yet how alterations in physiologic parameters, such as hepatic blood flow, plasma protein binding and hepatocellular enzymatic activity, influence the hepatic clearance and oral availability of drugs is poorly understood. What appears to be lacking is a meaningful model which interrelates these physiologic variables with hepatic clearance. Without such a model there is little chance of quantitatively predicting the effect of altered physiological states on hepatic clearance and hence the pharmacokinetics of drugs. And it is only through an understanding of the quantitative elements of drug disposition that advances in rational drug therapy are likely to be made.

The purpose of this investigation was several fold. The first objective was to examine the mathematical properties of two widely conceived models of hepatic clearance in order to establish parameters which could be used to discriminate between them and to predict the influence of altered physiologic parameters on various pharmacokinetic parameters. The second and principal objective was to study the effect of blood flow on the disposition of lidocaine, its monodeethylated metabolite, monoethyl-glycinexyliidide and antipyrine in the perfused rat liver in situ preparation. Lidocaine was chosen as it is very highly cleared by rat

liver, and theoretically the influence of blood flow on the availability or the effluent drug concentration of a highly cleared drug was found to be the best discriminator between the two models of hepatic clearance. Monoethylglycine xylidide was studied as an example of a metabolite which was also well cleared. Antipyrine was chosen as an example of a poorly cleared compound. The final objective was to integrate the present findings with those in the literature, and examine the consequences of a model of hepatic clearance in pharmacokinetics and therapeutics.

IV. EXPERIMENTALA. Material

The name and structure of the compounds used are listed in Table 3 below.

Table 3. List of Compounds Used

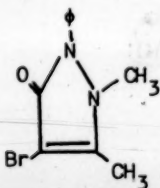
Names and Structures	Purpose	Source or Reference
Lidocaine hydrochloride monohydrate (2-diethylamino-2',6'-acetoxylidide)	Example of a highly cleared compound	Astra, Worcester, Mass. 01606
2-diethylamino-3'-bromo-aceto-anilide (Br-DEA)	Internal standard for lidocaine assay in blood and bile	Levy, R. Ph.D. Thesis U.C.S.F. 1971
2-ethyl-2-isobutyl-2',6'-acetoxylidide (WI2174)	Internal standard for lidocaine assay in liver, blood and bile	Astra, Worcester, Mass. 01606

Cont'd Table 3

Names and Structures	Purpose	Source or Reference
Monoethylglycine xylidide (MEGX) (2-ethylamino-2'-acetoxyxylidide)	Metabolite of lidocaine, and example of a moderately cleared compound	Astra, Worcester, Mass. 01606
2-ethylamino-3'-methoxyaceto-anilide	Internal standard for MEGX assay in bile, blood and liver	Astra, Worcester Mass. 01606
Antipyrine (2,3-dimethyl-1-phenyl-3-pyrazoline-5-one)	Example of a poorly cleared compound	Merck & Co. Inc. Rahway, New Jersey

Cont'd Table 3.

Names and Structures	Purpose	Source or Reference
4-bromo-antipyrine (bromo-2,3-dimethyl-1-phenyl-3-pyrazoline-5-one)	Internal standard for antipyrine assay	Gift, Dr. R. Sawchuck, University of Minnesota



All solvents were "Analytical Reagent" grade quality and distilled prior to use, with the exception of anhydrous ether.

Other materials, supplies and apparatus which were used are listed in Appendices I and II.

B. PROCEDURE

I. Biological

The perfusion medium used in the perfused liver in situ preparation consists of red blood cells, glucose, dextran, albumin and electrolytes, as listed in Table 4.

Table 4. Composition of the Perfusion Medium

Bovine Serum Albumin (Tyrode Solution)	1%
Dextran T-40	3%
Red Blood Cells	20%
Glucose	300 mg%
Kreb Ringer Bicarbonate	q.s. 100%

Composition of Kreb Ringer's Bicarbonate (KRB) Solution

0.9% NaCl (0.154M)	100 parts
1.15% KCl (0.154M)	4 parts
1.22% CaCl ₂ (0.110M)	3 parts
2.11% KH ₂ PO ₄ (0.154M)	1 part
3.82% MgSO ₄ · 7H ₂ O (0.154M)	1 part
1.3% NaHCO ₃ (0.154M)	21 parts 130 parts

The mixture was gassed vigorously with 5% CO₂ for 1 hour before use (45).

a. Preparation of the Perfusion Medium

The red blood cells used were separated from outdated human whole blood stored in citrate-phosphate-dextrose. Blood was filtered through a safti-filter blood administration set into culture tubes (25 X 150 mm) to half the volume and sterile normal saline solution was added to the remaining volume of the tube. The tube was capped and inverted gently 2-3 times and centrifuged for 10 minutes at 2000 rpm. The diluted plasma layer was aspirated off, discarded and any protein aggregates at the interphase visible were removed by suction. The washing was repeated twice with normal saline, followed by washing with lactated Ringer solution until the top aqueous layer was clear and free of protein aggregate at the interphase. The lactated Ringer solution of the last wash was removed by suction, and the red blood cells were filtered through a fine mesh (white organdy) into a graduated cylinder. The dextran, weighed out in a beaker, was wetted with a small volume of KRB, and was dissolved with the aid of a magnetic stirrer. The dissolved dextran solution was filtered through Whatman #1 filter paper and mixed well with the other ingredients (albumin, glucose and the remaining required volume of KRB). This solution was buffered to pH = 7.4 either with carbon dioxide gas or sodium hydroxide solution. Drugs was added to the solution at this stage and mixed well before admixture of the red blood cells. After the addition of the red blood cells the solution was stirred gently with a glass rod and was ready for perfusion.

b. The Apparatus

The liver perfusion apparatus, modelled after the design by Dr. Carl Mondon (Mount Zion Hospital, San Francisco) was built by Dr. G. Reichert ~~Reichert~~ and Mr. N. O. Henry of the School of Pharmacy, University of California at San Francisco (Figures 19-21). Basically, it is a box (2' wide X 3' long X 2' high), housing a humidifier, a manifold outlet for a gas supply, motor-driven rotating discs, a heating unit with light source, a temperature indicator, and a thermostatic probe. The top of the box is composed of three easily removable transparent plexi-glass sheets placed one next to another. The front door of the perfusion box facilitates the addition or removal of material. The blood medium, well mixed by rotating in a 1000 ml round flask in the reservoir (fitted onto the discs), is pumped using a Peristaltic Finger Pump (Figure 21A) (usual settings: the rate selection, 1, "v" speed control from 50 to 110) through a Bentley by-pass filter (Figure 21B), then a hollow fiber oxygenator (gas is kept at 1 L/min) (Figure 21C) and finally through a bubble trap (Figure 21C) before reaching the liver. The bubble trap consists of a 14 gauge hypodermic needle fitted halfway through the syringe (Figure 21C) and secured in position with epoxy glue. The top part of the syringe is fitted with a size 5 rubber stopper through which a 19 gauge needle is inserted to monitor the pressure with a manometer. A level of blood is kept in the syringe so that the bubbles formed will merely float on top of the level and will not appear in the outlet. All the connections

Figure 19. Schematic representation of the assembly of the perfusion Apparatus.

R₁ and R₂ are rotating reservoirs 1 and 2

P, the Harvard Peristaltic Pumps

S, a four-way stopcock

O, hollow fiber oxygenator

F, blood filter

B, bubble trap

Pr, manometer

O₂, oxygen 95%, carbon dioxide 5%

The big square represents the perfusion box where the temperature is maintained at 37°C ± 2°C.

The arrows indicate the direction of blood flow.

For one-through (single-passage) experiments (non-recirculating of medium), the effluent blood from the liver is collected in a beaker and the medium is not returned to the reservoir. For recirculating experiments, the effluent blood from the liver is returned to the reservoir.

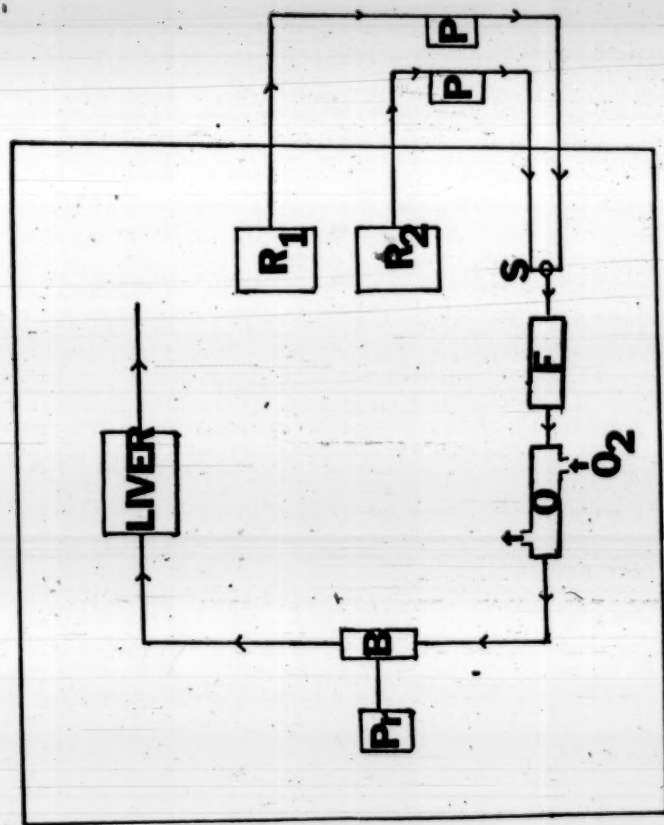


Figure 20. The Liver Perfusion Apparatus.

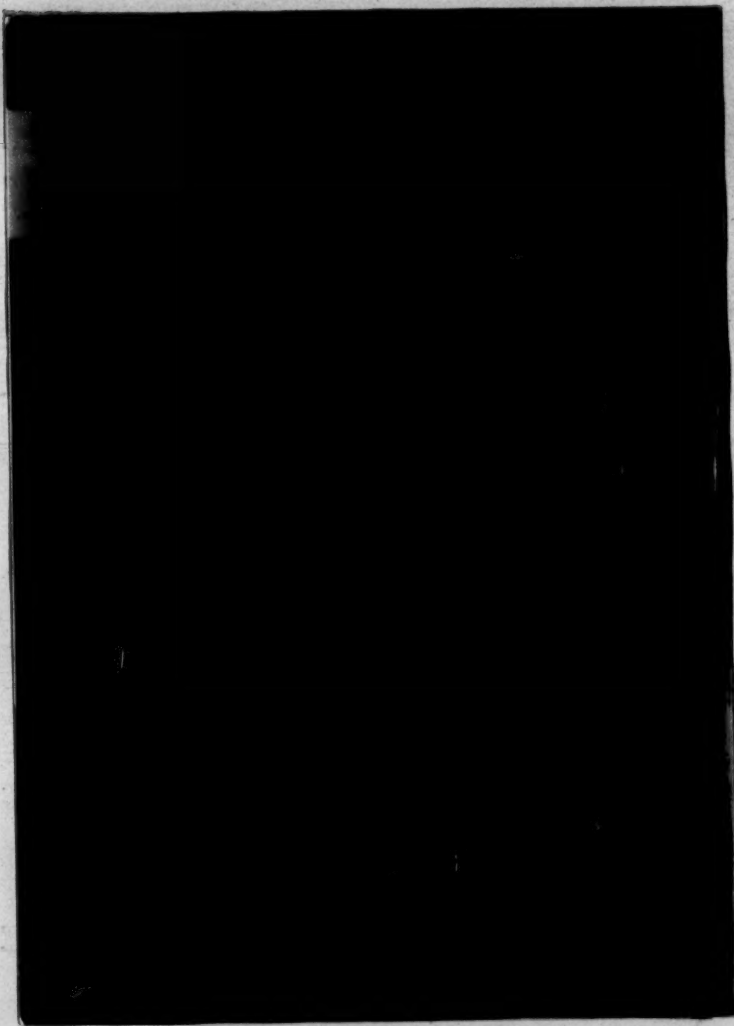
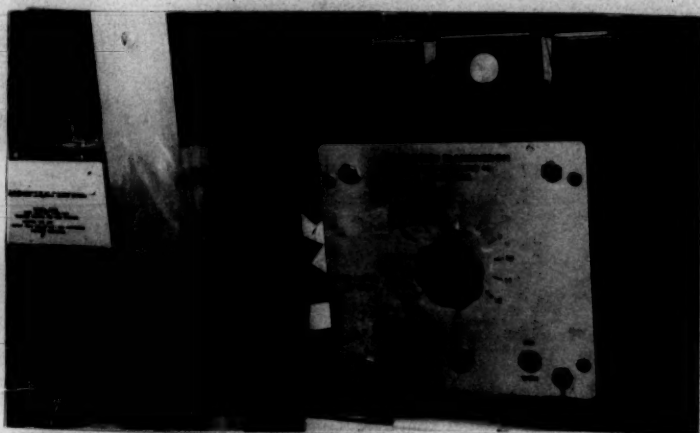


Figure 21. Parts of the Perfusion Apparatus

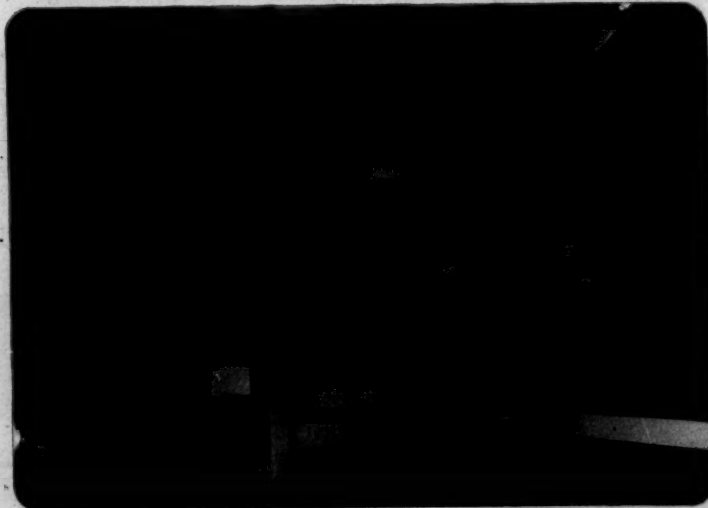
- A) Harvard Peristaltic Pump**
- B) Bentley by-pass filter**
- C) Oxygenator and bubble trap**



(A)



(B)



(C)

are made with polyethylene tubing (PE 240) and Luer-stub adapters. The section of tubing passing through the pump comes from the safti-blood administration set. Three-way and four-way stopcocks are inserted where necessary to facilitate the selection of the medium from the reservoirs.

c..Operative Procedure

Male Sprague-Dawley (200-450 gm) rats fed ad libitum were used as liver donors. Nembutal^R 50 mg/Kg was given intraperitoneally to the rat to induce anesthesia. The rat was weighed and placed on a surgical board (10 1/2" X 10 1/2") above the perfusion box. The fur of the animal was wetted with normal saline and a mid-line incision was made into the skin from the lower abdomen to the neck region. Another mid-line incision was made along the linea alba into the musculature up to the xiphoid process which was in turn removed. Bleeding was minimized by clamping the major vessels of the abdominal wall near the xiphoid process before mid-transverse incisions to the right and left of the mid-line were made. The intestines were displaced to the animal's left with a 4" X 4" gauze wetted with a normal saline so that liver, portal vein, right kidney, the lower inferior vena cava, and the bile duct were visible.

Bile duct cannulation was mostly done with PE 20 tubing and with PE 10 tubing for small bile ducts. Cannulation of the bile duct was done by first tying the distal end of the bile duct. Using fine

scissors, a small incision was then made in the bile duct and the bevelled side of the tubing was introduced into the region where bile oozed out. The tubing was pushed into the point where the duct arose from its branches and secured with a ligature (Deknatel 0-0 silk).

The gastroduodenal vein was tied at its junction with the portal vein. Two loose ligatures were passed around the portal vein at intervals of 3-4 mm below where the vein divided to enter the separate lobes of the liver. After tying the ligatures at the inferior vena cava at a point just above the right renal vein, and at the distal end of the portal vein, the portal vein was cannulated with a 16 gauge 2 1/2" catheter placement unit, a double cannula from which the sharpened central cannula could be withdrawn after insertion into the vein. The remaining teflon catheter was secured in place by tying the loose ligatures. The catheter, filled with the backflow of rat blood was connected to the outflow from the bubble trap. The pump and timer were activated. The thorax was opened by a transverse incision just above and along the line of insertion of the diaphragm with curved scissors. Two longitudinal cuts towards the head from the two ends of the transverse incision were also made. The sternum was cut and the rib cage totally removed, exposing the lungs and the heart. The right atrium was cut with fine scissors and a 14 gauge 2 1/2" catheter placement unit. Only the teflon catheter was inserted through the atrium into the inferior vena cava to collect the hepatic venous blood. Ligatures were made to secure this

outflow catheter. The outflow was either (1) returned to the reservoir in recirculating experiments or (2) collected into a separate beaker in once-through (single passage) experiments where the medium was not recirculated.

The surgical board, with the rat perfused in situ was then lowered into the perfusion chamber and maintained at a temperature of $37^{\circ}\text{C} \pm 2^{\circ}\text{C}$. To minimize drying, a piece of Saran wrap was placed above but not in contact with the liver.

d. Method and Time of Sampling

1) Blood

a) Single Passage (Steady State Experiments)

Single passage experiments were conducted using lidocaine and MEGX. During each steady state condition, a constant influent drug concentration was used. A ml aliquot was taken from the reservoir at zero time and at the end of each steady state condition (or at the end of the experiment) and at every time new medium containing the same concentration of drug was added to the reservoir. The samples were stored in screwcapped 2-dram clear glass sample vials until analyzed. The influent drug concentration (CI) was taken as the mean of the individual concentrations. Blood samples (12 mls) were taken from the outflow

leaving the liver and stored in screwcapped 3-dram clear glass sample vials until analyzed. Four samples were taken during the last 10 minutes of each steady state period (usually 30 minutes). The steady state effluent blood concentration (Co) was taken as the mean of the concentration of these four samples.

b) Recirculating Experiments

Recirculating experiments were conducted using antipyrine. Samples (2-4 ml) taken from the reservoir at zero time and at appropriate times thereafter, were stored in a 2-dram clear glass screwcapped vial until analyzed.

2) Bile

Bile, collected in toto in 2-dram screwcapped glass vials, was stored until analyzed.

3) Liver

At the end of the experiment, the liver was quickly removed surgically from the rat carcass and submerged in ice cold methanol. After blotting, the liver was weighed in a previously tared vial and reduced to fine pieces by scissoring action before 10N NaOH (8-18 gm) was added and the total weight recorded. The macerated liver was then frozen (-10°C). Just prior to analysis, the liver was thawed out and reduced to fine particles

using a teflon tissue homogenizer (50 ml capacity).

All blood, bile and liver samples were stored in the refrigerator (0°C) until analyzed, usually one or two days after the experiment.

2. Chemical

a. Lidocaine Assay in Blood, Bile and Liver

An appropriate aliquot was pipetted (blood, bile) or weighed out (liver) and placed in a screwcapped (teflon-lined) culture tube (16 X 150 mm). The sample size was chosen on the basis of the expected lidocaine content to get comparable peak heights of lidocaine with its internal standard. All samples were adjusted to the same volume (6 or 12 ml for blood analysis and 2 gm for liver analysis) by the addition of blank blood or blank liver tissue such that the volume ratio of blood or tissue to the organic phase within the same set of analysis remained constant. 200 mcL of a 10 mg/L solution of internal standard (Br-DEA for blood and bile and WI2174 for liver, blood and bile) in phosphate buffer was added to each tube. The assay procedure, similar to that of Benowitz and Rowland (108) is as follows:

- (1) 200 mcL 2N NaOH and 6 ml of anhydrous ether were added to the culture tube containing lidocaine and the internal standard. The tube was then capped tightly and shaken in a tilt-type mixer for 10 minutes.

- (2) The tube was centrifuged at 2000 rpm for 10 minutes.
- (3) The ether layer was transferred via a Pasteur pipette to a nipple-bottomed tube (nipple of 0.5 cm o.d. and 2-3 cm length fused onto a 16 X 150 mm culture tube) containing 200 mcl 0.5N HCl.
- (4) The ether-acid mixture was vortexed manually by repetitive inversion for one minute. Special care was taken to ensure constant mixing.
- (5) After centrifugation for 10 minutes at 2000 rpm, the ether layer was aspirated off and discarded.
- (6) A fresh 2 ml ether was added to the tube and vortexed again for approximately 15 seconds.
- (7) After centrifugation for 10 minutes at 2000 rpm, the ether layer was again aspirated off and discarded. Care was taken at this step to ensure all the ether was removed.
- (8) To the acid layer was added 200 mcl 2N NaOH and 25 mcl distilled carbon disulphide (CS_2). The tube was then immediately capped and vortexed for 1 minute.
- (9) After centrifugation at 2000 rpm for 10 minutes, the carbon disulphide layer appeared as a bubble at the bottom of the nipple.

(10) About 5 mcl of the CS₂ layer was sampled carefully with a 10 mcl Hamilton microliter syringe, making sure that none of the aqueous layer was included and 3 mcl was injected into a gas chromatograph.

Figure 22 illustrates gas-chromatographic tracings obtained by taking a blank blood sample (6 ml) (A) and the same volume of blood containing lidocaine and Br-DEA, (B) and WI2174 as the internal standard (C), through the extraction procedure. A Varian 1200 model gas chromatogram equipped with a flame ionization detector was used. Separation was accomplished using 6' long 1/8" o.d. glass column packed with 3% OV-17 on 100-120 mesh Gas Chrom Q. Injector port, column and detector temperatures were 265°, 190° and 270°C respectively. Carrier gas (nitrogen), air and hydrogen flow were 25, 300 and 25 mls/min respectively.

Figure 23 represents calibration curves for 0.125 -2.0 mcg samples of lidocaine hydrochloride monohydrate with 1 mcg of Br-DEA as the internal standard in blood, and with 1 mcg WI2174 as internal standard in blood and the liver. The peak height ratio of lidocaine/Br-DEA and lidocaine/WI2174 are found to be linear with the amount of lidocaine used and have been used for quantitative purposes.

Figure 22. Chromatograms obtained when blank blood (A), 1 mcg lidocaine hydrochloride monohydrate and 1 mcg Br-DEA in blood (B), and 1 mcg lidocaine hydrochloride monohydrate and 1 mcg WI2714 in blood (C) were taken through the assay procedure. Attenuation is at 64 and range 10^{-10} amp/mv.

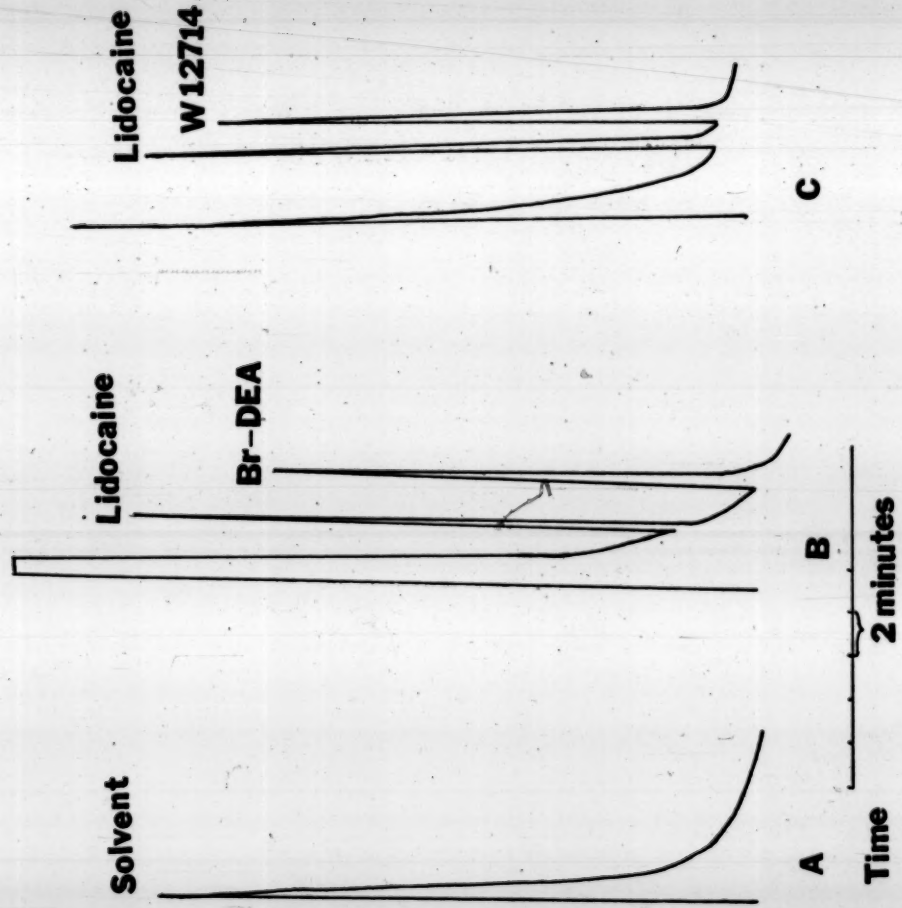


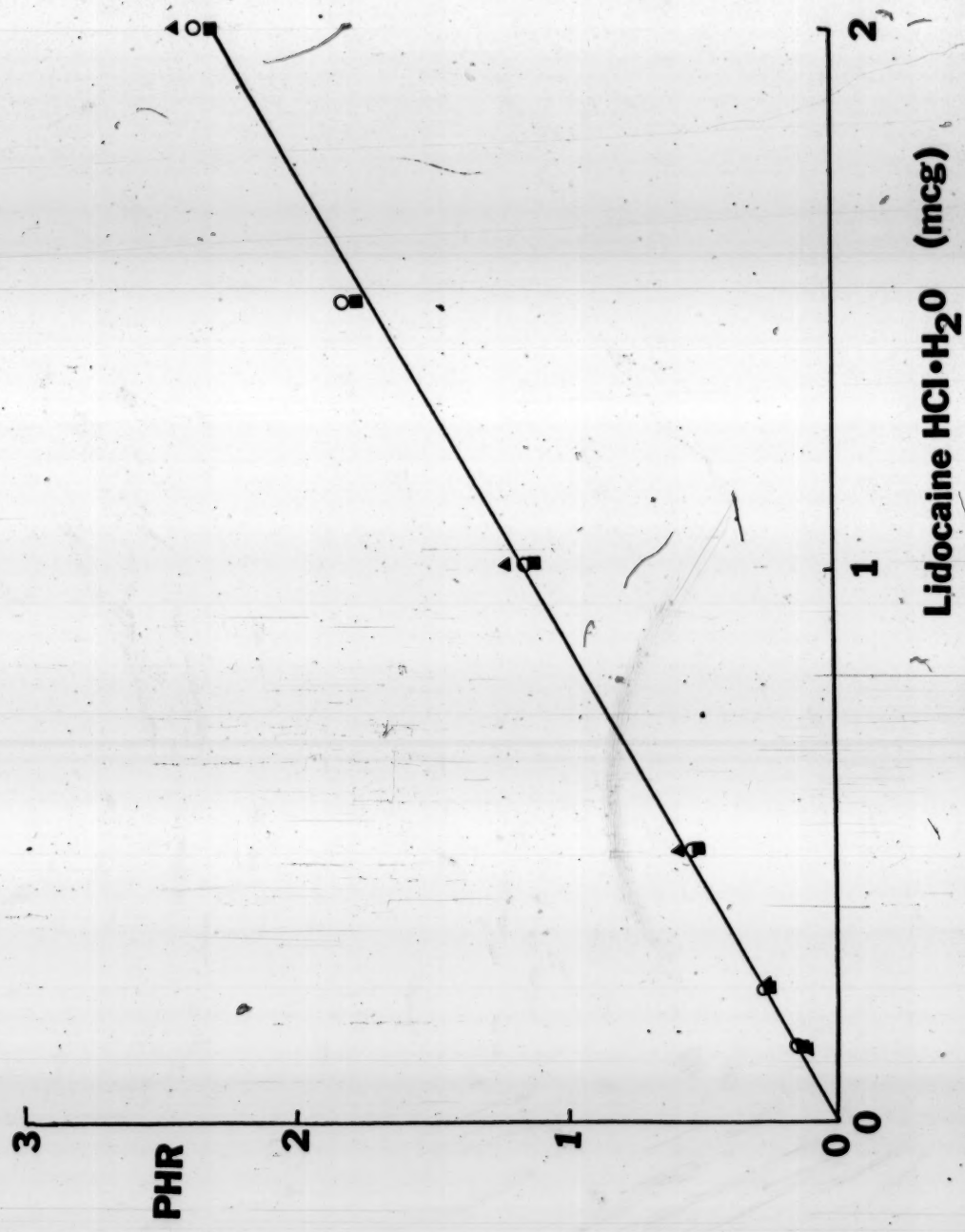
Figure 23. Calibration curve for lidocaine

The peak height ratio (PHR) of lidocaine to its internal standard is plotted against the amount of lidocaine hydrochloride monohydrate (0.125-2.0 mcg) added to biological sample.

(■) represents the calibration curve of lidocaine/Br-DEA
in blood

(○) represents the calibration curve for lidocaine/WI2714
in blood.

(▲) represents the calibration curve for lidocaine/WI2714
in liver tissue.



b. Antipyrine Assay in Blood and Bile

An aliquot of blood (0.5-2.0 ml) or bile (0.5 ml) was pipetted into a screwcapped (teflon-lined) culture tube (16 X 150 mm). The volume used was based on the expected antipyrine concentration present to give comparable peak heights of antipyrine to its internal standard 4-bromo-antipyrine. All the samples were made up to the same volume with blank blood such that the volume ratio of blood to the organic phase within the same set of analysis remained constant. The assay procedure is similar to that described by Huffman (109) and other investigators (110, 111). The procedure is as follows:

- (1) 200 μ l 2N NaOH and 7 ml distilled dichloromethane (CH_2Cl_2) were added to the tube containing antipyrine and 4-bromo-antipyrine (500 μ l of 20 mg/L solution of internal standard in phosphate buffer) and capped.
- (2) The top aqueous layer and the interphase were aspirated off.
- (3) The remaining CH_2Cl_2 was transferred via a Pasteur pipet into a nipple tube containing small clean carborundum boiling chip and evaporated to dryness under a stream of nitrogen and in a warm water bath (45°C).

(4) The sides of the nipple tube was rinsed with 0.5 ml of CH_2Cl_2 and again evaporated to dryness.

(5) The residue was dissolved in 50 μl of distilled water and vortexed for 30 seconds.

(6) 1-3 μl of the aqueous solution was injected into a gas chromatograph.

Figure 24 illustrates gas-chromatographic tracings obtained when a blank blood sample (A) and the same volume of blood containing antipyrine and its internal standard were taken through the assay procedure. A Varian 1200 model gas chromatograph equipped with a flame ionization detector was used and separation was accomplished using a 6' long 1/8" o.d. glass column packed with 3% OV-17 on 100-120 mesh Gas Chrom Q. Injector port, column, and detector temperatures were 235, 230 and 270°C respectively. Gas flows for nitrogen, air, and hydrogen were 25, 300 and 25 mls/min respectively.

Figure 25 is a calibration curve for antipyrine (0.625-10.0 mcg) obtained by plotting the peak height ratio of antipyrine to 4-bromoantipyrine against amount of antipyrine and is found to linear in the range examined.

Figure 24. Chromatograms obtained when blank blood (A) and blood containing 5 mcg antipyrine and 10 mcg 4-bromoadantpyrine (B) were taken through the antipyrine assay. Attenuation is at 128 and range 10^{-10} amp/mv.

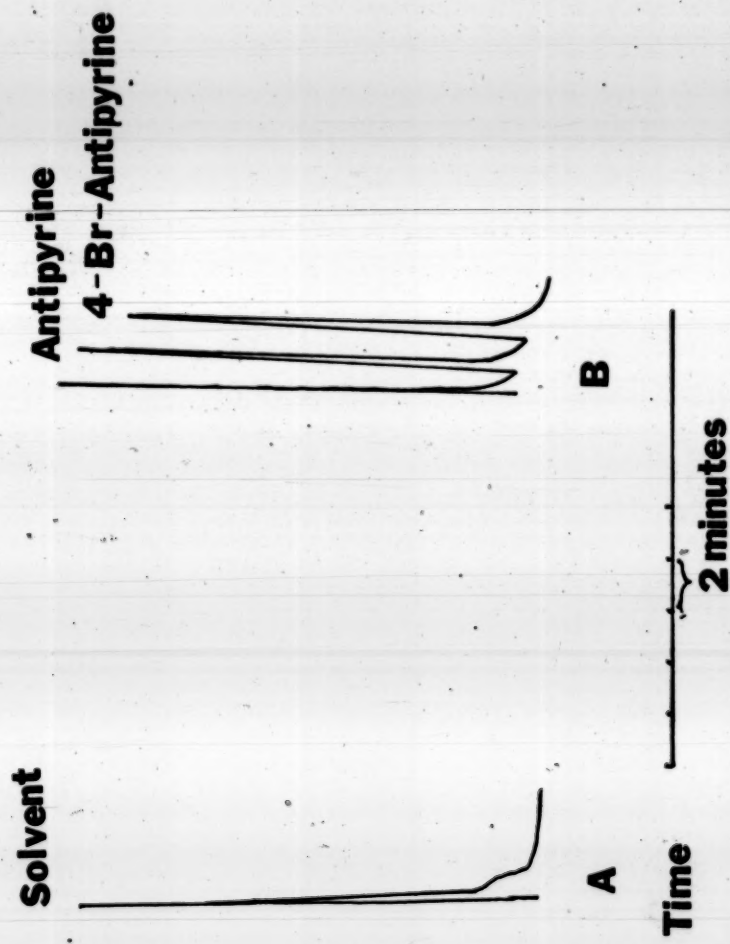


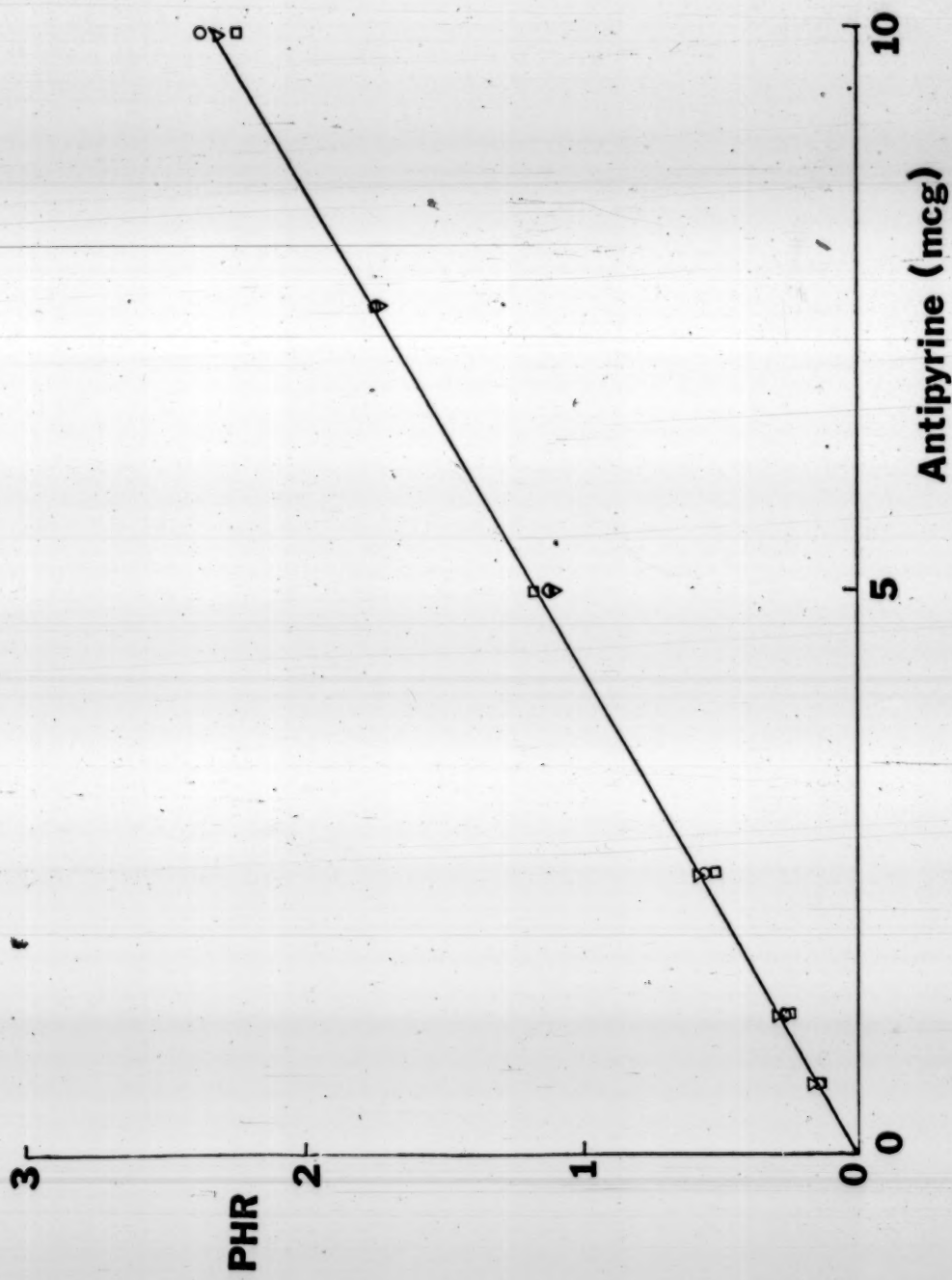
Figure 25. Calibration curve for antipyrine

The peak height ratio (PHR) of antipyrine to its internal standard (4-bromo-antipyrine) is plotted against the amount of antipyrine (0.625-10.0 mcg).

(○) represents the calibration curve of antipyrine in blood.

(□) represents the calibration curve of antipyrine in plasma.

(△) represents the calibration curve of antipyrine in water.



C. MEGX Assay in Blood, Bile and Liver

MEGX in blood, bile and liver were extracted using the same procedure as reported by Halkin *et al* (112). An appropriate aliquot was pipetted (blood, bile) or weighed out (liver) and placed in a screwcapped (teflon-lined) culture tube (16 X 150 mm). The sample size (0.25-2000 mcL for blood and 2 gm for liver) was chosen on the basis of expected MEGX content to get comparable peak heights of MEGX and its internal standard. All samples were adjusted to the same volume (2 ml or 2 gm) by the addition of blank blood or blank liver tissue to give the same volume ratio with the organic phase for the same set of analysis. 100 mcL of 5 mg/L solution of internal standard in phosphate buffer solution was used for all samples. The assay procedure is as follows:

- (1) To the sample containing MEGX and its internal standard, 200 mcL 2N NaOH and 2 ml distilled pentyl acetate were added in a culture tube (16 X 150 mm) and mixed for 10 minutes in a tilt-type mixer.
- (2) After centrifugation at 2000 rpm for 10 minutes, the pentyl acetate was transferred via a Pasteur pipet to a nipple-bottomed tube containing 200 mcL 0.5N H_2SO_4 and then the tube was capped and vortexed manually for 1 minute to ensure thorough and complete mixing.
- (3) After centrifugation at 2000 rpm for 10 minutes, the pentyl acetate layer was aspirated off.

- (4) A fresh 1 ml pentyl acetate was added. The mixture was vortexed again and centrifuged.
- (5) After centrifugation at 2000 rpm for 10 minutes, the pentyl acetate layer was again aspirated off.
- (6) 200 mcl 2N NaOH and 300 mcl pentyl acetate were added to the remaining aqueous layer and vortexed for 1 minute.
- (7) After centrifugation, 25 mcl of a freshly prepared 2% solution of pentafluorobenzoyl chloride in chromatographic grade benzene was added.
- (8) The tube was allowed to stand for 5 minutes, and then gently capped and allowed to stand for another 10 minutes.
- (9) The tube was vortexed and centrifuged for 10 minutes.
- (10) 1-3 mcl of the pentyl acetate layer was injected into a gas chromatograph equipped with a Scandium Tritide electron capture detector.

A Varian 1200 series gas chromatograph fitted with a Scandium Tritide electron capture detector and a 6' long $\frac{1}{8}$ " o.d glass column packed with 3% OV-17 on Gas Chrom Q on 100-120 mesh was used. Carrier

gas flow (5% methane in argon) was 20 ml/min. Injector port, column and detector temperatures were 250, 245 and 300°C respectively. Typical chromatograms of blank blood sample (A) and MEGX and its internal standard in blood (B) taken through the extraction procedure were shown in Figure 26. A typical calibration curve obtained by adding known amounts of MEGX (50-750 ng) and 500 ng of its internal standard taken through the assay procedure is shown in Figure 27. The ratio of the response of the derivatized MEGX to that of the derivatized internal standard was found to be proportional to the amount of MEGX examined.

d. Protein Determination

The amount of protein present in a sample was determined by a modification of the Lowry method (113). The procedure is as follows:

- (1) 100 μ l sample was placed into a plastic microfuge tube.
- (2) 150 μ l 15% trichloroacetic acid solution was added, the tube was capped, vortexed well and allowed to stand for 15 minutes.
- (3) The tube was vortexed again and centrifuged.
- (4) The tip of the microcentrifuge tube containing the protein precipitate was cut off and collected in a disposable culture tube (12 X 75 mm).

Figure 26. Chromatograms obtained when 2 ml blank blood (A), and the same volume of blood containing 750 ng of MEGX and 500 ng internal standard (B) were taken through the assay. Attenuation is at 4 and range 10^{-10} amp/mv.

Internal Standard

MEGX

B

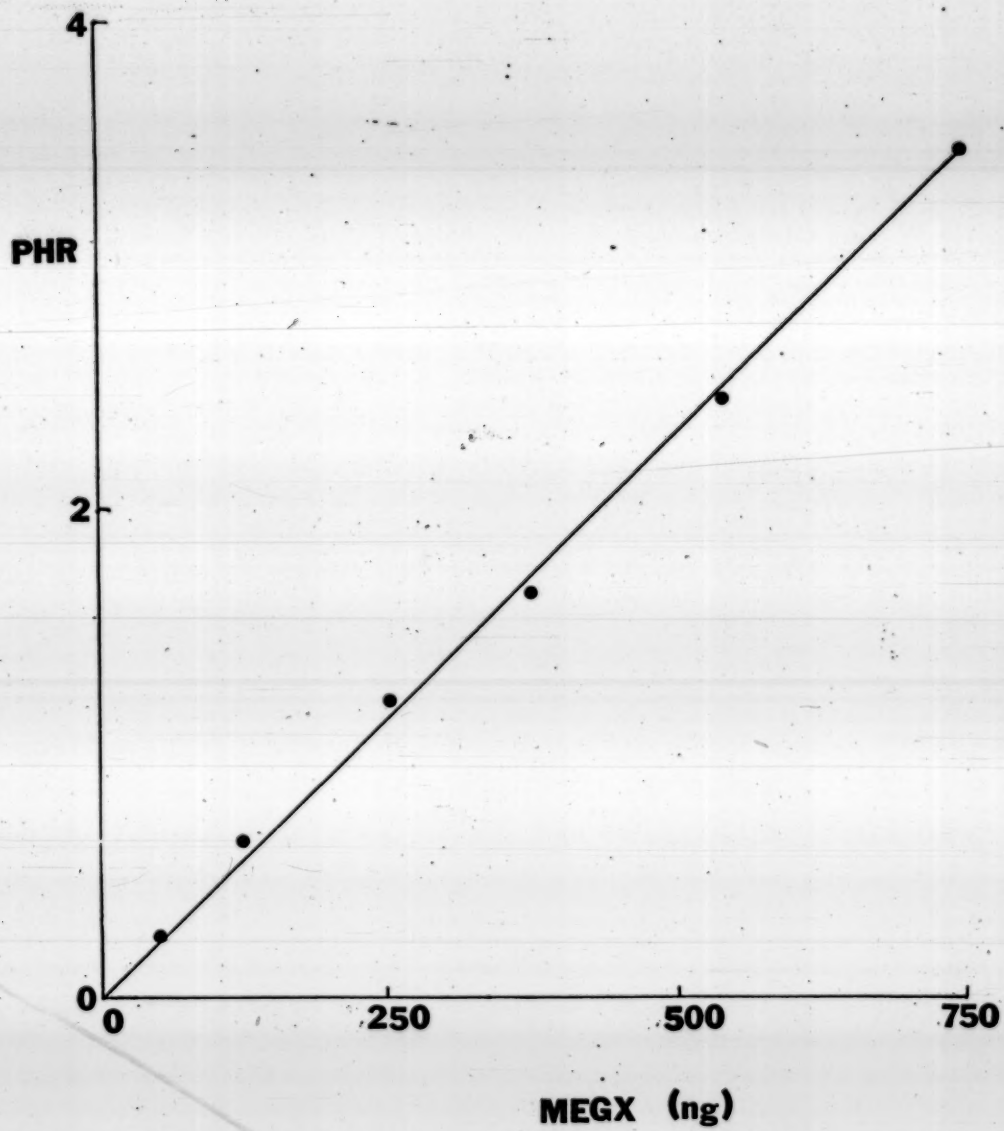
Solvent

Time 2 minutes

A

Figure 27. Calibration curve for MEGX in blood

The peak height ratio (PHR) of derivatized MEGX to its derivatized internal standard is plotted against the amount of MEGX (62.5-750 ng)



- (5) The inner walls of the remaining part of the microfuge tube were washed down with one ml of solution (15 parts 2% sodium carbonate in 0.1N NaOH and 0.3 parts 0.5% cupric sulfate pentahydrate in 1% potassium sodium tartrate), and the washings (containing any precipitate) were collected into the culture tube.
- (6) The culture tube was in turn vortexed and allowed to stand for 10 minutes.
- (7) After standing for an additional 10 minutes, and while vortexing slightly, 100 mcl IN Folin Reagent was added.
- (8) The resulting reaction was allowed to proceed for one hour, and the absorbance of the sample was then read at 750 nm on a Cary 15 Spectrophotometer at sensitivity = 4.
- (9) The amount of protein was estimated by reference to a calibration curve.

The calibration curve was constructed in the following manner: A 4:100 dilution of "plasma" from the perfusate (1% albumin, 3% dextran and 300 mg% glucose in Kreb-Ringer Bicarbonate Solution) is made by diluting 400 mcl of the "plasma" to 10 ml with normal saline. From this solution, 0.8, 0.6, 0.4, 0.2, 0.1 and 0.05 ml were diluted to

1 ml with normal saline. A blank was constituted with normal saline instead of the protein solution. The samples were treated in the procedure described earlier. A typical calibration curve is shown in Figure 28 where the optical density is plotted against the protein content.

e. Analysis of the Biochemistry of the Perfusion Medium

A sample of blood (10 ml) was taken from the unused perfusion medium at zero time and at various times from the effluent venous blood from the rat liver during the experiment. The samples were allowed to stand for 1 hour and centrifuged. The "plasma" layer of the perfusate was pipetted off and sent to ICN Medical Laboratories, Portland, Oregon for "Serum Profile" examination. This test entails the quantitation of glucose, uric acid, creatinine, blood urea nitrogen (BUN, albumin, globulins, cholesterol, electrolytes (P, Cl, Na, K, Ca) and enzymes (alkaline phosphatase, lactic acid dehydrogenase (LDH), serum glutamic oxaloacetic transaminase (SGOT), and serum glutamic pyruvate transaminase (SGPT). The assays are completed within a day of arrival.

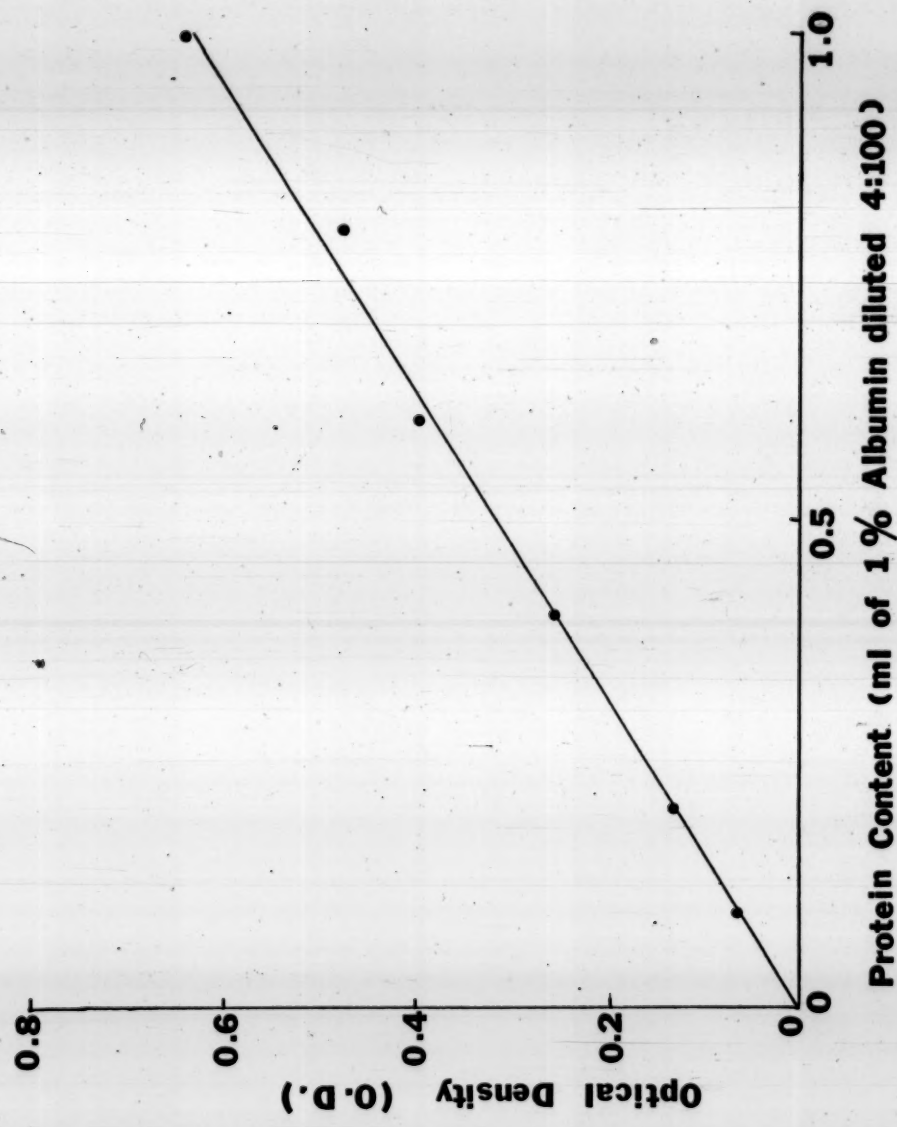
3. Physical

a. Method of Protein Binding Determination

The binding of lidocaine and monoethylglycine xylidide to the perfusate medium was studied in vitro using the Dianorm^R equilibrium dialysis system. This apparatus consists of twenty teflon cells, each made into two

Figure 28. Calibration curve for protein

Absorbance is read at 750 nm on a Cary 15 Spectrophotometer at sensitivity = 4. Sodium chloride solution is "reference" blank solution.



compartments (half cells) of volume 1 ml each by placing a section (2" X 2") of visking cellulose tubing of thickness 0.025 mm in between them. The tubing was prepared as follows:

- (1) 2" strips were cut and soaked in distilled water. One side of the tubing was cut and gently opened so that the material was thoroughly soaked in water on both sides.
- (2) After soaking for 30 min, the membranes were transferred to a 30% ethanol solution and soaked for another 30 minutes.
- (3) The ethanol was removed by washing the membranes in running distilled water for 15 minutes.
- (4) This was repeated before soaking the membranes in Kreb Ringer Bicarbonate solution for 30 minutes before they were finally ready for use.

The cells, packed so that the entire system was water tight were mounted on a motor-driven unit to ensure thorough mixing (25 rpm). The temperature was maintained at $37^{\circ}\text{C} \pm 1^{\circ}\text{C}$ by immersing the unit in a constant temperature water bath.

The procedure involved with equilibrium dialysis is as follows:

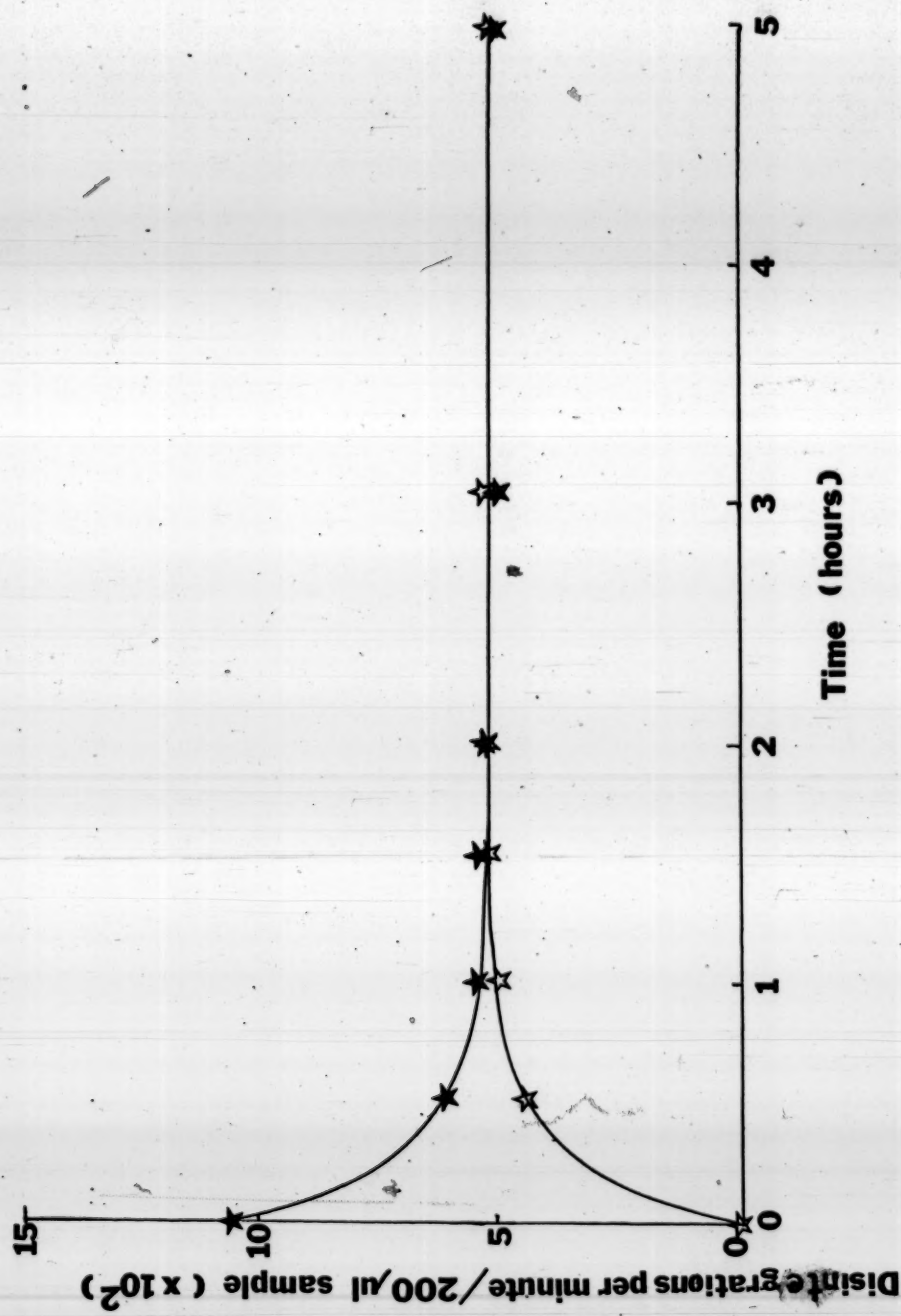
- (1) One ml solution containing the drug in "plasma" was introduced into one half cell with a disposable tuberculin syringe, and one ml of Kreb Ringer Bicarbonate solution was simultaneously injected into the corresponding half cell. Both solutions were buffered to pH = 7.4 (with HCl or NaOH).
- (2) The cells were tightly sealed and placed into the constant temperature water bath, and the motor-driven units were activated.
- (3) After the attainment of equilibrium, the units were removed.
- (4) The content in each half cells was collected and assayed.

The attainment of equilibrium was investigated in a preliminary study. Equilibrium was taken to be achieved when the ratio of the concentration of drug in buffer to that in "plasma" remained constant with time. 100 mcl lidocaine carbonyl ^{14}C (specific activity 5.48 mg/0.1 mC in 10 ml 0.1N HCl) was added to 10 ml of a solution containing 7.05 mg/L lidocaine in "plasma". Six cells were prepared according to the procedure described above. The solution on the "plasma" side was prepared in the following manner: Samples were retrieved at different times up to 5 hours. The radioactive counts from 200 mcl of "plasma" and buffer were counted in 10 ml aquasol in a potassium clear glass scintillation vial. The counts per minute were converted to disintegration (per minute (dpm) (corrected for quenching using AES ratio). Figure 29 shows that the

Figure 29. Attainment of equilibrium during equilibrium dialysis

- ★ dpm in "plasma" side
- ★ dpm in buffer side





equilibrium was attained as early as two hours. Thus all subsequent experiments were done for a period of 3 hours. Also material balance indicated that there was no binding of lidocaine to the membranes or cells.

The binding of lidocaine to "plasma" proteins was studied using the radioactive drug. 2 ml lidocaine solution (0.005-36.36 mg/L) was spiked with 10 mcl of radioactive lidocaine (5.48 mg/0.1 mC in 10 ml 0.1N HCl) prior to equilibrium dialysis. In the MEGX binding studies (0.3-45.0 mg/L), the drug was assayed by the gas chromatographic method. The degree of binding (α) is estimated as the concentration of drug in the buffer side to that in the "plasma" side at equilibrium.

b. Measurements of Oxygen Tension and pH

Measurement of pO_2 and pH were performed using a Radiometer. Blood samples (2-3 mls) were obtained from the arterial side (immediately after exit from the oxygenator) and the venous side (immediately after exit from the liver) in an air-free manner via four-way or three-way stopcocks connected to the apparatus. The samples collected in 3 ml plastic disposable syringes were capped and frozen immediately in ice. Prior to pO_2 measurements, the instrument was zeroed with "Natural Gas" (without oxygen content) and then calibrated with air. The sample was thawed out by leaving the syringe 2-3 minutes at room temperature and warming

with the hands. Then the sample (1-2 ml) was injected into the oxygen electrode, and the stabilized reading was taken as the correct pO_2 . The electrode was then flushed with distilled water.

Prior to pH measurements, the pH electrode was calibrated using standard pH buffers (pH = 6.975). A small volume (0.5 ml) of the thawed blood sample was injected into the electrode and the stabilized reading was taken at the pH of the blood. The electrode was washed with gentle injections of distilled water between measurements. Recalibration of pO_2 and pH electrodes were performed prior to each measurement.

c. Measurement of Perfusion Pressure

The perfusion pressure was monitored using a Tycoaneroid Sphygmomanometer connected to the apparatus via the bubble trap as shown in Figure 21C.

d. Electron Microscopy

Electron microscopy was only performed on one liver preparation which was considered to be representative of the others. The work was kindly performed by Dr. Tunde Felke, Department of Anatomy, University of California at San Francisco.

V. RESULTS AND DISCUSSIONA. AnalyticalI. Biological

The perfused rat liver preparation is an in vitro preparation closest to the in vivo situation. It is relatively inexpensive and the environment of the preparation can easily be manipulated. Direct sampling of material is also provided in this preparation. However, the perfusion medium used is artificial and deficient in hormones and other endogenous substances which may alter the metabolic activities of the system. The rat liver perfused in situ technique is preferred over the isolation technique as the time of anoxia during surgery is reduced to a minimum and the handling of the organ is avoided. However only short term experiments (< 4 hours) can be performed in this in situ preparation as the liver is in contact with a decaying carcass. In this in situ preparation, hepatic blood flow measurements (for the entire liver) rather than perfusion flow rates (blood flow per gm liver) are made as the weight of the liver is not assessed until the end of the experiment. However an estimation of liver weight is approximately given by 3.5% of the body weight. The liver weights are estimated to be 10-12 gm from rat donors (200-350 gm) and value of 10-12 mls/min is chosen as the normal blood flow to the liver.

The once-through technique (non-recirculating of medium) is preferred to the recirculating experiment when the conditions permit. Accumulation of metabolites and toxic end products is avoided. Also as the composition of the perfusion medium is held constant, (delivering adequate oxygen supply, nutrients and constant drug concentration to the organ), steady state situations can be studied and different conditions can be set up consecutively, with the liver serving as its own control. This drastically reduces the number of experiments needed (114). A big drawback to once-through experiments is that large volumes of perfusate are required which tend to shorten the duration of the experiment because of expenses involved.

2. Chemical

a. Lidocaine Assay

The slopes of the standard curve prepared from blood, plasma, water (in 2N NaOH) and liver (in 2N NaOH) were not significantly different at a confidence level of 0.95 (Figure 23).

1) Stability and Reproducibility

A standard curve with lidocaine hydrochloride monohydrate (0.0625-2 mcg) and 1 mcg WI2714 as the internal standard in blood, taken through the assay procedure was found to remain constant in its slope

for day 1 and upon reinjection of the same samples for days 2 and 3, indicating that lidocaine was stable in carbon disulfide for at least three days after the extraction procedure.

The stability of lidocaine in liver tissue (stored in 10N NaOH) was tested by repeating the liver analysis six months after the first analysis. Six samples of the liver tissue were assayed for lidocaine. No significant differences were found between the measurements as shown in Table 5 inferring the stability of lidocaine in strong base. This supports the findings of Benowitz and Rowland (108). Initially Br-DEA was used as the internal standard, but subsequently it was found to be unstable in 10N NaOH (used in liver assay). The latter is probably due to hydrolysis. Instead WI2714 was used as it is stable in strong base and has a shorter retention time than Br-DEA.

Table 5. Stability of Lidocaine in Liver Tissues Stored in 10N NaOH

Amount of Lidocaine in Liver Tissue (mcg)	
First Analysis	Second Analysis (6 months later)
27.1	28.5
15.0	21.5
31.4	28.8
39.1	39.5
23.8	25.3
68.9	72.9

Large sample sizes (15 ml) were used for analysis of the effluent

drug concentration and small sample sizes (0.25 ml) were used for some measurements of influent lidocaine levels. The peak height ratio (PHR) was tested against different volume ratios of blood/organic solvent. No significant differences were detected in the PHR using a ten fold difference in the volume ratio although the percent of lidocaine extracted varied with the volume of organic solvent used. Apparently the extraction of the internal standard varied to the same degree.

To assess the reproducibility of the assay, five blood samples with 1 mcg lidocaine hydrochloride monohydrate and 1 mcg WI2714 as the internal standard were taken through the assay procedure. The mean was 1.20 with a % coefficient of variation \pm 14.3%. The reproducibility of the assays between and within days was assessed from the slopes of nine calibration curves from nine sets of analyses on different days. The mean of these nine slopes was found to be 1.30 with a % coefficient of variation \pm 6%.

2) Specificity

The specificity of the lidocaine assay was tested for possible interference by MEGX by taking a mixture of 20 mcg MEGX, 0.125 mcg lidocaine hydrochloride monohydrate and 1 mcg WI2714 in blood through the assay procedure. The purpose of this was to demonstrate the possible contribution to the lidocaine peak due to the presence of a large amount of metabolite (MEGX) generated during lidocaine metabolism. The interference by consti-

tuents in blood was also ascertained by taking blank blood containing 1 mcg WI2714 through the assay procedure. In neither instance was the lidocaine to internal peak height ratio affected.

3) Sensitivity

The minimum amount of lidocaine detected by the assay procedure was found to be 50 ng at attenuation 32 at 10^{-12} amp/mv.

b. Antipyrine Assay

The slopes of the standard curves prepared from blood, plasma and water were not significantly different at a confidence level of 0.95 (Figure 25).

1) Stability and Reproducibility

A standard curve with antipyrine (0.625-10 mcg) and 10 mcg 4-bromo-antipyrine as the internal standard in blood taken through the assay procedure was found to remain constant in its slope for day 1 and upon reinjection of the same samples for days 2 and 3, indicating that antipyrine is stable for at least three days after the extraction procedure. The stability of antipyrine in phosphate buffer was demonstrated by the presence of reproducible slopes when the same stock solution was used as standards at different times.

To assess the reproducibility of the assay, four blood samples with 10 mcg antipyrine and 10 mcg 4-bromo-antipyrine were taken through the assay procedure. The mean PHR is 2.36 with a % coefficient of variation $\pm 2.1\%$. The reproducibility of the assays between and within days was assessed from the slopes of four calibration curves (on four sets of analyses on four separate days). The mean of these four slopes was found to be 0.23 with a % coefficient of variation $\pm 0.84\%$.

2) Specificity

The interference by constituents in blood was tested by taking blank blood containing 10 mcg 4-bromo-antipyrine through the assay procedure. It was found that blank blood did not contribute any interfering substances to the assay.

3) Sensitivity

The minimum amount of antipyrine detected by the assay at attenuation 32 and 10^{-12} amp/mv was found to be 125 ng.

c. MEGX Assay

The slopes of the standard curve prepared from blood and plasma for MEGX (50-750) and its internal standard (500 ng) taken through the assay procedure were found to be linear and did not differ significantly

(confidence level of 0.95) from one another (slope = 7.0) (Figure 27).

The slope of the standard curve prepared from water (slope = 5.5) using the same concentration was linear but significantly different from that obtained from blood and plasma. This can be due to the more favorable solubility or partition of MEGX into water than blood or plasma during its initial extraction with the organic layer whereas the partition of the internal standard into plasma, blood or water and the organic layer is the same.

1) Stability and Reproducibility

The stability of the derivatized MEGX and its internal standard was tested by the preparation of a standard curve with MEGX (50-750 ng) and 500 ng internal standard in blood taken through the assay procedure. The slope of the calibration curve for day 1 after the assay procedure was 6.5. Upon reinjection of the same samples, the slopes of the curve for days 2 and 3 remained linear, but were 7.0 and 9.0 respectively. This change in slope may be due to the deterioration of the derivatized internal standard upon standing, or due to its slow partition into the aqueous layer upon standing, increasing the peak height ratio with time. The stability of MEGX in phosphate buffer solution was proven because reproducible slopes were obtained when using MEGX from the same stock solution at different times as standard.

To assess the reproducibility of the assay, six samples containing

125 ng MEGX and 500 ng internal standard in blood were taken through the assay procedure. The mean peak height ratio was found to be 1.70 with a % coefficient of variation \pm 8.8%.

Attempts to develop a liver analysis proved unsuccessful because of interfering substances.

2) Specificity

The gas chromatographic assay for MEGX proved to be specific. The presence of a large amount (10 mcg) of lidocaine (the parent compound) did not change the peak height ratio of the derivatized form of 25 ng MEGX (the metabolite) and 500 ng internal standard taken through the assay procedure. Blank blood containing 500 ng internal standard did not contribute interfering peaks to the quantitation of MEGX.

3) Sensitivity

The minimum amount of the MEGX detected by the assay was found to be 10 ng at attenuation 32 and 10^{-12} amp/mv.

B. Discussion of the Experimental Procedure

I. Protein Binding

It was shown from theoretical analysis that binding to perfusate constituents can profoundly influence the hepatic clearance and availability of a drug (See Theoretical). Accordingly, the binding of lidocaine and MEGX to perfusate constituents was determined.

The blood to plasma concentration ratio (λ) and degree of protein binding of (α) of lidocaine and MEGX in various influent and effluent "plasma" and blood samples are shown in Tables 6 and 7 respectively. Throughout the respective concentration range studied (0.0036-36.00 mg lidocaine/L and 0.8-45.0 mg MEGX /L), neither lidocaine nor MEGX appear to bind significantly to components (plasma or red blood cells) of the perfusate. The mean of α for lidocaine and MEGX are 0.94 ± 0.4 and 1.00 ± 0.06 respectively. The lack of substantial binding of lidocaine to albumin had been reported (115) and it now appears to be so for MEGX and also for the binding of these amines to dextran. The value of unity for λ for lidocaine and MEGX also implies the lack of substantial binding of the same amines to washed red blood cells. Therefore, changes in protein (albumin), dextran and red blood cell composition should not influence the hepatic clearance or availability of these amines.

Table 6. Binding of Lidocaine to Perfusion Components

Lidocaine* concentration (mg/L) before equilibrium dialysis		λ^{***}	Counts/200 mci**		
blood "plasma"			buffer side after equilibrium dialysis	"plasma" side after equilibrium dialysis	
2.93	3.21	0.913	537	601	0.89
3.64	3.88	0.938	583	651	0.90
8.58	8.46	1.012	538	581	0.93
19.04	20.68	0.921	674	737	0.93
36.33	35.50	1.023	560	624	0.89
0.005	0.004	1.25	536	603	0.89
0.013	0.13	1.0	596	624	0.95
0.011	0.012	0.917	516	548	0.94
0.156	0.154	1.013	521	539	0.97
0.150	0.149	1.007	652	677	0.96
2.874	2.972	0.967	529	519	1.02
2.906	2.912	0.998	593	617	0.96
8.744	8.451	1.035	559	564	0.96

Mean $\bar{X} = 0.999$ 0.938

n = 13 13

S.D. = ± 0.068 ± 0.0385 Level of confidence = 0.95 = 0.45
(df = 12)

not significant

Level of Confidence 0.95
(df = 12)

not significant

*assayed by gas chromatographic method

**not corrected for quenching; counting efficiency of samples do not differ

*** $\lambda = C_p/C_p$ **** $\alpha = \frac{C \text{ unbound, plasma}}{C \text{ total, plasma}} = \frac{\text{cpm/200 mci buffer side}}{\text{cpm 200 mci "plasma" side}}$

Table 7. Binding of MEGX to Perfusate Components

Concentration of MEGX (mg/L)		Concentration of MEGX (mg/L)			λ^*
buffer side after equilibrium	"plasma" side after equilibrium	Blood	"Plasma"		
16.94	16.42	0.484	0.441		0.911
15.44	16.09	0.484	0.449		0.928
6.76	6.86	0.484	0.449	Mean \bar{X} =	0.9195
7.11	7.47	0.484	0.449	n =	2
2.84	3.33	0.484	0.449	S.D. =	± 0.0120
1.46	1.49	0.484	0.449	Level of Confidence =	0.95
1.58	1.44	0.484	0.449	(df = 1)	not significant
0.66	0.63	0.484	0.449		
0.66	0.64	0.484	0.449		
0.77	0.77	0.484	0.449		
0.831	0.752	0.484	0.449		
0.364	0.369	0.484	0.449		
0.354	0.343	0.484	0.449		
Mean \bar{X} =		1.0808			
n =		14			
S.D. =		± 0.0630			
Level of Confidence =		0.95			
(df = 13)		not significant			

$$^*\lambda = C_B/C_p$$

$$^{**}\alpha = \text{fraction free} = \frac{C \text{ unbound, plasma}}{C \text{ total, plasma}} = \frac{C_{\text{buffer side}}}{C_{\text{plasma side}}}$$

The binding of antipyrine to perfusate components was not examined as it was reported by Brodile et al (17) that antipyrine does not bind significantly to plasma proteins nor blood cells. Thus the values of α and λ are taken as one.

When the values of α and λ are known, the ratio $\frac{C_{\text{blood cell}}}{C_{\text{unbound, plasma}}}$ can be calculated from Equation 18. Benowitz et al (116) estimated the ratio of plasma water lidocaine to erythrocyte water lidocaine in the rhesus monkey to be 0.92, knowing $C_{\text{blood cell}}/C_p = 3.3$, $\alpha = 0.4$ and the water content in erythrocytes 70%. Since the blood to plasma concentration, (λ) and the degree of protein binding (α) are both unity for lidocaine in the perfusate medium, $C_{\text{blood cell}}/C_{\text{unbound, plasma}}$ is also one (Equation 18). When the water content in erythrocyte is again taken as 70%, the ratio of plasma water lidocaine to erythrocyte water lidocaine in the perfusate medium (containing human red blood cells) is thus 0.7. This difference may be due to different membrane characteristics of the red blood cell in humans as compared to rhesus monkeys such that movement of molecules in water crossing membranes is different.

2. Discrimination between Models I and II by Changing Hepatic Blood Flow of a Highly Cleared Drug at a Concentration to the Liver below the Km of the System

a. Lidocaine, a Highly Cleared Compound

On theoretical grounds, the term A' is essentially constant at

concentrations of drug to the liver below the K_m of the system. The greatest discrimination between Models I and II is noted by studying the changes of perfusion (hepatic blood flow per gm of tissue) on the availability ($\frac{C_0}{C_1}$) of a highly cleared compound. Under linear conditions, extraction is independent of the influent concentration (C_1), the effluent concentration (C_0) of a highly cleared compound is equally as good a discriminator. The latter parameter is used to discriminate between the two models with blood flow changes.

Lidocaine is chosen as the model compound because preliminary data indicated that its extraction ratio by the liver is very high in man (118) in dog (120) and in rhesus monkey (116, 121). The mean extraction ratio for lidocaine in the perfused rat liver preparation was found by the present investigation to be greater than 0.995. This appears to be the highest extraction ratio ever recorded. In addition, certain aspects of its metabolism are well defined (122, 126), in particular the conversion to monoethylglycine xylidide (MEGX) (125-127). As an analytical procedure existed for this deethylated metabolite (112, 124, 128), the formation of metabolite with blood flow and lidocaine concentration can also be examined. The insignificant binding of lidocaine and MEGX to plasma and red blood cell constituents (Pages 124-125) rendering the hepatic clearance of these compounds insensitive to changes in perfusate composition, is another virtue in the use of lidocaine.

b. Viability, Stability and Steady State

Before any interpretations can be made, the viability and stability of the preparation must be established. The criterion used for viability was that the hepatic extraction ratio of the drug remained constant with time. Figure 30 illustrates the attainment of this criterion when a constant influent lidocaine concentration (3.53 mg/L) was delivered at a constant flow rate of 10 ml/min/liver. The effluent concentration of the drug was very low (0.0115 mg/L) and the extraction ratio very high (0.997) over the entire period of study. The high extraction persisted from the first point of sampling (7 minutes) onwards, indicating that the preparation was stable and viable. As the low effluent concentration persisted from 7 minutes (the first sampling point), steady state conditions must have been established within 7 minutes. In subsequent experiments, the attainment of steady state was ensured by maintaining a blood flow for 30 minutes before a change (either blood flow or concentration) was imposed. The effluent concentration was taken as the mean of four samples taken within the last ten minutes of the interval. The bile concentration and volume were low and constituted only a negligible route of elimination. This is shown in Table 8 which summarizes the results of five studies.

Figure 30. Viability of the preparation as indicated by the constancy of the effluent drug concentration and hence extraction ratio with time when influent concentration of lidocaine (3.53 mg/L) was delivered at a constant blood flow rate (10 mls/min) to the perfused rat liver in situ preparation.

$$C_l = 3.53 \text{ mg/L}$$

C_0 Lidocaine (mg/L)

0.01
0.02

0 50 100

Time (minutes)



Table 8. Lidocaine Elimination by Bile

Total Volume of bile (ml)	Lidocaine Concentration in bile (mg/L)	Amount of Lidocaine Elimination	Total Amount* of Lidocaine infused into via bile (mcg)	% Elimination via bile liver (mcg)
1.5	1.469	2.204	556	0.40
3	1.378	4.134	4546	0.09
2	0.945	1.89	2654	0.07
2	1.152	2.304	684	0.34
2.5	1.108	2.77	872	0.32

$$* \text{Total amount of lidocaine infused} = \sum_{k=1}^n \dot{V}_B \cdot C_{lk} \cdot t_k$$

where \dot{V}_B = blood flow

C_l = influent lidocaine concentration

t = time interval for steady state period

n = total number of steady state periods

The biochemistry of the medium, the oxygen tension, perfusion pressure as well as electron microscopy were also performed to establish the viability of the preparation. The biochemical results for three liver preparations are tabulated in Table 9. The electrolytes remained relatively constant. The lack of potassium leakage (from liver cells to the blood) indicated the absence of severe rupture of cell membrane. However, the rise in the levels of some enzymes pointed to the occurrence of cell leakage (129) and indicated that the liver suffered some degenerative changes during perfusion. No globulin should be present in the medium. The reading may be an erroneous one.

Table 9. The Biochemistry of the Perfusate Medium

Test	Rat #1			Rat #2			Rat #3		
	Time=0'	73'	143'	0'	160'	187'	210'	0'	120'
Glucose (mg%)				0.6	0.8	0.6	0.8		
Uric Acid (mg%)				0.1	0.3	0.3	0.2		
Creatinine (mg%)				0	1	0	1		
BUN (mg%)	32	31	140	20	47	28	42	44	90
LDH (I.U.)	7.0	11	29	33	76	105	65	5	11
SGOT (I.U.)				5	81	10	57	8	28
SGPT (I.U.)	8	8	39	10	10	9	10	9	60
Bilirubin Total (mg%)	0.06	0.11	0.07	0.006	0.1	0.08	0.2	0.03	0.2
Alk. Phosphatase (I.U.)	9	8	8	7	2	6	1	1	0.1
Cholesterol (mg%)	0	0	0	0	0	0	6	5	10
Total Protein (G%)	3.8	2.9	2.8	5.0	4.8	5.3	4.7	5.6	5.9
Albumin (G%)	0.7	0.6	0.7	1.0	0.9	1.0	1.0	0.9	1.0
Phosphorus (MEQ/L)	2.1	2.5	2.5	2.1	2.5	2.5	2.3	2.2	2.7
Chlorides (MEQ/L)	1.7	1.24	1.22	1.13	1.20	1.08	1.20	1.17	1.21
Sodium (MEQ/L)	144	140	146	147	148	148	147	143	146
Potassium (MEQ/L)	5.1	4.9	5.0	5.1	5.1	5.3	5.3	4.9	4.8
Ca Total (MEQ/L)	4.1	4.0	4.2	3.9	3.8	3.9	3.8	4.0	4.1
Globulin (G%)	3.2	2.3	2.1	4.0	3.9	4.3	3.7	4.7	4.9
A/G Ratio	0.19:1	0.26:1	0.3:1	0.3:1	0.2:1	0.2:1	0.2:1	0.2:1	0.2:1

The oxygen tension and pH of arterial and venous blood were measured at different flow rates in some studies. Table 10 shows the results of these measurements.

Table 10. Oxygen Tension in Arterial and Venous Blood at Various

Flow Rates						
Study #	Blood Flow (mls/min)	Arterial Blood Oxygen tension (mm Hg)	pH	Venous Blood Oxygen tension (mm Hg)	pH	
1	16	331	7.38	16	7.12	
	14	380	7.23	14	7.08	
	12	337	7.14	12	7.09	
	10	359	7.24	10	6.98	
	16	403	7.11	16	6.98	
2	12	238	7.42	16	6.914	
	10	177	7.0023	13	6.912	
	12	175	7.408	13	6.949	
	14	170	7.202	12	7.1	
	16	257	7.094	15	7.052	
3	12	175	7.15	11.3	7.08	
	10	202	7.18	11	7.09	
	12	171	7.32	13.5	7.18	
	14	151	7.15	16.5	7.067	
	12	145	7.22	15	7.106	
4	16	123	7.18	17	7.09	
	19	365	not measured	32	not measured	
	16	392	"	28	"	
	13	401	measured	20.6	measured	
	10	391	measured	16.7	measured	
	19	296	measured	20.2	measured	

At an oxygen pressure of about 100 mm Hg, approximately 97% of the hemoglobin is combined with oxygen (for 0.45 hematocrit) (130). The blood perfusate medium has a lower hematocrit of 0.2 whereas the oxygen blood perfusate medium has a lower hematocrit of 0.2 whereas the oxygen

hemoglobin is combined with oxygen (for 0.45 hematocrit) (130). The blood perfusate medium has a lower hematocrit of 0.2 whereas the oxygen blood perfusate medium has a lower hematocrit of 0.2 whereas the oxygen

blood perfusate medium has a lower hematocrit of 0.2 whereas the oxygen pressure for arterial blood under all flow rates greatly exceeded the value of 100 mm Hg. It was thus inferred that complete saturation of the hemoglobin by oxygen did indeed take place. The high arterial oxygen tension measured in the arterial samples in the preparation greatly exceeded the value of 45 mm Hg, a value reported by Cumming and Mannerling (64) to be the minimum arterial oxygen tension for "unhindered" (normal) hexobarbital metabolism in the isolated rat liver preparation. Thus the oxygen supply evidenced by the high arterial oxygen tension was considered adequate to maintain the liver preparation in a viable state.

The pH of the arterial and venous blood averaged 7.22 ± 0.121 and 7.05 ± 0.78 respectively from the sixteen measurements. Although the pH of the perfusate was initially adjusted to 7.4, the arterial blood had a pH of 7.22. This may be due to the presence of 5% carbon dioxide in the gas supply for oxygenation (95% oxygen and 5% carbon dioxide) which may dissolve in the blood or be carried by the hemoglobin. The pH may possibly be maintained at 7.4 if 100% oxygen is used in the gas supply. Another method would be to titrate the medium with base to a pH of 7.4 during the experiment. The venous pH is not significantly different from the arterial pH, yet one can still see a decrease towards acidity due to the accumulation of acidic end-products of endogenous metabolism.

The perfusion pressure was monitored distant to the liver (see Figures 20 and 21C). Consequently it served only as a semi-quantitative measure of the actual pressure within the liver. Nonetheless, the monitored pressure reflected changes in liver resistance to the pump action, and at a constant blood flow, the pressure of the system should be constant. This was demonstrated in one experiment where blood flow was kept constant at 10 mlis/min. The pressure during the entire experiment remained the same (18-20 mm Hg). On increasing liver blood flow, perfusion pressure should increase according to Poiseuille's law (59). If liver blood flow is returned to the original flow rate, the pressure should also return to its original value. An increase in pressure in this instance would indicate a loss of its elasticity and integrity of cellular structure. Table II illustrates the flow-pressure relationship, confirming that there are no hysteresis effects.

Table II. Flow-Pressure Relationship of the Perfused Rat Liver in situ
Preparation

Blood Flow (mls/min)	Perfusion Pressure (mm Hg)
10	20-22
12	22-24
10	20-22
14	28-30
10	21-22
16	32-33
10	21-22

Electron microscopy was performed only once. The liver, chosen randomly, was fixed with osmium tetroxide, microtomed and screened by an electron microscope. The electron micrographs indicated that the mitochondria, cristae, ribosomes, endoplasmic reticulum and the nuclei were still intact after three hours of perfusion. Lysosome elements were also abundant. Some glycogen stores were left, and there was no extensive vacuolization, a process that accompanied cell damage and loss of integrity of cellular structure (131). In some instances, microvilli were destroyed and some endothelial lining damaged. All these findings indicated that the liver preparation retained most of its identifiable cellular structures. However the slight vacuolization showed a trend towards deterioration of the liver preparation (132).

c. Linearity

Discrimination between the two models is simplified when operating under linear kinetic conditions (independent of concentrations). To test for linearity, the concentration of lidocaine to the liver was varied from 0.95 to 7 mg/L at intervals of 30 minutes while maintaining a constant blood flow of 10 mls/min. The stability of the system was checked by repeating the initial input condition at the end of the experiment. The data (Table 12) shows no significant trend in either the availability, (Co/Ci) or the extraction ratio with varying influent drug concentration, indicating that the system is linear and stable at concentrations below

7 mg/L and at a hepatic blood flow 10 mls/min. Subsequently, to ensure linearity, an influent lidocaine concentration at or below 4 mg/L was always employed.

Table 12. Constant Extraction of Lidocaine with Influent Concentration below 7 mg/L

Lidocaine concentrations (mg/L) Influent (Cl)	Effluent (Co)	Availability (Co/Cl)	Extraction Ratio (Cl-Co)/Cl
7.00	0.0431 ± 0.00758	0.0062	0.9938
5.73	0.0256 ± 0.00292	0.0045	0.9995
3.00	0.0152 ± 0.00081	0.0051	0.00089
1.95	0.0094 ± 0.00125	0.0048	0.9952
0.95	0.0039 ± 0.00084	0.0041	0.9959
6.53	0.0571 ± 0.00809	0.0087	0.9913

$n = 4 \pm S.D.$ $n = 4 \pm S.D.$

d. Experimental Design

Initially, experiments were conducted in the following manner. Blood flow to the liver was varied from 16,12,8 and 4 mls/min and then returned to the original flow rate of 16 mls/min, with each steady state period being a 30 minutes interval. In some experiments, the order of blood flow was reversed from 4 to 16 mls/min and back to 4 mls/min. The choice of 16 mls/min as the upper limit was based on preliminary data suggesting that the preparation deteriorated at flow rates above 16 mls/min. Table 13

shows the effects of such changes in blood flow on the steady state extraction of lidocaine at a constant influent concentration of 3.75 mg/L.

Table 13. Influence of Hepatic Blood Flow on the Extraction of Lidocaine

Flow rate (mls/min)	Lidocaine effluent concentration (mg/L)	Extraction ratio (ER)
16	0.0449 \pm 0.0045	0.9987
12	0.0245 \pm 0.00142	0.9935
8	0.0187 \pm 0.0033	0.9950
4	0.0914 \pm 0.0144	0.9756
16	0.0264 \pm 0.0008	0.9930

$n = 4 \pm$ S. D.

As theoretically predicted, decreasing blood flow from 16 to 8 mls/min decreased the effluent drug concentration. Unexpectedly, on further decreasing the blood flow rate to 4 mls/min, the extraction of the drug fell.

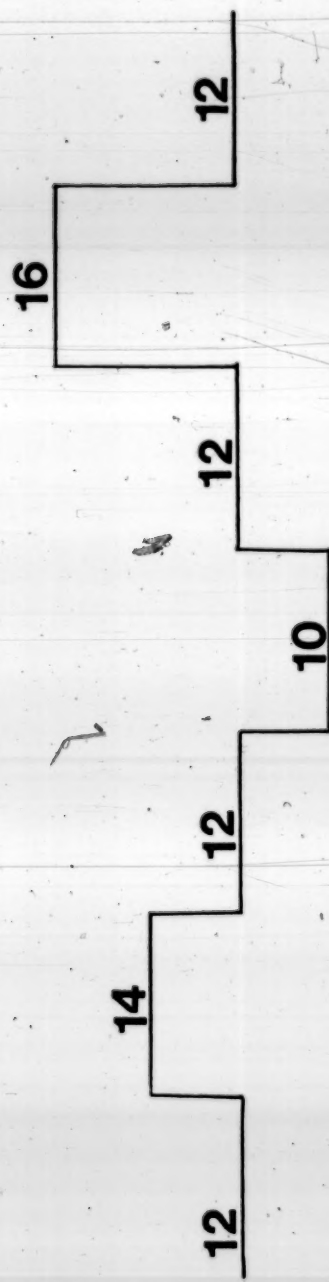
This paradox may be due to partial collapse of the hepatic vascular bed at low perfusion pressures (59) which result from low blood flow rates to the liver. Under these conditions, the effective areas of sinusoids in contact with blood are reduced, leading to a decrease in extraction of the drug. When the effective areas of the sinusoids are in maximal contact with blood, a limiting state of hepatic vasculature called Poiseuille's region is reached. In this region, the ratio of blood flow to pressure is a constant and further increases in pressure beyond this value do not open up new channels of perfusion within the hepatic vasculature. (59). Such a state must have been reached at flow rates of

8, 12 and 16 mls/min for increases in pressure did not increase the extraction ratio (due to increase in effective perfusion). Rather, the behavior of the extraction ratio was in agreement with the predictions.

Because of these potential physiological constraints, subsequent experiments were conducted with 10 mls/min as the minimum value such that the flow changes were from 16, 14, 12, 10 (descending order) and back to 16 mls/min again (ascending order). This design seemed to alleviate the deviations due to the collapse of the vasculature at low pressures (low flow rates). However another separate problem arose. Namely, that the viability of the preparation fluctuated from one steady state to another, causing difficulty in the interpretation of the data.

To overcome the last problem, the following design was developed. In this design, a control flow, e.g. 12 mls/min is chosen to perfuse the rat liver at a constant influent drug concentration. After 25 minutes of perfusion, the flow is randomly changed to 10, 14 or 16 mls/min for a further 25 minutes before returning the flow back to the control flow (12 mls/min). This procedure is repeated for each change in blood flow. An example is shown in Figure 31. This design provides the most meaningful interpretation of the data.

Figure 31. Schematic representation of the design of experiments used to discriminate between two models of hepatic drug clearance with alterations in blood flow. Each period of perfusion is 25 minutes. A control flow rate of 12 mls/min is chosen and interrupted at random by flow rates of 10, 14 or 16 mls/min.



← 25 →
Minutes

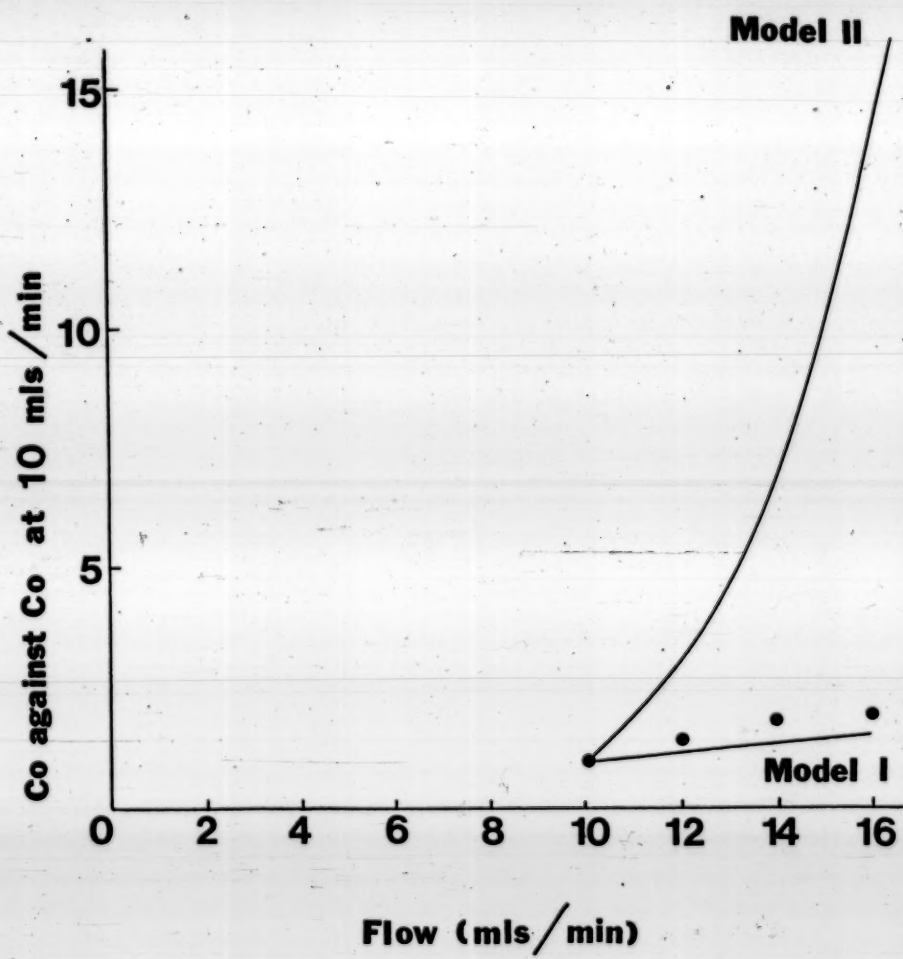
e. Results and Treatment of Data for the Flow-Change Experiments Conducted
at Constant Influent Lidocaine Concentrations at or below 4 mg/L

The enzyme activity of the system during the flow-change is considered the same as the average of that of the control flow periods immediately before and after the change. The effects of flow changes on hepatic extraction are then easily interrelated and interpreted even when the viability of the preparation fluctuates slightly. An example of a typical experiment is shown in Figure 32 (Study I in Appendix IX) where the control flow rate was 10 mls/min. The effluent lidocaine concentration at a particular flow rate is compared to the average effluent lidocaine concentration during the control flow rate and plotted against blood flow. Predictions of the effluent drug concentrations for Models I and II are made in the following manner:

Hepatic blood flow (to the entire liver) rather than the perfusion rate is used as in the perfused rat liver in situ preparation as the weight of the liver is not known until the end of the experiment. Furthermore the liver weight obtained at the end of the experiment may be overestimated due to edema or liver enlargement. Most important of all, the predictions within a liver preparation can be made using either blood flow or perfusion rate.

The average effluent lidocaine concentration of the control flow flanking a particular blood flow is used to calculate the extraction

Figure 32. The predicted and observed lidocaine data for Models I and II when blood flow is changed to 12, 14 and 16 mls/min from the control flow rate of 10 mls/min (Study I - Appendix IX). The lines represent predicted data for Models I and II and the points are experimental.



ratio and the term A' as in Equation 19 for Model I and Equation 27 for Model II. These A' terms are in turn used to predict the extraction ratio and effluent drug concentration at that particular flow for each model. From Figure 32 it is seen that the observed data are predicted more accurately by Model I.

A series of eight additional experiments were performed in the same manner using 12 ml/min as the control flow and 10, 14 and 16 as the randomly chosen flow changes. The results of these nine experiments are tabulated in Appendix IX. The observed and predicted results for Models I and II for these nine experiments which were performed on different rat livers with different orders of flow and at different times were grouped together as shown in Figure 33 for Model I and Figure 34 for Model II.

The straight line with slope = 1 represents the perfect correlation. The data (predicted versus observed effluent lidocaine concentration) for Models I and II are fitted individually to a straight line by regression analyses and the resultant slopes obtained are then compared to the straight line with slope = 1. Table 14 summarizes the generated statistics.

Figure 33. Predicted versus observed effluent lidocaine concentrations for Model I for a series of nine experiments performed at a low influent lidocaine concentration (4 mg/L) with alterations of blood flow. The line with slope = 1 indicates a perfect fit. The predicted and observed data are given in Appendix IX-A-B-C.

Model I

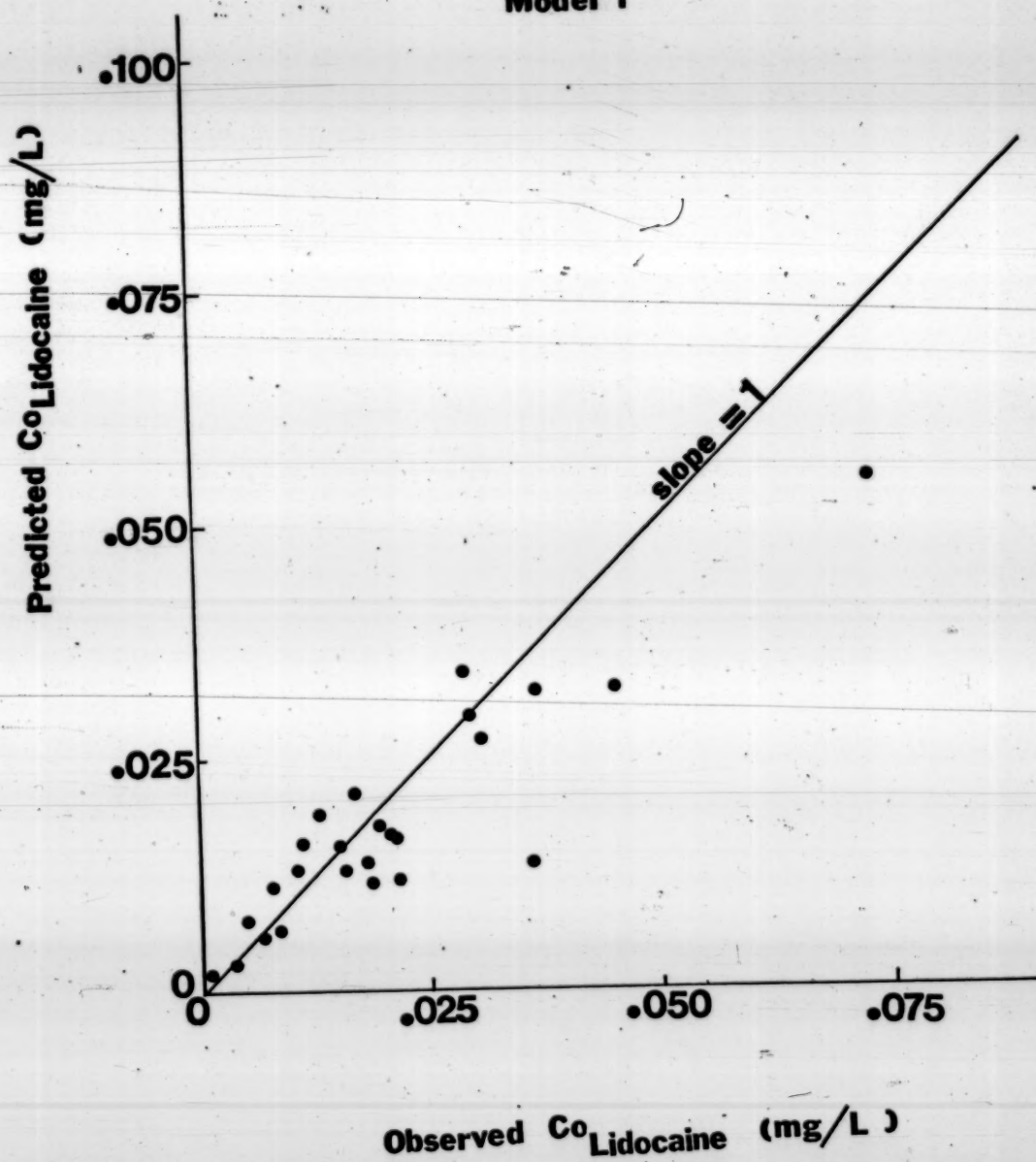


Figure 34. Predicted versus observed effluent lidocaine concentration for Model II for a series of nine experiments performed at low influent lidocaine concentration (4 mg/L) with alterations of blood flow. The line with slope = 1 indicates a perfect fit. The predicted and observed data are given in Appendix IX-A-B-C.

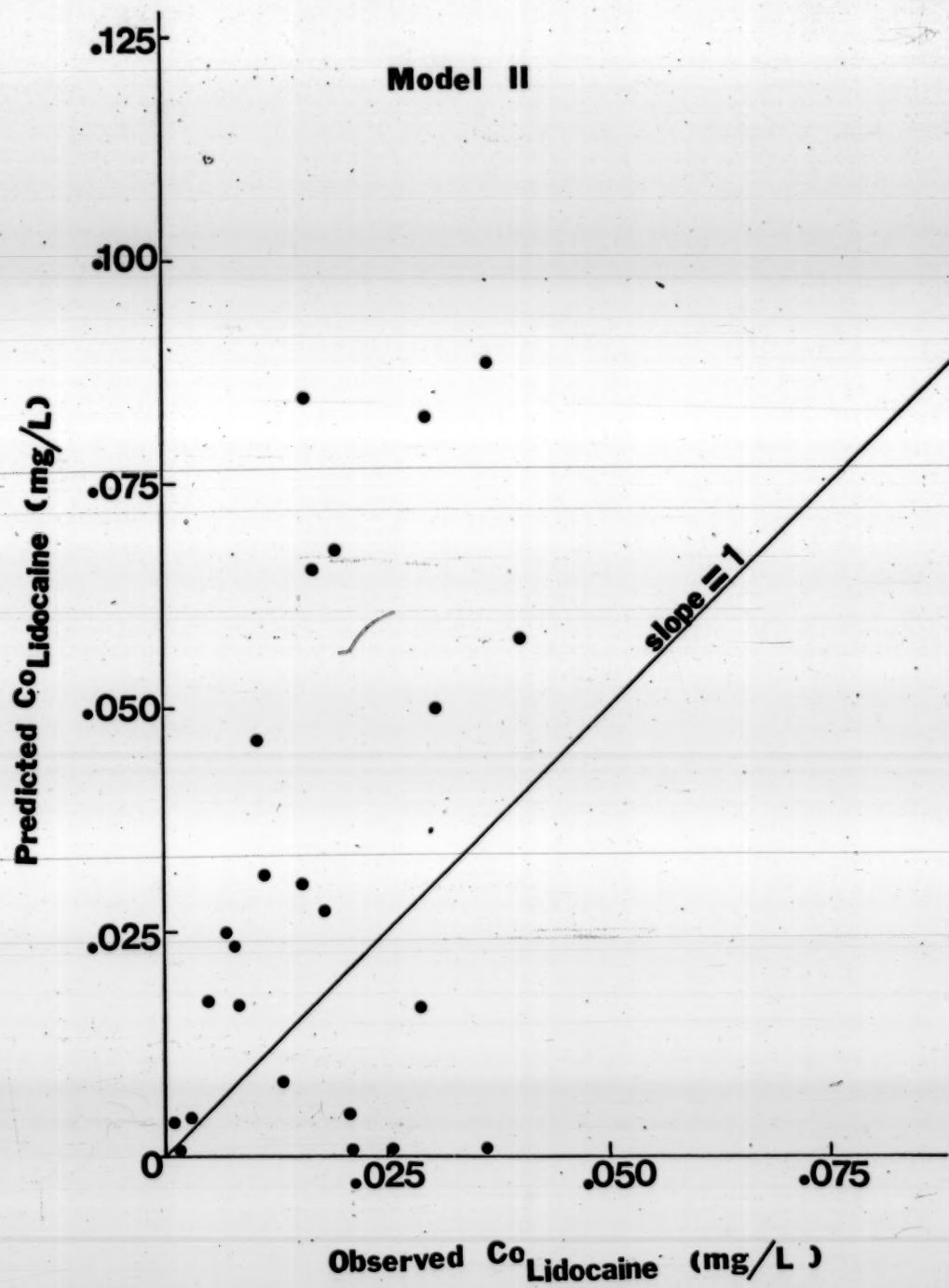


Table 14. Regression Analyses of Data and Comparison of the Slopes to Slope = 1

Statistical Parameter	Model I	Model II
n	25	25
s_x^2	0.0001389	0.00117
s_y^2	0.000234	0.0002341
$s_{y,x}^2$	0.000047	0.0001438
slope (m)	1.16635	0.28684
Intercept (b)	0.00012	0.01018
corr. coeff. (r)	0.8986	0.6415
$s_{y,p \cdot x}^2$ *	0.0000235	0.0000719
$s_{y,p \cdot x}$	0.004848	0.00848
t**	1.40083	9.96494
df	46	46
level of confidence	95%	95%
	not significant	not significant

$$*s_{y,x,p}^2 = \frac{(n_1 - 2)s_{y,x_1}^2 + (n_2 - 2)s_{y,x_2}^2}{(n_1 + n_2 - 4)}$$

s_{y,x_1}^2 calculated above from
Models I & II.

$s_{y,x_2}^2 = 0$ as there is perfect

as there is perfect

correlation

$$** t = \frac{(m - 1)}{\sqrt{\frac{1}{(n_1 - 1)s_{x_1}^2} + \frac{1}{(n_2 - 1)s_{x_2}^2}}} \quad df = (n_1 + n_2 - 4)$$

The t statistics for Models I and II are 1.4008 and 9.9649 respectively, with 46 degrees of freedom. This value of t ($df = 46$) is not significant for Model I at 95% confidence interval whereas it is for Model II. Based on this finding, Model II is rejected as to having a slope equal to one and Model I is accepted as having a slope equal to one at 95% level of confidence. Although a statistical analysis is performed to accept or reject the data based on the "goodness of fit" to the straight line with $slope = 1$ for perfect correlation of observed and prediction results, it is inappropriate to quote such statistical parameters. This is so because the data are derived from different populations whose means and variances may be different (134).

f. Mass Balance with Liver Analysis

From theoretical analysis, discrimination between the two models is best perceived with the use of a highly extracted compound (extraction is due to metabolism and not hepatic uptake) with blood flow changes. Under steady state conditions uptake is essentially complete, and the rate of loss of the drug should be accounted for only by metabolism. Since steady state conditions were achieved within 7 minutes as shown in one study, (Page 129) and it is inconceivable that lidocaine is taken up by the liver to a great extent. However, to confirm the point that the removal of lidocaine during its passage through the liver is indeed by metabolism, liver analysis was performed in seven livers and the results are given in Table 15.

Table 15. Liver Analysis of Lidocaine and the Partition of Lidocaine in Liver With Respect to the Effluent Drug Concentration in Blood

Total amount of lidocaine infused*	Amount of lidocaine in liver at end of experiment**	Fraction of dose in liver at end of experiment	Wet weight of liver at end of experiment (gm)	Lidocaine conc. in effluent blood after correction for steady state condition (Co) (mg/L)	Amount of lidocaine in liver at the end of experiment (C _L) (mcg/gm liver)	Concentration of R _L /B ***
9871	28.45	0.0029	13.241	0.0243	28.41	2.146
9870	21.55	0.0022	9.9985	0.0120	21.532	2.154
8820	28.81	0.0033	15.0361	0.00572	28.80	1.916
10038	38.04	0.0038	13.285	0.0330	37.99	2.860
10060	39.50	0.0039	13.67	0.0278	39.46	2.886
10685	25.31	0.0024	10.70	0.0435	25.24	2.359
11736	72.88	0.0062	11.146	0.0799	72.76	6.528
						81.7

* Total amount of infused = $\sum_{k=1}^n V_B \cdot k \cdot C_{L,k} \cdot t \cdot k$ where n is the number of steady state conditions and the t the duration for the steady state period.

** Amount of lidocaine in liver (wet weight) = amount of lidocaine assayed \times $\frac{\text{Total weight of liver} + \text{ION NaOH}}{\text{Weight (liver + ION NaOH) used}}$

*** (Amount of lidocaine in (wet weight) liver - $1.5 \times (Co)$ mcg; hepatic blood volume is taken as 1.5 ml

**** Partition coefficient for liver = $\frac{\text{conc. of drug in liver (C}_L\text{)}}{\text{conc. of drug in effluent blood (Co)}}$

From mass balance, the total amount of lidocaine infused equals the amount of drug in the liver, the total amount eliminated by biliary excretion and the total amount metabolized. It was shown earlier that the biliary route did not contribute significantly to the removal of lidocaine, and it is shown here that liver uptake of lidocaine is also insignificant (an average value of 0.35% of dose is present in the liver). Furthermore, this estimation of 0.35% is an overestimation for the amount of lidocaine present in the liver as only wet weights of the liver (containing blood) were assayed and that the liver was not flushed with blank blood or saline prior to storage. This finding confirmed that lidocaine does possess a high extraction ratio (>0.995) and this high value is totally attributed to metabolism.

Knowing the amount of lidocaine in liver (corrected for lidocaine in blood), one can easily calculate the steady state partition coefficient ($R_{L/B}$) (Table 15). This is done by dividing the amount of lidocaine per gm of liver tissue by the steady state effluent lidocaine blood concentration of the last steady state condition for the perfused rat liver preparation. A mean value of 132.7 ± 97.3 was obtained. This value is very high compared to the value reported by Benowitz *et al* (116). They reported a value of 0.61 for partition coefficient ($R_{L/p}$), the amount of lidocaine per gm liver to the effluent plasma concentration in the rhesus monkey. Even when a correction of the plasma concentration to blood concentration is made, this value is substantially less than the $R_{L/B}$ value in the rat liver preparations. A value of one is anticipated

for $R_{L/B}$ for lidocaine as α and λ are both unity for the binding to the perfusate medium. The experimental value is ($R_{L/B} = 132$) extremely high. A possible explanation for this high value is that the amount of lidocaine in the blood is underestimated by taking the volume of blood (1.5 ml) multiplied to the concentration of drug in the effluent. The liver may have stopped its eliminating activity when it is immersed in methanol so that the amount of drug that is actually in the blood is underestimated hence leading to an overestimation of the amount of lidocaine per gm of liver tissue.

3. Clearance of a Poorly Cleared Compound with Changes in Blood Flow

Previous studies had shown the effects of blood flow on the availability of a highly cleared compound as (lidocaine). Theoretical considerations have shown that poorly cleared compounds are poor discriminators for models of hepatic drug clearance with blood flow changes (Page 69). Theoretical analysis has also shown that the clearance for these poorly cleared compounds would approach the eliminating capacity, term A' of the system and hence be independent of hepatic blood flow (Pages 39 and 46). The clearance of a compound with low extraction ratio should be tested with changes in hepatic and blood flow if the model(s) holds true, then hepatic blood flow should exert no influence on the clearance of such a compound.

The influence of hepatic blood flow on the hepatic clearance of a

poorly cleared compound was investigated using antipyrine which is reported to have a low hepatic extraction ratio (135). Although the degree of plasma protein binding and blood cell partitioning of a poorly cleared compound influence its clearance, antipyrine is essentially unbound and evenly distributed in total body water (117), and hence the parameters α and λ do not affect its clearance.

Preliminary once-through perfusion studies confirmed that the extraction ratio of antipyrine is low with a value of 0.08. Indeed the difference between the influent and effluent drug concentration was so small that it lay within the sensitivity of the assay. To circumvent this problem, the recirculating perfusion method was used. In the system employed, a bolus of drug was added initially to the reservoir. As the influent blood passed through the liver, drug was being removed. The effluent blood, containing less drug than the influent blood (before the latter transited through the liver) returned to the reservoir. Thus the concentration of drug in the reservoir decreased with time due to removal of drug by the liver. This situation resembled a two-compartment model, where the liver was an eliminating compartment connected to the reservoir, a non-eliminating compartment (Page 19), the sampling compartment being the reservoir.

Under a constant flow rate of 10 ml/min to the liver, the concentration of antipyrine in the reservoir declined exponentially with

time (Figures 35 and 36). As predicted upon a change in blood flows, the clearance and hence the slope of the exponential decline of concentration with time (Figures 37 and 38). The various parameters for these four experiments are summarized in Table 16.

Figure 35. Exponential decay of the concentration of antipyrine in the reservoir with time under constant blood flow (10 mls/min) to the liver preparation in a recirculating experiment (Study 1).

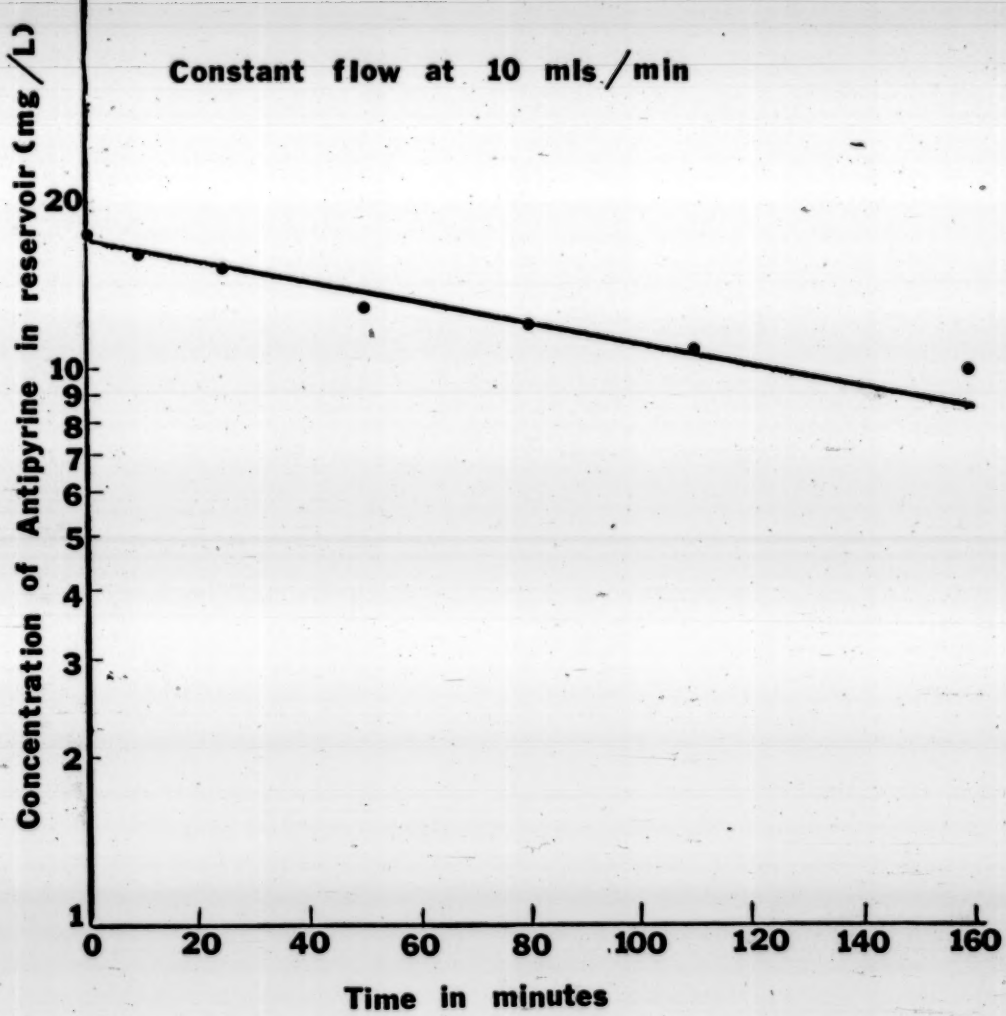


Figure 36. Exponential decay of the concentration of antiyprine in the reservoir with time under constant blood flow (10 ml/min) to the liver preparation in a recirculating experiment (Study 11).

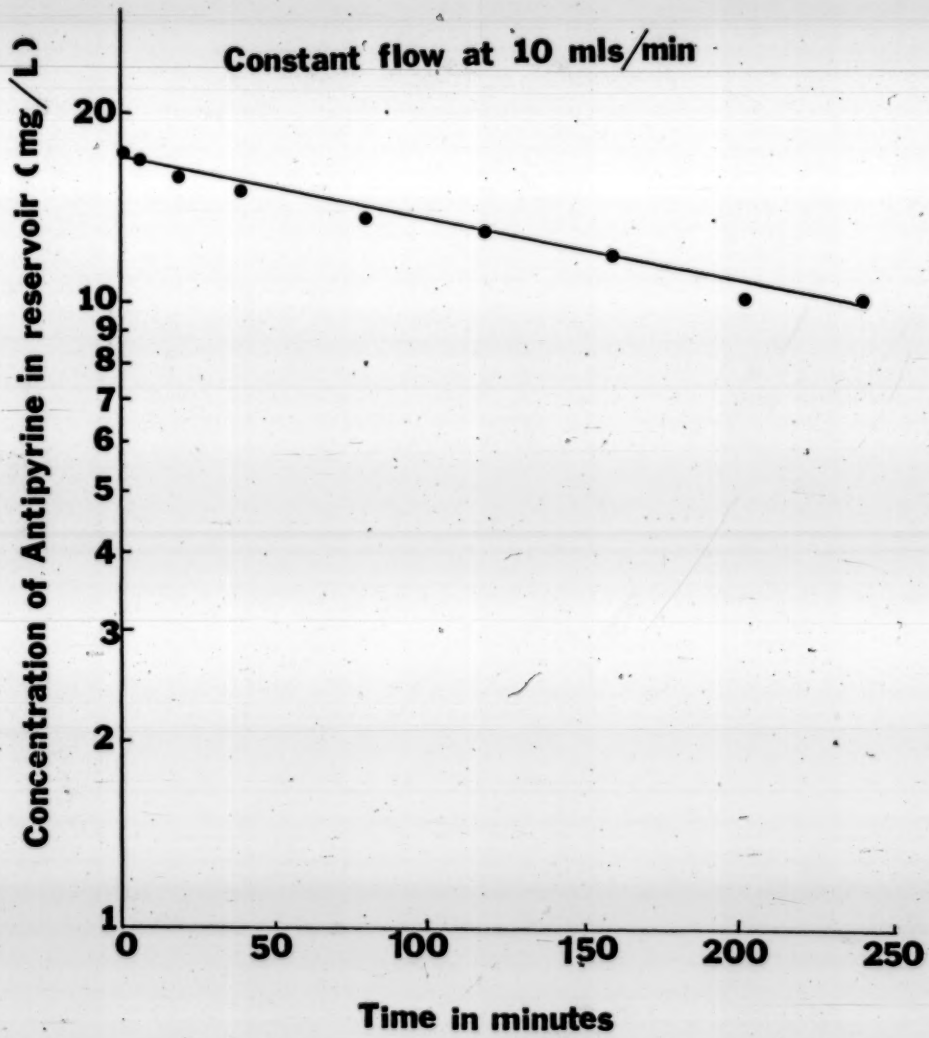


Figure 37. The lack of effect of changes in hepatic blood flow on the exponential decay of the concentration of antipyrine in the reservoir with time in a recirculating experiment (Study III).

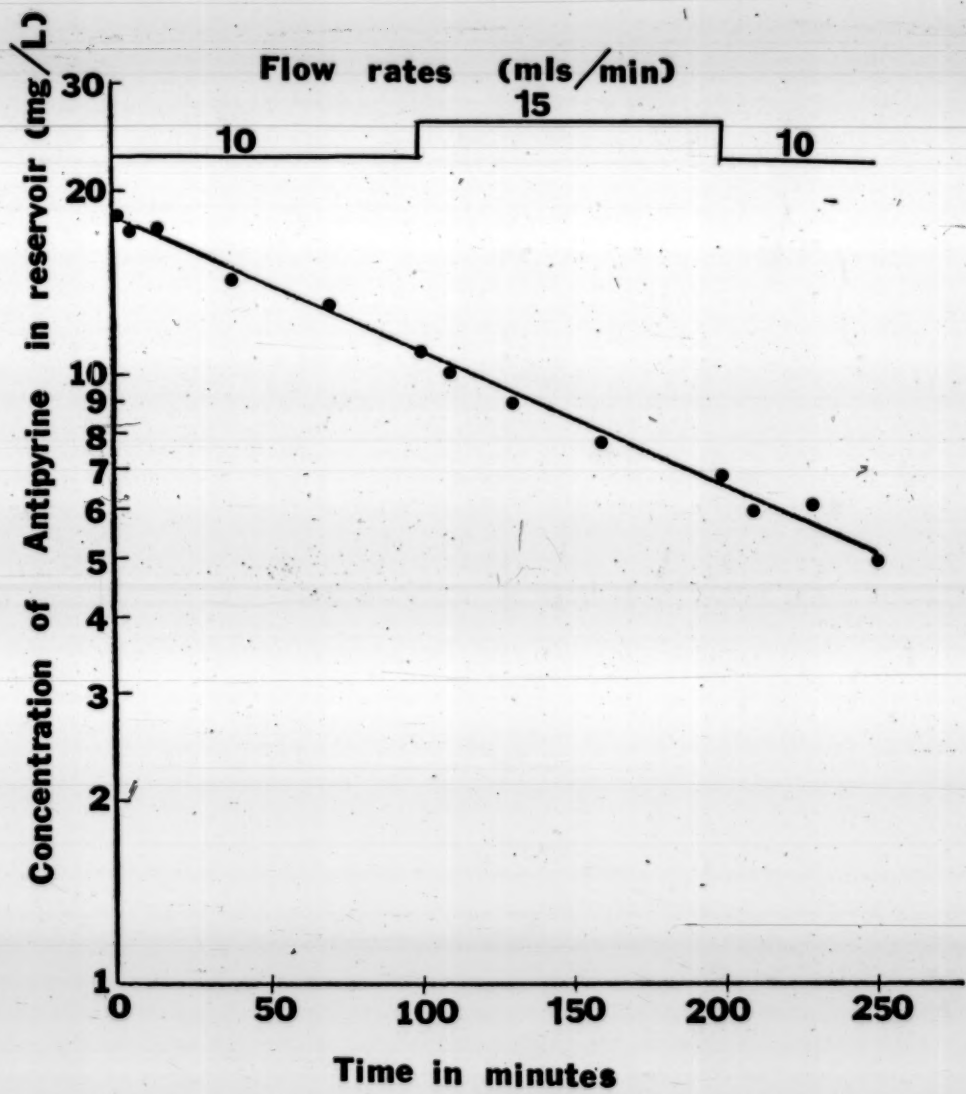


Figure 38. The lack of effect of changes in hepatic blood flow on the exponential decay of the concentration of antipyrine in the reservoir with time in a recirculating experiment (Study IV).

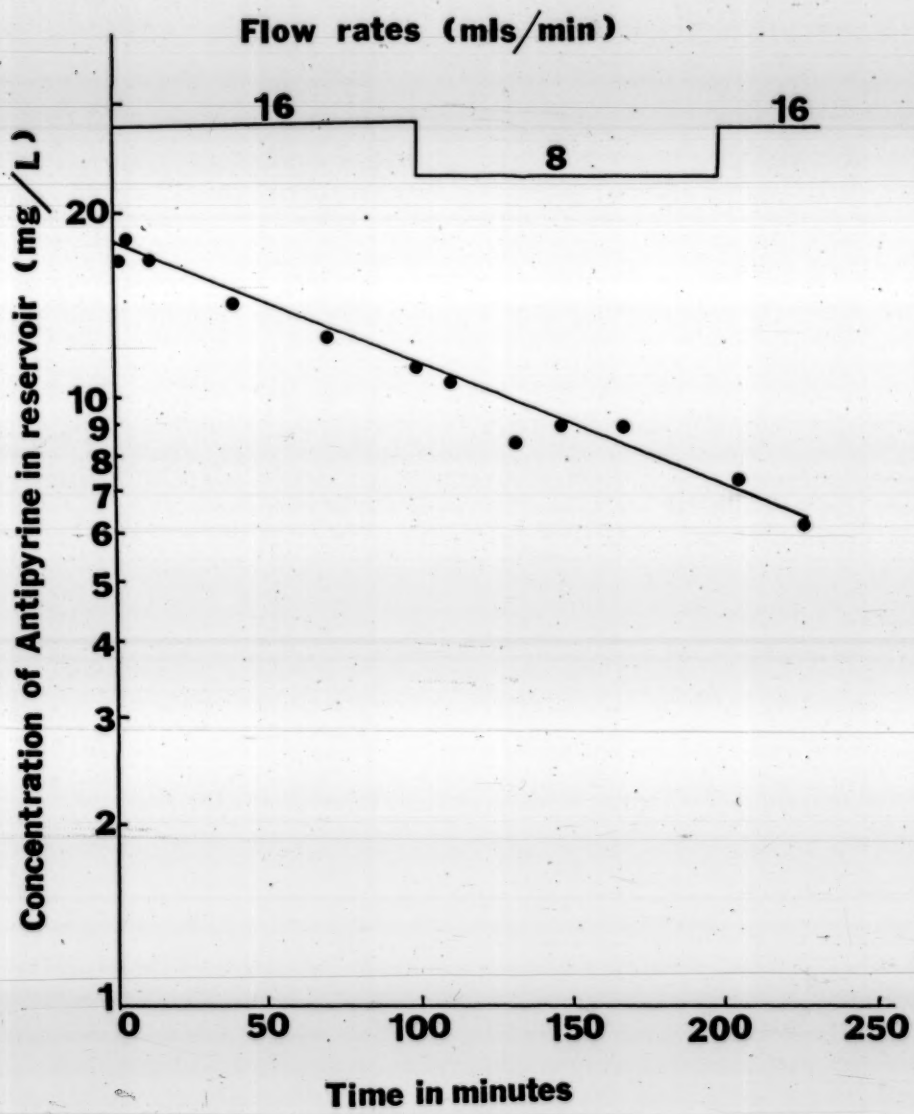


Table 16. Various Parameters Calculated for Antipyrine in Recirculating Experiments

Preparation Study Fig. #	Dose (mcg)	Volume of reservoir (mls)	Blood Flow (mls/min)	Half-life (min)	$\frac{C_p(0)}{C_p(t)}$ * (mg/L)	V_d^{**} (mls)	Clearance*** (mls/min)	Extraction Ratio	Effective Volume (mls)	$V_L \cdot R_L / B$
				$t_{1/2}$		\dot{V}_{cl}	ER			
I	35	2777	160	10	145	17.2	161.4	0.7714	0.9771	1.4
II	36	3190	180	10	280	16.5	193.3	0.4784	0.0478	13.3
III	37	2742	150	10	136	18.0	152.3	0.7761	0.078	2.3
					15				0.0571	
					10				0.078	
IV	38	2707	140	16	178	18.0	150.4	0.586	0.0366	10.4
					8				0.0732	
					16				0.0366	

* extrapolated concentration at zero time

$$** V_d = \frac{\text{Dose}}{C_p(0)}$$

$$*** \dot{V}_{cl} = \frac{0.693}{t_{1/2}}$$

$$**** ER = \frac{\dot{V}_{cl}}{V_B}$$

The volume of distribution (V_d) of antipyrine in the perfused rat liver in situ preparation is the total volume that antipyrine distributes in. This volume relates the concentration of drug at a certain time to the amount of drug in the reservoir at that instant. At time zero, the product of V_d and the concentration at zero time ($C_p(0)$) give the total amount (Dose) at zero time. The V_d is in fact the sum of all the volumes in the compartments. In the liver preparation, it is given by the sum of the volume of the reservoir (V_R) and the effective volume of the liver ($V_L \cdot R_{L/B}$) (14) where V_L is the volume of the liver and $R_{L/B}$ is the partition coefficient of the compound between the liver and effluent venous blood.

The effective volume of the liver is the volume of the liver that the drug (with concentration as sampled from the reservoir) appears to distribute in. When the value of V_L is given, one can easily calculate the partition coefficient of the drug into the liver and effluent venous blood. There is considerable variation in the effective liver volume in the preparation as seen in Table 16. A very likely explanation for this would be due to error in the measurement of the volume of the reservoir (V_R). This volume is given by the ml's of perfusate used in the experiment. It is very conceivable that some volume is lost before the blood circuit is completed in the recirculating experiment such that there is an over-estimation of the volume of perfusate used, leading to an underestimation of the effective volume of the liver. Furthermore $R_{L/B}$ should have a value of one since antipyrine distributes in total body water (117).

4. Discrimination Between Models I and II by Changing the Influent
Lidocaine Concentration Delivered at Constant Blood Flow to the
Liver When Operating Under Non-linear Conditions

To examine the possibility of capacity limiting the hepatic microsomal enzyme system, varying concentrations of lidocaine (3-84 mg/L) were delivered at a constant blood flow rate of 10 ml/min to the rat liver. The stepwise increase (or decrease) in influent concentration was carried out at 30 minutes intervals. During the last steady state period prior to the termination of the experiment the influent lidocaine concentration was returned to the original value (influent concentration of the first steady state period) to check for the viability of the preparation. Two studies were carried out in this manner (Table 17). In Study I, lidocaine influent concentration was increased stepwise from 3 to 36 mg/L and then returned to the original influent concentration at around 3.6 mg/L. In Study II, lidocaine influent concentration was decreased stepwise from 84 to 4 mg/L and returned to the influent concentration of the second steady state period. The reversal in order (stepwise influent concentration decrease) for Study II as compared to Study I (stepwise influent concentration increase) was to demonstrate that previous exposure of the liver to high concentrations did not give rise to a "wash out" effect when followed by perfusion with blank blood (containing no drug) or blood containing less drug.

Table 17. Effect of Influent Lidocaine Concentration on its Hepatic Extraction Under Constant Blood Flow (10 mls/min) - Studies I and II

Study #	Lidocaine concentration (mg/L)		Velocity of removal (mcg/min) $v = \dot{V}_B (C_I - C_O)$	Extraction Ratio
	Influent	Effluent		
I	2.9228	0.0043 \pm 0.0009	29.185	0.9985
	3.6357	0.0116 \pm 0.0010	36.241	0.9968
	8.4771	0.1629 \pm 0.0139	81.134	0.9808
	19.0355	2.8770 \pm 0.0466	161.585	0.8489
	36.3312	9.0172 \pm 1.5097	273.14	0.7518
	3.5976	0.2738 \pm 0.1125	33.238	0.9239
	84.255	20.38 \pm 0.7027	638.75	0.7581
II	38.625	9.3007 \pm 0.3867	293.243	0.8086
	19.1239	3.6608 \pm 0.3867	154.631	0.8086
	9.1121	1.4217 \pm 0.2733	76.904	0.8440
	4.4279	0.2122 \pm 0.0566	42.157	0.9521
	39.904	7.3751 \pm 0.9412	325.289	0.8152

$n = 4 \pm$ S.D.

These two studies demonstrated saturation kinetics for lidocaine with decreasing extraction ratio on increasing the influent concentration. The data is presented in a linearized form as in Equation 11 for Model I and Equation 26 for Model II. Regression analyses of $\text{Co}/(\text{Cl}-\text{Co})$ versus Co for Model I and $\ln(\text{Co}/\text{Cl})$ versus $(\text{Cl}-\text{Co})$ for Model II were performed. No attempt to show the plots was made because of scaling difficulties. Line fitting was performed by the least square method. The assumption used in the linearized transformations to arrive at values of V_{max} and K_m was that the system behaved as a one enzyme system.

The data was also fitted by NONLIN (136) for Model I (Studies I and II) as in Equation 10 (the velocity of removal (v) against the effluent lidocaine concentration (Co)) and for Model II as in Equation 26 (velocity of removal (v) against $\ln(\text{Co}/\text{Cl})$). The underlying assumption was only a one-enzyme existed for lidocaine metabolism.

The results of the regression analyses on the linear transformations and curve fitting by NONLIN for Models I and II were summarized in Table 18.

Table 18. Regression Analyses and Curve Fitting by NONLIN Performed
on Studies I and II for Models I and II

Regression analyses of linearized transformations (n = 6)

Study #	Model fitted	Vmax (mcg/min)	Km (mg/L)	A'* (mls/min)	r**
I	I	285.78	0.8705	328.3	0.9633
II	I	961.54	14.3365	67.07	0.7731
I	II	330.2	6.196	53.38	0.7522
II	II	1295.3	56.32	22.998	0.6416

NONLIN Curve Fitting (n = 6)

Study #	Model fitted	Vmax (mcg/min)	Km (mg/L)	A'* (mls/min)	R ²⁺	Cor ⁺⁺	S ⁺⁺⁺
I	I	398.6	4.65	85.72	0.939	0.984	6.255
II	I	838.1	13.0	64.45	0.966	0.965	3.973
I	II	120.95	1.48	81.72	0.662	0.752	7.387
II	II	406.5	12.44	32.68	0.683	0.642	10.85

* calculated by Vmax/Km

** correlation coefficient

$$+ R^2 = \frac{\sum \text{observed}^2 - \sum \text{dev}^2}{\sum \text{observed}^2}$$

++ cor = correlation between observed and predicted results

+++S = s^2 (sum of square deviations)

From linear regression analyses of the data from the two studies, very poor correlation was obtained for Model II whereas an improved correlation was obtained for Model I as indicated by the correlation coefficient, r ($r = 0.9633, 0.7331$ for Model I and 0.7522 and 0.6416 for Model II). This meant that when the observed data was transformed and plotted according to Models I and II in a linearized form, the transformed data fitted to a straight line better for Model I than for Model II.

For the NONLIN curve fitting procedure, the same function (velocity of removal) as the y variable was fitted against the effluent drug concentration (C_0) for Model I and $\ln(C_0/C_1)$ for Model II. In the first instance, a curve similar to a plot of the velocity versus substrate concentration was obtained (C_0 reflects the substrate concentration C_L according to Model I). In the second instance, a straight line was obtained as predicted by Equation 26 for Model II.

The sum of square deviations (S) is less for Model I than in Model II for the two studies. The correlation between observed and predicted results (cor) was extremely good for Model I and poor for Model II. Also the parameter (R^2) which is the ratio of the sum of squares due to regression to the total sum of squares indicated a good fit for Model I and a poor one for Model II. In the non-linear case, this parameter (R^2) is analogous to the multiple correlation coefficient in the linear regression case, the latter being an indicator of how close the regression plane fits the data (136).

The two fitting procedures all pointed towards poor correlation for Model II and a much improved correlation for Model I under non-linear conditions (high concentration at the enzyme site $>K_m$).

Different A' values were obtained for the different fitting procedures for the two studies fitted to the two models. A large discrepancy existed between the values of A' (calculated from V_{max} and K_m) from the two studies fitted to the models using different fitting procedures. The manner in which the properties of the generated statistics differ for the straight line curve fitting procedure and the NONLIN curve fitting procedure is unknown. However one common observation was made. The values of A' are lower than the anticipated values for Models I and II (predicted values of A' for lidocaine with ER 0.995 at a blood flow of 10 mls/min/liver are 1990 and 52.98 mls/min for Models I and II respectively). This observation led to the suspicion that one or a combination of the following was occurring.

- (1) The liver preparation was deteriorating. In Study I, the extraction of lidocaine during the last period of perfusion did not return to the original extraction (higher extraction) of lidocaine. In this case, the K_m will not be affected whereas the V_{max} would decrease as the functional liver mass decreases. This may lead to a smaller A' .

(2) The high concentration of lidocaine is toxic to liver tissues.

In this case, once again, the functional liver mass is decreased due to high concentrations of lidocaine which is toxic to the liver tissues, and this would effectively reduce V_{max} whereas the K_m would not be affected.

(3) The kinetics of lidocaine is not a simple one enzyme system nor a multiple system with very close V_{max} 's and K_m 's (the individual V_{max} and K_m are not significantly different from the mean V_{max} and K_m). For multiple enzyme systems with widely different V_{max} 's and K_m 's under conditions where the concentration at the liver is high, some metabolic pathways may become capacity limited while the others may still operate linearly (137). In this case, it is hard to dissect the influence of one metabolic pathway on another and obtain discrete values for V_{max} and K_m .

(4) There is end product inhibition. At high lidocaine influent concentrations, high concentrations of metabolite(s) are generated, and these may competitively or non-competitively inhibit lidocaine metabolism. In the case where the inhibition is competitive (can be overcome by substrate), the K_m is not affected while the V_{max} is decreased to $V_{max}/(1 + \frac{[I]}{K_I})$ where $[I]$ is the concentration of the inhibitor and K_I is the

~~dissociation~~ dissociation constant for the enzyme-inhibitor complex. In the case where the inhibition is non-competitive (cannot be overcome by substrate), the V_{max} is not affected whereas the K_m estimated is given by $K_m (1 + \frac{I}{K_I})$ (138).

It is probable that for the lidocaine experiments at high influent concentrations to the liver, some degree of inhibition does occur, plus there is saturation of the enzyme sites by the substrate lidocaine. The preparation itself may deteriorate with time, and all these lead to a much lower estimate of the parameters V_{max} and K_m and hence the term A' compared to the values predicted by the models.

Indeed in the two studies, concentration of MEGX was as high as 30 mg/L. The MEGX appearing in the perfusate ranged from 0.25-30 mg/L and constituted 0.08-55% of the influent lidocaine concentration (3-84 mg/L). The percent of MEGX generated from lidocaine is actually higher as MEGX is further metabolized. It was also found that the higher the concentration of lidocaine used, the higher the concentration of MEGX in the perfusate. This increased percentage of effluent MEGX may be due to:

- (1) Saturation of a metabolic pathway other than MEGX at high lidocaine doses such that the percentage of lidocaine metabolized to MEGX is increased.

(2) The metabolism of the generated MEGX is inhibited by high concentration of lidocaine.

(3) The MEGX metabolic pathway is capacity limited by the high concentration of MEGX generated with high concentrations of lidocaine.

Table 19. Generation of MEGX with High Concentration of Lidocaine
Studies I and II

Study #	Influent Lidocaine concentration (mg/L)	Effluent concentration of MEGX (mg/L)	Fraction of MEGX in effluent in terms of influent lidocaine*
	(C _I Lidocaine)	(C _{MEGX})	
I	2.9228	not detectable	-
	3.6357	0.2545 ± 0.0284	0.0795
	8.4771	1.3369 ± 0.0810	0.1791
	19.0355	6.5024 ± 0.2149	0.3879
	36.3312	12.1943 ± 0.2962	0.3812
	3.5976	0.9589 ± 0.2130	0.3027
II	84.255	29.6437 ± 1.0785	0.3996
	38.625	14.7645 ± 2.0518	0.4342
	19.1239	9.2279 ± 1.3512	0.5480
	9.1121	3.9699 ± 0.3835	0.4948
	4.4279	0.7947 ± 0.1663	0.2038
	39.904	13.3937 ± 1.7147	0.3812

n = 4 ± S.D.

* corrected for molecular weight

The presence of a high concentration of metabolite is known to inhibit the metabolism of the parent compound in some instances (139,140). The possibility of end product inhibition was explored. Three studies were conducted using a low influent concentration of lidocaine (below the K_m of the system) delivered at a constant blood flow of 10 ml/s/min to the liver. The MEGX concentration appearing in the effluent from the low influent lidocaine concentration should be a negligible though detectable quantity. Varying influent concentrations (0-13 mg/L) of MEGX were added in a stepwise manner at 25 minute intervals to the perfusate. The results are tabulated in Table 20.

In all instances, there was some evidence of inhibition of lidocaine metabolism by MEGX although the results were highly variable. In two studies (Studies I and II), the inhibition is very marked and was almost complete at high influent MEGX concentrations (11 mg/L) while in the third study (Study III) the degree of inhibition was slight despite the presence of a high influent concentration of MEGX (13 mg/L). As can be seen from the previous two studies (Page 161, Table 17) where high lidocaine concentrations (3-84 mg/L) were delivered to the liver, the lowest extraction ratio observed was 0.75 (Table 17) while high effluent concentrations MEGX (12-14 mg/L) were generated. It should be borne in mind that this effluent MEGX concentration represents the minimum concentration at the enzymatic site, since the MEGX formed is further metabolized within the liver. Thus it is unlikely that MEGX at influent concentration below 11 mg/L (the MEGX concentration at the enzyme site

is lower than than the influent MEGX concentration as the compound has to reach the enzyme site from the perfusate) can totally inhibit the metabolism of lidocaine. However further studies are needed to substantiate the above finding.

Table 20. Inhibition of Metabolism of Lidocaine by MEGX - Studies I, II and III

Study #	Influent concentration (mg/L)		Effluent concentration (mg/L)		ER, Lidocaine	
	Lidocaine	MEGX	Lidocaine	MEGX		
I	2.9937	0	0.0055 ± 0.0013	0.0272 ± 0.0025	0.9982	
	2.9937	0.7573	0.0282 ± 0.0091	0.1066 ± 0.0152	0.9906	
	2.9937	2.4237	0.1142 ± 0.0254	0.6293 ± 0.0582	0.9619	
	2.9937	5.3427	0.6593 ± 0.0273	2.0582 ± 0.0772	0.7798	
	2.9937	11.2906	2.7140 ± 0.1116	6.6486 ± 0.4502	0.0934	
	2.9937	0	0.0061 ± .0011	0.0726 ± 0.0328	0.9980	
II	3.41	0	0.0318 ± 0.0120	0.0713 ± 0.0123	0.9907	
	3.41	0.6843	0.1037 ± 0.0102	0.1908 ± 0.098	0.9696	
	3.41	2.4147	0.3729 ± 0.0738	0.9279 ± 0.1038	0.8906	
	3.41	5.4878	0.9266 ± 0.1012	2.4249 ± 0.1909	0.7283	
	3.41	11.2361	2.8868 ± 0.397	5.7186 ± 0.5515	0.1534	
	3.41	0	0.1338 ± 0.0285	0.2007 ± 0.0346	0.9608	
III	3.2751	0	0.0044 ± 0.0003	0.1654 ± 0.0222	0.9987	
	3.2751	6.436	0.0214 ± 0.0045	3.7255 ± 0.2017	0.9935	
	3.2751	12.0170	0.0398 ± 0.0038	6.1180 ± 0.7017	0.9878	
	3.2751	12.176	0.0738 ± 0.0154	9.5000 ± 2.1436	0.9775	
	3.2751	13.362	0.0741 ± 0.0033	13.148 ± 0.8916	0.9774	
	3.2751	0	0.0029 ± 0.0038	0.1840 ± 0.1368	0.9991	

n = 4 ± S.D.

n = 4 ± S.D.

5. Further Discrimination between Models I and II by the Formation of the Metabolite (MEGX) from the Parent Compound (Lidocaine) with Flow Changes under Linear Conditions

Before any attempt to correlate the generation of MEGX from lidocaine with flow changes was made, the behaviour of MEGX itself was explored.

a. Linearity of MEGX Extraction Under Constant Blood Flow

The results of six preparations where changing concentrations of MEGX were delivered at constant blood flow of 10 ml/min are tabulated in Appendix X. Steady state conditions were observed within 15 minutes or less (first point of sampling). The extraction ratio of MEGX varied between 0.32-0.91 from high to low concentrations (20.9-0.46 mg/L) in different liver preparations. From experiments III, IV and V, it is estimated that the system is linear when the influent concentration of MEGX is below 1.5 mg/L. To ensure linearity, all subsequent experiments designed to be operating linearly were operated at an influent MEGX concentration of 0.5 mg/L.

b. Effect of Flow Changes on the Extraction of MEGX Under Linear Kinetic Conditions

The behaviour of the extraction ratio with respect to flow changes under linear kinetic conditions (0.5 mg/L) was investigated by the method used previously for lidocaine (Page 142). The control flow rate was taken

as 10 ml/s/min and increases to 12, 14 or 16 ml/s/min were chosen randomly. The results of these experiments are tabulated in Appendix XI.

The observed changes in the effluent concentration of MEGX and the extraction ratio were not in full agreement with the predicted changes for the two models. For two studies (Studies III and IV), the extraction of MEGX with increasing blood flow was reduced as anticipated. For the remainder four studies, there was complete reversal. The extraction ratio was observed to increase with increasing blood flow. The observed and predicted data (calculation same as lidocaine Page 142) for the effluent MEGX concentration were compared as shown in Figures 39 and 40 for Models I and II. The predicted values were much higher than the observed data for both models. The data were fitted to a straight line for each model individually and the slopes of the lines were compared to the line with slope = 1 which represents the best correlation between observed and predicted data (same method as lidocaine (Page 147)). The generated statistics are tabulated in Table 21.

Figure 39. A plot of the predicted and observed effluent MEGX concentrations with blood flow changes at constant low influent MEGX concentrations for Model I.

The line with slope = 1 represents the best correlation between observed and predicted data. The observed and predicted data for effluent MEGX concentrations for the six experiments are given in Appendix XI-A-B.

Model I

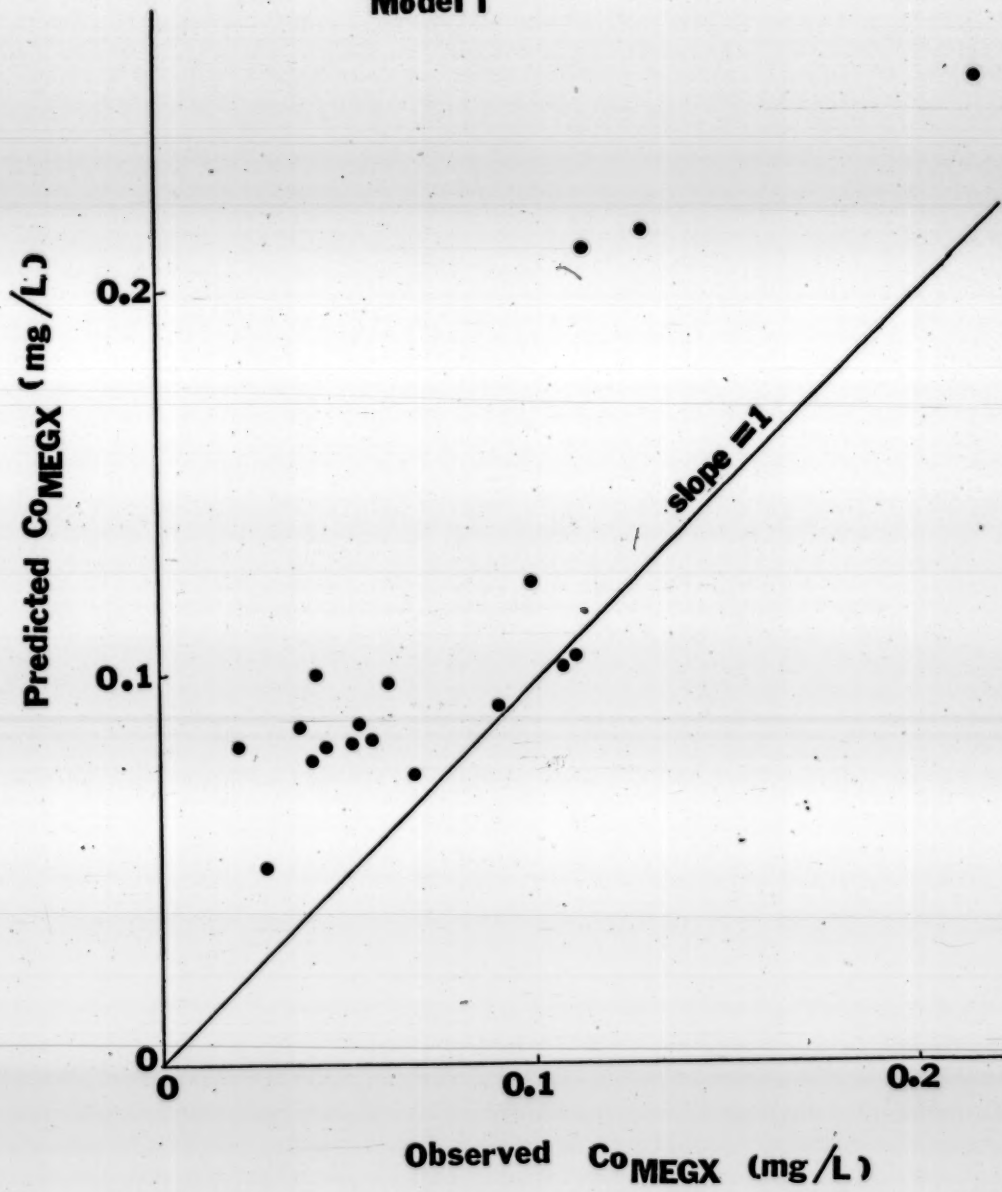


Figure 40. A plot of the predicted versus observed effluent MEGX concentrations with blood flow changes at constant low influent MEGX concentrations for Model II.

The line with slope = 1 represents the best correlation between observed and predicted data for MEGX effluent concentrations for the six experiments are given in Appendix XI-A-B.

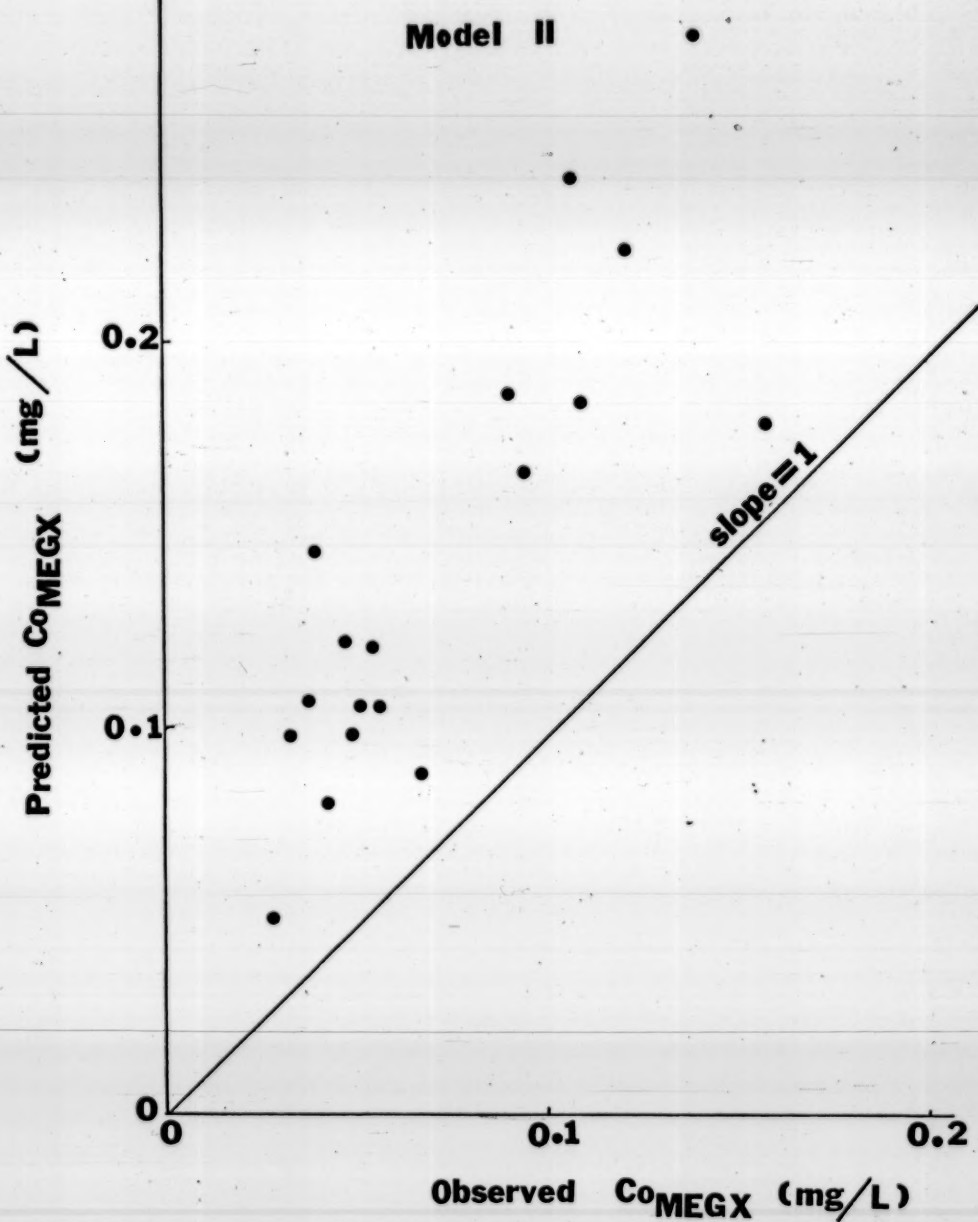


Table 21. Statistical Parameters from Regression Analyses and the
 Comparison of Slopes on the Predicted and Observed
 Effluent MEGX Concentrations for Models I and II.

Regression Analyses on Predicted and Observed Effluent MEGX Concentration

Statistical Parameter	Model I	Model II
n	18	18
(Observed data) \bar{X}	0.69633	0.69633
s_x^2	0.0011862	0.0011862
(Predicted data) \bar{Y}	0.1056944	0.13894
s_y^2	0.0024249	0.0031862
slope m	0.5722852	0.52932
Intercept b	0.009146	0.0039129
Correlation coefficient r	0.8182	0.86747

Comparison of Slopes

n	18	18
$s_{y \cdot x}^2$	0.002164	0.002093
$s_{y \cdot x \cdot p}^2$	0.001082	0.001046
t	1.3058	1.4611
(df)	32	32
Confidence level	95%	95%
	significant	significant

The t statistic with 32 degrees of freedom is seen to be statistically significant at 95% confidence level for both models. The reason why Model I failed to predict MEGX clearance while it adequately predicted lidocaine clearance is unknown. One may speculate this poor correlation between observed and predicted data may be due to changes in biliary excretion with blood flow changes. However preliminary data indicated that MEGX was eliminated only to a very small degree into the bile, and hence this cannot be used to explain the poor prediction of Model I for MEGX. No explanation can be afforded at this point and further investigation is needed. Model II failed to predict MEGX clearance as well as lidocaine clearance and was within anticipations.

c. Generation of MEGX from Lidocaine at a Constant Low Concentration of Lidocaine to the Liver with Changes in Blood Flow

An attempt was made to correlate the appearance of the metabolite generated at constant influent concentration of the parent compound with changes in blood flow for Models I and II. The MEGX concentration in the perfusate was assayed in the nine experiments where lidocaine at low concentrations were delivered at different flow rates to the liver (Page 144 and Appendix IX-A-B-C). The results for MEGX from these nine experiments were tabulated in Appendix XIII-A-B-C. Predictions of the metabolite appearing in the effluent with a constant influent concentration of the parent compound delivered at various

flow rates were calculated for Models I and II. Predictions for Model I were calculated as follows:

It is assumed that the fraction (f) of lidocaine metabolized to MEGX is constant when operating under linear kinetic conditions and that Model I can adequately describe the clearance of MEGX.

Now the rate of elimination of lidocaine is given by:

$$\dot{V}_B \cdot (C_{I_p} - C_{O_p}) = A'_{I_p} \cdot C_{O_p} \quad \text{Equation 51}$$

Assuming the kinetics of MEGX are also linear, its metabolism at the site of formation is independent of its concentration at the site so that

$$\dot{V}_B \cdot C_{O_M} = f \cdot \dot{V}_B \cdot (C_{I_p} - C_{O_p}) - A'_{I_M} \cdot C_{O_M} \quad \text{Equation 52}$$

rate of appearance of MEGX in effluent blood	rate of formation of MEGX from lidocaine	rate of elimination of MEGX
--	--	--------------------------------

where subscripts P and M represent the parent compound lidocaine

and the metabolite MEGX and A' is given by $\sum_{i=1}^n \frac{V_{max,i}}{K_m,i}$ under linear conditions.

Equation 52 can be transformed into

$$\frac{\dot{V}_B}{C_{oM}} = \frac{A'_M}{f \cdot (C_{l_p} - C_{o_p} - C_{oM}/f)} \quad \text{Equation 53}$$

An assessment of f can be done in the following manner. The extraction ratio of MEGX under linear conditions was found to be 0.9 when MEGX was given alone (Appendix X). The MEGX generated from lidocaine metabolism was further eliminated before its appearance in the effluent perfusate. Thus what appeared is only 0.1 times what was formed from lidocaine. On this basis the MEGX generated from lidocaine (Appendix XII) under linear kinetic conditions is estimated to be approximately 30-40%. The assumption used is that lidocaine does not interfere with the metabolism of MEGX and vice versa.

A direct assessment of the value of f can be made as shown in Equation 54 when the effluent concentrations of lidocaine and MEGX at two different known flow rates (1 and 2) are known. The viability of the preparation is again assumed to be constant.

$$\frac{\dot{V}_{B1} / \dot{V}_{B2}}{C_{oM1} / C_{oM2}} = \frac{(C_{l_p} - C_{o_p2} - C_{oM2}/f)}{(C_{l_p} - C_{o_p1} - C_{oM1}/f)} \quad \text{Equation 54}$$

Subscripts 1 and 2 denote conditions at flow rates 1 and 2.

Since the effluent concentration of lidocaine (C_{Op}) and MEGX (C_{OM}) are very small, and f is a substantial term, C_{Op} and C_{OM}/f should be negligible compared to the constant influent lidocaine concentration (C_I) then $\frac{A'_M}{f(C_I - C_{Op} - C_{OM}/f)}$ is essentially a constant.

$$\text{Thus } \frac{\dot{V}_{B_1}}{C_{OM_1}} = \frac{\dot{V}_{B_2}}{C_{OM_2}} \quad \text{Equation 55}$$

The effluent concentration of the metabolite therefore increases with increasing blood flow for Model I. The prediction for the effluent MEGX concentration for Model I are tabulated in Appendix XII-A-B-C.

Under linear kinetic conditions, where A' is essentially constant predictions for Model II were made as follows:

$$(A' = \sum_{i=1}^n \frac{V_{max,i}}{K_m,i}) \text{. Then at any point } x \text{ along the tube, the rate of}$$

change of lidocaine concentration at point x (similar to Equation 21) is given by:

$$\frac{dC_{Op}}{dx} = - \frac{C_{Op} A'_{t,P}}{\dot{V}_{B_1} t \cdot L} \quad \text{Equation 56}$$

where subscript t represents the tube, and subscript P represents lidocaine and L represents the length of the tube. The same assumptions that the fraction of lidocaine metabolized to MEGX is constant when operating under linear kinetic conditions and that Model II adequately describes the clearance of MEGX are again made. The rate of change of MEGX concentration at point x is now given by the difference of its formation and elimination:

$$\frac{dC_{x,M}}{dx} = \frac{(f \cdot A'_{t,P} \cdot C_{x,P} - A'_{t,P} \cdot C_{x,M})}{V_{B,t} \cdot L} \quad \text{Equation 57}$$

where subscript M denotes the metabolite MEGX.

Taking Laplace transforms of Equation 56

$$\bar{C}_{x,P} = \frac{C_{i,P}}{\left(s + \frac{A'_{t,P}}{V_{B,t} \cdot L} \right)} \quad \text{Equation 58}$$

and then substitution of Equation 58 into the Laplace transform of Equation 57

$$\bar{C}_{x,M} = \frac{f \cdot C_{i,P} \cdot A'_{t,P}}{V_{B,t} \cdot L \cdot \left(s + \frac{A'_{t,P}}{V_{B,t} \cdot L} \right) \left(s + \frac{A'_{t,M}}{V_{B,t} \cdot L} \right)} \quad \text{Equation 59}$$

The anti-Laplace transform of the concentration of MEGX at point x along the tube is given by:

$$C_{xM} = \frac{f \cdot Cl_P \cdot A'_{t,P}}{A'_{t,M} - A'_{t,P}} \left(e^{-\left(\frac{A'_{t,P}}{V_{B,t}} \cdot \frac{x}{L} \right)} - e^{-\left(\frac{A'_{t,M}}{V_{B,t}} \cdot \frac{x}{L} \right)} \right) \quad) \text{ Equation 60}$$

$$= \frac{f \cdot A'_{t,P} \cdot Cl_P \cdot e^{-\left(\frac{A'_{t,P}}{V_{B,t}} \cdot \frac{x}{L} \right)}}{\left(A'_{t,M} - A'_{t,P} \right)} \left[1 - e^{-\left(\frac{\left(A'_{t,P} - A'_{t,M} \right)}{V_{B,t}} \cdot \frac{x}{L} \right)} \right] \quad]$$

Equation 60

When $x=L$ and integrating all the tubes, the effluent MEGX concentration (C_{oM}) is given by:

$$C_{oM} = \frac{f A'_{t,P} Cl_P \cdot e^{-\left(\frac{A'_{t,P}}{V_B} \right)}}{\left(A'_{t,M} - A'_{t,P} \right)} \left(1 - e^{-\left(\frac{\left(A'_{t,P} - A'_{t,M} \right)}{V_B} \right)} \right) \quad) \text{ Equation 61}$$

$$= \frac{f A'_{t,P} C_{oP}}{\left(A'_{t,M} - A'_{t,P} \right)} \left(1 - e^{-\left(\frac{\left(A'_{t,P} - A'_{t,M} \right)}{V_B} \right)} \right) \quad) \text{ Equation 61}$$

When the eliminating capacity of the metabolite ($A'_{t,M}$) greatly exceeds the eliminating capacity of the parent compound ($A'_{t,P}$) (the rate limiting step is the formation of the metabolite from

the parent compound) the term in the exponent becomes a negative number. In such cases, the value of one minus the exponential term becomes a constant and is not much affected by changes in blood flow. Also the greater the difference between A'_M and A'_P the less influence is the flow term in the exponential. On this basis, a prediction of the effluent metabolite concentration at different flow rates can be made as follows:

$$\frac{C_{O_M 1}}{C_{O_M 2}} = \frac{C_{O_P 1}}{C_{O_P 2}} \quad \text{Equation 62}$$

where the subscripts 1 and 2 denote conditions at flow rates 1 and 2.

In the case for MEGX (ER is 0.9), A'_M is 23 mls/min at a blood flow of 10 mls/min and this value is much less than the eliminating capacity for lidocaine (ER 0.999, A'_P is 69 mls/min at blood flow of 10 mls/min). Thus the above method cannot be applied to predict the effluent metabolite concentration at different flow rates. Instead the following method is used.

A rearrangement of Equation 61 and substitution of $g = A'_M - A'_P$ and $k = f \cdot A'_P$ give the simplified equation

$$\frac{C_{oM}}{C_{oP}} = \frac{k}{g} \left(1 - e^{-\frac{g}{V_B}} \right) \quad \text{Equation 63}$$

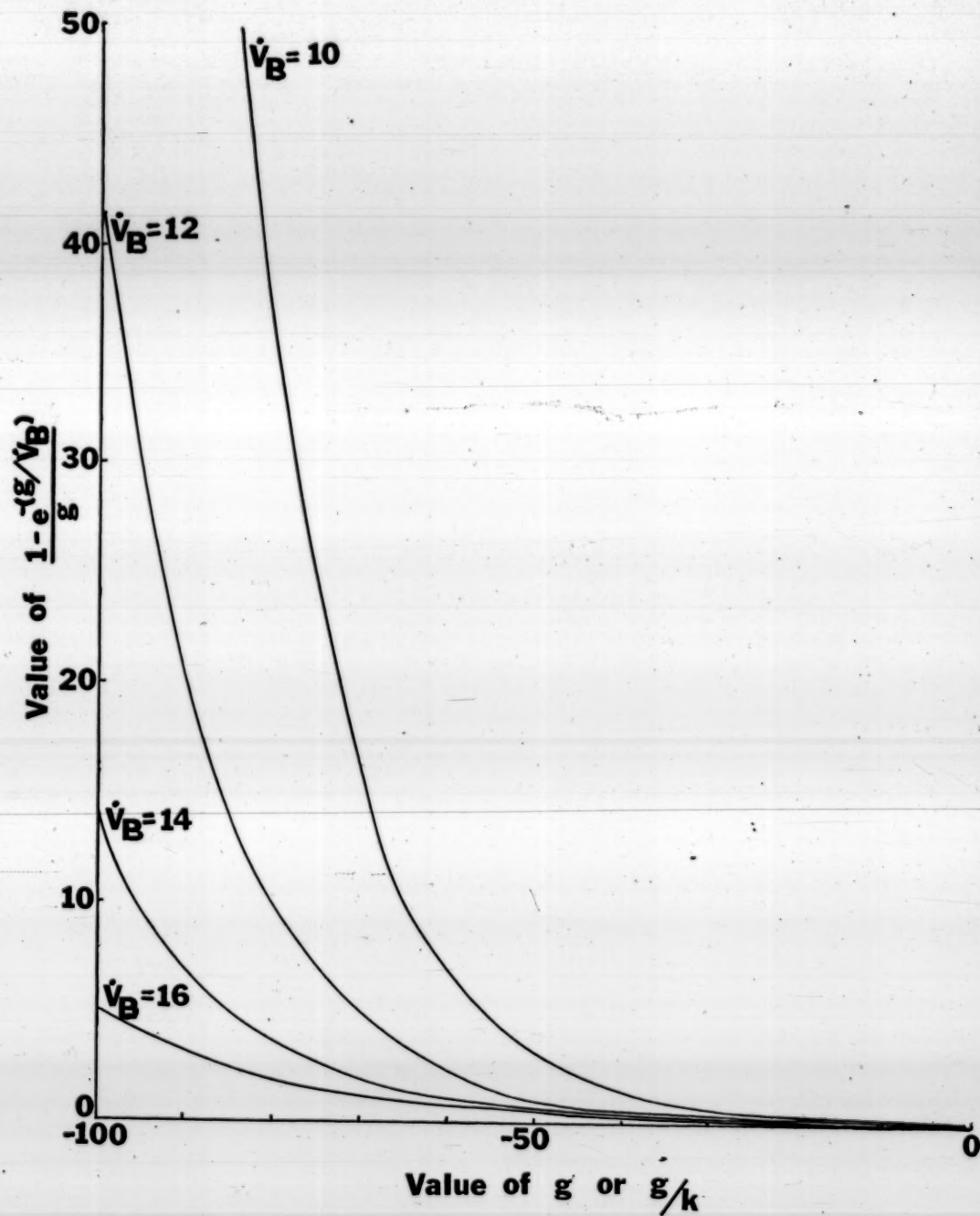
Using different values of g to give values of $(1 - e^{-(g/V_B)})/g$ at one flow rate, and at different flow values, a series of graphs is constructed. (Figure 41). If the ratio (C_{oM}/C_{oP}) the effluent concentrations of the metabolite and the parent compound is known and this value is equal to $\frac{k}{g} (1 - e^{-\frac{g}{V_B}})$, (Equation 63), the

value of g or g/k can be ascertained by the intersection of this value (on the y axis) and the curve at that flow rate. A prediction of the $\frac{C_{oM}}{C_{oP}}$ at a different flow rate can be made in the same manner.

Knowing the ratio at one flow rate, the intersection of this value (on the y axis) and the curve at that flow will give the value of g or g/k on the x axis. Using this newly found value of g or g/k , the intersection of this and the curve for the next flow rate will give the ratio of (C_{oM}/C_{oP}) at that particular flow rate (value given on the y axis). This method predicts the ratio of the effluent concentrations of the metabolite and the parent compound instead of predicting the effluent concentration of the metabolite alone. The reason why this is adopted is that no other solution is found. The predicted and observed ratio of the effluent concentrations for MEGX and lidocaine for Model II are tabulated in Appendix XII A-B-C.

UNI

Figure 41. A plot of $(1-e^{-\frac{g}{V_B}})/g$ against g for blood flows at 10, 12, 14 and 16 mls/min. The numbers next to the curves indicate the plot at that particular flow rate.



The predicted and observed results for Model I (effluent MEGX concentration) and Model II (ratio of effluent MEGX and lidocaine concentrations) were plotted individually and the correlation of the observed and predicted data was shown in Figures 42 and 43 for Models I and II respectively.

The data were fitted to a straight line for each model and the slope of the line was compared to the line with slope = 1 (perfect correlation). The statistics generated are tabulated in Table 22.

Table 22. Statistical Parameters from Regression Analyses and the Comparison of Slopes on the Predicted and Observed Data for Model I (Effluent MEGX Concentration) and Model II (Ratio of the Effluent MEGX and Lidocaine Concentrations).

Regression Analyses on Predicted and Observed Data for Models I and II

Statistical Parameter		Model I	Model II
n		25	25
(Observed data)	\bar{X}	0.1556	12.57
	s_x^2	0.006242	93.528
(Predicted data)	\bar{Y}	0.2195	19.929
	s_y^2	0.063932	1305.7
slope	m	1.401679	1.81896
Intercept	b	0.0299	5.4634
correlation coefficient r		0.765	0.4886

Cont'd Table 22

Comparison of Slopes from the Predicted Versus Observed Data Plots for Models I and II to the Line with Slope of One.

Statistical Parameter	Model I	Model II
n	25	25
$s^2_{y,x}$	0.021264	1039.6
$s^2_{y,x,p}$	0.010632	519.8
t	1.0662	1.203
(df)	46	46
Confidence level	95%	95%
	not significant	not significant

The t statistic for Models I and II are 1.0662 and 1.203 respectively with 46 degrees of freedom. These values of t are not significant for Models I and II at 95% confidence interval. Thus the slopes of the fitted lines equal one at 95% confidence interval.

The intercept of the line for Model II is -5.4634 and deviates much from the intercept of zero for the line with slope = 1 (best correlation). If the fitted straight line for Model II is forced through zero, a slope which is significantly different from one is suspected. Furthermore the correlation between predicted and observed data is very poor. Contrastingly, the intercept of the line for Model I is -0.0299 and does not deviate much from the intercept

Figure 42. Predicted MEGX effluent concentrations versus the observed data for Model I for the same nine experiments performed with low influent lidocaine concentration with alterations in blood flow. The line with slope = 1 represents a perfect correlation. The results are tabulated in Appendix ~~XIIA-B-C~~

Model 1

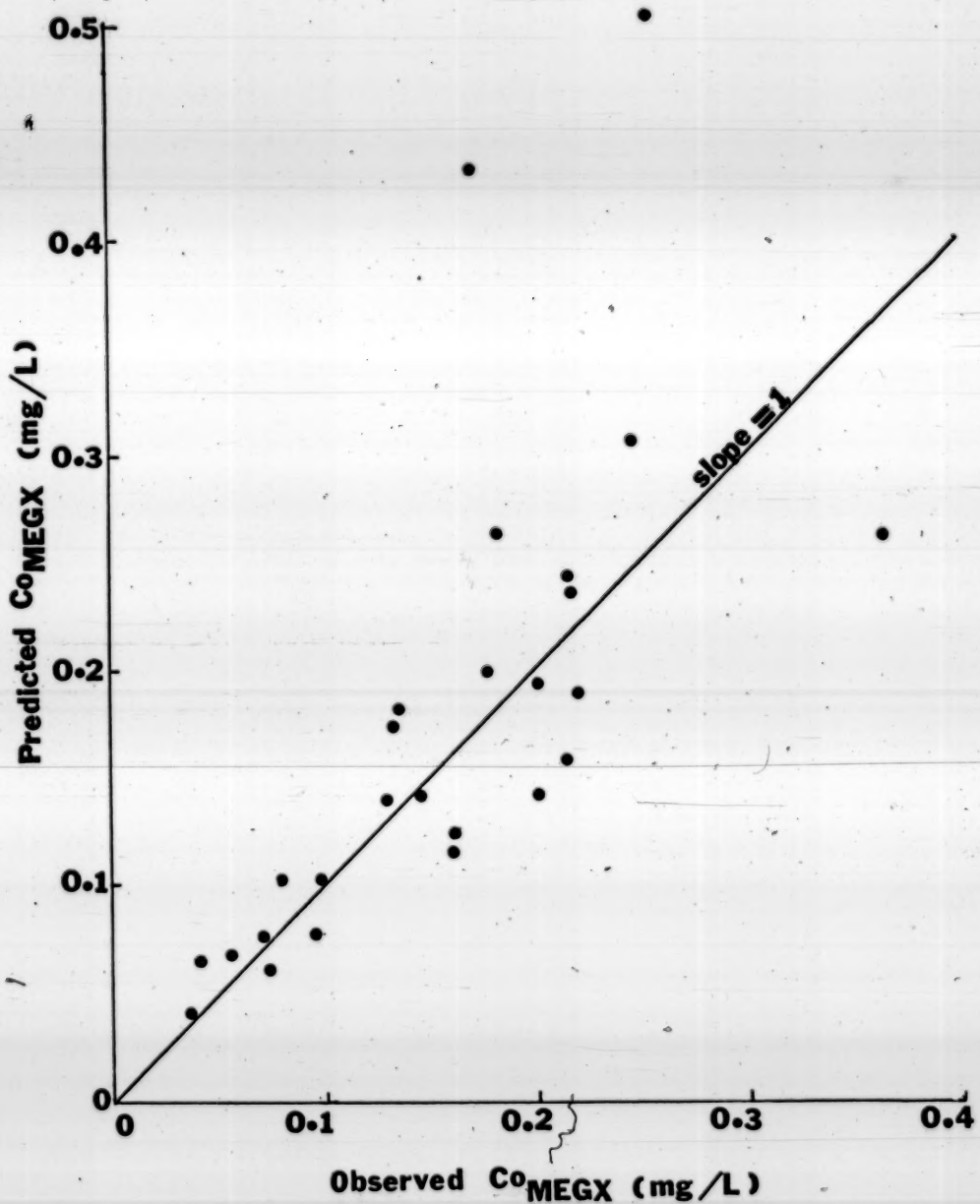
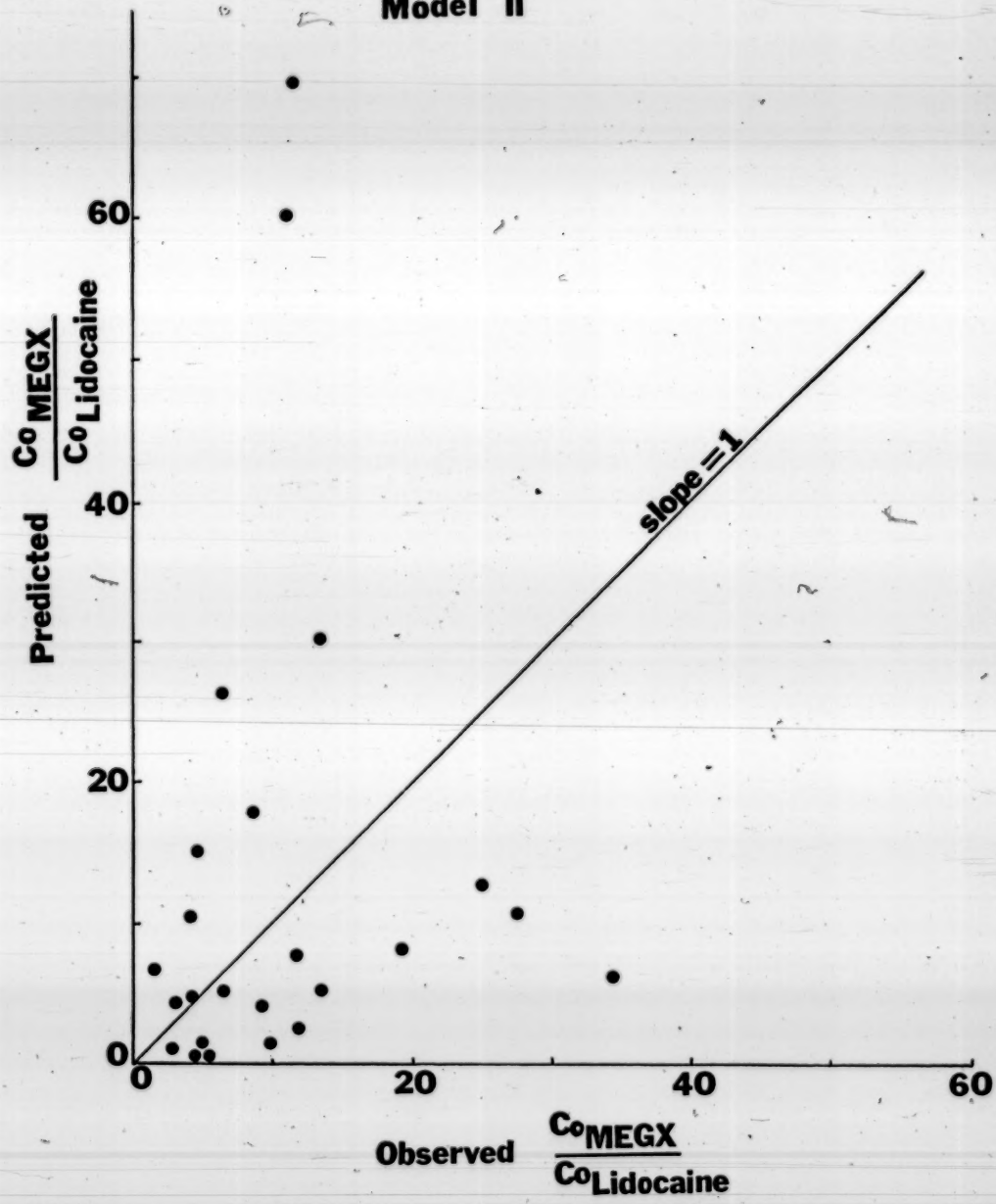


Figure 43. Predicted ratio of the effluent MEGX and lidocaine concentrations versus the observed ratio for Model II for the same nine experiments performed with low influent lidocaine concentration with alterations in blood flow. The line with slope = 1 represents a perfect correlation.

The results are tabulated in Appendix XII-A-B-C

Model II



of zero from the line with slope = 1 (best correlation). Even if the fitted straight line for Model I is forced through zero, a slope which may not be significantly different from one is suspected. The correlation between predicted and observed data is still poor, but a much better correlation is seen for Model I compared to Model II (0.4886 for Model II and 0.765 for Model I). On this basis, Model I is the better model to predict the appearance of the concentration of the metabolite in the effluent blood when a constant low influent concentration of the parent compound (below K_m) is delivered at varying blood flows to the liver.

As shown above, Model I is the better model to predict the appearance of metabolite(s) in the perfusate. Its predictive properties on dosage regimens as chronic drug administration where the potential of metabolite accumulation is more likely is as follows:

Under constant oral administration of a drug, the steady state concentration of the parent compound depends only on the rate of administration (Dose/ τ) and the term A' and is independent of blood flow to the eliminating organ (Table I). Under steady state conditions, the rate of formation of the metabolite from the parent compound equals its rate of elimination. If f is the fraction of the parent compound that is converted to the metabolite, then

f. rate of removal of parent compound = rate of elimination of metabolite

Equation 64

Under linear kinetic conditions, A' and f are constants and when $\frac{f}{A'} = 1$ for the metabolite and the parent compound, substitution of

$C_{B,ss,oral}$ = $(Dose/\tau)/A'_P$ (Equation 34) into Equation 64 gives

$$f \cdot \dot{V}_B \cdot \frac{A'_P}{A'_P + \dot{V}_B} \cdot \frac{Dose/\tau}{A'_P} = \dot{V}_B \frac{A'_M}{\dot{V}_B + A'_M} \cdot C_{B,ss,M,oral} \quad \text{Equation 65}$$

and the steady state concentration of the metabolite is estimated by:

$$C_{B,ss,M,oral} = \frac{f \cdot (Dose/\tau)}{A'_P + \dot{V}_B} \cdot \frac{A'_M + \dot{V}_B}{A'_M} \quad \text{Equation 66}$$

At high hepatic extraction of the parent compound as well as the metabolite, i.e., A'_P and A'_M greatly exceed blood flow, then the steady state metabolite concentration is given by the constant $f \cdot (Dose/\tau)/A'_P$ and is independent of blood flow.

When a drug is given by constant infusion (rate = R^o) its steady state blood concentration is inversely related to its clearance when operating under linear kinetic conditions

$(C_{B,ss,inf} = \frac{R^o}{V_{cl}})$. Again if f is the fraction of drug that is converted to the metabolite, the rate of formation of the metabolite

is f times the rate-in (R^0) of the parent compound. Thus the steady state metabolite concentration is given by:

$$C_{B,ss} = \frac{f \cdot R^0}{V_B \cdot ER_M} = \frac{f \cdot R^0}{V_B} \cdot \frac{A'_M + \dot{V}_B}{A'_M} \quad \text{Equation 67}$$

$$= \frac{f \cdot A'_P}{A'_P + \dot{V}_B} \cdot \frac{A'_M + \dot{V}_B}{A'_M} \cdot C_{B,ss, P,inf}$$

The manner in which the steady state metabolite concentration following constant drug infusion of the parent compound changes with blood flow will depend on how A'_M is related to \dot{V}_B . In cases where A'_M is much greater than blood flow, then the steady state levels of the metabolite increases with decreasing flow. In cases where A'_M is much less than flow, then the steady state metabolite concentration is constant ($f \cdot R^0 / A'_M$) and independent of blood flow.

6. Fitting of Data from the Literature into the Models

The only data that are available in the literature which examine the relationship between the extraction ratio and blood flow are that of Brauer (101) and Whitsett (141). Their data are fitted into the two models.

Brauer's data were obtained from the isolated rat liver preparation in which chromic phosphate was perfused into the rat liver (101). The extraction ratio of the compound by the liver was assessed under steady state conditions by directly measuring $\text{CrPO}_4-\text{P}^{32}$ in hepatic venous and portal venous specimens obtained at the same time. Upon a change in perfusion flow rate, a new steady state extraction ratio was achieved 8-10 minutes after the change. The extraction efficiency for CrPO_4 was determined after equilibration of each preparation at two or three different perfusion rates for each preparation. Viability of the preparation was checked by the final clearance curve at the original perfusion rate to confirm the healthy survival of the tissue. A series of experiments was performed where flow rate varied from 0.5 to 6 mls/min/gm liver and 29 data points were generated. This set of data is very comprehensive as a wide range of flow rates was examined.

The effect of hepatic blood flow on the hepatic removal rate of oxyphenbutazone as reported by Whitsett and coworkers (141) was studied in the intact dog. Blood flow was controlled by proper cannulation, shunting (redirection of blood) and pumping, and measured by flow probes. Simultaneous blood samples were drawn from a peripheral artery and the hepatic vein to determine hepatic drug extraction (oxyphenbutazone is not excreted by the kidneys nor the bile to a great extent). Hepatic blood flow was altered between 0.46 to 2 ml/min/gm liver. Arterial and venous blood concentrations of oxyphenbutazone and hepatic blood flow were each determined at least

ten times. However there was no mention of the establishment of steady state conditions.

The NONLIN computer program (136) was used to fit the data from Brauer and Whitsett. The results of computer fitting are shown in Figures 44 and 45 for data from Brauer and Whitsett respectively and tabulated in Table 23.

Table 23. Computer fitting by NONLIN of data from Brauer and Whitsett.

Study	Model fitted	R ² *	Cor.**	S***
Brauer	I	0.987	0.944	0.067363 with 28 df.
	II	0.985	0.942	0.072115 with 28 df.
Whitsett	I	0.992	0.994	0.052366 with 3 df
	II	0.975	0.989	0.0901045 with 3 df

$$* R^2 = \frac{\sum \text{Observed}^2 - \sum \text{dev}^2}{\sum \text{Observed}^2}$$

** Cor = the correlation between observed and predicted values

$$*** S = s^2$$

In both cases, the data fitted both models very well. From the statistics generated, no significant difference (at 95% confidence interval) was found in the statistical parameters.

Figure 44. NONLIN computer curve fitting of the data from Brauer for Models I and II.

The lines represent computer generated lines.
The dots are experimental points.

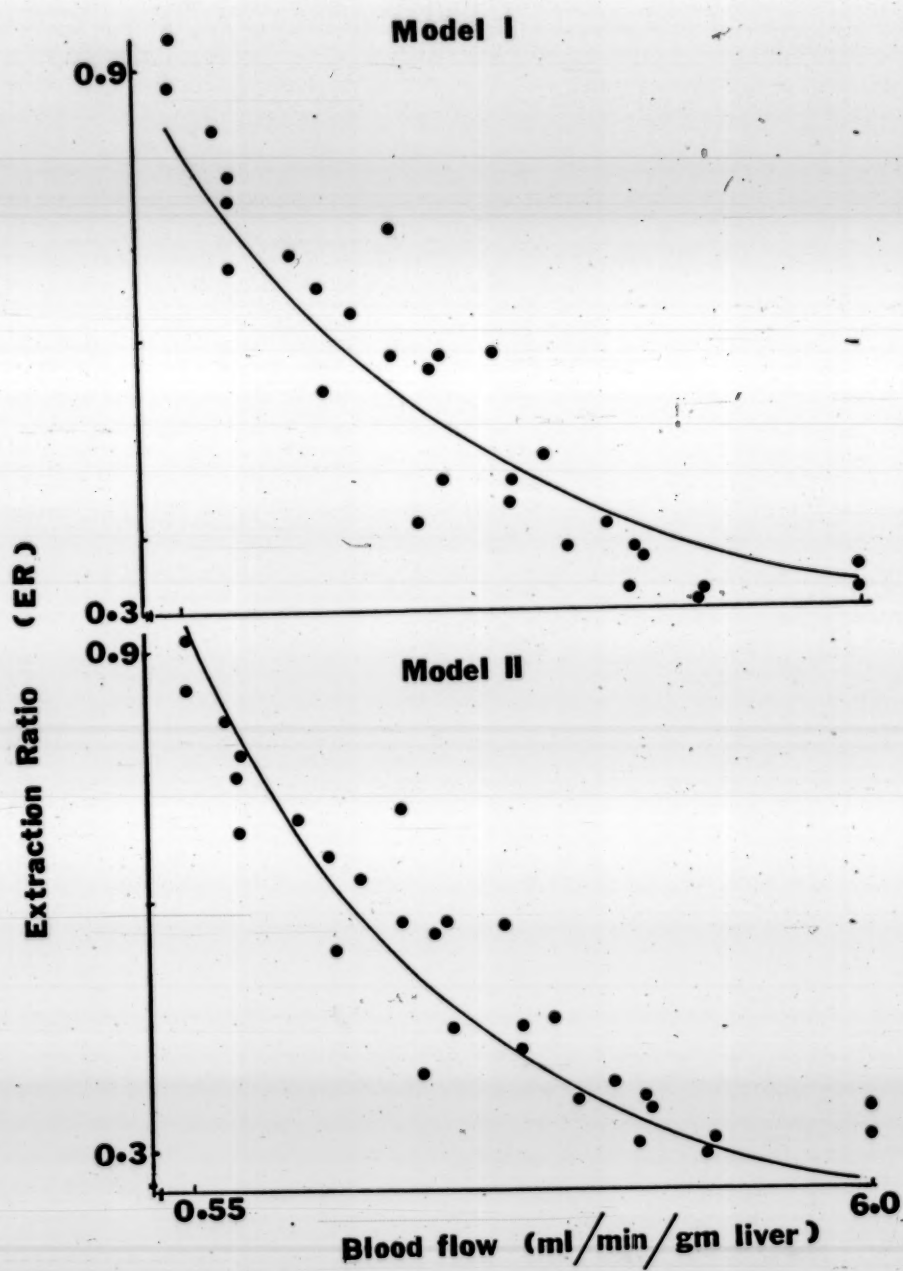
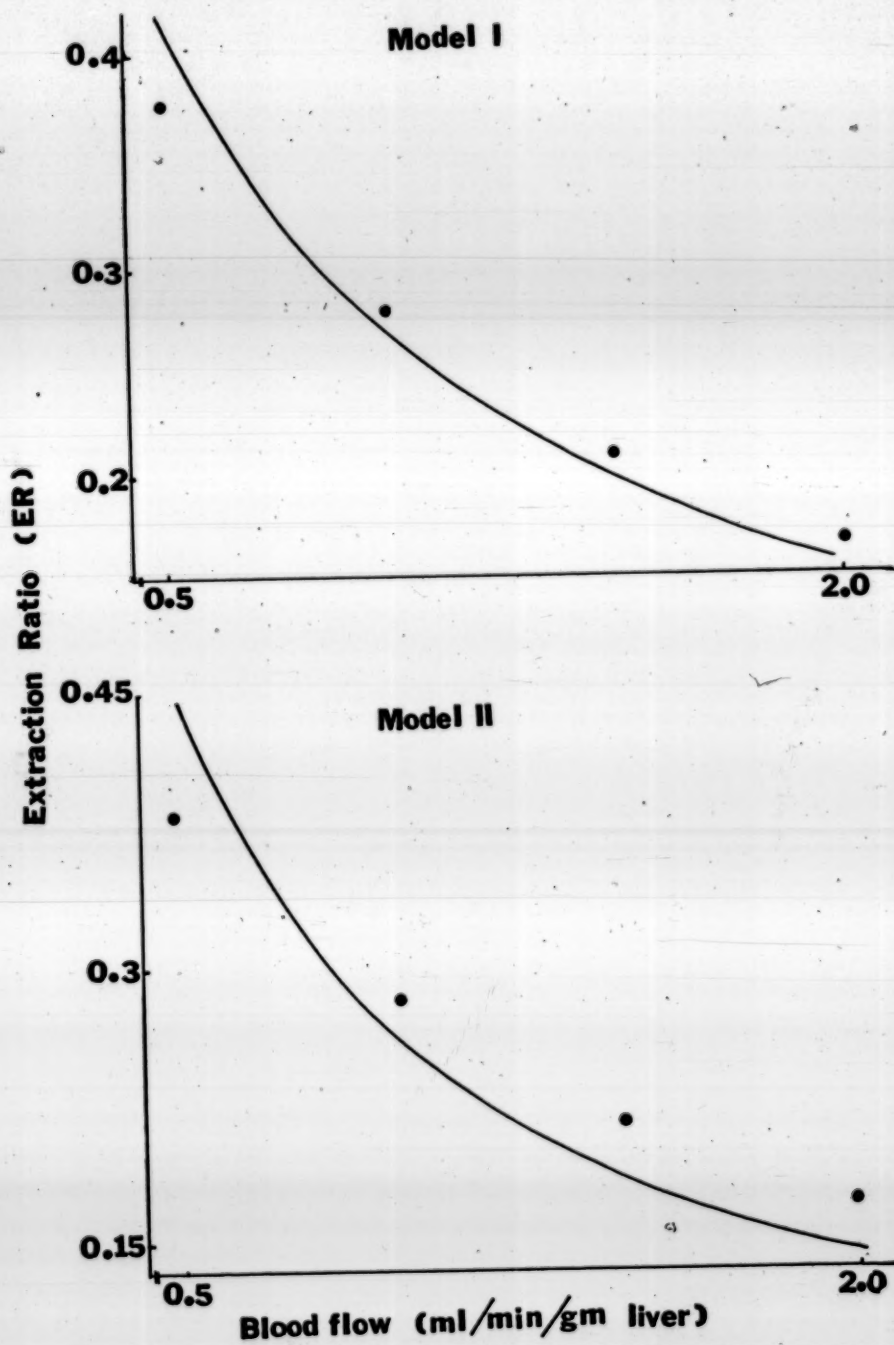


Figure 45. NONLIN computer curve fitting of the data from Whitsett for Models I and II.

The lines represent computer generated lines.

The dots are experimental points.



While the sum weighted square deviations of the fitted equations should be minimal, the scatter of the observed data points about the theoretical curve should be randomly distributed for proper selection of a model. In this instance, the sums of square deviations are not significantly different and this criterion does not serve as a means to distinguish between the models. Thus the scatter of the observed data points about the theoretical curve was examined.

The nature of scatter of experimental points about fitted curves was investigated by the examination and analysis of residuals (142). An unweight residual is defined by the following equation:

$$(\text{unweighted residual}) = (\text{observed value}) - (\text{calculated value})$$

A weighted residual is given by

$$(\text{weighted residual}) = (\text{unweighted residual}) \times (\text{weight})^{\frac{1}{2}}$$

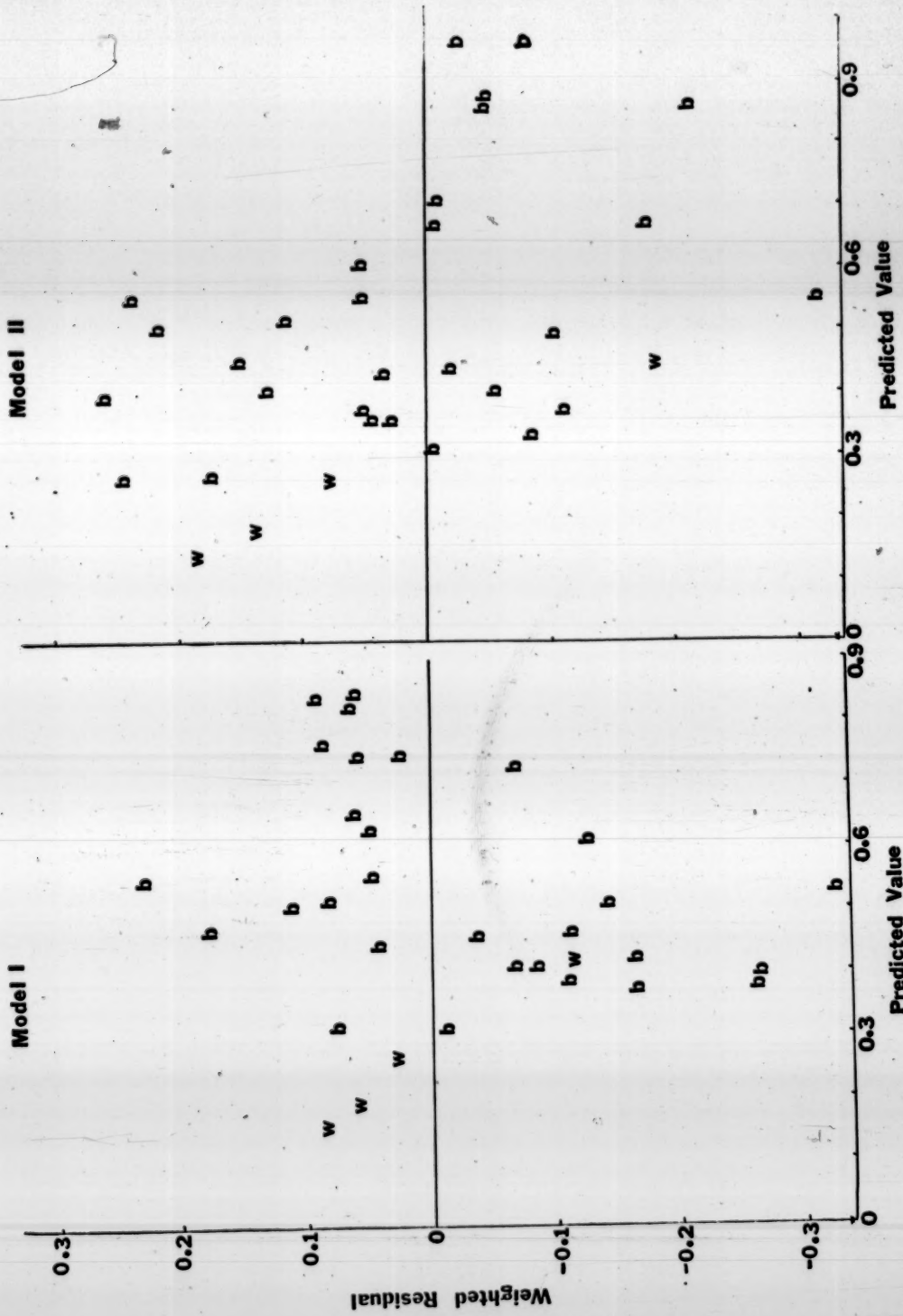
where the weight is frequently defined as $1/(\text{observation})^2$.

The sum of the squared weighted residuals is the quantity minimized in a least-square analysis. An appropriate method to examine scatter is to plot (weighted residual) against (calculated value). A residual plot was constructed (Figure 46) from the data obtained from Brauer and Whitsett fitted to Models I and II.

Figure 46. Plot of weighted residual against predicted value of the data from Brauer and Whitsett for Models I and II.

b. represents data from Brauer

w. represents data from Whitsett.



In both instances, there exist a fairly random distribution of weighted residuals. Therefore the models are considered "consistent" (142). Although a model is "consistent", it still may be "non-unique" or "ill-conditioned". This condition exists when the amount of information contained in the data is inadequate to define the model chosen. Thus the two models fit the data equally well; the models are equally probable and it is impossible on the basis of least-squares fit alone to choose between them (142).

VI. CONCLUSION

The attempt to discriminate between the two models of hepatic drug clearance has elucidated that Model I (where the liver is a well stirred compartment with the concentration of drug in the liver in equilibrium with the effluent drug concentration) is the better fit. The studies were carried out with changes in the availability or the effluent drug concentration with hepatic blood flow of a highly cleared compound (lidocaine) with only negligible binding to protein and blood cells and at low concentrations of lidocaine to the liver (under linear kinetic conditions). The data corresponded closely to the predictions of Model I. Linearized transformation of data obtained from a high influent concentration of lidocaine (above K_m) and at constant blood flow gave a better fit for Model I than for Model II. All the data with lidocaine and MEGX point to an acceptance of Model I to describe hepatic drug clearance.

Physiologically, Model II appears to be the more appropriate model to describe hepatic clearance of drugs. One can easily conceive of the passage of blood, carrying drug, and being channelled into sinusoids and metabolized by liver hepatocytes during the transit through the liver as if the liver sinusoids are a series of identical parallel tubes with a sheet of cells lining the tubes and enzymes distributed evenly within the cells. Thus it is reasonable

7

to think that the concentration of drug in blood varies from point to point along the flow path. Consequently, the material balance for a reaction component must be made for a differential element of volume or flow, a situation analogous to a steady state plug flow reactor in engineering (143). However this flow is orderly with no mixing with any element ahead and after it. There may be lateral mixing, but no mixing or diffusion along the path. This pattern of circulation may be applied to most organs, but not to the liver. As stated earlier (Introduction Chapter), the hepatic vasculature is a highly ramified network with cross anastomoses shunts and indirect paths in addition to "bulk flow". Any element of blood within the sinusoidal bed can reach another part of the sinusoidal bed within the organ without leaving this section of the vascular tree. The portal vein, hepatic artery and the sinusoids are interconnected by direct and obscure pathways. In this respect, the liver can be viewed operationally as a well stirred tank (Model 1) with a uniform composition throughout at any instant of time, a situation analogous to a mixed reactor (or backmix reactor, or the ideal stirred tank reactor, or the constant flow stirred tank reactor) in engineering (143) so that the exit stream from this reactor has the same composition as the fluid within the reactor. The assumption of the model by Kety (144) for the exchange of inert gas at the lungs and tissues is similarly based, in that the effluent concentration is in equilibrium with that within the tissues. This theory has been applied to the quantitation of hepatic blood flow

by substances such as Xenon-133 (145, 146).

Furthermore for Model II, the rate of elimination cannot be explained based on the assumptions of Model II alone and the concept of manifolding has been added to explain some of the deviations from the model (104). In the case of the perfect manifold, a single plate of cells with the inflow divided into streams perpendicular to the plate (in contrast to the assumptions of Model II of a plug flow through a tube with a sheet of cells lining the tube and enzymes evenly distributed within the cells) is present and results in an elimination corresponding to that of a homogenous phase (104), a situation resembling Model I.

Thus Model I is not only physiologically sound, but the predictions also correlate well with the data obtained for lidocaine, MEGX and antipyrine. Operationally it should be accepted as a model to predict drug clearances as well as other pharmacokinetic parameters.

A. Implications of Model I in Pharmacokinetics and Therapeutics Under Linear Kinetic Conditions

According to Model I, hepatic drug extraction and hence clearance are influenced by hepatic blood flow, plasma protein binding, blood cell partitioning and the eliminating capacity of the system (Equations 19 and 20). Other pharmacokinetic

parameters such as availability, area under the curve and the steady state blood concentration of the drug for certain dosage regimens as functions of flow, binding and eliminating capacity are tabulated in Table I.

I. Hepatic Blood Flow

Hepatic blood flow is known to be affected by a number of factors including posture (60), disease state (e.g. congestive heart failure (61, 112, 147)) vasoactive substances (148, 149, 150, 151) stress (151, 152) and hormones (42). The influence of changes in hepatic blood flow on pharmacokinetic parameters is examined in the light of Model I.

Model I predicts a reduction of extraction ratio with increasing blood flow (Equation 19). Consistent with this hypothesis is Brauer's data on colloidal chromic phosphate extraction in the isolated perfused rat liver preparation over a wide range of hepatic blood flow (101). Whitsett's data for oxyphenbutazone extraction by the intact dog liver with changes in hepatic blood flow (141) correlated well with predictions from Model I (Page 194). According to the predictions of Model I, the extraction ratio for highly cleared compounds is independent of blood flow (extraction ratio approaches one) as in the case of lidocaine (148). For very poorly extracted compounds, the extraction ratio changes inversely with blood flow.

(Page 39). For drugs with intermediate extraction ratios, the extraction ratio varies nonlinearly with blood flow (141) as shown in Equation 19.

The effect of hepatic blood flow on clearance of compounds has frequently been reported. For highly extracted compounds (extraction ratio approaching one), clearance is determined by blood flow. In cases where blood flow to the liver is reduced, clearance is correspondingly decreased. Reduction in clearance of highly extracted compounds such as lidocaine (61, 147, 148), indocyanine green (153) and propranolol (154) have been reported in cases of reduced hepatic blood flow. Increases in clearance of these highly extracted compounds associated with an increase in hepatic blood flow have also been reported (63, 155). For poorly cleared compounds, clearance according to Model I is independent of blood flow (clearance approaches the term A'). The clearance of antipyrine, a poorly extracted compound is not affected by an increase (40%) in hepatic blood flow (63). Drugs with intermediate extraction ratios will have clearances which change nonlinearly with blood flow (Equation 20).

The relationship of blood flow and availability was shown previously in Table I. The manner in which availability changes with hepatic blood flow depends on the extraction ratio of the drug. For a highly extracted compound, increasing the blood flow

will cause a proportionate increase in the availability (A' greatly exceeds blood flow). For a drug that is poorly extracted, availability is virtually independent of blood flow (flow greatly exceeds the term A'). For drugs with intermediate extraction ratios, availability is predicted to change nonlinearly with blood flow. Unfortunately, there is not any experimental evidence in existence to support this concept.

The area under the blood-concentration-time curve is not only inversely related to the clearance of a drug, a comparison of the areas under the curve obtained from a single oral and a single intravenous dose also gives a measure of the availability of the single oral dose when the clearance of the drug is constant. There is no mention however, of the effect of blood flow on the area under the curve when the drug is given orally or intravenously which in turn can affect the quantitation of availability. Environmental factors as posture and intake of food are some inconspicuous causes altering hepatic blood flow and hence influence clearance. Such factors may not be controlled, and may alter the values for availability in the area comparisons.

According to Model I, the area under the blood-concentration-time curve following a single oral dose is not altered by hepatic blood flow but strictly depends on the dose and the term A' or hepatic eliminating capacity of the system (Table I) irrespective of the

extraction ratio of the drug. Thus a discrepancy occurring in the areas would be due solely to the difference in hepatocellular activity (Term A') of the individuals rather than differences in hepatic blood flow. The same theoretical analysis for the area under the curve was also given by Perrier and Gibaldi (105). The area under the curve for an oral dose remains unchanged irrespective of the blood flow to the liver and the extraction ratio of the drug. One can view that the rate of absorption, the availability and clearance of the drug are altered to the same degree so that the effects of flow on availability and clearance are cancelled. Thus the shape of the area under the curve may change, but the value of the area should remain unchanged.

Whereas if the drug is given intravenously, the intravenous area under the curve is inversely related to the clearance (Table I). The manner in which blood flow influences the intravenous area under the curve is related to its influence on clearance. For highly cleared compounds, where clearance approaches the limiting value of blood flow, the intravenous area under the curve changes inversely with blood flow whereas for poorly cleared compounds, the area under the curve is not altered. For drugs with intermediate extraction ratios, the area under the curve following an intravenous dose will change nonlinearly with blood flow.

This aspect of changes in area with hepatic blood flow following an intravenous dose for highly cleared compounds deserves attention. If quantitation of the availability of such highly cleared compounds is done by the method of a comparison of the oral area under the curve to the intravenous area under the curve and the latter is much influenced by blood flow, then availability measurements may be quite different even when it is repeated in the same individual where the blood flows under the conditions are different. A control of posture and intake of food should be stipulated to nullify the effect of flow differences which may give rise to differences in the measurements of availability. Unfortunately there is no evidence to support this concept.

The steady state blood concentration of a drug following constant infusion is inversely proportional to its clearance under steady state conditions (Table 1) and a situation analogous to the area under the curve for an intravenous dose with blood flow is seen here for the steady state blood concentration on constant infusion with flow changes. Again, it is in cases for drugs with high extraction ratios that blood flow exerts its greatest influence on the steady state blood concentrations following constant infusion. This was seen in the studies by Stenson and coworkers (61) correlating the cardiac index to arterial steady state lidocaine concentration on constant infusion that a linear relationship existed between the arterial lidocaine concentration and estimated

hepatic blood flow (a linear relationship exists between cardiac indices and extracted hepatic blood flow). For poorly cleared compounds, where blood flow does not affect clearance, the steady state concentration upon infusion is not altered by flow changes. For drugs with intermediate extraction ratios, the steady state concentration upon constant drug infusion changes nonlinearly with flow as given in Table I.

According to Model I, the steady state concentration of a compound following constant oral administration is given by the rate of drug administration divided by the hepatocellular activity of the system (A') and is not influenced by blood flow for drugs of different extraction ratios (Table I). This situation is analogous to the area under the curve for a single oral dose described earlier (Page 206). Again, the sole source of variation in the plateau concentration in a population of subjects receiving the same rate of administration is not in the differences in blood flow in the subjects but in the intrinsic hepatocellular activity of the system (A'). Nortriptyline, desmethylimipramine (156) and propranolol are examples of drugs which exhibit large interpatient variations in the steady state plasma or blood concentration. These drugs also happen to be highly cleared by the liver and exhibit a "first-pass" effect. This had led to the notion that large interpatient variations in the plateau levels are more likely to occur with drugs that display a large first pass effect. According

To Model I, it is not so important whether a drug is highly cleared or not, but rather whether there are large variations in the value of A'.

2. Protein Binding and Blood Cell Partitioning

The binding of a drug to plasma proteins and blood cells influences its disposition (distribution and elimination) and response as the free drug is considered the moiety that equilibrates between tissues and gets eliminated as well as the species eliciting pharmacologic effects and toxicities. A drug that is bound to plasma proteins and/or blood cells can be displaced from its binding sites competitively by another species present in high enough concentrations and with similar or stronger affinity constants, or non-competitively by modification of the binding characteristic favoring dissociation of the binding complex. In cases where the concentration of the drug greatly exceeds the number of binding sites available, then the fraction unbound increases precipitously with concentration.

The model predicts that plasma protein binding and blood cell partitioning affect the extraction ratio in the manner shown in Equation 19. Many drugs that are highly bound are also highly cleared. Examples are bromosupthalein BSP (62), lidocaine (147) and propranolol (75). For such compounds, although the drug can be rapidly removed from the site, dissociation from plasma proteins

and blood cells is even more rapid so that binding does not rate limit elimination, and all drug, whether bound or unbound, is available for elimination as the drug moves through the sinusoids. Mathematically, this condition exists when α' greatly exceeds blood flow. For the poorly cleared compounds, increasing the fraction free should directly increase the extraction ratio and clearance (flow greatly exceeds $\frac{\alpha}{\lambda} A'$ and ER approaches $\frac{\alpha}{\lambda} A'$). Indeed the work of Levy et al (76) showed that for the highly protein bound and poorly cleared drug, warfarin, (<< 1%), its plasma clearance was directly proportional to the fraction unbound. A similar conclusion was obtained by examining the clearance of warfarin with albumin concentration in the perfused rat liver in situ preparation (157). For drugs with intermediate extraction ratios, the degree of protein binding and blood cell partitioning influences the extraction ratio and clearance nonlinearly as shown in Equations 19 and 20.

Other pharmacokinetic parameters are also examined with respect to the influence of plasma protein binding and blood cell partitioning. The relationship of the availability of a compound with α and λ is shown in Table I. For drugs with high extraction ratios, the degree of protein binding bears an inverse relationship with $\frac{\alpha}{\lambda}$ ($\frac{\alpha}{\lambda} A'$ greatly exceeds blood flow). For a poorly extracted drug, availability is unaffected by the degree of binding or partitioning (flow greatly exceeds $\frac{\alpha}{\lambda} A'$), and for drugs with intermediate extraction ratios,

availability changes nonlinearly with the degree of plasma protein binding and blood cell partitioning as shown in Table I.

The area under the blood-concentration-time curve for a single oral dose as predicted by Model I is given in Table I. It is seen that the area under the blood-concentration-time curve for a single oral dose varies inversely with $\frac{\alpha}{\lambda}$ for drugs irrespective of the extraction ratio. When the area under the curve is based on the concentration of drug unbound in the plasma, (AUC unbound, plasma_{oral}) it is found to be constant (Dose/A') with $\frac{\alpha}{\lambda}$. On the other hand, when the area under the blood-concentration time curve a single intravenous dose with α and λ is examined (Table I), the binding parameters (α and λ) do not influence the area under the blood-concentration time curve for highly extracted compounds ($\frac{\alpha}{\lambda} A'$ greatly exceeds flow) whereas for the poorly extracted compounds, the area under the curve varies inversely with $\frac{\alpha}{\lambda}$ (flow exceeds $\frac{\alpha}{\lambda} A'$). For drugs with intermediate extraction ratios, the area changes nonlinearly with α and λ as in Table I. When the area under the curve is based on the concentration of the drug unbound in the plasma (AUC unbound, plasma_{IV}), it is found to be equal to

$$\frac{\alpha A'}{\lambda} \text{Dose} / \left(\frac{\alpha A'}{\lambda} + V_B \right)$$
. The availability of a drug via a certain route of administration as measured by a comparison of the area under the blood-concentration-time the curve to that of the intravenous area

under the blood-concentration-time can also be calculated by comparing the area under the curve based on the unbound drug concentration in plasma to that of the intravenous dose. In this respect, the problem that may arise when protein binding and blood cell partitioning are changing from study to study is alleviated.

Model I predicts that the steady state blood concentration on constant oral administration is inversely related to the hepatocellular activity (A') and $\frac{\alpha}{\lambda}$, as in Table I, irrespective of the extraction ratio of the drug. When the steady state concentration is expressed as the unbound concentration in plasma, it is found to be constant and independent of α and λ and equals $Dose/A'$. Similar theoretical analysis was arrived at by Rowland (73). When the drug is given by constant infusion, the plateau blood concentration is given as in Table I. The manner in which α and λ influence the steady state blood concentration will depend on the extraction ratio of the drug (relation of $\frac{\alpha}{\lambda} A'$ to flow). For drugs that are highly cleared, where clearance approaches blood flow, the steady state concentration is independent of the binding parameters. In contrast, for drugs with low extraction ratios, the steady state blood concentration upon constant infusion varies inversely with $\frac{\alpha}{\lambda}$ (flow greatly exceeds $\frac{\alpha}{\lambda} A'$). In this instance, the steady state concentration when expressed as the unbound plasma concentration would be a constant ($Dose/A'$) and independent of α and λ . This was again incorporated in Rowland's analysis (73). For drugs with

intermediate extraction ratios, the steady state blood concentration changes nonlinearly with α and λ as shown in Table I.

While it is important to examine the influence of protein binding and blood cell partitioning on the various pharmacokinetic parameters as previously mentioned, it is more important to examine the unbound drug levels and see the influence of the binding parameters on the unbound concentration. As stated previously (Page 209), it is the unbound species that equilibrates within tissue, exerts pharmacological responses and exhibits toxicities.

3. Hepatocellular Activity or Eliminating Capacity of the System

(Term A')

Much discussion has been devoted to the influence of blood flow and plasma protein binding and blood cell partitioning. Equally important is the hepatocellular activity (term A') which is comprised of the enzymatic constants V_{max} and K_m ($A' = V_{max}/K_m$). Phenobarbital and lindane are well known inducers which effectively reduce the half-life of poorly extracted compounds such as antipyrine (158,148). Phenobarbital was known to induce microsomal enzymes and effectively increase the V_{max} values for the metabolism of diphenylhydantoin (159, 160). Furthermore, A' can be modified by the presence of inhibitory substances (metabolites) as shown previously (Page 165).

According to Model I, theoretical analysis has shown that the extraction ratio of a drug depends on the relationship of hepato-cellular activity (A') of the system to the blood flow as in Equation 19. When the value of A' is low with respect to blood flow, the extraction ratio of the drug is low, and vice versa (when A' exceeds flow, extraction ratio is high and approaches the value of one), and for values of A' comparable to blood flow, the extraction ratio of the drug has intermediate values.

The effect of the term A' on other pharmacokinetic parameters is tabulated in Table I. The influence of A' on the availability of a compound depends again on the value of A' with respect to blood flow. Should A' be much greater than flow (highly cleared compound), then the availability is inversely related to A' . Contrastingly should A' be much less than flow, then availability is essentially complete (equals one) and independent of A' . If A' and blood flow have comparable values, then the availability will be an intermediate value.

As shown previously (Pages 210 and 211) the area under the curve based on unbound drug in the plasma for a single oral dose as well as the steady state unbound plasma concentration following constant oral administration of a drug are all inversely related to the term A' . Variations in A' will be inversely translated into these parameters. The area under the blood-concentration-time curve

following a single intravenous dose and the steady state concentration of the drug in blood following constant infusion are indirectly related to A' through their inverse relationship with clearance and extraction ratio (Table I). When the extraction ratio of the compound is high, then clearance approaches blood flow and slight alterations in A' do not affect clearance. Whereas in situations where clearance of a compound approaches A' (poorly cleared compound), then altering A' will change the pharmacokinetic parameters (area and steady state concentration) in a reciprocal manner. Drugs having intermediate extraction ratios will change in a nonlinear fashion with A' as in Table I.

4. Generation of Metabolite

The formation of metabolites from the parent compound plays an important role in pharmacology and toxicology. There are cases when the metabolites generated are active or more active than the parent compound (161) or that they are toxic and exhibit toxic side effects that are undesirable (162). The potential for an unpredicted increase in activity or toxicity is augmented when the metabolites are generated in high amounts and the levels are not monitored. Furthermore, complications such as end product inhibition may occur. An example is oxyphenbutazone, an active metabolite of phenylbutazone which is capable of inhibiting the metabolism of its parent compound (139). Another example is the inhibition of metabolism of diphenylhydantoin by its major metabolite 5-(p-hydroxy-phenyl)-5-

phenylhydantoin (163, 164).

Model I predicts the formation of metabolites which may or may not be intermediates for further metabolism. The potential for drug toxicity and unpredicted pharmacologic effect is greatest when drugs are given on a chronic basis.

The prediction according to Model I on the steady state metabolite concentration in blood upon constant oral administration is shown in Equation 66. Under conditions where the binding parameters are linear and in the case where the elimination of the metabolite is rate limiting ($A'M$ is much less than flow and $A'p$ greatly exceeds flow), the steady state metabolite concentration increases with blood flow. In cases where the rate of formation of the metabolite is rate limiting ($A'p$ is much less than flow and $A'M$ greatly exceeds flow), then the steady state metabolite concentration decreases with blood flow. In cases where the eliminating capacity for the parent compound as well as the metabolite are large ($A'p$ and $A'M$ greatly exceed blood flow), then the metabolite concentration is constant and is independent of blood flow.

According to the predictions by Model I, the steady state metabolite concentration in blood following constant infusion is given by Equation 67. Under conditions where binding parameters are linear, and in the case where the eliminating capacity of the metabo-

lute is great compared to blood flow, the steady state metabolite concentration decreases with increasing flow and vice versa. Indeed Halkin and co-workers (112) quantitated the metabolite MEGX following constant infusion of the parent drug lidocaine in patients with and without heart failure and found an increase in the levels of the metabolite with decreased hepatic blood flow. This finding is coincidental with the predictions of Model I that the metabolite itself must also be highly cleared. Although the data available is limited, it appeared from the kinetics of MEGX that it is also highly cleared in man. In cases where the eliminating capacity of the metabolite is low (flow exceeds $A'M$) the steady state metabolite concentration is not expected to change with blood flow according to predictions by Model I.

Model I also affords a method for the estimation of f , the fraction of the parent compound that is converted to the metabolite under linear kinetic conditions. Following constant infusion (rate, R^0) and when the metabolite is very slowly cleared, the fractional conversion from the parent compound can be estimated by $\frac{A'M}{R}$ times the steady state concentration of the metabolite at that infusion rate. In cases where the metabolite is highly cleared ($A'M \gg V_B$) a plot of the steady state metabolite concentration versus the reciprocal of blood flow for a given rate of infusion (Equation 67) gives a slope equal to f , rate of infusion. Thus f can be easily estimated.

5. Estimation of in vivo Vmax and Km

The in vitro method of incubating enzyme(s) in its purified form or enzyme system(s) with substrate in the presence or absence of cofactors has provided a method for the estimation of the in vitro enzymatic parameters (Vmax and Km) governing the reaction (165). The Vmax and Km of the system can be estimated by the conventional Lineweaver-Burk or Eadie-Hofstee type plots where the slopes and the intercepts of these plots give the values of Vmax and Km (166). While it is relatively simple to interpret data from the in vitro situation (the substrate concentration is given by the initial concentration of substrate and the velocity of reaction is given after the cessation of reaction), the estimation of enzymatic parameters from in vivo situations has been a complicated task. Obviously an accurate assessment of the velocity of the reaction for an in vivo system can be assessed from steady state studies but the substrate concentration is not easily determined. As shown by Winkler and coworkers, the effects of using different "substrate" concentrations (liver hepatocyte concentration, influent concentration, the average of the influent and effluent concentration and the geometric mean of the influent and effluent concentration) in the estimation of Km and Vmax of galactose furnished different Km values but arrived at the same value for Vmax in the isolated perfused pig liver preparation under steady state conditions (54). The values of Vmax are identical for the different "substrate" concentrations used in

their study. This is in accordance with the fact that at very high substrate concentrations, the mean concentration in the liver does not differ from the input or output concentrations, while the error rises when the perfusate concentration becomes smaller. The K_m values found using different expressions for "substrate" concentrations are considerably different as compared to the K_m obtained for the real substrate (hepatocyte) concentration, e.g., for the arterial (input) concentration as substrate, an overestimation of three fold is found (54).

Lundquist and Wolthers (167) estimated the in vivo K_m and V_{max} for the metabolism of ethanol in man to be 2.03 mM and 79.6 μ moles / min (equivalent to 9.227 gm/hr) which correlated very favourably when compared to the in vitro estimates K_m and V_{max} obtained using liver alcohol dehydrogenase, the enzyme which is generally believed to be responsible for the first stage of the metabolism of ethanol. Makar and Mannerling (168) were also able to demonstrate a close correlation of the in vivo and in vitro estimates of K_m and V_{max} in the rat and monkey using ethanol as the substrate. As can be seen in these two studies, a good correlation between in vivo and in vitro estimates exists even when the plasma concentration of ethanol is used in the estimation. This is so because ethanol, being a very small molecule, distributes essentially in total body water such that the blood, plasma and liver concentration are considered the same. Substitution of the

plasma concentration for the substrate concentration (liver concentration) still provides the true estimates of K_m and V_{max} .

Model I provides a method for the estimation of the in vivo enzymatic parameters as the effluent concentration of the compound in blood is in equilibrium with that in the liver. In this model, the velocity of drug removal can be expressed in terms of the effluent drug concentration (C_o).

$$\text{velocity of removal } (v) = \frac{V_{max} \cdot C_o}{\frac{\lambda}{\alpha} K_m + C_o} \quad \text{Equation 68}$$

where α is the plasma protein binding parameter and λ is the blood partitioning parameter. Lineweaver-Burk type plots of the velocity of removal quantitated by blood flow times the concentration difference ($V_B \cdot (C_i - C_o)$) against the effluent drug concentration in blood will furnish estimations for V_{max} and the apparent K_m (apparent K_m equals the true K_m times $\frac{\lambda}{\alpha}$). In instances where $\frac{\alpha}{\lambda} = 1$, i.e., the drug distributes evenly in all tissues, then K_m can be assessed directly. In cases where $\frac{\alpha}{\lambda} \neq 1$, and when the binding parameters (α and λ) are known, K_m can still be estimated.

This method, however suffers from a limitation for drugs that are highly cleared, i.e. drugs which have clearance values approaching hepatic blood flow. The true clearance values of these highly extracted compounds may greatly exceed the value of blood flow, but the measured quantity for clearance is the limiting value

of blood flow. In this region, then clearance ceases to be a measure of K_m and V_{max} . An example of such an error is given by the method of van Ginneken and coworkers (169). Their method of back extrapolation of the linear portion of the curve to estimate K_m and V_{max} suffers the same limitation for a compound that is cleared very rapidly (or drugs with high extraction ratios). When the log concentration versus time profile is linear (concentration of substrate is low compared to K_m), the slope of this straight portion does not reflect the true clearance parameters (V_{max} and K_m) but rather measures blood flow divided by the volume of distribution (V_B/V_d) for a drug with high extraction ratio as the clearance is limited by blood flow when true value greatly exceeds the latter. An analysis of their data for ethanol showed that the elimination rate constant(k) can be calculated by the hepatic blood flow (1.5 L/min) divided by the volume of distribution (36.7L) to be 2.1429 hr^{-1} as compared to their reported estimated value of 2.33 hr^{-1} . When their estimated K_m value (4.5652 mM) is compared to that obtained from Lundquist and Wolthers (167) an overestimation of 2.25 times is seen. The V_{max} is still estimated by their method at $C_L \gg K_m$ where clearance is no longer blood flow limited, rather it is capacity limited, and should reflect the true clearance parameters. The effect of blood flow on the estimation is also stressed by Dedrick and Forrester (170).

7

For poorly cleared compounds, Model I as well as the method provided by van Ginneken *et al* (169) are adequate to estimate the parameters of K_m and V_{max} .

Another possible source of error that may arise in the estimation of the enzymatic parameters is when the arterial concentration is used instead of the venous concentration in the estimation of K_m and V_{max} . This can be demonstrated in the following example in a situation where a drug is introduced by constant infusion at a rate (R^o) and when steady state conditions are reached, the rate in = rate out.

$$R^o = \dot{V}_B \cdot (C_A - C_V) = \frac{V_{max} C_V}{K_m + C_V} \quad \text{Equation 69}$$

C_A and C_V are the steady state concentrations of drug in the arterial and venous blood respectively. For simplicity sake, the concentration of drug in the liver is set equal to the venous concentration, i.e., $\frac{\alpha}{\lambda} = 1$. The venous blood concentration at steady state is given by:

$$C_V = \frac{R^o}{(V_{max} - R^o)} \cdot K_m \text{ true} \quad \text{Equation 70}$$

$$= - \frac{R^o}{\dot{V}_B} \cdot C_A$$

If instead, the arterial side is sampled, then the steady state arterial concentration is given by:

$$C_A = \frac{R^o}{(V_{max} - R^o)} \cdot \frac{(V_{max} - R^o + \dot{V}_B \cdot K_m \text{ true})}{\dot{V}_B}$$

$$= \frac{R^o}{(V_{max} - R^o)} \cdot K_m \text{ app} \quad \text{Equation 71}$$

One can see that instead of the true K_m , the apparent K_m is measured.

$$K_m \text{ app} = \frac{V_{max} - R^o + \dot{V}_B K_m \text{ true}}{\dot{V}_B} \quad \text{Equation 72}$$

or

$$K_m \text{ true} = K_m \text{ app} \cdot \frac{(R^o - V_{max})}{\dot{V}_B} \quad \text{Equation 73}$$

All the above is based on drug elimination describable by a simple Michaelis-Menten kinetics with only an uni-enzyme system characterized by its V_{max} and K_m . Cases where multi-enzyme systems with alternate routes of metabolism or extrahepatic elimination present are not considered in the analysis. Cases where the biotransformation process is subjected to substrate inhibition and complete product inhibition (171) are also not considered in the above analysis.

B. Qualifying Remarks

So far a model for hepatic drug clearance is examined and accepted to have predictive properties. This model is adequate to describe the kinetics of a drug in the body when the drug is totally hepatically cleared, or when the majority of elimination occurs in the liver. However, a drug can also be eliminated to a good extent extrahepatically, usually via the renal route of elimination. In such instances, the model (though still holds true) may not be adequate to reflect total body clearance of the drug (total body clearance is the sum of the individual clearances). Changes of blood flow, protein binding or the eliminating capacity of the enzyme system may or may not affect extrahepatic clearance to the same degree as the hepatic clearance. It is difficult to dissect what portion of changes is associated with hepatic clearance or extrahepatic clearance when a change in the total body clearance is observed. Furthermore, gut wall metabolism in the gastrointestinal tract is not considered in the model. An error can easily arise when the sum of the clearances due to gut wall metabolism and that due to hepatic elimination is taken as the hepatic clearance of the drug. These factors should be taken into consideration when one is applying the model to predict drug clearance or other pharmacokinetic parameters. The best predictions are obtained when the model is applied to drugs that are totally hepatically cleared.

Appendix I, Material and Supplies

Nembutal ^R (Sodium Pentobarbital) Injectable 50 mg/ml	Abbott Labs. Chicago, Illinois
Pentafluorobenzoyl chloride	Pierce Chemical Co. Rockfield, Illinois
Sodium Chloride Solution 0.9% (Normal Saline)	Travenol Lab. Inc. Deerfield, Illinois
Lactated Ringers Solution, U.S.P.	Travenol Lab. Inc. Deerfield, Illinois
Polyethylene tubing PE 240	Clay Adams Co. Parsippany, New Jersey
Dextran T 40	Pharmacia Fine Chemicals Inc. Piscataway, New Jersey
Bovine Serum Albumin 25% (Tyrode's Solution)	Sigma Chemical Co. St. Louis, Missouri
Intramedic ^R Luer-Stub Adapters Gauge 15	Clay Adams Co. Parsippany, New Jersey
Three-way and Four-way Stopcocks	Clay Adams Parsippany, New Jersey
Detrose Injectable U.S.P. 50%	Travenol Labs. Inc. Deerfield, Illinois
Aquasol	New England Nuclear Corp. Boston, Massachusetts
Folin Reagent	Harleco Philadelphia, Pennsylvania
Out Dated Human Whole Blood	Irwin Memorial Blood Bank San Francisco, California
Safti Blood Administration Set Code 889-84	Cutter Labs. Berkeley, California
Whatman #1 Filter Paper	W & R Balston Ltd. England

Appendix II. Materials and Supplies Cont'd

Hollow Fiber Oxygenator

Edwards Labs.
Santa Ana, California

Bentley Partial Bypass

Coast Medical Corp.
Walnut Creek, California

Rats, Sprague-Dawley

Simmonson
San Francisco, California

Cathlon IV Catheter Placement Unit
14 Gauge, 2 1/2"

Jelco Lab.
Raritan, New Jersey

Cathlon IV Catheter Placement Unit
16 Gauge 2 1/2"

Jelco Lab.
Raritan, New Jersey

Surgical Silk 0-0

Daknetal
San Jose, California

Microfuge tubes

Beckman Instruments Inc.
Palo Alto, California

Carbogen (95% oxygen, 5% carbon Dioxide)

Ohio Medical Products
Madison, Wisconsin

Appendix II. Equipment

Vari-Whirl Mixer

Van-Lab.
Scientific Supplies Co.
U.S.A.

"Tilt-Type" Mixer

Linson Instruments
Stockholm, Sweden

Beckman Research pH Meter
Model 1019

Beckman Instruments Inc.
Palo Alto, California

Tricarb Scintillation Counter

Nuclear Chicago

Cary 15

Beckman Instruments Inc.
Palo Alto, California

Microfuge Centrifuge

Beckman Instruments Inc.
Palo Alto, California

Oxygen Electrodes

Radiometer
Copenhagen

Tyco Aneroid Sphygmomanometer

American Hospital Supplies
South San Francisco, California

Peristaltic Pump
Model 1202

Harvard Apparatus Co.
Millis, Massachusetts

Gas Chromatograph
Varian Series 1200

Varian
Palo Alto, California

Centrifuge
HN-S Centrifuge

International Equipment Co.
Needham Heights, Massachusetts

Magnestir
Pyro-magnestir

Lab-Line Instruments Inc.
Melrose Park, Illinois

Dianorm

Scientific and Medical Instrumentation
CH-Esslinger Switzerland

Perfusion Apparatus

Home Built by Mr. Norman O. Henry
University of California
School of Pharmacy
San Francisco, California

Appendix IIIA. Predicted values of steady state extraction ratio, clearance and availability with changes in blood flow - Model I*

Reference Point**	(A')***	Hepatic Blood Flow (ml/min/gm liver)									
		1.0					1.5				
		ER _I	v _{cI}	F _I	ER _I	v _{cI}	ER _I	v _{cI}	F _I	ER _I	v _{cI}
0.1	0.1111	0.1818	0.0909	0.8182	0.1000	0.1	0.9000	0.0690	0.1035	0.9310	0.0526
0.2	0.25	0.3333	0.16665	0.66667	0.2000	0.2	0.8000	0.1429	0.21435	0.8571	0.1052
0.3	0.42857	0.4615	0.23075	0.5385	0.3000	0.3	0.7000	0.2220	0.333	0.778	0.1111
0.4	0.66667	0.5714	0.287	0.4286	0.4000	0.4	0.6000	0.3077	0.46155	0.6923	0.2222
0.5	1.00	0.66667	0.33335	0.3333	0.5000	0.5	0.5000	0.4000	0.6000	0.6000	0.8889
0.6	1.50	0.7500	0.375	0.2500	0.6000	0.6	0.4000	0.5000	0.75	0.5000	0.353
0.7	2.3333	0.8235	0.41175	0.1765	0.7000	0.7	0.3000	0.6087	0.91305	0.3913	0.8235
0.8	4.00	0.8889	0.44445	0.1111	0.8000	0.8	0.2000	0.7273	1.09095	0.2727	0.7500
0.9	9.00	0.9474	0.4737	0.0526	0.9000	0.9	0.1000	0.8571	1.28565	0.1429	0.6364
0.95	19.00	0.9744	0.4872	0.0256	0.9500	0.95	0.0500	0.9286	1.3902	0.0732	0.1818
0.99	99.00	0.9950	0.4975	0.0050	0.9500	0.99	0.0100	0.9851	1.47765	0.0149	0.0952
0.995	199.00	0.9975	0.49875	0.0025	0.9950	0.995	0.0050	0.9925	1.48875	0.0075	0.0198
0.999	999.00	0.9995	0.499975	0.0005	0.9990	0.999	0.0010	0.9985	1.49775	0.0015	0.0100
										0.9980	0.0020

* \bar{A} is taken as 1 for all calculations

** ER at blood flow = 1.0 ml/min/gm liver. This value is used to calculate the term (A') which in turn is used to predict changes with blood flows at 0.5, 1.5 and 2.0 ml/min/gm liver.

*** Hepatocellular activity calculated from reference point.

Appendix III B. Predicted values of the AUC following a single oral and intravenous dose and the steady state blood concentration following constant oral administration and constant intravenous infusion of the drug with changes in blood flow - Model 1*

Reference ^a (A ₁) *** Point**	0.5			1.0			1.5			2.0			Hepatic Blood Flow (ml/min/gm liver)		
	AUC _{oral}	AUC _{IV}	and C _{B,ssInf}	AUC _{oral}	AUC _{IV}	and C _{B,ssInf}	AUC _{oral}	AUC _{IV}	and C _{B,ssInf}	AUC _{oral}	AUC _{IV}	and C _{B,ssInf}	AUC _{oral}	AUC _{IV}	and C _{B,ssInf}
0.1	0.1111	9.001	11.001	9.001	10.0	9.001	9.001	9.662	9.001	9.001	9.665	9.001	9.506	9.001	9.506
0.2	0.25	4.00	6.001	4.00	5.000	4.00	4.00	4.665	4.00	4.00	4.665	4.00	4.500	4.00	4.500
0.3	0.42857	2.3333	4.334	2.3333	3.333	2.3333	3.003	2.333	3.003	2.333	2.333	2.333	2.833	2.333	2.833
0.4	0.66667	1.50	3.500	1.50	2.500	1.50	2.000	2.167	2.000	2.000	2.167	2.000	2.00	2.00	2.00
0.5	1.00	1.00	3.000	1.00	2.000	1.00	1.00	1.667	1.00	1.00	1.667	1.00	1.500	1.00	1.500
0.6	1.50	0.66667	2.667	0.66667	1.667	0.66667	1.333	0.66667	1.333	0.66667	1.333	0.66667	1.167	0.66667	1.167
0.7	2.333	0.4286	2.429	0.4286	1.429	0.4286	1.095	0.4286	1.095	0.4286	1.095	0.4286	0.929	0.4286	0.929
0.8	4.00	0.25	2.250	0.25	1.250	0.25	0.917	0.25	0.917	0.25	0.917	0.25	0.750	0.25	0.750
0.9	9.00	0.1111	2.111	0.1111	1.111	0.1111	0.778	0.1111	0.778	0.1111	0.778	0.1111	0.611	0.1111	0.611
0.95	19.00	0.0526	2.053	0.0526	1.053	0.0526	0.526	0.0526	0.526	0.0526	0.526	0.0526	0.533	0.0526	0.533
0.99	99.00	0.01010	2.010	0.01010	1.010	0.01010	0.01010	0.01010	0.01010	0.01010	0.01010	0.01010	0.510	0.01010	0.510
0.995	199.0	0.00503	2.005	0.00503	1.005	0.00503	0.00503	0.00503	0.00503	0.00503	0.00503	0.00503	0.505	0.00503	0.505
0.999	999.0	0.00100	2.001	0.00100	1.001	0.00100	0.00100	0.00100	0.00100	0.00100	0.00100	0.00100	0.501	0.00100	0.501

* \bar{a} is taken as 1 for all calculations.

** ER at blood flow = 1.0 ml/min/gm liver, this value is used to calculate the term (A₁) which in turn is used to predict changes with blood flows at 0.5, 1.5 and 2.0 ml/min/gm liver.

Single oral and IV dose 1 mcg; rate of constant drug administration for oral and intravenous infusion - 1 mcg/min units for 1) AUC (mg/L)-min 2) C_{B,ss} "mg/L

***Hepatocellular activity (A₁) calculated from reference point

Appendix IVA. Predicted values of the steady state extraction ratio, clearance and availability with changes in blood flow - Model II *

Refer- ence point **	Hepato- cellular activity (A'_{II})	Hepatic Blood Flow at			2.0		
		ER_{II}	V_{cII}	F_{II}	ER_{II}	V_{cII}	F_{II}
0.1	0.10536	0.1900	0.095	0.8100	0.1000	0.1	0.9000
0.2	0.2231	0.3600	0.18	0.6400	0.2000	0.2	0.8000
0.3	0.35667	0.5100	0.255	0.4900	0.3000	0.3	0.7000
0.4	0.51083	0.6400	0.32	0.3600	0.4000	0.4	0.6000
0.5	0.6931	0.7500	0.375	0.2500	0.5000	0.5	0.5000
0.6	0.91629	0.8400	0.42	0.1600	0.6000	0.6	0.4000
0.7	1.20397	0.9100	0.455	0.0900	0.7000	0.7	0.3000
0.8	1.60844	0.9600	0.48	0.0400	0.8000	0.8	0.2000
0.9	2.30259	0.9900	0.495	0.0100	0.9000	0.9	0.1000
0.95	2.99573	0.9975	0.49875	0.0025	0.9500	0.95	0.0500
0.99	4.60517	0.9999	0.4995	0.0001	0.9900	0.99	0.0100
0.995	5.29832	0.9998	0.49998	0.000025	0.9950	0.995	0.0050
0.999	6.90776	0.9999	0.49999	0.000001	0.9990	0.999	0.0010

^a Is taken as 1 for all calculations

** ER at blood flow=1.0 ml/min/gm liver. This value is used to calculate the term (A'_{II}) which in turn is used to predict changes with blood flows at 0.5, 1.5 and 2.0 ml/min/gm liver

Appendix IVB.
Predicted values of the AUC following a single oral and intravenous dose and the steady state blood concentration following constant oral administration and constant intravenous infusion of the drug with changes in blood flow - Model II*

Reference**	Hepatocellular Activity (A _{II}) calculated from reference point	Hepatic Blood Flow (ml/min/gm liver)		AUC _{oral II}		AUC _{IV II}		AUC _{oral II}		AUC _{IV II}		AUC _{oral II}		AUC _{IV II}	
		1.0	0.5	AUC _{oral II}	AUC _{IV II}										
0.1	0.1054	8.5263	10.526	9.000	10.000	9.1667	9.833	9.2476	9.747						
0.2	0.2231	3.5556	5.556	4.00	5.00	4.157	4.824	4.2348	4.735						
0.3	0.35667	1.9216	3.922	2.333	3.333	2.4839	3.151	2.5619	3.062						
0.4	0.51083	1.125	3.125	1.50	2.500	1.6433	2.310	1.7183	2.218						
0.5	0.6931	0.6667	2.667	1.00	2.000	1.1351	1.802	1.2071	1.361						
0.6	0.91629	0.381	2.381	0.6667	1.667	0.7918	1.458	0.9606	1.361						
0.7	1.20397	0.1978	2.198	0.4286	1.429	0.5413	1.208	0.6055	1.105						
0.8	1.60994	0.0834	2.083	0.25	1.250	0.3465	1.013	0.4045	0.904						
0.9	2.2059	0.0202	2.083	0.050	0.050	0.1111	0.111	0.1828	0.849	0.2512	0.731				
0.95	2.99573	0.0050	2.000	0.026	0.026	0.053	0.053	0.1047	0.821	0.144	0.644				
0.99	4.65017	0.0002	2.000	0.01010	0.01010	0.0324	0.0324	0.0699	0.656	0.556	0.556				
0.995	5.29832	0.00005	2.00005	0.00503	0.00503	0.02008	0.02008	0.0687	0.687	0.03805	0.538				
0.999	6.9078	0.000002	2.000002	0.00100	0.00100	0.00673	0.00673	0.0673	0.0673	0.01632	0.516				

* $\frac{\alpha}{\lambda}$ is taken as 1 for all calculations

**ER at blood flow = 1.0 ml/min/gm liver. This value is used to calculate the term (A'II) which in turn is used to predict changes with blood flow at 0.5, 1.5 and 2.0 ml/min/gm liver.

Single oral and IV dose- 1 mcg; Rate of constant drug administration for oral and intravenous infusion - 1 mcg/min.
Units for 1) AUC = (mg/L)·min 2) C_{B,ss} = mg/L

Appendix X VA. Ratio of predicted steady state extraction ratios, clearances and availability for models I and II with changes in blood flow*

		Hepatic blood flow (ml/min/gm liver)					
		0.5			1.0		
		ER _I /ER _{II} **	F _I /F _{II} ***	ER _I /ER _{II}	F _I /F _{II}	ER _I /ER _{II}	F _I /F _{II}
0.9568	1.0101	1.0000	1.0000	1.0177	0.9987	1.0253	0.9987
0.9257	1.0417	1.0000	1.0000	1.0340	0.9946	1.0521	0.9938
0.9049	1.0990	1.0000	1.0000	1.0491	0.9868	1.0808	0.9843
0.8929	1.1906	1.0000	1.0000	1.0662	0.9732	1.1091	0.9682
0.8889	1.3332	1.0000	1.0000	1.0811	0.9524	1.1379	0.9428
0.8929	1.3625	1.0000	1.0000	1.0939	0.9210	1.1663	0.9035
0.9045	1.9611	1.0000	1.0000	1.1029	0.8731	1.1906	0.8426
0.9259	2.7775	1.0000	1.0000	1.1053	0.7974	1.2060	0.7453
0.9590	5.2600	1.0000	1.0000	1.0921	0.6633	1.1965	0.5749
0.9768	10.2400	1.0000	1.0000	1.0723	0.5393	1.1681	0.4259
0.9951	50.00	1.0000	1.0000	1.0330	0.3209	1.0891	0.1980
0.9975	100.0	1.0000	1.0000	1.0224	0.2565	1.0653	0.1414
0.9995	500.0	1.0000	1.0000	1.0086	0.1500	1.0306	0.0632

* $\frac{\alpha}{X}$ is taken as 1 for all calculations

** ER_I/ER_{II} = $\dot{V}_{clI}/\dot{V}_{clII}$

*** F_I/F_{II} = C_{0I}/C_{0II}

Appendix VB. Ratio of predicted areas under the blood concentration time curve and the steady state concentration following constant oral administration and constant infusion for Models I and II with changes in blood flow*

		Hepatic Blood Flow (ml/min/gm liver)		2.0	
		0.5	1.0	1.5	2.0
		$\frac{\text{AUC}_{\text{oral I}}}{\text{AUC}_{\text{oral II}}}$ **	$\frac{\text{AUC}_{\text{IV I}}}{\text{AUC}_{\text{IV II}}} \text{ ***}$	$\frac{\text{AUC}_{\text{oral I}}}{\text{AUC}_{\text{oral II}}}$	$\frac{\text{AUC}_{\text{IV I}}}{\text{AUC}_{\text{IV II}}}$
		$\frac{\text{AUC}_{\text{oral I}}}{\text{AUC}_{\text{oral II}}}$	$\frac{\text{AUC}_{\text{IV I}}}{\text{AUC}_{\text{IV II}}}$	$\frac{\text{AUC}_{\text{oral I}}}{\text{AUC}_{\text{oral II}}}$	$\frac{\text{AUC}_{\text{IV I}}}{\text{AUC}_{\text{IV II}}}$
1.0557	1.0451	1.0000	1.0000	0.9819	0.9826
1.1250	1.0801	1.0000	1.0000	0.9622	0.9679
1.2142	1.1050	1.0000	1.0000	0.9394	0.9651
1.3333	1.1200	1.0000	1.0000	0.9128	0.9381
1.5000	1.1249	1.0000	1.0000	0.8810	0.9251
1.7498	1.1201	1.0000	1.0000	0.8420	0.9143
2.1688	1.1051	1.0000	1.0000	0.7918	0.9065
2.9976	1.0802	1.0000	1.0000	0.7215	0.9052
5.5000	1.0450	1.0000	1.0000	0.6078	0.9164
10.520	1.0238	1.0000	1.0000	0.5024	0.9326
50.505	1.0050	1.0000	1.0000	0.3118	0.9685
100.50	1.0024	1.0000	1.0000	0.2502	0.9781
500.50	1.0005	1.0000	1.0000	0.1487	0.9915

* $\frac{\alpha}{\lambda}$ is taken as 1 for all calculations

** $\text{AUC}_{\text{oral I}} / \text{AUC}_{\text{oral II}} = \text{C}_{\text{B,ssoral I}} / \text{C}_{\text{B,ssoral II}}$

*** $\text{AUC}_{\text{IV I}} / \text{AUC}_{\text{IV II}} = \text{C}_{\text{B,ssinf I}} / \text{C}_{\text{B,ssinf II}}$

Appendix VI A. Predicted steady state extraction ratio for a given fraction of drug unbound in plasma and at constant blood flow (1.0 ml/min/gm liver) - Model I*

Reference Point**	$(A'_{\text{I}})^{***}$	ER_{I} predicted at $\frac{\alpha}{\lambda} =$
0.1	0.1111	0.1
0.2	0.25	0.2
0.3	0.42857	0.3
0.4	0.66667	0.4
0.5	1.00	0.5
0.6	1.50	0.6
0.7	2.33333	0.7
0.8	4.00	0.8
0.9	9.00	0.9
0.99	99.00	0.99
0.999	999.00	1.0

* $\dot{V}_{\text{Cl}}_{\text{I}}$ is obtained by multiplying calculated values of ER_{I} by blood flow (1.0 ml/min/gm liver)

** ER at blood flow = 1.0 ml/min/gm liver at $\frac{\alpha}{\lambda} = 1$

*** (A'_{I}) calculated from reference point

Appendix VI B, Predicted availability for a given fraction of drug unbound in plasma and at constant blood flow (1.0 ml/min/gm liver) - Model I

Reference Point*	$(A'_1)**$	(F_1) predicted at $\frac{\alpha}{\lambda} =$	0.1	0.2	0.3	0.4	0.5	0.6	0.7	0.8	0.9	1.0
0.1	0.1111	0.9889	0.9783	0.9677	0.9575	0.9474	0.9375	0.9278	0.9184	0.9091	0.9000	
0.2	0.25	0.9762	0.9524	0.9392	0.9091	0.8699	0.8696	0.8511	0.8333	0.8163	0.8000	
0.3	0.42857	0.9589	0.9211	0.8861	0.8537	0.8235	0.7955	0.7692	0.7447	0.7217	0.7000	
0.4	0.6667	0.9375	0.8824	0.8333	0.7895	0.7500	0.7143	0.6818	0.6522	0.6250	0.6000	
0.5	1.00	0.9091	0.8333	0.7692	0.7143	0.6667	0.6250	0.5882	0.5556	0.5263	0.5000	
0.6	1.500	0.8696	0.7692	0.6897	0.625	0.5714	0.5263	0.4878	0.4545	0.4255	0.4000	
0.7	2.3333	0.8108	0.6818	0.5882	0.5172	0.4615	0.4167	0.3797	0.3488	0.3226	0.3000	
0.8	4.00	0.7143	0.5556	0.4545	0.3846	0.3333	0.2941	0.2632	0.2381	0.2174	0.2000	
0.9	9.00	0.5263	0.3571	0.2703	0.2174	0.1818	0.1562	0.1370	0.1220	0.1099	0.1000	
0.99	99.00	0.0917	0.0481	0.0326	0.0246	0.0198	0.0166	0.0142	0.0125	0.0111	0.0100	
0.999	999.00	0.0099	0.0050	0.0033	0.0025	0.0017	0.0014	0.0012	0.0011	0.0010		

*ER at blood flow = 1.0 ml/min/gm liver and at $\frac{\alpha}{\lambda} = 1$

** (A'_1) calculated from reference point

Appendix VI.C. Predicted area under the blood-concentration-time curve for single oral dose for a given fraction of drug unbound in plasma and at constant blood flow (1.0 ml/min/gm liver) - Model I*

Reference Po Int**	(A'1)***	AUC _{oral1} (mg/L)	Predicted at $\frac{\alpha}{\lambda} =$	
0.1	0.1111	0.1 9.000 4.5 3.000 2.000 1.3333 1.000 0.7778 0.5833 0.4667 0.3889 0.3333 0.2500 0.2000 0.1667 0.1333 0.10714 0.08571 0.06250 0.04625 0.03125 0.02125 0.01587 0.01389 0.01234 0.01111 0.00144 0.00168 0.00126 0.00112 0.00010 0.00012 0.00011	0.2 0.5 0.4 0.3 0.250 1.8 1.5 0.8000 0.6667 0.57143 0.5000 0.3333 0.2917 0.2593 0.2333 0.21428 0.1875 0.1667 0.14286 0.1250 0.1111 0.09524 0.08333 0.0741 0.06667 0.06122 0.053571 0.04167 0.03571 0.03125 0.02777 0.02222 0.01852 0.01389 0.01234 0.01111 0.00144 0.00168 0.00126 0.00112 0.00010 0.00012 0.00011	0.5 0.6 0.7 0.8 0.9 1.0 1.250 1.2857 1.4444 0.4000 0.2593 0.2333 0.1667 0.14286 0.1250 0.1111 0.1000 0.0741 0.06667 0.04268 0.04762 0.04268 0.03571 0.03125 0.02777 0.02222 0.01852 0.01389 0.01234 0.01111 0.00144 0.00168 0.00126 0.00112 0.00010 0.00012 0.00011

*Steady state blood concentration of drug following constant oral administration (CB_{ssoral1}) in mg/L = $AUC_{oral1} \frac{\alpha}{\lambda}$

** ER at blood flow = 1.0 ml/min/gm liver at $\frac{\alpha}{\lambda} = 1$

*** (A'1) calculated from reference point
Single oral dose = 1 mcg; rate of administration = 1mcg/min

Appendix VID. Predicted values of the area under the blood-concentration-time curve following a single intravenous dose for a given fraction of drug unbound in plasma and at constant blood flow (1.0 ml/min/gm) - Model 1*

Reference Point**	(A'1)**	AUC _{IVI}	($\text{mg}/\text{L}\cdot\text{min}$) predicted at $\frac{\alpha}{\lambda} =$
0.1	0.1111	0.1	0.2
0.2	0.25	90.09	46.083
0.3	0.42857	42.017	21.008
0.4	0.66667	24.331	14.327
0.5	1.00	16.000	8.503
0.6	1.50	11.001	6.000
0.7	2.33333	7.669	4.333
0.8	4.00	5.285	3.143
0.9	9.00	3.500	2.250
0.99	99.00	2.111	1.051
0.999	999.00	1.00	1.00

*Steady state drug concentration in blood ($C_{BSS,inf}$, in mg/L) following constant infusion of drug = AUC_{IVI}

**ER at blood flow = 1.0 ml/min/gm liver at $\frac{\alpha}{\lambda} = 1$

*** (A'1) calculated from reference point
single intravenous dose = 1 mcg; rate of infusion = 1 mcg/min)

Appendix VIIA. Predicted steady state extraction ratio for a given fraction of drug unbound in plasma and at constant blood flow (1.0 ml/min/gm liver) - Model II*

Reference Point**	$(A'_{II})^{***}$	ER_{II} predicted at $\frac{a}{\lambda} =$
0.1	0.10536	0.1
0.2	0.2231	0.0105
0.3	0.35667	0.0209
0.4	0.51083	0.0436
0.5	0.6391	0.0971
0.6	0.91629	0.1294
0.7	1.20397	0.1134
0.8	1.60944	0.1487
0.9	2.30259	0.2057
0.99	4.60517	0.3690
0.999	6.90776	0.4988

* $\dot{V}_{c_{II}}$ is obtained by multiplying the calculated values of ER_{II} by blood flow (1.0 ml/min/gm liver)

** ER at blood flow = 1.0 ml/min/gm liver and at $\frac{a}{\lambda} = 1$

*** (A'_{II}) calculated from reference point

Appendix VII B. Predicted availability for given fraction of drug unbound in plasma and at constant blood flow (1.0 ml/min/gm liver) - Model II

Reference Point*	(A'')**	F _{II} predicted at $\frac{\alpha}{\lambda} = 1$	F _{II} predicted at $\frac{\alpha}{\lambda}$	F _{II} predicted at $\frac{\alpha}{\lambda} = 0.9$	F _{II} predicted at $\frac{\alpha}{\lambda} = 0.8$	F _{II} predicted at $\frac{\alpha}{\lambda} = 0.7$	F _{II} predicted at $\frac{\alpha}{\lambda} = 0.6$	F _{II} predicted at $\frac{\alpha}{\lambda} = 0.5$	F _{II} predicted at $\frac{\alpha}{\lambda} = 0.4$	F _{II} predicted at $\frac{\alpha}{\lambda} = 0.3$	F _{II} predicted at $\frac{\alpha}{\lambda} = 0.2$	F _{II} predicted at $\frac{\alpha}{\lambda} = 0.1$	
0.1	0.10536	0.1	0.2	0.3	0.4	0.5	0.6	0.7	0.8	0.9	0.9	0.9	1.0
0.2	0.2221	0.9895	0.9791	0.9689	0.9587	0.9487	0.9387	0.9289	0.9192	0.9095	0.9095	0.9095	0.9095
0.3	0.35667	0.9779	0.9564	0.9352	0.9146	0.8944	0.8747	0.8554	0.8365	0.8181	0.8181	0.8181	0.8181
0.4	0.51083	0.9650	0.9311	0.8985	0.8670	0.8367	0.8073	0.7791	0.7518	0.7254	0.7254	0.7254	0.7254
0.5	0.6391	0.9502	0.9029	0.8579	0.8152	0.7746	0.7360	0.6994	0.6645	0.6317	0.6317	0.6317	0.6317
0.6	0.91629	0.9126	0.8326	0.7597	0.6931	0.6325	0.5771	0.5266	0.4804	0.4384	0.4384	0.4384	0.4384
0.7	0.120397	0.8866	0.7860	0.6968	0.6178	0.5477	0.4856	0.4305	0.3817	0.3384	0.3384	0.3384	0.3384
0.8	1.60944	0.8513	0.7248	0.6170	0.5253	0.4472	0.3807	0.3241	0.2759	0.2349	0.2349	0.2349	0.2349
0.9	2.30559	0.7943	0.6310	0.5012	0.3891	0.3162	0.2512	0.1995	0.1585	0.1259	0.1259	0.1259	0.1259
0.99	4.60517	0.6310	0.3891	0.2512	0.1585	0.1000	0.0631	0.0398	0.0251	0.0158	0.0158	0.0158	0.0158
0.999	6.90776	0.5012	0.2512	0.1259	0.0631	0.0316	0.0159	0.0079	0.0040	0.0020	0.0020	0.0020	0.0020

*ER at blood flow = 1.0 ml/min/gm liver and at $\frac{\alpha}{\lambda} = 1$

** (A'') calculated from reference point

Appendix VII C. Predicted area under the blood-concentration time curve for single oral dose for a given fraction of drug unbound in plasma at constant blood flow (1.0 ml/min/gm liver)
- Model II*

Reference Point**	$(A'_{II})^{***}$	$AUC_{oral,II}$ ((mg/L)-min) predicted at $\frac{\alpha}{\lambda} =$
0.1	0.1	0.2
0.1	0.10526	4.6847
0.2	0.2231	4.4249
0.3	0.35667	2.7671
0.4	0.51083	1.9080
0.5	0.6391	1.3925
0.6	0.91629	1.0442
0.7	1.20397	0.7818
0.8	1.60944	0.5725
0.9	2.30259	0.3865
0.99	4.60517	0.1710
0.999	6.90776	0.1005
		0.3
		0.4
		2.3213
		1.432
		1.3514
		0.8852
		0.6037
		0.4411
		0.3151
		0.4328
		0.6728
		0.3161
		0.2298
		0.3673
		0.2634
		0.1710
		0.0637
		0.0355
		0.0144
		0.5
		1.5313
		0.8470
		0.6519
		0.5124
		0.4198
		0.3437
		0.2788
		0.2327
		0.1981
		0.1376
		0.5116
		0.3527
		0.2642
		0.1713
		0.1349
		0.1601
		0.1365
		0.1721
		0.1211
		0.0944
		0.0809
		0.0615
		0.0480
		0.0335
		0.04062
		0.00111
		0.00674
		0.00326
		0.00161
		0.00080
		0.00040
		0.9
		1.0

* Steady state blood concentration of drug ($Q_{B,ss,oral,II}$ in mg/L) following constant oral administration
= $AUC_{oral,II}$

**ER at blood flow = 1.0 ml/min/gm liver at $\frac{\alpha}{\lambda} = 1$

*** (A'_{II}) calculated from reference point

Single oral dose = 1 mcg; rate of administration for constant oral administration = 1 mcg/min

Appendix VII D. Predicted area under the blood-concentration-time curve following a single intravenous dose for a given fraction of drug unbound in plasma and at constant blood flow (1.0 ml/min/gm liver) - Model II*

Reference Point**	$(A'_{11})^{***}$	$AUC_{IV_{11}}$	$((mg/L)\cdot\text{min})$	predicted at $\frac{\alpha}{\lambda} =$
0.1	0.10536	0.1	0.2	0.5
0.2	0.2231	95.238	47.847	0.6
0.3	0.35667	45.25	32.154	0.7
0.4	0.51083	28.57	15.43	0.8
0.5	0.6391	20.08	11.71	0.9
0.6	0.91629	14.93	7.52	1.0
0.7	1.20397	11.44	4.16	1.05
0.8	1.60944	8.82	4.67	1.50
0.9	2.30259	6.725	3.50	2.33
0.99	4.60517	4.861	2.61	3.33
0.999	6.90776	2.71	2.71	2.50

* Steady state drug concentration in blood ($C_{B,ss,inf_{11}}$ in mg/L) following constant infusion for drug = $AUC_{IV_{11}}$

** ER at blood flow = 1.0 ml/min/gm liver and at $\frac{\alpha}{\lambda} = 1$

*** (A'_{11}) calculated from reference point

Single intravenous dose = 1 mcg; rate of infusion = 1 mcg/min

Appendix VIII A. Ratio of predicted steady state extraction ratios and clearances with changes in in the ratio $(\frac{\alpha}{\lambda})$ and at constant blood flow (1.0 ml/min/gm liver)*

$\frac{\alpha}{\lambda}$	$\frac{\alpha}{\lambda} =$					
	0.1	0.2	0.3	0.4	0.5	0.6
1.0571	1.0383	1.0381	1.0291	1.0253	1.0196	1.0155
1.1041	1.0917	1.0772	1.0644	1.0521	1.0407	1.0297
1.1743	1.1451	1.1272	1.1000	1.0808	1.0612	1.0448
1.255	1.2111	1.1731	1.1391	1.1091	1.0822	1.0585
1.3567	1.2883	1.2296	1.1801	1.1379	1.1023	1.0713
1.492	1.3787	1.2913	1.2219	1.1665	1.1201	1.082
1.672	1.4869	1.3582	1.2632	1.1906	1.1339	1.0892
1.9213	1.6148	1.4243	1.2964	1.206	1.1398	1.0901
2.3029	1.7423	1.4629	1.2811	1.1965	1.1269	1.0781
2.4615	1.5582	1.2919	1.1591	1.0891	1.0496	1.0267
1.985	1.3288	1.1403	1.0647	1.0306	1.0143	1.0066

$$* \frac{ER_I}{ER_{II}} = \frac{\frac{V_{CL}}{V_{CL}}}{\frac{V_{CL}}{V_{CL}}}$$

Appendix VIII B. Ratio of the predicted availability and effluent drug concentrations for Models I and II with changes in the ratio $\frac{\alpha}{\lambda}$ and at constant blood flow (1.0 ml/min/gm liver)*

$$F_I/F_{II} \text{ at } \frac{\alpha}{\lambda} =$$

0.1	0.2	0.3	0.4	0.5	0.6	0.7	0.8	0.9	1.0
0.9994	0.9992	0.9988	0.9987	1.0093	0.9987	0.9988	0.9991	0.9996	1.0000
0.9983	0.9958	0.9947	0.9940	0.9939	0.9942	0.9950	0.9962	0.9978	1.0000
0.9937	0.9893	0.9862	0.9847	0.9842	0.9854	0.9873	0.9906	0.9949	1.0000
0.9868	0.9773	0.9713	0.9685	0.9682	0.9705	0.9748	0.9815	0.9899	1.0000
0.9744	0.9572	0.9468	0.9425	0.9429	0.9473	0.95555	0.9674	0.9821	1.0000
0.9529	0.9239	0.9079	0.9017	0.9034	0.9120	0.0263	0.9461	0.9706	1.0000
0.9145	0.8674	0.8441	0.8372	0.8426	0.8581	0.8820	0.9138	0.9533	1.0000
0.8391	0.7666	0.7366	0.7322	0.7453	0.7725	0.8121	0.8630	0.9255	1.0000
0.6626	0.5659	0.5393	0.5587	0.5750	0.6218	0.6867	0.7696	0.8729	1.0000
0.1453	0.1236	0.1298	0.1552	0.1980	0.2631	0.3568	0.4980	0.7025	1.0000
0.0198	0.0199	0.0262	0.0396	0.0633	0.1076	0.1772	0.3000	0.5000	1.0000

$$* \frac{F_I}{F_{II}} = \frac{C_{0I}}{C_{0II}}$$

Appendix VIIC. Ratio of predicted areas under the blood-concentration-time curve following a single oral dose and the steady state blood concentration of drug in blood following constant oral administration with changes in the ratio ($\frac{a}{X}$) and at constant blood flow (1.0 ml/min/gm liver)*

$$\text{AUC}_{\text{oral I}} / \text{AUC}_{\text{oral II}} \text{ at } \frac{a}{X} =$$

	0.1	0.2	0.3	0.4	0.5	0.6	0.7	0.8	0.9	1.0
0.955	0.961	0.963	0.969	0.973	0.980	0.984	0.989	0.995	1.000	
0.904	0.912	0.924	0.934	0.945	0.955	0.966	0.977	0.988	1.000	
0.846	0.964	0.879	0.895	0.911	0.928	0.945	0.963	0.981	1.000	
0.786	0.807	0.828	0.850	0.783	0.897	0.921	0.947	0.973	1.000	
0.718	0.743	0.770	0.799	0.828	0.859	0.892	0.927	0.962	1.000	
0.638	0.670	0.703	0.738	0.775	0.814	0.856	0.901	0.949	1.000	
0.548	0.583	0.622	0.663	0.708	0.757	0.810	0.868	0.931	1.000	
0.437	0.475	0.517	0.565	0.618	0.678	0.745	0.820	0.905	1.000	
0.288	0.325	0.369	0.436	0.481	0.552	0.637	0.737	0.857	1.000	
0.059	0.079	0.100	0.134	0.182	0.250	0.348	0.4906	0.698	1.000	
0.010	0.015	0.023	0.037	0.061	0.104	0.179	0.313	0.554	1.000	

$$* \frac{\text{AUC}_{\text{oral I}}}{\text{AUC}_{\text{oral II}}} = \frac{C_{B,\text{ssoral I}}}{C_{B,\text{ssoral II}}}$$

Appendix VIII D. Ratio of Predicted Areas, under the blood-concentration-time curve following a single dose and the steady state blood concentrations of drug in blood following constant intravenous infusion with changes in the ratio $\frac{\alpha}{\chi}$ and at constant blood flow (1.0 ml/s/min/gm liver)*

$AUC_{IV_1}/AUC_{IV_{II}}$	at $\frac{\alpha}{\chi} =$	0.1	0.2	0.3	0.4	0.5	0.6	0.7	0.8	0.9	1.0
0.9459	0.9631	0.9629	0.9118	0.9753	0.9808	0.9847	0.9904	0.9956	1.000		
0.9286	0.9159	0.9234	0.9395	0.9505	0.9609	0.9711	0.9809	0.9902	1.000		
0.8516	0.8732	0.8912	0.9090	0.9252	0.9424	0.9571	0.9722	0.9865	1.0000		
0.7968	0.8256	0.8525	0.8780	0.9105	0.9240	0.9447	0.9644	0.9830	1.0000		
0.7371	0.7763	0.8133	0.8473	0.8787	0.9075	0.9335	0.9579	0.9796	1.0000		
0.6702	0.7253	0.7770	0.8186	0.8574	0.8926	0.9199	0.9522	0.9775	1.0000		
0.5993	0.6726	0.7362	0.7919	0.8297	0.8817	0.9180	0.9499	0.9768	1.0000		
0.5204	0.6192	0.7020	0.7712	0.8292	0.8774	0.9169	0.9508	0.9778	1.0000		
0.4352	0.5738	0.6833	0.7807	0.8358	0.8876	0.9279	0.9588	0.9816	1.0000		
0.4063	0.6420	0.7745	0.8628	0.9181	0.9531	0.9741	0.9873	0.9951	1.0000		
0.5037	0.7528	0.8741	0.9400	0.9700	0.9862	0.9931	0.9970	0.9990	1.0000		

$$* \frac{AUC_{IV_1}}{AUC_{IV_{II}}} = \frac{C_{B,ss,inf_1}}{C_{B,ss,inf_{II}}}$$

Appendix IXA. Alterations of blood flow at low influent lidocaine concentration to the liver
(Studies I, II and III)

Study	Blood flow (mls/min)	Average effluent lidocaine concentration (mg/L)	Extraction Ratio	Predictions			
				Model I	Model II	Model III	Co II (mg/L)
I	10	0.00575 \pm 0.00037	0.9987				
Cl=4.378 (mg/L)	12	0.008425 \pm 0.00071	0.9980	7774.4	0.00675	66.609	0.01701
	10	0.0055 \pm 0.00054	0.9987				
	16	0.01621 \pm 0.00152	0.9963	5506.5	0.01269	63.144	0.06709
	10	0.010375 \pm 0.00061	0.9976				
	14	0.01962 \pm 0.00109	0.9955	3464.5	0.01762	58.5	0.06709
	10	0.01483 \pm 0.00386	0.9966				
II	12	0.0126 \pm 0.00216	0.9917				
Cl=4.309 (mg/L)	14	0.0305 \pm 0.00325	0.9927	2161.9	0.02772	62.39	0.04999
	12	0.0352 \pm 0.00993	0.9918				
	10	0.0291 \pm 0.00315	0.9932	1230.9	0.03472	55.68	0.01646
	12	0.0480 \pm 0.1467	0.9889				
	16	0.0733 \pm 0.00454	0.9830	1244.5	0.05469	55.81	0.13161
	12	0.0343 \pm 0.00259	0.9920				
	12	0.1347 \pm 0.01819	0.9692				
III	14	0.0403 \pm 0.00607	0.9908				
Cl=4.368 (mg/L)	12	0.0278 \pm 0.00294	0.9936	1869.2	0.0324	60.655	0.05761
	10	0.0134 \pm 0.00055	0.9969				
	12	0.0186 \pm 0.00074	0.9957	2256.6	0.01935	62.903	0.00813
	16	0.0931 \pm 0.00470	0.9787				
	12	0.0243 \pm 0.00312	0.9944	2441.7	0.02855	63.847	0.08111

n = 4 \pm S.D.

Appendix IXB. Alterations of blood flow at low influent lidocaine concentration to the liver (Study IV, V & VI).

Study	Blood flow (mls/min)	Average effluent lidocaine concentration (mg/L)	Extraction Ratio	Predictions		
				Model I A' (mls/min)	Co ₁ (mg/L)	Model II A' (mls/min)
IV $C_1=4.387$ (mg/L)	12	0.0049 ± 0.00103	0.9989	5359.6	0.01142	73.269
	14	0.0078 ± 0.00038	0.9982	5359.6	0.01142	73.269
	12	0.0147 ± 0.00230	0.9966	3257.7	0.02165	67.291
	16	0.9170 ± 0.00054	0.9961	3257.7	0.02165	67.291
	12	0.0175 ± 0.00209	0.9960	3556.9	0.01237	68.35
	10	0.0211 ± 0.00275	0.9951	3556.9	0.01237	68.35
	12	0.0120 ± 0.00083	0.9973			
V $C_1=4.626$ (mg/L)	12	0.0049 ± 0.00042	0.9989	8089.3	0.00799	78.18856
	14	0.0051 ± 0.00034	0.9989	8089.3	0.00799	78.18856
	12	0.0088 ± 0.00204	0.9981	5482.5	0.01346	73.54116
	16	0.0108 ± 0.00082	0.9977	5482.5	0.01346	73.54116
	12	0.0114 ± 0.00338	0.9975	4176.2	0.01105	70.24132
	10	0.0190 ± 0.0007	0.9959	4176.2	0.01105	70.24132
	12	0.0151 ± 0.0007	0.9967			
VI $C_1=4.076$ (mg/L)	12	0.00189 ± 0.00019	0.99954	19319	0.00211	88.63
	10	0.00162 ± 0.00013	0.9996	19319	0.00211	88.63
	12	0.00317 ± 0.00024	0.99922	14876	0.00383	85.42
	14	0.00333 ± 0.00014	0.99918	0.99917	0.00608	81.53
	12	0.0034 ± 0.00014	0.99818	10713	0.00608	81.53
	16	0.0074 ± 0.00042	0.9986			
	12	0.00572 ± 0.00039				

$n = 4 \pm S.D.$

Appendix IX.C. Alteration of blood flow at low influent lidocaine concentration to the liver (Study VII, VIII, & IX)

Study	Blood flow (mls/min)	Average effluent lidocaine concentration (mg/L)	Extraction Ratio	Predictions		Model II Co _{II}
				Model I A _I (mls/min)	Co _I (mg/L)	
VII Cl=4.563 (mg/L)	12	0.0208 ± 0.00503	0.9954			
	10	0.0364 ± 0.00193	0.9920	3266.7	0.01393	67.32
	12	0.0126 ± 0.00163	0.9972			0.00544
	14	0.0115 ± 0.00017	0.9975	3984.6	0.01598	69.71
VIII Cl=4.455 (mg/L)	12	0.0148 ± 0.00067	0.9968			
	10	0.0369 ± 0.00148	0.9919	2278.9	0.03181	63.02
	12	0.0330 ± 0.00249	0.9928			0.08886
	14	0.0280 ± 0.00689	0.9937			
IX Cl=4.728 (mg/L)	12	0.0207 ± 0.00291	0.9953	2741.4	0.01618	65.22
	10	0.0108 ± 0.00126	0.9976			0.00654
	12	0.0155 ± 0.00108	0.9965	4004.2	0.01551	69.75
	14	0.0158 ± 0.00114	0.9965			0.03053
IX Cl=4.728 (mg/L)	12	0.0299 ± 0.00128	0.9933	2438.3	0.02902	63.82
	10	0.0278 ± 0.00336	0.9938			0.08244
	12					
	14					
IX Cl=4.728 (mg/L)	12	0.0172 ± 0.00139	0.9964	3945.1	0.01195	69.59
	10	0.0212 ± 0.00537	0.9955			0.00449
	12	0.0115 ± 0.00532	0.9976			
	14	0.0183 ± 0.00083	0.9961	4886	0.01351	72.14
IX Cl=4.728 (mg/L)	12	0.00117 ± 0.0007	0.9975			0.02734
	10	0.1200 ± 0.02676	0.9746	2043.1	0.03673	61.72
	12	0.0435 ± 0.00599	0.9908			0.0998
	14					

n = 4 ± S.D.

Appendix XA. Extraction of MEGX with Altering Concentrations under Constant Blood Flow
(10 ml/s/min) - Studies I, II and III

	MEGX Influent concentration (mg/L)	MEGX Effluent concentration (mg/L)	Extraction Ratio MEGX
Study I	11.1974	5.8336 ± 0.1893	0.4790
	20.8667	14.5735 ± 0.7369	0.3177
	11.1373	6.0966 ± 0.1136	0.4526
Study II	2.1308	0.4033 ± 0.2256	0.8107
	3.3223	0.9713 ± 0.1172	0.7076
	4.9771	1.8006 ± 0.3280	0.6382
	1.8843	0.3947 ± 0.04002	0.7905
Study III	0.6274	0.0643 ± 0.01362	0.8974
	1.3299	0.1782 ± 0.01735	0.8660
	2.2064	0.2852 ± 0.01476	0.8707
	3.2305	1.2632 ± 0.05322	0.6090
	4.9356	1.9428 ± 0.2077	0.6063
	0.6274	0.2107 ± 0.03364	0.6641
	6.4909	2.8524 ± 0.2541	0.5606

n = 4 ± S.D.

Appendix XB. Extraction of MEGX with Altering Concentrations under Constant Blood Flow (10 ml/s/min) - Studies IV, V, and VI

	MEGX Influent Concentration (mg/L)	MEGX Effluent Concentration (mg/L)	Extraction Ratio MEGX
Study IV	0.6216	0.0647 ± 0.010046	0.8959
	0.7524	0.0766 ± 0.008124	0.8982
	1.3532	0.2072 ± 0.01027	0.8468
	1.7901	0.2291 ± 0.01924	0.8720
	2.7638	0.5321 ± 0.01855	0.8075
	0.7542	0.1421 ± 0.00915	0.8111
Study V	1.8112	0.2327 ± 0.02267	0.8715
	1.1002	0.09968 ± 0.00204	0.9094
	0.7765	0.09800 ± 0.01241	0.8738
	0.4598	0.06236 ± 0.00759	0.8614
	1.8112	0.2322 ± 0.01668	0.8718
Study VI	3.0804	0.9143 ± 0.00293	0.7032
	1.8504	0.3397 ± 0.02054	0.8164
	1.4085	0.2262 ± 0.01233	0.8394
	1.6714	0.1667 ± 0.01003	0.8544
	2.2903	0.0942 ± 0.00518	0.8597
	3.1318	1.2005 ± 0.01550	0.6167
	9.218	4.2403 ± 0.2463	0.5400

n = 4 ± S.D.

Appendix XI A. Alteration of Blood Flow at Low Concentrations of MEGX to the Liver
Studies I, II and III

Study	Influent MEGX Concentration (mg/L)	Blood Flow (mls/min)	Effluent MEGX Concentration (mg/L)	Extraction Ratio	A ₁ (mls/min)	Predictions		
						Model I Co ₁ (mg/L)	Model II Co ₁ (mg/L)	Co ₁ (mg/L)
I	0.554	10	0.0317 ± 0.0033	0.9427	121.28	0.499	25.75	0.0648
		12	0.0274 ± 0.0048	0.9505				
		10	0.0527 ± 0.0304	0.9048				
		14	0.0304 ± 0.00787	0.9451	101.25	0.0697	24.1015	0.0991
		10	0.0468 ± 0.00962	0.9155				
		16	0.0434 ± 0.00164	0.9216	100.36	0.0803	24.012	0.1235
II	0.449	10	0.0811 ± 0.00482	0.8192				
		12	0.0487 ± 0.00538	0.8914	51.51	0.0848	18.17	0.0988
		10	0.0649 ± 0.00938	0.8553				
		14	0.0517 ± 0.00315	0.8847	64.34	0.0846	20.06	0.1071
		10	0.0559 ± 0.00403	0.8754				
		16	0.0537 ± 0.00478	0.8803	72.39	0.0872	21.09	0.1202
III	0.526	10	0.1321 ± 0.01326	0.7491				
		14	0.1069 ± 0.0081	0.7969	39.02	0.1056	14.82	0.1825
		10	0.0824 ± 0.00528	0.8435				
		16	0.0923 ± 0.00708	0.8247	52.18	0.1235	18.28	0.1678
		10	0.0867 ± 0.00848	0.8353				
		12	0.0889 ± 0.00906	0.8311	56.33	0.0923	18.93	0.1086
		10	0.0718 ± 0.00478	0.8636				

n = 4 ± S.D.

Appendix XIB. Alteration of Blood Flow at Low Concentrations of MEGX to the Liver
Studies IV, V and VI

Study	Influent MEGX Concentration (mg/L)	Blood Flow (mls/min)	Effluent MEGX Concentration (mg/L)	Extraction Ratio	Predictions			
					Model A ₁	Model C ₀	Model A ₁₁	Model C ₀₁₁
IV	0.551	10	0.0481 ± 0.00229	0.9128	90.18	0.0741	23.04	0.1062
		14	0.0591 ± 0.00308	0.8929	77.88	0.0736	21.74	0.0900
		10	0.0619 ± 0.0047	0.8878	68.05	0.1049	17.83	0.181
		12	0.0655 ± 0.00285	0.8813				
		10	0.0634 ± 0.00422	0.8851				
		16	0.1063 ± 0.00814	0.8074				
		10	0.0777 ± 0.00263	0.8592				
		14	0.0789 ± 0.00759	0.8570				
		10	0.1351 ± 0.00711	0.7845	27.59	0.211	13.24	0.2435
		14	0.1051 ± 0.00421	0.8324				
V	0.627	10	0.1985 ± 0.00721	0.6834	26.54	0.1952	12.96	0.2129
		12	0.1200 ± 0.00475	0.8086	31.33	0.212	14.1937	0.2582
		10	0.1446 ± 0.01203	0.7694				
		16	0.1382 ± 0.00975	0.7796				
		10	0.1587 ± 0.00908	0.7469				
		10	0.0511 ± 0.00307	0.9028				
VI	0.526	10	0.0402 ± 0.00245	0.9235	85.99	0.0644	22.616	0.0799
		12	0.0585 ± 0.00725	0.8887				
		10	0.0361 ± 0.00238	0.9313				
		14	0.0599 ± 0.00368	0.8886				
		10	0.0395 ± 0.00179	0.9248				
		16	0.0760 ± 0.00453	0.8554				

n = 4 ± S.D.

Appendix XIIA. Appearance of MEGX in Effluent Perfusion from Lidocaine (Low Concentrations) with Blood Flow Changes - Studies I, II and III

Study	Blood Flow (mls/min)	Effluent Lidocaine Concentrations (mg/L)	MEGX Co ₂ Lidocaine	Predictions			
				Co ₂ MEGX *	Co ₂ Lidocaine	Co ₂ MEGX I (mg/L)	Co ₂ Lidocaine I Co ₂ MEGX II
Cl=4.3787 mg/L							
I	10	0.00575 ± 0.00037	0.03680 ± 0.00725	7.3306	0.0084		
	12	0.008425 ± 0.00071	0.0377 ± 0.00356	5.1254	0.0099	0.0413	3.18
	10	0.0055 ± 0.00054	0.0319 ± 0.00676	6.6433	0.0084		
	16	0.01621 ± 0.00152	0.0778 ± 0.00858	5.5973	0.0204	0.0605	0.795
	10	0.010375 ± 0.00061	0.0436 ± 0.00720	4.8134	0.0091		
	14	0.01962 ± 0.00109	0.0780 ± 0.00595	4.5536	0.0204	0.0704	0.9086
II	10	0.01483 ± 0.00386	0.0570 ± 0.00450	4.4025	0.0149		
	12	0.0126 ± 0.00216	0.1681 ± 0.00359	15.1508	0.0443		
	14	0.0305 ± 0.00325	0.1378 ± 0.00828	5.311	0.0363	0.1806	4.5428
	12	0.0352 ± 0.0093	0.1415 ± 0.03151	4.5654	0.0373		
	10	0.0291 ± 0.00315	0.1298 ± 0.01066	5.0658	0.0342	0.1413	15.332
	12	0.0480 ± 0.01467	0.1975 ± 0.02366	4.673	0.0521		
III	16	0.0733 ± 0.00454	0.1939 ± 0.00935	3.0166	0.0511	0.2345	1.3628
	12	0.0343 ± 0.00259	0.1542 ± 0.00966	5.1057	0.0407		
	10	0.1347 ± 0.00607	0.1703 ± 0.00695	4.6246	0.1426		
	12	0.0278 ± 0.00294	0.1926 ± 0.02346	4.7992	0.0443	0.4324	5.2242
	10	0.0134 ± 0.00055	0.1597 ± 0.0662	7.8682	0.0501		
	12	0.0186 ± 0.00074	0.1071 ± 0.0155	13.5352	0.0416	0.1249	
Cl=4.368 mg/L	16	0.0931 ± 0.00470	0.2152 ± 0.02513	6.5395	0.0278		
	12	0.0243 ± 0.00312	0.0996 ± 0.00504	2.6252	0.0560	0.1379	1.3628
				4.6550	0.0259		
						$n = 4 \pm S.D.$	

*corrected for molecular weights

n = 4 ± S.D.

Appendix XIIB. Appearance of MEGX in Effluent Perfusion From Lidocaine (Low Concentrations) with Blood Flow Changes - Studies IV, V and VI

Study	Blood Flow (mls/min)	Lidocaine	Effluent Concentrations		COMEGX *		COMEGX *		Predictions	
			MEGX	COMEGX	COMEGX	Oil Lidocaine (mg/L)	COMEGX	COMEGX *	Oil Lidocaine (mg/L)	COMEGX *
IV Cl=4.3868 mg/L	12	0.0049 ± 0.00103	0.1224 ± 0.00446	28.6116	0.0320	8.177	0.0348	0.0320	0.0348	8.177
	14	0.0078 ± 0.00038	0.1336 ± 0.00605	19.6168	0.0464		0.01930	13.8616	0.0464	
	12	0.0147 ± 0.00230	0.1779 ± 0.01307	12.4173	0.0481		0.0179	12.4173	0.0481	
	16	0.0170 ± 0.00054	0.1843 ± 0.02716	14.3076	0.0571		0.01569	11.6494	0.0560	
	12	0.0175 ± 0.00209	0.2186 ± 0.05025	11.6494	0.0560		0.0110	15.0811	0.0412	
	10	0.0211 ± 0.00275	0.2146 ± 0.05025	11.6494	0.0560		0.0110	15.0811	0.0412	
V Cl=4.6245 mg/L	12	0.0049 ± 0.00042	0.0367 ± 0.00364	8.5788	0.0090		0.005364	9.2530	0.0102	0.0637
	14	0.0051 ± 0.00034	0.0412 ± 0.00286	9.4235	0.0179		0.00364	9.4235	0.0179	0.0637
	12	0.0088 ± 0.00204	0.0724 ± 0.01334	10.4313	0.0246		0.00286	10.4313	0.0246	0.1047
	16	0.0108 ± 0.00082	0.0993 ± 0.01562	8.4900	0.0209		0.00207	8.4900	0.0209	0.1047
	12	0.0114 ± 0.00338	0.0845 ± 0.0120	6.5046	0.0267		0.00521	6.5046	0.0267	0.1047
	10	0.0190 ± 0.0007	0.1079 ± 0.00397	6.8875	0.0225		0.00397	6.8875	0.0225	0.0731
VI Cl=4.0756 mg/L	12	0.00189± 0.00019	0.0707 ± 0.01637	42.8464	0.0199		0.0019	42.8464	0.0199	
	10	0.00162± 0.00013	0.05578± 0.01220	39.4385	0.0157		0.0013	39.4385	0.0157	
	12	0.00317± 0.00013	0.0937 ± 0.0435	33.8561	0.0263		0.0013	33.8561	0.0263	
	14	0.00333± 0.00014	0.0803 ± 0.02361	27.8714	0.0226		0.0014	27.8714	0.0226	0.1019
	12	0.0034 ± 0.00014	0.0809 ± 0.01505	27.2538	0.0227		0.0014	27.2538	0.0227	0.1019
	16	0.0074 ± 0.00042	0.2258 ± 0.06809	34.9192	0.0635		0.0042	34.9192	0.0635	
VII	12	0.00572± 0.00038	0.3752 ± 0.07608	75.1318	0.1054		0.0038	75.1318	0.1054	6.7006
	12									

n = 4 ± S.D. n = 4 ± S.D.

*corrected for molecular weights

Appendix XIIC. Appearance of MEGX in Effluent Perfusion from Lidocaine (low Concentrations) with Blood Flow Changes - Studies VII, VIII and IX

Study#	Blood Flow (mls/min)	Effluent Concentrations (mg/L)	Co _{MEGX} Co _{Lidocaine}		Predictions Co _{MEGX} Co _{Lidocaine}	
			MEGX	Lidocaine	Co _{MEGX} Co _{Lidocaine}	Co _{MEGX} (mg/L)
Co_{MEGX}						
VII C1=4.5628 mg/L	12	0.0208 ± 0.00503	0.4103 ± 0.05361	22.5941	0.1030	0.2437
	10	0.0364 ± 0.0019	0.2158 ± 0.03351	7.1439	0.0542	5.4514
	12	0.0126 ± 0.00163	0.1744 ± 0.03123	15.8538	0.0438	
	14	0.0115 ± 0.00017	0.2557 ± 0.0298	25.4677	0.0642	12.7198
	12	0.0148 ± 0.00267	0.6899 ± 0.06097	53.3927	0.1752	
	16	0.0369 ± 0.00148	0.3946 ± 0.02055	12.2486	0.0991	1.3065
VIII C1=4.4513 mg/L	12	0.0350 ± 0.00249	1.2699 ± 0.5503	44.0771	0.3188	7.9499
	12	0.0280 ± 0.006689	0.1815 ± 0.02105	7.4246	0.0467	
	10	0.0207 ± 0.00291	0.591 ± 0.01380	8.8035	0.0409	0.1152
	12	0.0108 ± 0.00126	0.0948 ± 0.03169	10.0541	0.0244	38.046
	14	0.0155 ± 0.00108	0.1428 ± 0.01041	10.5525	0.0367	4.6564
	12	0.0158 ± 0.00114	0.1477 ± 0.01810	10.7073	0.0580	
IX C1=4.7279 mg/L	16	0.0299 ± 0.00128	0.1766 ± 0.01584	6.7651	0.0597	0.1987
	12	0.0278 ± 0.003356	0.1503 ± 0.0109	6.1926	0.0387	1.8171
	12	0.0172 ± 0.00139	0.2964 ± 0.02912	19.7382	0.0627	
	10	0.0212 ± 0.005537	0.1994 ± 0.0198	10.7733	0.0422	0.1919
	12	0.0115 ± 0.00532	0.1642 ± 0.04167	16.3544	0.0398	60.1921
	14	0.0183 ± 0.00083	0.2186 ± 0.1301	13.6822	0.0530	0.1873
Co_{Lidocaine}						
VII C1=4.5628 mg/L	12	0.0017 ± 0.0007	0.1567 ± 0.01600	15.3405	0.0380	5.6785
	16	0.1200 ± 0.02676	0.3667 ± 0.04873	3.5002	0.0888	0.2603
	12	0.0435 ± 0.00059	0.2336 ± 0.00942	6.1509	0.0566	4.5428

 $n = 4 \pm S.D.$ $n = 4 \pm S.D.$

*corrected for molecular weights

REFERENCES

1. Gréhant, N.,
Physiologique des reins par le dosage de l'urée dans le
sang et dans l'urine
J. Physiol. Pathol. Gen. 6:1, 1904.
2. Ambard L., and Weill A.
Les lois numériques de la sécrétion rénale de l'urée et du
chlorine de sodium
J. Physiol. Pathol. Gen. 14:753, 1912.
3. Addis T.
Ratio between the urea content of the urine and blood after
administration of large quantities of urea
J. Urol. 1:263-287, 1917.
4. Möller E., McIntosh J. R., Van Slyke D.D.
Studies of urea excretion
J. Clin. Invest. 6:427-465, 1929.
5. Lewis A.E.
The concept of hepatic clearance
Am. J. Clin. Pathol. 18:789-795, 1948.
6. Shore P.A., Brodie B.B. and Hogben C.A.M.
The gastric secretion of drugs: A pH partition hypothesis
J. Pharmacol. Exp. Ther. 119:361-369, 1957.
7. Heinemann H.O and Fishman A.P.
Nonrespiratory function of the mammalian lung
Physiological Reviews 49:1-47, 1969.
8. Vane J.R.
The Role of the lung in the metabolism of vasoactive substances
in "Pharmacology and Pharmacokinetics" edited by Teorell T.,
Dedrick R.L. and Condliffe P.G., Plenum Press 1974.
9. Litterest C.L., Mamnaugh E.G., Reagan R.L. and Gram T.E.,
Comparison of in vitro drug metabolism by lung, liver and
kidney in several common laboratory species
Drug Metabolism and Disposition 3:259-265, 1975.
10. Mehendale H.M. and El-Bassilouni E.A.
Uptake and disposition of aldrin and dieldrin by the perfused
rabbit lung
To be published.

11. Rowland M.
The Influence of route of administration on drug availability
J. Pharm. Sci. 101:70-74, 1972.
12. Wagner J.G., Northam J. I, Always C.D. and Carpenter O.S.
Blood levels of drug at the equilibrium state after multiple dosing
Nature 201:1301-1302, 1965.
13. Westlake, W.J.
Time integral of drug concentration in the central (plasma) compartment
J. Pharm. Sci. 59:722-723, 1970.
14. Rowland M., Benet L.Z. and Graham G.G.
Clearance concepts in pharmacokinetics
Journal of Pharmacokinetics and Biopharmaceutics 1:123-136, 1973.
15. Jusko W.J. and Gibaldi M.
Effects of change in elimination on various parameters of the two compartment open model
J. Pharm. Sci. 61:1270-1273, 1972.
16. Jelliffe R.W.
An improved method of digoxin therapy
Ann. Int. Med. 69:1301-1302, 1968.
17. Orme B.M. and Cutler R.E.
The relationship between kanamycin pharmacokinetics: Distribution and renal function
Clin. Pharmacol. Ther. 10:543-550, 1969.
18. Cutler R.E. and Orme B.M.
Correction of serum creatinine concentration and kanamycin half-life
JAMA 209:539-542, 1969.
19. McHenry M.C., Gavan T.L., Gifford R.W., Geurkink N.A., van Ommen R.A., Town M.A. and Wagner J.G.
Adjustments based on endogenous creatinine clearance and serum creatinine concentration
Ann. Int. Med. 74:192-197, 1971.
20. Wagner J.G.
Biopharmaceutics and Relevant Pharmacokinetics First Ed.
Drug Intelligence Publications 1971.
21. Rowland M.
Drug Administration and Regimens in "Clinical Pharmacology" Chapter
Edited by Melmon K.L. and Morrelli H., McMillan 1972.

22. Koelle G.B.
Neuromuscular blocking agents in "The Pharmacological Basis of Therapeutics"
Fourth Ed., edited by Goodman L.S. and Gilman A.
McMillan Company, 1971.
23. Doyle F.P., Nayakir J.H.C., Smith H.C. and Stove E.R.
New penicillins stable towards both acid and penicillinase
Nature 192:1183-1184, 1961.
24. Kakemi K, Sesaki H., Mayashi M. and Nadi T.
Absorption and excretion of drugs XXXVII. Effects of Ca^{++} on the absorption of tetracycline from the small intestine
Chem. Pharm. Bull. 16:2206-2212, 1968.
25. Sweeney W.M., Hardy S.M., Dornbusch A.C. and Rüegsegger J.M.
Absorption of tetracycline in human beings as affected by certain excipients
AM & CT IV: 642-656, 1957.
26. Shand D.G. and Nies A.S.
The almost complete hepatic extraction of propranolol during Intravenous administration in the dog
Life Sci. 10:1417-1421, 1971.
27. Gibaldi M., Boyes R.N., Feldman S.
Influence of first pass effect on availability of drugs
J. Pharm. Sci. 60:1338-1340, 1971.
28. Shannon J.A. and Smith H.W.
The excretion of inulin, xylose and urea by normal and phlorinized man
J. Clin. Invest. 14:393-401, 1935.
29. Ham J.M., Pirola R.C., Elmslie R.G.
Function of the isolated Pig Liver Surg. Gynecol. & Obstet. 129:470-474, 1969.
30. Berk P.D., Blaschke T.F. and Waggoner J.G.
Defective bromosulphthalein clearance in patients with constitutional hepatic dysfunction (Gilbert's Syndrome)
Gastroenterology 63:472-481, 1972.
31. Sereny G., Kalant H. and Endrenyi L.
Evaluation of high dose bromosulphthalein clearance test in the diagnosis of minimal alcohol liver disease
J. Med. 3:41-59, 1972.

32. Paumgartner B., Probst P., Kraines R. and Leevy C.M.
Kinetics of Indocyanine green removal from the blood
Ann. N.Y. Acad. Sci. 170:134-147, 1970.
33. Clarkson M.J. and Richards T.G.
Steady state plasma clearance of bromosulphthalein and
Indocyanine green measured by single injection.
Res. Vet. Sci. 8:454-462, 1967.
34. Rasmoe K., Juul-Nielsen J., Iversen-Hansen R.,
Schmidt A. Winkler and Tygstrup N.
The functional pattern of the isolated perfused pig liver
Scand. J. Gastro. suppl. 149-154, 1971.
35. Tygstrup N., Funding J., Juul-Nielsen J., Kelding S.,
Koudahl, G., Rasmoe K., and Winkler K.
The function of the perfused and *in vivo* pig liver.
Scand. J. Gastro. supp. 131-138, 1971.
36. Tengstrom B.
The discriminatory ability of a galactose tolerance test
and some other tests in the diagnosis of cirrhosis of the
liver, hepatitis and biliary obstruction
Scand. J. Clin. Invest. 23:159-169, 1969.
37. Branch R.A., Herbert C.M. and Read A.E.
Determinants of serum antipyrine half-lives in patients with
liver disease
Gut 14:569-573, 1973.
38. Dobson E.L., and Jones H.B.
The behavior of intravenously injected particulate material
Acta Med. Scand. suppl. 273, 1952.
39. Jeunet F.S., Shoemaker W.J., Good R.A.
Isolable double perfusion of the liver in the study of the
reticuloendothelial system
Nature 215:61, 1967.
40. Agarwal M.K., Hoffman W.W. and Rosen F.
The effect of endotoxin and thorotrast on inducible enzymes in
the isolated perfused rat liver.
Biochem. Biophys. Acta 177:250, 1969.
41. Behnke A.R., Jr.
The liver in relation to the body as a whole in "Liver Function"
edited by Brauer R.W., Washington
American Institute of Biological Sciences, 1958.

42. Greenway C.V. and Stark R.D.
Hepatic vascular beds
Physiological Reviews 51:23-65, 1971.
43. Brauer R.W., Leong G.F. and Pessotti R.L.
Vasomotor activity in the isolated perfused rat liver
Am. J. Physiol. 174:304, 1953.
44. Fischer A.
Dynamics of circulation in "The Liver" edited by Rouiller C.
N.Y. Academic Press, 1963
45. Ross B.D.
Perfusion Techniques in Biochemistry
A Laboratory Manual, Clarendon Press, Oxford 1972.
46. Brauer R.W.
Liver circulation and function
Physiological Reviews 43:115-213, 1963.
47. Brauer R.W.
"Liver Function", page 7 Publication #4,
American Institute of Biological Sciences,
Washington, D.C. 1958.
48. Williams R.T.
"Detoxification Mechanisms"
N.Y. Wiley 1959.
49. Smith R.L.
"The Excretory Function of the Bile", The Elimination of Drugs
and Toxic Substances in Bile
Chapman and Hall, London 1973.
50. Boyes R.N., Adams H.J. and Duce B.R.
Oral absorption and disposition kinetics of lidocaine
hydrochloride in dogs
J. Pharmacol. Exp. Ther. 174:1-8, 1970.
51. Boyes R.N., Scott D.B., Jebson P.L., Godman M.J. and
Julian D.G.
Pharmacokinetics of lidocaine in man
Clin. Pharmacol. Ther. 12:115-116, 1971.
52. Shand D.G. and Rangno R.E.
The disposition of propranolol I. Elimination during oral
absorption in man.
Pharmacology 7:159-168, 1972.

53. Brauer R.W.
Hepatic blood flow and its relation to hepatic function
Am. J. Digestive Diseases 8:564-576, 1963.
54. Winkler K., Kelding S. and Tygstrup N.
Clearance as a quantitative measure of liver function in
"The Liver: Quantitative Aspects of Structure and Function"
page 144-155, Karger-Basel, 1973.
55. Anderson, M.N. and Kuchiba K.
Measurement of acute changes in liver function and blood flow
Arch. Surg. 100:541-545, 1970.
56. Bradley E.L.
Measurements of hepatic blood flow in man
Surgery 75:783-789, 1974.
57. Larsen J.A.
Elimination of ethanol as a measure of hepatic blood flow
In the cat. I. Experiments with single injection of ethanol
Acta Physiol. Scand. 57:201-208, 1963.
58. Brauer R.W.
Liver
Annual Review of Physiology 18:253-278, 1956.
59. Brauer R.W., Leong G.F., McElroy R.F., Jr., and Holloway R.J.
Hemodynamics of the vascular tree of the isolated rat liver
preparation
Am. J. Physiol. 186:537-542, 1956.
60. Culbertson J.W., Wilkins R.W., Ingelfinger F.J. and Bradley E.E.
The effect of upright position upon the hepatic blood flow
M.J. Clin. Invest. 30:325, 1951.
61. Stenson R.E., Constantino R.T. and Harrison D.C.
Interrelationships of hepatic blood flow, cardiac output
and blood levels of lidocaine in man
Circulation 43:205-211, 1971.
62. Bradley S.E., Ingelfinger F.J. and Bradley G.P.
Hepatic circulation in cirrhosis of the liver
Circulation 5:410-419, 1952.
63. Branch R.A., Shand D.G., Wilkinson G.R. and Nies A.S.
Increased clearance of antipyrine and d-propranolol after
phenobarbital treatment in the monkey
J. Clin. Invest. 53:1101-1107, 1974.

64. Cumming J.F. and Mannerling G.J.
Effect of phenobarbital administration on the oxygen requirement for hexobarbital metabolism in the isolated perfused rat liver and the intact rat
Biochem. Pharmacol. 19:973-978, 1970.
65. Raøl A., Hansen F.V., Kelding S., Tygstrup N., Tønnensen K and Winkler W.K.
Effect of hypoxia on the function of the isolated perfused pig liver
Digestion 10:375-376, 1974.
66. Brauer R.W., Holloway R.J. and Leong G.F.
Temperature effects on radiocolloid uptake by the isolated rat liver
Am. J. Physiol. 189:24-30, 1957.
67. Hobbs K.E.F., Hunt A.C., Palmer D.B., Badric F.E., Morris A.M., Mitra S.K., Peacock J.H., Immelman E.J. and Riddell A.G.
Hypothermic perfusion as a method of short-term porcine liver storage
Brit. J. Surg. 55:862, 1968.
68. Elmslie R., Pirola R.C., Coroneos N. and Ham J.M.
Function of the liver after isolated cold perfusion
Surg. Gynecol. & Obstet. 131:694-696, 1970.
69. Wardell W.M.
Redistribution Drug Interactions: A Critical Examination of Putative Clinical Examples in "Drug Interactions"
Edited by Morselli P.L, Garattini S. and Cohen S.N.
Raven Press 1974.
70. Reidenberg M.M. Oder-Cederlof I., von Bahr C., Borgå O. and Sjöqvist F.
Protein binding of diphenylhydantoin and desmethylimipramine in plasma from patients with poor renal function
N. Engl. Med. 285:264-268, 1971.
71. Hooper W.D., Bochner F., Eadie M.J., Tyer J.H.
Plasma protein binding of diphenylhydantoin. Effects of sex hormones, renal and hepatic disease
Clin. Pharmacol. Ther. 15:276-282, 1974.
72. Blaschke T.F., Meffin P.J., Melmon K.L. and Rowland M.
Influence of acute viral hepatitis on phenytoin kinetics and protein binding
Clin. Pharmacol. Ther. 17:685-691, 1975.
73. Rowland M. and Matin S.
Kinetics of drug-drug interaction
Journal of Pharmacokinetics and Biopharmaceutics 1:553-567, 1973.

74. Rowland M. Thomson, Melmon K.L. and Guilchard A.
The disposition kinetics of lidocaine in man
Ann. N.Y. Acad. Sci. 179:383-398, 1971.
75. Evans G.H., Shand D.G.
Disposition of propranolol VI. Independent variation in steady state circulating drug concentrations and half-life as a result of plasma drug binding in man
Clin. Pharmacol. Ther. 14:494-500, 1973.
76. Levy G. and Yacobi A.
Effect of protein binding on the elimination of warfarin
J. Pharm. Sci. 63:805-806, 1974.
77. Friedman M. and Byers S.O.
Clearance of allantoin in the rat and dog as a measure of glomerular filtration rates
Am. J. Physiol. 151:192, 1947.
78. Wan S.H. and Riegelman S.
Renal contribution to overall metabolism of drugs. I. Conversion of benzoic acid to hippuric acid
J. Pharm. Sci. 61:1278-1283, 1972.
79. Wan S.H. and Riegelman S.
Renal contribution to overall metabolism of drugs. II.
Biotransformation of salicylic acid to salicyluric acid
J. Pharm. Sci. 61:1284-1287, 1972.
80. Rowland M. and Riegelman S.
Pharmacokinetics of acetylsalicylic acid and salicylic acid after intravenous administration in man
J. Pharm. Sci., 57:1313-1319, 1968.
81. Brauer R.W., Pessotti R.L. and Pizzolato P.
Isolated rat liver preparation. Bile production and other basic properties
Proc. Soc. Exp. Biol. 78:174-181, 1951.
82. Brauer R.W., Holloway R.J. and Leong G.F.
Changes in liver function and structure due to experimental passive congestion under controlled hepatic vein pressures
Am. J. Physiol. 186:537-542, 1956.
83. Herz R., Cueni B., Bircher J. and Paumgartner B.
The excretory capacity of the isolated rat liver, an in vitro-
in vivo comparison
Nauyn-Schmiedeberg's Arch Pharmacol. 277:297-304, 1973.

84. Miller L.L., Bly C.G., Watson M.L. and Bale W.F.
The dominant role of liver in plasma protein synthesis. A direct study of the isolated perfused rat liver with the aid of lysine^{4-C}
J. Exp. Med. 94:431, 1941.
85. Green M. and Miller L.L.
Protein catabolism and protein synthesis in perfused livers of normal and alloxan diabetic rats
J. of Biol. Chem. 235:3202-3208, 1960.
86. Ryoo H. and Tarver H.
Studies on protein synthesis with a new liver perfusion apparatus
Proceedings of the Society for Experimental Biology and Medicine 128:760-772, 1968.
87. Hoffenberg R., Gordan A.H., Black E.G. and Louis L.N.
Plasma protein catabolism by the perfused rat liver
Biochem. J. 118:401-404, 1970.
88. Mortimore G.E., Tletze F.
Studies on the mechanism of capture and degradation of insulin ¹³¹I by the cyclically perfused rat liver.
Ann. N.Y. Acad. Sci. 82:329-344, 1959.
89. Williamson J.R., Garcia A., Renold A.E. and Cahill G.F., Jr.
Studies on the perfused rat liver I. Effect of glucagon and insulin on glucose metabolism
Diabetes 15:183-187, 1966.
90. Mortimer G.E.
Effect of insulin on potassium transfer in isolated rat liver
Am. J. Physiol. 200:1315-1319, 1961.
91. Mayes P.A. and Felts J.M.
Liver function studied by liver perfusion
Proc. Eur. Soc. Drug Toxicity, 7:16-29, 1966.
92. von Bahr C., Borgå O., Fellenius E. and Rowland M.
Kinetics of nortriptyline NT in rats *in vivo* and in the isolated perfused liver: Demonstration of a "first pass" appearance of NT in the liver
Pharmacology 9:177-186, 1973.
93. von Bahr C., Sjögqvist F. and Levy G.
Relation between drug elimination kinetics in intact animals and isolated perfused liver system: phenylbutazone
J. Pharm. Pharmac. 22:867-868, 1970.

94. Briemmer D.D. and van Rossum J.M.
Pharmacokinetics of (+) and (-) and plus or minus hexobarbitone
on man after oral administration
J. Pharm. Pharmac. 25:762-764, 1973.
95. Briemmer D.D. and van Rossum J.M.
Pharmacokinetics of the enantiomers of hexobarbital studied in the
same intact rat in the same isolated perfused rat liver
Eur. J. Pharmacol. 26:321, 1974.
96. Bickel M.H. and Minder R.
Metabolism and biliary excretion of the lipophilic drug molecules,
imipramine and desmethylimipramine in the rat - I. Experiments
in vivo and with isolated perfused livers
Biochem. Pharmacol. 19:2425-2435, 1970.
97. Bickel M.H. and Minder R.
Metabolism and biliary excretion of the lipophilic drug molecules,
imipramine and desmethylimipramine in the rat II. Uptake in bile
micelles
Biochem. Pharmacol. 19:2437-2443, 1970.
98. Bartósek I., Mussini E., Garattini S.
Reduction of nitrazepam by the rat liver
Biochemical Pharmacology 18:2263-2264, 1969.
99. Stitzel R.E., Tephly T.R. and Mannerling G.J.
Inhibition of drug metabolism: VI-Inhibition of hexobarbital metabolism
in the isolated perfused liver of the rat
Molecular Pharmacology 4:15-19, 1968.
100. Kelding S., Tønnesen K., Vallø-Hansen F., Vinterby A. and Tygstrup N.
Modification of galactose elimination kinetics by ethanol in the
perfused pig liver in "Regulation of Hepatic Metabolism", pages 324-333
Munksgaard, Copenhagen 1973.
101. Brauer R.W., Leong G.F. McElroy R.F. and Holloway R.J.
Circulatory pathways in the rat liver as revealed by page 32
chromic phosphate colloid uptake in the isolated perfused
liver preparation.
Am. J. Physiol. 184:593-598, 1956.
102. Wilkinson G.R., Shand D.G.
Commentary. A physiological approach to hepatic drug clearance
Clin. Pharmacol. Ther. 18:377-390, 1975.
103. Goresky C.A., Ziegler W.H. and Bach C.G.
Capillary exchange modelling. Barrier limited and flow limited
distribution
Circulation Research 27:739-764, 1970.

104. Winkler K., Bass S., Kelding S. and Tygstrup N.
The effect of hepatic perfusion on the assessment of kinetic constants in "Regulation of Hepatic Metabolism"
edited by Lundquist F. and Tygstrup N., pages 797-807,
Munksgaard, Copenhagen, 1974.
105. Perrier D. and Gibaldi M.
Clearance and biologic half-life as indices of intrinsic hepatic metabolism
J. Pharmacol. Exp. Ther. 191:17-24, 1974.
106. Nies A.S., Shand P.G. and Branch R.A.
Hemodynamic Drug Interaction
Cardiovasc. Clinics 6: 45-53, 1974.
107. Wilkinson G.R.
Pharmacokinetics of drug disposition. Hemodynamic considerations
Annual Review of Pharmacology 15:11-27, 1975.
108. Benowitz N. and Rowland M.
Determination of lidocaine in blood and tissues
Anesthesiology 39:639-641, 1974.
109. Huffman D., Shoeman D.W. and Azarnoff D.L.
Correlation of the plasma elimination of antipyrine and appearance of 4-hydroxy-antipyrine in the urine of man
Biochemical Pharmacology 23:197-210, 1974.
110. Litcher M., Black M., Arias I.M.
The metabolism of antipyrine in patients with chronic renal failure
J. Pharmacol. Exp. Ther. 187:612-619, 1973.
111. Prescott L.F. and Adjepon-Yamoah K.J. and Roberts C.
Rapid gas-liquid chromatographic estimation of antipyrine in plasma
J. Pharm. Pharmac. 25:205-207, 1973.
112. Halkin H., Meffin P., Melmon K.L. and Rowland M.
Influence of congestive heart failure on blood levels of lidocaine and its active monodeethylated metabolite
J. Clin. Pharmacol. 17:669-676, 1975.
113. Lowry O.H., Rosenbrough N.J., Farr A.L. and Randall R.J.
Protein measurements with the Folin Phenol reagent
J. Biol. Chem. 193:265-275, 1951.
114. Lindros K.O.
The once through perfusion technique-advantages and limitations
in "Alfred Benzon Symposium VI: Regulation of Hepatic Metabolism"
edited by Lundquist F. and Tygstrup N., Academic Press, 1974.

115. Tucker G.T., Bridenbaugh P.O., Moore D.C.
Plasma binding of anilide-type local anesthetic to human plasma:
Relationship between binding, physicochemical properties
Anesthesiology 33:287-303, 1970.
116. Benowitz N., Forsyth R.P., Melmon K.L. and Rowland M.
Lidocaine disposition in monkeys and man. I. Prediction by
a perfusion model
Clin. Pharmacol. Ther. 16:87-98, 1974.
117. Brodie B.B., Axelrod J.
The fate of antipyrine in Man
J. Pharmacol. Exp. Ther. 98:97-104, 1950.
118. Boyes R.N., Scott D.B., Jebson P.J., Godman M.J. and Julian D.G.
Lidocaine pharmacokinetics in man
Clin. Pharmacol. Ther. 12:105-116, 1971.
119. Tucker G.T. and Boas R.A.
Pharmacokinetic Aspects of Intravenous Regional Anesthesia
Anesthesiology 34:538-549, 1971.
120. Boyes R.N., Adams H.J., Duce B.R.
Oral absorption and disposition kinetics of lidocaine hydrochloride
in dogs
J. Pharmacol. Exp. Ther. 174:1-8, 1970.
121. Benowitz N., Forsyth R.P., Melmon K.L. and Rowland M.
Lidocaine disposition of monkey and man. II. Effects of
hemorrhage and sympathomimetic drug administration
Clin. Pharmacol. Ther. 16:99-108, 1974.
122. Hollunger G.
On the metabolism of lidocaine. I. Properties of enzyme system
responsible for the oxidative metabolism of lidocaine
Acta Pharmacol. et Toxicol. 17:356-364, 1960.
123. Hollunger G.
On the metabolism of lidocaine. II. Bioconversion of lidocaine
Acta Pharmacol. et Toxicol. 17:365-373, 1960.
124. DiFazio C.A. and Brown R.E.
Lidocaine metabolism in normal and phenobarbital pretreated dogs
Anesthesiology 30:238-243, 1972.

125. Adjepon-Yamoah K.K. and Prescott L.F.
Lidocaine metabolism in man.
Brit. J. Pharmacol. 47:672P-673P, 1973.
126. Mather L.E. and Thomas J.
Metabolism of lidocaine in man.
Life Science 11:915-919, 1972.
127. Keenaghan J.B. and Boyes R.N.
The tissue distribution, metabolism and excretion of lidocaine in
rats, guinea pigs, dogs and man
J. Pharmacol. Exp. Ther. 180:454-463, 1972.
128. Strong J. M. and Atkinson A.J., Jr.
Simultaneous measurement of plasma concentration of lidocaine
and its deethylated metabolite by mass fragmentography
Analytical Chemistry 44:2287-2290, 1972.
129. Bartósek I., Gualtani A. and Garattini S.
Long-term perfusion of isolated rat liver
Pharmacology 8:244-258, 1972.
130. Guyton A.C.
"Function of the human body"
Second Edition Saunders Company, 1965.
131. Schmucker D.L. and Curtis J.C.
A correlated study of the fine structure and physiology of the
perfused rat liver.
Lab. Invest. 30:201-212, 1974
132. Private Communications with Dr. T. Felke, Department of Anatomy,
University of California at San Francisco, California 1975.
133. Dixon W.J. and Massey F.J.
Introduction to statistical analysis, pages 207-208 Third Edition.
McGraw Hill Book Company, 1969.
134. Private Communications with Dr. S.L. Beal, Senior Statistician
University of California at San Francisco, 1975.
135. Rowland M.
Application of clearance concepts to some literature data on drug
metabolism in the isolated perfused liver preparation and in vivo.
European J. Pharmacol. 17:352-356, 1972.

136. Metzler C.M
A User's Manual for NONLIN
Technical Report 7292/69/7292/025 Upjohn Co., Kalamazoo, Michigan
Nov. 25, 1969.
137. Levy G.
Pharmacokinetics of salicylate elimination in man.
J. Pharm. Sci. 54:959-967, 1965.
138. Wood W.B., Wilson J.H., Benbow R.M. and Hood L.E.
"Biochemistry. A Problem Approach"
Benjamen Inc., 1974.
139. Jähnchen E. and Levy G.
Inhibition of phenylbutazone elimination by its metabolite
oxyphenbutazone
P.S.E.B.M. 141: 963-965, 1972.
140. Ashley J.J. and Levy G.
Inhibition of diphenylhydantoin elimination by its major metabolite
Res. Comm. Chem. Pathol. Pharmacol. 4:97-306, 1972.
141. Whitsett T.L., Dayton P.G. and McNay J.L.
The effect of hepatic blood flow on the hepatic removal rate of
oxyphenbutazone in the dog
J. Pharmacol. Exp. Ther. 177:246-255, 1971.
142. Boxenbaum H.G., Riegelman S. and Elashoff R.M.
Statistical estimations in pharmacokinetics
Journal of Pharmacokinetics and Biopharmaceutics 2:123-148, 1973.
143. Levenspiel O.
"Chemical Reaction Engineering" Second Edition
Wiley and Sons, Inc., 1972.
144. Kety S.S.
Theory and applications of the exchange of inert gas at the lungs
and tissues
Pharmacol. Rev. 3:1-41, 1951.
145. Larson S.M., Millar R.C., Chalmers T.C., Gelrud L.G., Kramer R.J.
and Johnston G.S.
Quantitation of hepatic blood flow by Xenon-133
In "The Liver: Quantitative Aspects of Structure and Function"
pages 96-106.
Karger-Basel, 1973.

146. Leevy C.N. Colakoglu S., TenHove W. and Stone R.
Clinical estimation of portal blood flow in man
in "The Liver: Quantitative Aspects of Structure and Function"
pages 107-117
Karger-Basel, 1973.
147. Thomson P.D., Rowland M. and Melmon K.L.
The influence of heart failure, liver disease and renal
failure on the disposition of lidocaine in man
Am. Heart Journal, 82:417-421, 1971.
148. Branch R.A., Shand D.G. and Nies A.S.
The reduction of lidocaine clearance by di-propranolol: An example
of hemodynamic drug interaction.
J. Pharmacol. Exp. Ther. 184:515-519, 1973.
149. Hoffbrand B.I. and Forsyth R.P.
Regional blood flow changes during nor-epinephrine, tyramine and
methoxamine infusions in the unanesthetized rhesus monkey
J. Pharmacol. Exp. Ther. 184:656-661, 1973.
150. Hoffbrand B.I., Forsyth R.P. and Melmon K.L.
Dose-related effects of isoprenaline on the distribution of
cardiac output and myocardial blood flow in conscious monkeys
Cir. Res. 7:664-669, 1973.
151. Benowitz N., Forsyth R.P., Melmon K.L. and Rowland M.
Lidocaine disposition kinetics in monkey and man.
II. Effects of hemorrhage and sympathomimetic drug administration
Clin. Pharmacol. Ther. 16:99-109, 1974.
152. Forsyth R.P., Hoffbrand B.I. and Melmon K.L.
Redistribution of cardiac output during hemorrhage in the
unanesthetized monkey
Cir. Res. 27:311-320, 1970.
153. Hood W.B. Jr., McCarthy B., Letac N. and Lown B.
Plasma clearance of indocyanine green following experimental infarction
in dogs
Proc. Soc. Biol. Med. 129:4-6, 1968.
154. Branch R.A., Nies A.S. and Shand D.G.
The disposition of propranolol. VIII. General implication of the
effects of liver blood flow in elimination from the perfused rat
liver
Drug Metabolism and Disposition 1:687-690, 1973.

155. Nies A.S., Shand D.G. and Branch R.A.
Hemodynamic Drug Interactions: The effects of altering hepatic blood flow on drug disposition, pages 231-240.
In "Drug Interactions" ed. by Morselli P.L, Garattini S. and Cohen S.N., Raven Press, 1974.
156. Alexanderson B. and Sjögqvist F.
Individual differences in the pharmacokinetics of monoethylated tricyclic antidepressants: Role of genetic and environmental factors and clinical importance
Annal. N.Y. Acad. Sci., 179-751, 1971.
157. Private Communications with Dr. G. Richelderfer, University of California San Francisco, 1973.
158. Kolmodin-Hedman B., Alexanderson B. and Sjögqvist F.
Effects of exposure of lindane on drug metabolism: Decreased hexobarbital sleeping-time and increased antipyrine disappearance rates in rats
Toxicology and Applied Pharmacology 20:299-309, 1971.
159. Kutt H.
Biochemical and genetic factors regulating dilantin metabolism in man
Ann. N.Y. Acad. Sci. 179:704-722, 1971.
160. Morselli P.L., Rizzo M. and Garattini S.
Interactions between phenobarbital and diphenylhydantoin in animals and epileptics
Annals N.Y. Acad. Sci., 179:88-107, 1971.
161. AMA Drug Evaluation
Second Edition page 518, Publishing Sciences Group.
Inc., 1973.
162. Schreiber E.C.
Metabolically oxygenated compounds: Function, conjugation and possible biological implications
J. Pharm. Sci. 63:1177-1190, 1974.
163. Ashley J.J. and Levy G.
Inhibition of diphenylhydantoin elimination by its major metabolite
Res. Comm. Pathol. Pharmacol. 4:297-306, 1972.
164. Ashley J.J., Levy G.
Kinetics of diphenylhydantoin elimination in rats
Journal of Pharmacokinetics and Biopharmaceutics 1:99-102, 1973.

165. Carter E.A. and Isselbacher K.J.
The role of microsomes in the hepatic metabolism of ethanol
Ann. N.Y. Acad. Sci. 179:282-294, 1971.
166. Lehninger A.L.
Biochemistry: The molecular basis of cell structure and function
Worth Publishers, 1970.
167. Lundquist F. and Wolthers H.
The kinetics of alcohol elimination in man
Acta Pharmacol. et Toxicol. 14:265-289, 1958.
168. Makar A.B. and Mannerling G.J.
Kinetics of ethanol metabolism in the intact rat and monkey
Biochem. Pharmacol. 19:2017-2022, 1970.
169. van Ginneken C.A.M., van Rossum J.M. and Fleurin H.L.J.M.
Linear and nonlinear kinetics of drug elimination
I. Kinetics on the basis of single capacity-limited pathways
of elimination with or without simultaneous supply-limited
elimination.
J. Pharmacokinetics and Biopharmaceutics 2:395-407, 1974.
170. Dedrick R.L and Forrester D.D.
Blood flow limitations in interpreting Michaelis constants for
ethanol oxidation in vivo.
Biochem. Pharmacol. 22:113-1140, 1973.
171. Perrier D., Ashley J.J. and Levy G.
Effect of product inhibition on kinetics of drug elimination
Journal of Pharmacokinetics and Biopharmaceutics 1:231-242, 1973.